SYNTHESIS AND EVALUATION OF NOVEL INHIBITORS OF THE CHK2 AND NF-κB PATHWAYS

By

Micah John Luderer

A THESIS

Submitted to
Michigan State University
in partial fulfillment of the requirements
for the degree of

MASTER OF SCIENCE

CHEMISTRY

2011

ABSTRACT

SYNTHESIS AND EVALUATION OF NOVEL INHIBITORS OF THE CHK2 AND NF-κB PATHWAYS

By

Micah John Luderer

The first chapter of this thesis describes synthetic efforts towards novel checkpoint kinase II inhibitors (Chk2). Inhibitors of Chk2 have the potential to protect healthy cells during ionizing radiation treatments by preventing the activation of p53, a cellular apoptotic pathway. Previously our group reported the synthesis of indoloazepine, a hymenialdisine derived natural product. Indoloazepine was found to be a more potent inhibitor of Chk2 compared to the natural product hymenialdisine. The main goal within this thesis was developing a synthesis for the constitutional isomer, *iso*-indoloazepine. Compared to indoloazepine, the inverted indole ring of *iso*-indoloazepine was believed to be capable of making an additional hydrogen bond to Glu-308 in the binding pocket of Chk2. *Iso*-indoloazepine and other analogs have been found to be selective inhibitors of Chk2.

The second chapter of this thesis describes synthetic work to further our understanding of how imidazolines inhibit the proteasome. Primarily, synthetic efforts were directed to resolve several racemic imidazolines into their individual enantiomers. This synthetic work was aimed to elucidate enantioselectivity of the proteasome.

DEDICATION

To my mother and father, my stepmother, my brothers and girlfriend with love.

ACKNOWLEDGMENTS

I kindly thank the entire faculty at Michigan State University for their instruction and support. I am fortunate to have been taught organic chemistry from many excellent professors, namely Dr. Jetze Tepe, Dr. Robert Maleczka, Dr. Babak Borhan, Dr. Greg Baker and Dr. Ned Jackson.

I greatly appreciate the NMR support I have received from Dr. Daniel Holmes over the years, and I am equally grateful to Dr. Richard Stables and his brilliant work with X-ray crystallography. Also, I would like to thank Dr. Dan Jones for his assistance with the mass spectrometry facility.

I kindly thank Dr. Jetze Tepe and his research group (Teri Lansdell, Jason Fisk, Christopher Hupp, Adam Mosey, Samantha Frawley, Thu Nguyen, Amanda Palumbo, Brandon Dutcher, Rahman Saleem, Ke Qu, Mike Kuszpit, Nicole Hewlett, Ben Weaver, Lauren Azevedo and Sujana Pradhan) for their advice and the opportunity to work in the laboratory beside them. More importantly, I thank all these people for the friendships I have made here at Michigan State University. In addition, special thanks to Chris Hupp for assistance with modeling studies, as well as Thu Nguyen and Teri Lansdell for performing all biological testing. Also, I am forever grateful to Michigan State University for financial support over the years and the wonderful opportunity to perform chemistry research.

Lastly I am thankful for my wonderful family (Jack, Connie, Monica, Nathan, and Adam), girlfriend Sarah, and friends Mike and Nicole. Without your constant support none of this is possible.

TABLE OF CONTENTS

LIST OF TABLES

LIST OF FIGURES

LIST OF SCHEMES

ABBREVIATIONS

Ac_2O – Acetic anhydride
AcOH – Acetic acid
Boc_2O – Di-*tert*-butyl dicarbonate
^{13}C NMR – Carbon Nuclear Magnetic Resonance Spectrosocopy
$CDCl_3$ – Deuterated chloroform
Chk2 - Checkpoint kinase 2
DCM - Dichloromethane
DIPEA – N,N-diisopropylethylamine
DMAP – 4-dimethylaminopyridine
DMF – N,N-dimethylformamide
DMSO-d_6 – Deuterated dimethylsulfoxide
EDCI – 1-Ethyl-3-(3-dimethylaminopropyl)carbodiimide
^{1}H NMR – Proton Nuclear Magnetic Resoance Spectroscopy
HRMS – High Resolution Mass Spectrometry
IR – Ionizing Radiation
MS – Mass Spectrometry
NaOAc – Sodium Acetate
PMB – 4-methoxybenzyl
SEMCl - 2-(Trimethylsilyl)ethoxymethyl chloride
TBAHS – Tetrabutylammonium hydrogensulfate
TEA - Triethylamine
THF - Tetrahydrofuran
Troc – 2,2,2-trichloroethyl chloroformate
TsCl – Tosylchloride

CHAPTER I: Synthesis of novel checkpoint kinase II inhibitors and evaluation of their efficacy for radiation oncology treatments

A. Cancer: An Epidemic

It is reasonable to assume that almost everyone throughout the course of their life will somehow be impacted by cancer. Cancer is a rapidly evolving disease, and with its evolvement comes an ever increasing complexity for treatment. This presents a constant challenge to both the physician and the scientist. With such a rapidly evolving disease, a physician must devise a personalized treatment with the highest probability for success. However, with the rapid evolution of cancer, this also places pressure on the scientist to find new therapeutic targets and develop more efficacious treatments. Although cancer is often used as a general term, it is important to note that over 100 forms of cancer exist.[1] In the latest national vital statistics report released in 2010, cancer was the second leading cause of death across the United States (Table I-1).[2] During 2006-2007, cardiovascular disease claimed 616,067 lives (25.4% of total deaths), whereas cancer claimed 562,875 lives (23.2% of total deaths). The results of

Table I-1: Summary of deaths from 2006-2007 in the United States.

Cause of Death from 2006-2007 in the United States	# of Deaths	% of Total Deaths
Cardiovascular Disease	616,067	25.4
Cancer	562,875	23.2
Stroke	135,952	5.6
Chronic lower respiratory disease	127, 924	5.3
Accidents (unintentional injuries)	123,706	5.1
Alzheimer's disease	74,632	3.1
Diabetes	71,382	2.9
Influenza and Pneumonia	52,717	2.2
Nephritis, Nephrotic Syndrome and Nephrosis	46,448	1.9
Septicemia	34,828	1.4
All other causes	576,843	23.8

all causes of death in the United States from 2006-2007 are summarized in Table **I-1**.

As one might expect, there is a disparity between cancer incidences between males and females. Figure I-1 presents data from the U.S. Department of Health and Human Services summarizing the most prevalent forms of cancers developed in males and females.[3] Prostate cancer has the highest incident rate in males, whereas breast

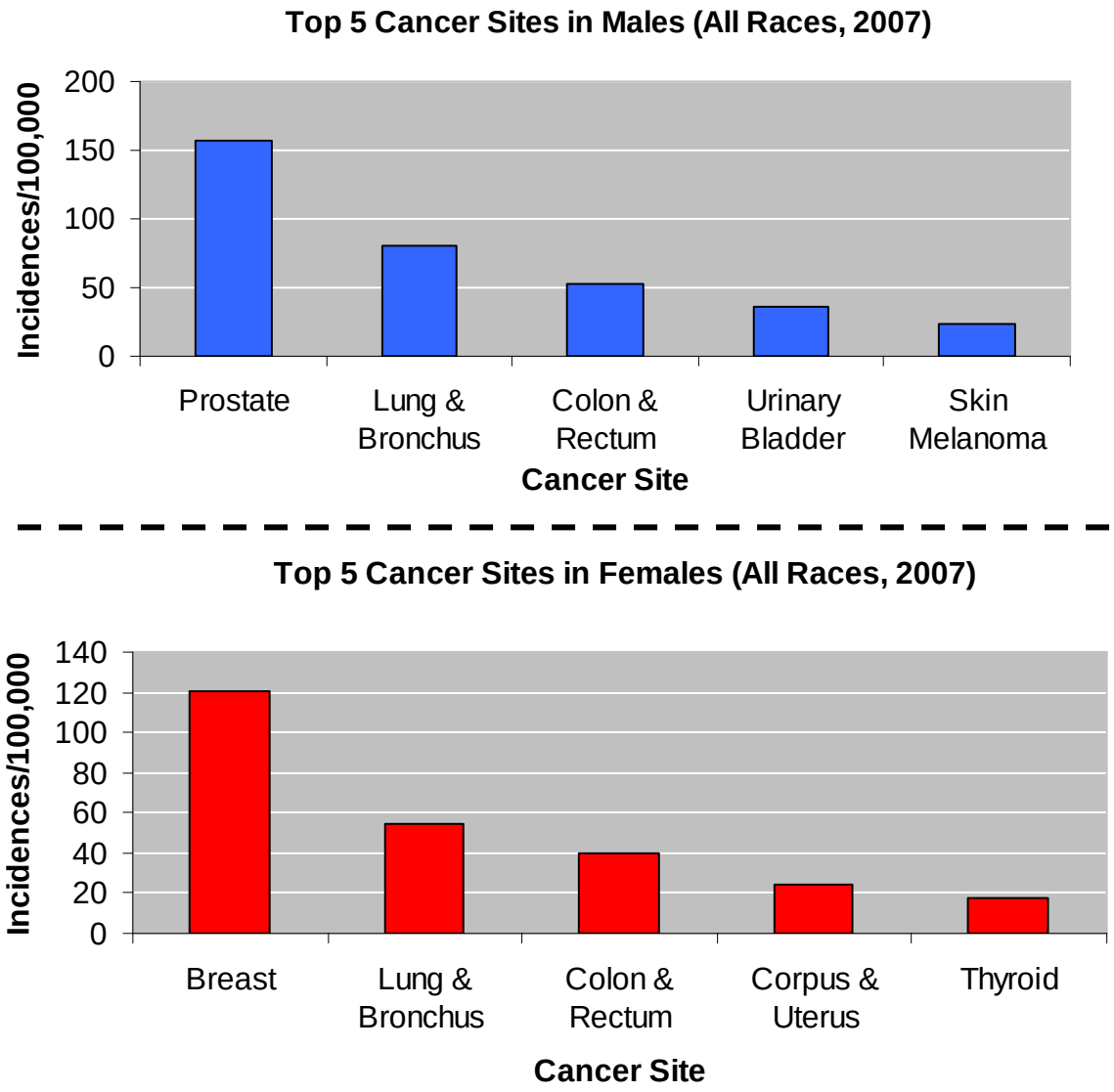

Figure I-1. Top 5 cancer sites for males (blue) and females (red) in the United State during 2007.*
**For interpretation of the references to color in this and all other figures, the reader is referred to the electronic version of this thesis.*

cancer is most prevalent in females. For both males and females, lung cancer has the second highest incident rate. This is especially shocking considering that the American Cancer Society estimates that 30% of cancers are tobacco related.[4] In other words, a significant percentage of lung and other cancers could be mitigated if the population abstained from using tobacco products. Additionally, the incidence of skin myelomas could be prevented by proper UV (ultra-violet) protection. It is quite possible in the near future that the leading cause of death in the United States will be cancer, especially considering the increasing number of drugs available to combat cardiovascular disease such as Lipitor ®.

It is reasonable that a substantial number of cancer incidences could be prevented by living healthier lifestyles, but this will not stop cancer all together. Unfortunately, a significant number of people will still be affected by cancer despite living perfectly healthy lifestyles. As of 2009, the National Cancer Institute estimates that males have 1 in 2 chance of developing cancer, while females have a 1 in 3 chance over their lifetime.[5] In order for cancer to be treated effectively, a continuously growing scientific understanding is a necessity.

Cancer may arise primarily from one of two factors: genetics or environmental factors.[4] Environmental factors contributing to cancer may be due to chemical exposure (such as Radon gas or tobacco), oxidative damage from UV radiation (sun exposure) or exposure to other higher energy radiations (X-ray or nuclear waste). Minimizing exposure to such environmental factors can potentially lower the incidence of certain cancers, such as skin melanomas.

However, there is also another, and perhaps more critical component to developing cancer: genetics. Regardless of living a perfectly healthy lifestyle, some individuals have a genetic predisposition for developing cancer. This can help elucidate the early onset of cancer seen, even when a young individual has been exposed to virtually no harmful environmental factors.[1] If a genetic mutation is passed on to one's offspring, the offspring are inherently at an increased risk for developing cancer sooner. Weinberg explains this as a "leapfrog" effect.[1] Normally, the process of developing a harmful mutation and the subsequent spreading throughout the body could take 3 to 4 decades. However, if the genetic mutation is introduced during embryonic development, the genetic mutation will be spread throughout the body and become ubiquitous.[1] In other words, the mutation has "leapfrogged" over the rate limiting step of spreading throughout the body. This effect illustrates the importance of understanding cancer at the genetic level in order to devise personalized, effective medical treatments.

It is believed that there are 2 major gene classes that are involved in the onset of cancer, proto-oncogenes and tumor suppressor genes.[1] A mutation in a proto-oncogene can result in a cell to over express growth-stimulatory proteins.[1] Alternatively, a mutation in a tumor suppressor gene will impair the cell's normal ability to express proteins that inhibit cell growth.[1] Coupled together, these mutations result in uncontrolled cell growth, or cancer. While these mutations can occur naturally over time, an individual that has been genetically predisposed to these mutations has an increased

risk for cancer onset. Understanding how both environmental and genetic factors facilitate the onset of cancer is imperative for developing novel treatments.

B. Current Treatments for Cancer

As of 2010, the National Institute of Health has estimated that the annual cost of fighting cancer was $263.8 billion dollars.[4] This statistic is perhaps more shocking considering that millions of people, just within the United States, are still losing this battle despite these expenditures.

Cancer treatments primarily can be broken down into radiation treatment and chemotherapy. Chemotherapy utilizes drugs to kill cancerous tissue, to slow cancer cell growth, and to also prevent metastasis as defined by the National Cancer Institute.[6] Alternatively, radiation therapy utilizes high radiation particles (X-rays or γ-rays) to destroy the DNA of the cancerous tissue.[6] Oftentimes a treatment plan will consist of both chemotherapy and radiation treatments. In the event that cancerous tissue has not metastasized (spread throughout the body), surgical removal is desirable if the tumor is an operable location.

Although the aforementioned treatments can be effective in the remission of cancer, these treatments are still imperfect. One difficulty with chemotherapy is specificity; many of the chemotherapeutics are cytotoxic, and selective delivery of a chemotherapeutic agent to cancerous tissue poses a challenge. Inevitably the chemotherapeutics will enter other major organ systems that can result in life threatening organ failure and other undesirable side effects (i.e. hair loss). In addition, chemotherapy is often associated with undesirable nausea and vomiting.[7] In some

cases, patients who have undergone chemotherapy once before will experience nausea and vomiting in anticipation of upcoming treatments.[7] This is not to say that chemotherapy cannot be totally effective. For instance, the development of cis-platin has been largely effective in treatment of testicular cancer.

In radiation treatment, it is inevitable that the ionizing radiation (IR) will damage the surrounding healthy tissue when targeting a tumor. Any healthy tissue that is in the path of radiation will be aversively affected. Radiation therapy generally is administered in one of two forms: external-beam radiation therapy or internal radiation therapy.[8] External-beam radiation therapy utilizes a linear particle accelerator to produce high energy photons (X-ray and γ-rays).[8] Computed tomography scans are used with the particle accelerator to maximize the precision at which the radiation is delivered to the tumor site. Radiation can be delivered to the patient from all possible angles by using Tomotherapy.[8] This type of radiation therapy has the advantage of being able to deliver the radiation from multiple angles, thus keeping the radiation dose within tolerance limits for the given tissue. Additionally, the exposure of sensitive areas in the body to radiation can be minimized.

In contrast, internal radiation therapy (also known as brachytheraphy) introduces radioactive particles at or near the cancerous tissue (sometimes permanently).[8] This method is advantageous for the treatment of internal structures (such as the prostate) that are structurally surrounded by sensitive tissue (i.e. bladder and testicles). However, this is an invasive technique and of course has limitations and is therefore not always applicable.

In order to mitigate the damage towards healthy tissues, the radiation therapy dose is fractionated and administered to the patient, typically every day over a period of several weeks. This is to allow for the normal DNA repair mechanisms to take place in healthy tissues, which typically take 6-12 hours.[9] Considering that healthy tissue is inevitably damaged, compounds are desirable that can protect healthy tissue during radiation treatments. These compounds, termed radioprotectors, offer the benefit of protecting healthy tissue during radiation treatment.[8] In order to be effective, a radioprotector must sensitize the cancerous tissue to the radiation treatment. In other words, the radioprotector must selectively protect healthy tissue, and not cancerous tissue. With this aim in mind, a therapeutic target is needed that can achieve this effect.

C. Elucidating the Chk1 and Chk2 Pathways as Attractive Therapeutic Targets for Radioprotection

Checkpoint kinase II (Chk2) is a therapeutic target that can achieve radioprotection for healthy cells during radiation treatments. The primary goal within this thesis was the development of a Chk2 inhibitor that would effectively be a radioprotector. In order to understand how a Chk2 inhibitor can be a radioprotector, the common cellular response pathways to DNA damage must be understood.

In response to DNA damage, two of the key kinase signaling cascades activated are ATR-Chk1 and ATM-Chk2 as delineated in Figure I-2.[10-12] Both ATM (ataxia-telangiectasia-mutated) and ATR (ataxia-telangiectasia and Rad3 related) are DNA damage sensor proteins.[11] ATM senses DNA double-strand breaks (DSBs) which commonly result from ionizing radiation.[11] In contrast, ATR responds to single-strand

breaks in DNA which commonly are caused by UV radiation.[13] Whereas ATM and ATR are DNA damage sensors, the primary role of Chk1 (Checkpoint Kinase I) and Chk2 is serving as signal transducers.

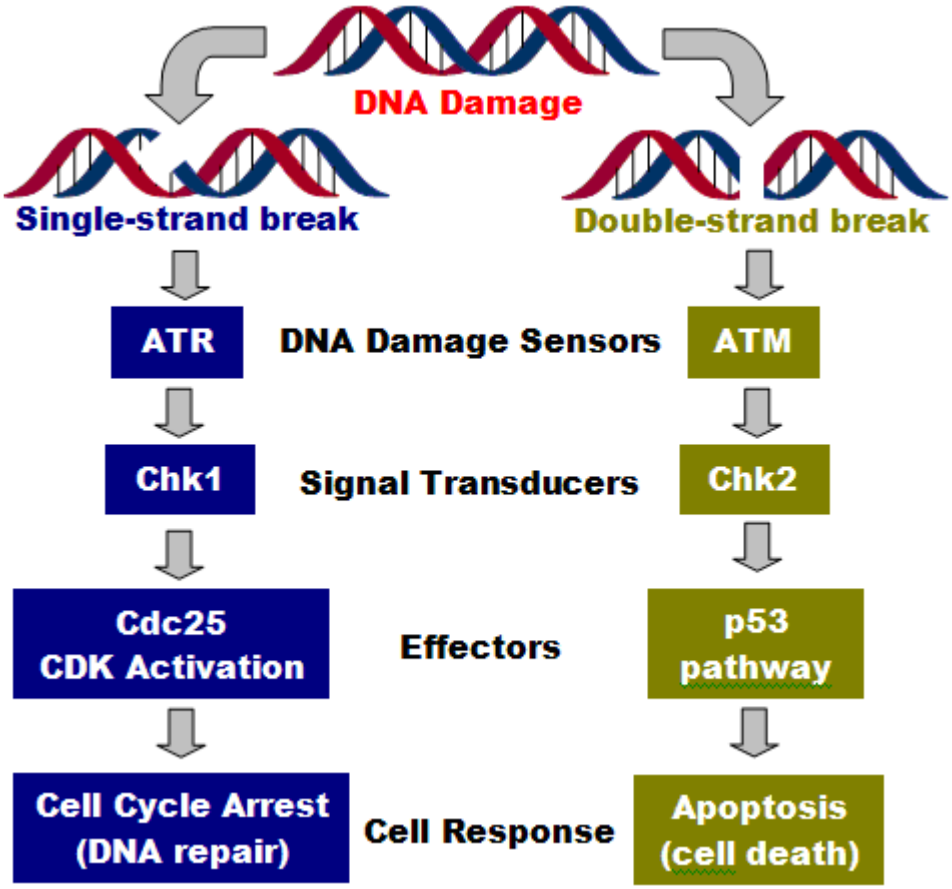

Figure I-2. Overview of Chk1 pathway (left) and Chk2 pathway (right).[12]

In short, it is the responsibility of Chk1 and Chk2 to begin the signal cascade and ultimately carry out the cell responses to the DNA damage.[12] Chk1 and Chk2 modulate effector molecules, such as p53 (a tumor suppressor protein) and Cdc25 that are downstream in the cascade (Figure I-2). The ATR-Chk1 and ATM-Chk2 pathways have very antagonistic effects on the cell cycle and the overall fate of the cell. In response to single-strand DNA damage, the Chk1 pathway ultimately leads to cell cycle arrest,

allowing for DNA repair and potential cell survival. Alternatively, when DNA DSBs are encountered, the Chk2 pathway ultimately leads to apoptosis, or cell death.

Looking at the ATR-Chk1 pathway in more detail (Figure I-2), ATR is responsible for the phosphorylation and subsequent activation Chk1. ATR is believed to phosphorylate Chk1 at Ser317 and Ser345.[10] After phosphorylation, Chk1 results in the phosphorylation of downstream effectors Cdc25a, Cdc25b and Cdc25c. Cdc25a-c are phosphotyrosine phosphatases, and their normal function is to dephosphorylate cyclin-dependent kinases (CDKs) that control transitions in the cell cycle.[12] Phosphorylation of Cdc25a-c by Chk1 renders them inactive and leads to their degradation.[12] Therefore the CDKs are not activated, and normal cell cycle transitions are inhibited resulting in a net cell cycle arrest. This promotes the cell to undergo other normal repair processes and thus promotes cellular survival.

Now considering the ATM-Chk2 pathway (Figure I-2), ATM activates Chk2 by phosphorylation of Thr68 on Chk2.[11,14] Therefore, activation of Chk2 has been described as being ATM-dependent.[14] Following phosphorylation of Thr68, homodimerization of Chk2 occurs resulting in autophosphorylation of Thr383 and Thr387.[15] This is the result of the Fork-head associated (FHA) domain of one Chk2 molecule recognizing the serine/threonine-glutamine (SQ/TQ)-rich domain of another.[16] Once activated, Chk2 will phosphorylate the downstream effector p53, which is a tumor suppressor protein.[10] Although disputable, it is believed Chk2 phosphorylates p53 at

Ser20, indicating that p53 is downstream of Chk2.[12] Upon activation of p53, cellular apoptosis is activated.

There are two conditions that must be satisfied in order to develop an effective checkpoint kinase inhibitor of the aforementioned pathways. If the inhibitor targets cancerous tissue, the inhibitor should selectively inhibit Chk1. If the Chk1 pathway is inhibited for cancerous cells, this will not allow for cell cycle arrest and repair of the damaged DNA, thereby promoting apoptotic pathways.[12] Alternatively, an inhibitor can be designed that selectively inhibits the Chk2 pathway in healthy tissue. If the Chk2 pathway is inhibited in healthy tissue, this will effectively block apoptosis of damaged cells and promote DNA repair and cellular survival.[12] For the remainder of this thesis, only Chk2 inhibitors will be discussed herein.

D. Proof of Principle for Inhibiting Chk2 and Current Inhibitors Thereof

An elegant study published by Motoyama et al further validated Chk2 as a desirable therapeutic target for radioprotection.[17] $Chk2^{-/-}$ knockout mice demonstrated significant resistance to sublethal doses of IR compared to wildtype $Chk2^{+/+}$ mice. This data is summarized in the survival curve found in Figure I-3. When $Chk2^{-/-}$, $Chk2^{+/-}$ and $Chk2^{+/+}$ mice were treated with 8 Gy of X-rays, two-thirds of the $Chk2^{+/-}$ and $Chk2^{+/+}$ mice had died 2 weeks post IR.[17] In contrast, two-thirds of the $Chk2^{-/-}$ mice survived after the equivalent IR exposure.[17] Additionally, the $Chk2^{-/-}$ mice were viable and no apparent

damage to their spleens was observed.[17] In sharp contrast, Chk1$^{-/-}$ exhibit embryonic lethality.[12]

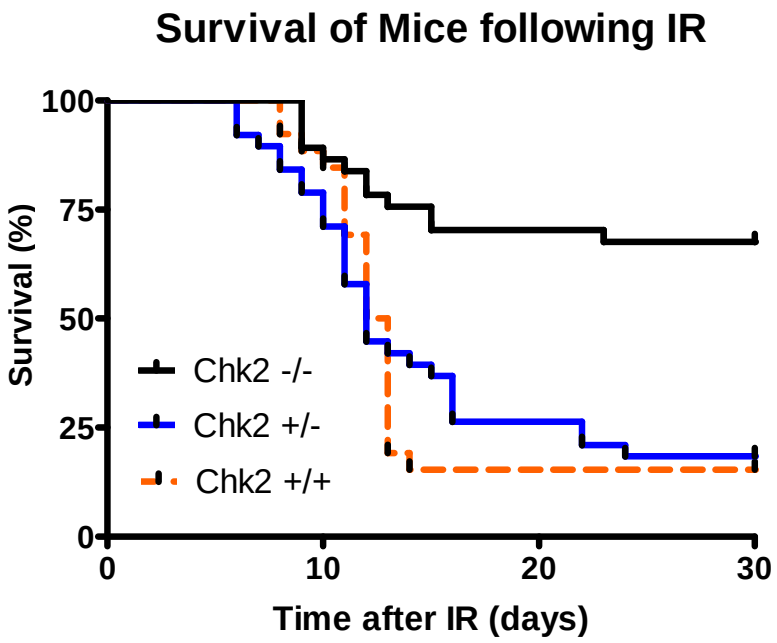

Figure I-3. Chk2$^{-/-}$ mice exemplified increased survival compared to Chk2$^{+/+}$ and Chk2$^{+/-}$ mice when irradiated with 8 Gy of X-rays.[17]

As mentioned previously, the ATM-Chk2 pathway ultimately leads to cell death (apoptosis). It is one of many controls that a cell has to prevent uncontrolled cell growth (cancer) as well as a safeguard to eliminate cells with genetic damage. During IR treatments, both healthy and cancer tissues are inevitably damaged. Therefore, if a small molecule could selectively inhibit the ATM-Chk2 pathway only for healthy cells, you would have an effective radioprotector. Whereas the cancerous tissue should undergo normal apoptotic pathways (i.e. Chk2) in response to the IR, the healthy tissue receives radioprotection when the Chk2 pathway is inhibited.

In order to be an effective Chk2 inhibitor, the Chk2 pathway must only be inhibited in healthy tissue. If Chk2 is simultaneously inhibited in the cancerous cells,

then the same radioprotection is being conferred to cancerous tissue and there is no net therapeutic gain. Fortunately, this condition is met considering that p53 is mutated in over 50% of cancer cell lines.[1,12] Since the p53 pathway is mutant in >50% of cancerous tissues, apoptosis of cancerous cells should not be inhibited. This is because the p53 pathway is not an active apoptotic pathway in a majority of cancers. Therefore the radioprotection achieved for healthy cells by inhibiting Chk2 should not be translated to the cancer cells.

There are a limited number of Chk2 inhibitors found throughout the literature and some examples are displayed in Figure I-4. Interestingly these molecules fall into

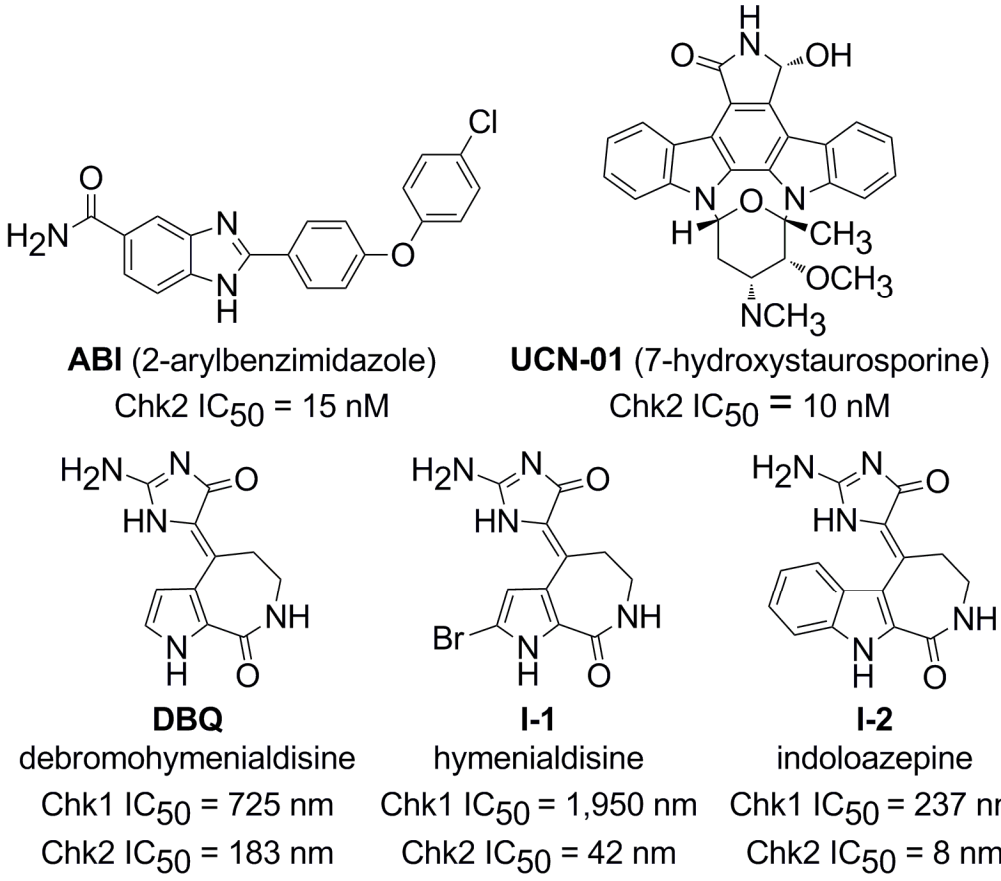

Figure I-4. Current inhibitors of Chk2 and their associated IC_{50} values.[18,20,21] Chk1 values are provided if available.

drastically different families of molecules. Johnson and Johnson has screened various novel benzimidazoles as Chk2 inhibitors and has identified 2-arylbenzimidazole (**ABI**) as a lead candidate (Chk2 IC_{50} = 15 nM).[18] Lead compound **ABI** was also tested at 10 μM concentrations and demonstrated <25% inhibition for 35 other kinases including Chk1.[18] Another inhibitor of Chk2 is indolocarbazole **UCN-01** (7-hydroxystaurosporine) which has underwent phase I clinical trials (Figure I-4).[19] **UCN-01** has been identified as a potent Chk2 inhibitor (IC_{50} = 10 nM) and has potential as a therapeutic.[20]

In addition to inhibitors **ABI** and **UCN-01**, the marine alkaloids hymenialdisine **I-1** and debromohymenialdisine (**DBQ**) have been shown to be potent inhibitors of Chk2 (Figure I-4). **DBQ** was isolated in 1980 from the marine sponge phakellia-flabellata.[22] Two decades later, following a screening of natural extracts, Roberge et al identified **DBQ** as an inhibitor of Chk2 (IC_{50} = 3.5 μM) and Chk1 (IC_{50} = 3.0 μM).[23] Hymenialdisine **I-1** was also discovered as an inhibitor of Chk2 (IC_{50} = 6 μM) but was only isolated in trace quantities.[23] The total synthesis of hymenialdisine **I-1** and **DBQ** was completed by Annoura and Tatsuoka in 1995 and by Horne et al in 2000.[24,25]

Knowing that the pyrrole based scaffold present in **DBQ** is a potent inhibitor of Chk2, the structurally related indole derivative could be envisioned. Following in 2004, Tepe and Sharma published the synthesis of indoloazepine **I-2**, the indole derivative of **DBQ** (Figure I-4).[26] Indoloazepine was shown to be a more potent Chk2 inhibitor (IC_{50} = 8 nM) than the natural products **DBQ** (IC_{50} = 183 nM) and hymenialdisine **I-1** (IC_{50} =

42 nm).[26] Additionally, indoloazepine **I-2** shows great selectivity (30 fold) for Chk2 over Chk1. Although hymenialdisine **I-1** also shows excellent selectivity for Chk2 over Chk1 (46 fold), its use has been limited as a therapeutic because it lacks selectivity towards other kinases.[12] Compared to hymenialdisine **I-1** and indoloazepine **I-2**, **DBQ** is the least potent inhibitor (IC_{50} = 183 nm) and has the poorest selectivity for Chk2 over Chk1 (4 fold).

E. Rationale for the Synthetic Efforts towards *iso*-indoloazepine

Based on the increased selectivity of indoloazepine **I-2** for Chk2 compared to **DBQ**, it was desirable to devise a synthesis of a structurally similar analog. It was hoped that an analog of **I-2** could be more potent and/or more selective for Chk2 over Chk1. The importance of the exocyclic amine present in the glycocyamidine ring of **I-2** was well understood by preparation of the hydantoin **I-3** and dimethylamine **I-4** analogs by Dr. Thu N.T. Nguyen (Figure I-5). Both **I-3** and **I-4** are inactive Chk2 inhibitors (IC_{50} > 10 μM, Figure I-5). In short, analogs **I-3** and **I-4** remove the possibility for hydrogen bonding that is critical for binding in the catalytic site of Chk2 (for a more detailed

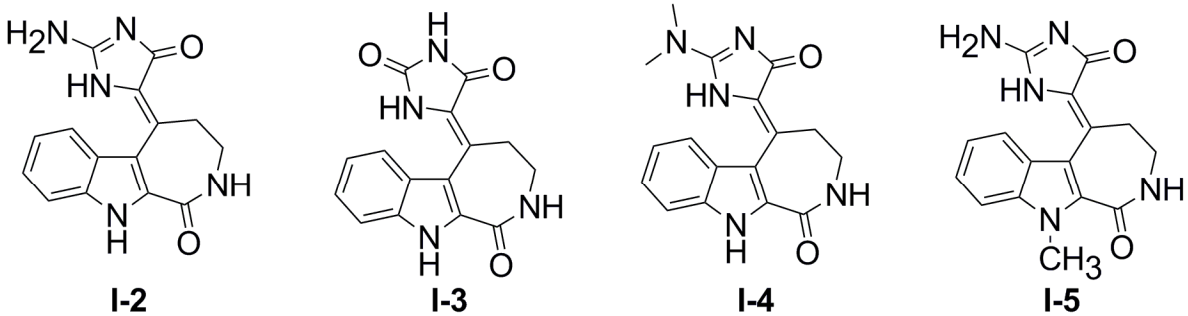

I-2 Chk2 IC_{50} = 13.5 nM | **I-3** Chk2 IC_{50} > 10 mM | **I-4** Chk2 IC_{50} > 10 mM | **I-5** Chk2 IC_{50} > 10 mM

Figure I-5. Various analogs of indoloazepine **I-2** and corresponding IC_{50} values.

discussion see section N). Additionally, the *N*-methylated indoloazepine derivative **I-5** also showed no Chk2 activity (IC_{50} > 10 μM, Figure I-5) indicating that methylation removes an important bonding interaction or creates steric repulsion in the binding pocket. In order to judiciously propose a new analog that could be a potent inhibitor of Chk2, an understanding of the Chk2 binding pocket was essential.

In 2006, Pearl et al reported the co-crystal structure of **DBQ** in the active site of Chk2.[15] This drastically elucidated the hydrogen bonding contacts that were critical in the binding of **DBQ**, and these contacts are found in Figure I-6. Consistent with the lack of inactivity observed with analogs **I-3** and **I-4** (Figure I-5), a key hydrogen bonding interaction for **DBQ** exists between ASN352 and GLU308.[15] Additionally, hydrogen

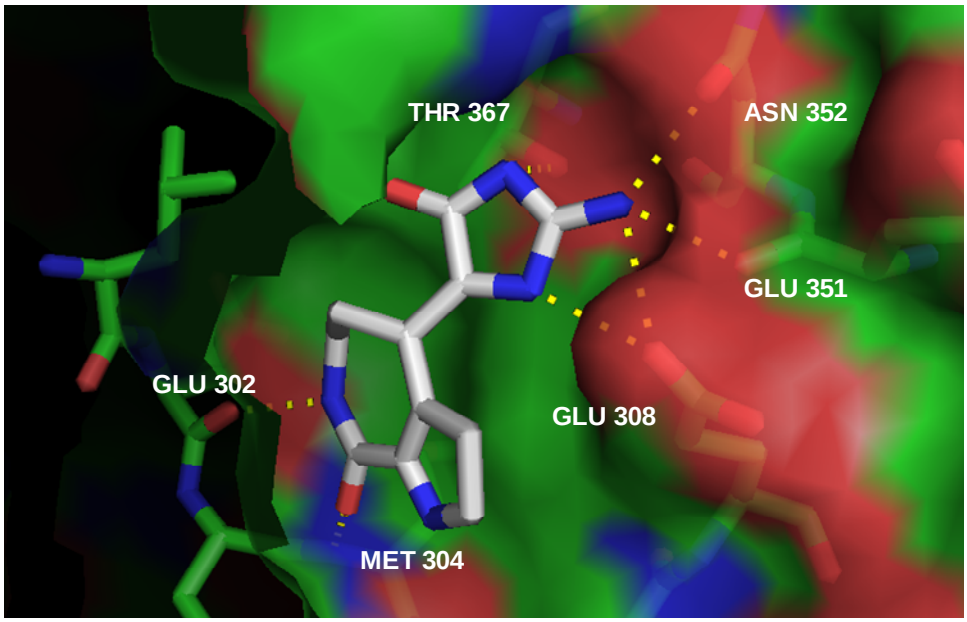

Figure I-6: Crystal structure of debromohymenialdisine (**DBQ**) in the Chk2 catalytic domain (PDB code: 2CN8). The enzyme residues are depicted in green stick form whereas the inhibitor is depicted in gray stick form. Nitrogen atoms are depicted in blue and oxygen in red. The yellow dashes represent hydrogen bonds. Green surface areas represent uncharged residues, positive residues are depicted in blue and negative residues are red.[15]

bonding interactions exist between the 7-membered lactam of **DBQ** and amino acids GLU302 and MET304.

Based upon the co-crystal structure of **DBQ**, it was therefore assumed that the structurally similar **I-2** utilized the same key polar contacts for its binding affinity. Indoloazepine **I-2** could easily be superimposed on **DBQ** in the co-crystal structure and acquire the same key hydrogen bonding contacts (Figure I-8 (right)). Therefore it was desirable to design an inhibitor that would still occupy this active sight and if possible have additional hydrogen bonding contacts that were not present in either **I-2** or **DBQ**.

An analog that was proposed to meet these requirements is *iso*-indoloazepine **I-6**. *Iso*-indoloazepine **I-6** is the constitutional isomer of indoloazepine **I-2** as shown in Figure I-7. The major structural difference between these isomers is that the indole ring is inverted. Figure I-8 displays both **I-2** and **I-6** modeled in the Chk2 binding pocket. The fact that the indole ring is inverted in **I-6** makes this an attractive synthetic target.

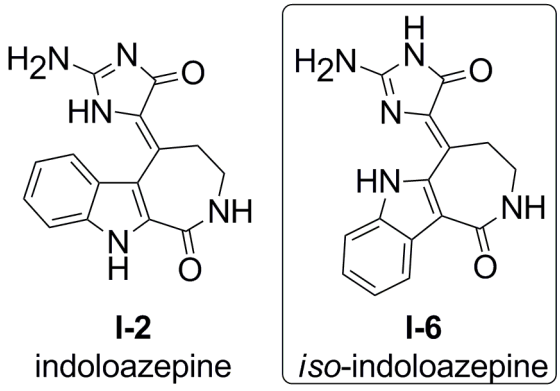

I-2 indoloazepine

I-6 *iso*-indoloazepine

Figure I-7. Indoloazepine **I-2** and the constitutional isomer *iso*-indoloazepine **I-6**.

As noted in Figure I-8, *iso*-indoloazepine **I-6** contains hydrogen bonding contacts between the glycocyamidine ring and amino acids GLU308 and ASN352. These same key hydrogen bonding contacts are also conserved in both the binding of **DBQ** and indoloazepine **I-2** to Chk2. However, since the indole nitrogen is inverted in **I-6**

(compared to indoloazepine **I-2**), an additional hydrogen bond contact is possible (Figure I-8 (left)). *Iso*-indoloazepine **I-6** is capable of forming a hydrogen bond between the indole N-H and GLU308 at a distance of 2.95 Å. In contrast, this hydrogen bond contact is not possible for **I-2** since the indole nitrogen is oriented in the opposite direction of GLU308 (Figure I-8 (right)).

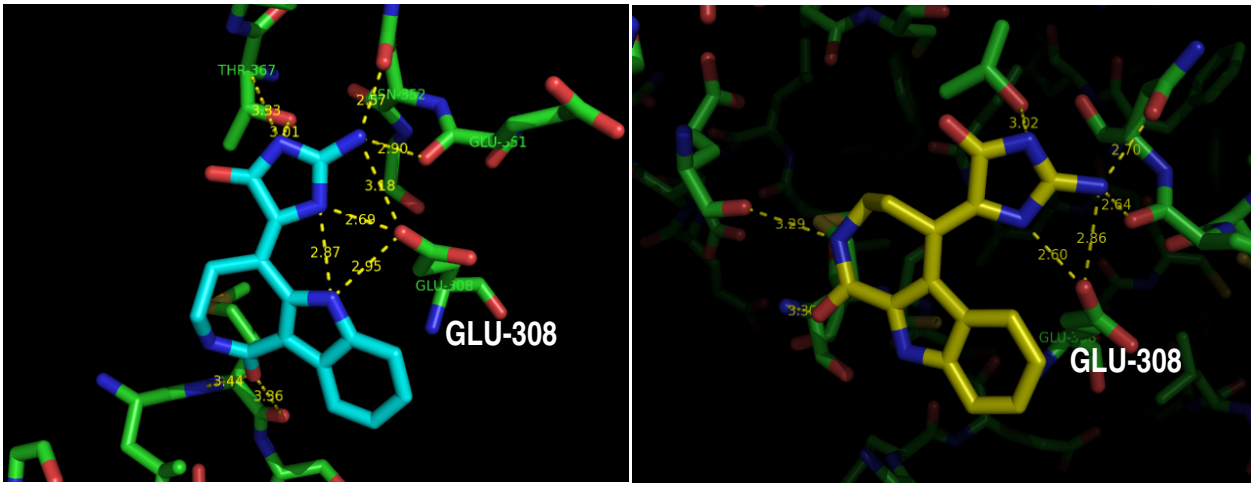

I-6 Polar Contacts **I-2 Polar Contacts**

Figure I-8. Hydrogen bonding contacts of *iso*-indoloazepine **I-6** (left) and indoloazepine **I-2** (right) in Chk2 catalytic site.

The importance of this indole proton is further illustrated by analog **I-5**, the N-methylated derivative of indoloazepine (Figure I-5). When the indole nitrogen is methylated, the Chk2 IC_{50} value is >10 μM. For this reason, the interaction of the indole N-H bond within the Chk2 binding pocket is of particular interest. Therefore, it is possible that this additional hydrogen bonding site found only with *iso*-indoloazepine **I-6** could make this isomer an equal or even more potent Chk2 inhibitor than **DBQ** or indoloazepine **I-2**.

Based on the previous modeling study, there was sound precedent to begin the synthesis of *iso*-indoloazepine **I-6**. The synthesis of **I-6** will be constructed from a simple

indole scaffold. The structure of indole along with the associated numbering convention is displayed in Figure I-9. Indole has a chemical reactivity similar to pyrrole (the scaffold of **DBQ**). One notable difference is the aromatic nitrogen proton is more acidic for pyrrole (pk_a = 17) compared to indole (pK_a = 21).

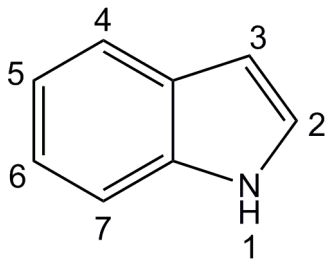

Figure I-9. Indole and the associated numbering convention for nomenclature.

When considering the previously reported syntheses of **DBQ**[24] and indoloazepine **I-2**[26], the key synthetic intermediate to each synthesis is the fused 7-membered lactam ring aldisine **I-7** and indoloaldisine **I-8**, respectively (Figure I-10). Therefore, based on these precedents, the key intermediate for the synthesis of *iso*-indoloazepine **I-6** was identified as *iso*-indoloaldisine **I-9** (Figure I-10). Considering indoloaldisine **I-8** (synthetic precursor of **I-2**), the amide carbonyl within the 7-membered ring is a substituent of the C-2 position (Figure I-10). In contrast, *iso*-indoloaldisine **I-9** will contain the amide carbonyl as a substituent of the C-3 position (Figure I-10). Note

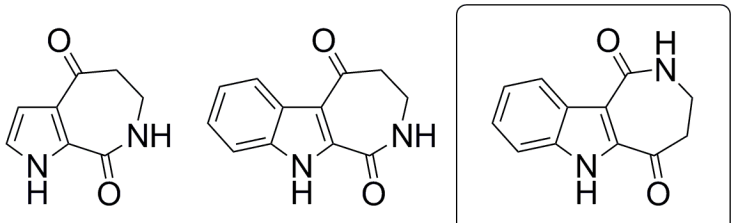

Figure I-10. Key intermediates **I-7** and **I-8** for the syntheses of **DBQ**[24] and indoloazepine **I-2**[26], respectively. Proposed key intermediate **I-9** for the synthesis of *iso*-indoloazepine **I-6**.

that since the synthetic precursors **I-8** and **I-9** are constitutional isomers, their respective final products indoloazepine **I-2** and *iso*-indoloazepine **I-6** will also be constitutional isomers.

Therefore, based on the precedent from the syntheses of **DBQ** and **I-2**, the first synthetic route towards *iso*-indoloaldisine **I-9** was planned. The first synthetic route attempted would utilize a Dieckmann condensation to form the 7-membered lactam ring found in **I-9**.

F. Synthetic Efforts towards an Intramolecular Dieckmann Condensation to Afford *iso*-indoloaldisine.

The first attempted synthetic route towards *iso*-indoloaldisine **I-9** (key intermediate for **I-2**) is outlined by the retrosynthesis presented in Scheme I-1. The key 7-membered ring intermediate **I-9** would be obtained from an intramolecular Dieckmann condensation. The necessary amide linkage would readily be assembled from the commercially available β-alanine ethyl ester, while the corresponding carboxylic acid

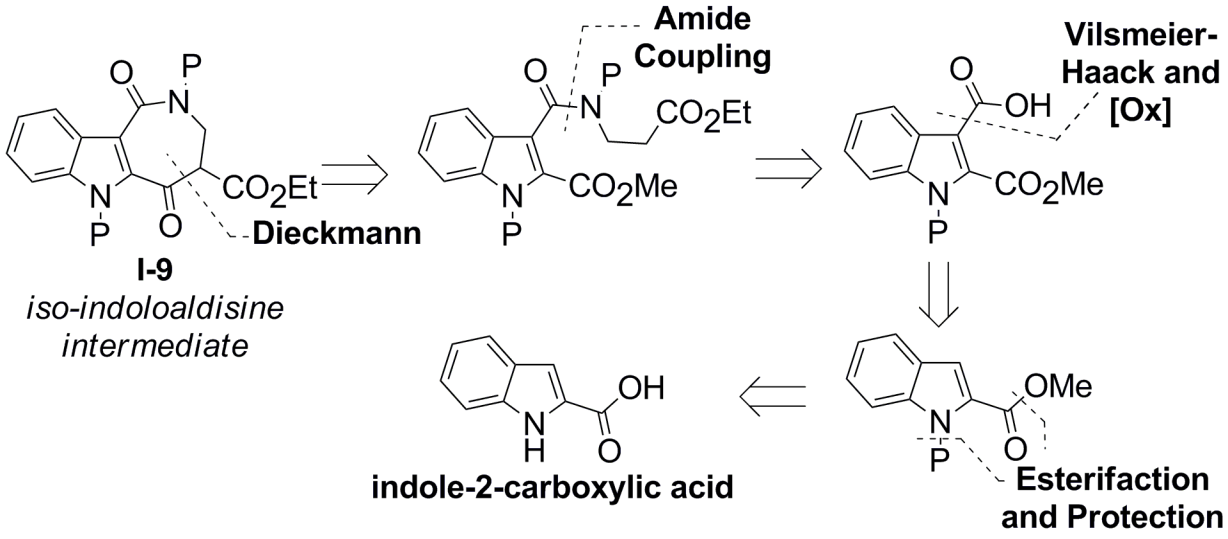

Scheme I-1. Proposed retrosynthesis for forming *iso*-indoloaldisine **I-9** intermediate. P = a protecting group.

would be the product of a Vilsmeier-Haack reaction and subsequent oxidation. The necessary starting material, indole-2-carboxylic acid, is commercially available. Several chemical transformations from **I-9** would yield the target compound *iso*-indoloazepine **I-6**.

The synthesis towards **I-9** begins with commercially available indole-2-carboxylic acid which quantitatively is converted to the corresponding methyl ester **I-10** using TMS-diazomethane (Scheme I-2). The purity of **I-10** is highly dependent on the 95:5 benzene/methanol solvent ratio. If insufficient methanol is added, a TMS-methyl acetate side product is formed approximately in a 1:1 ratio with the desired product.[27] Once the undesired product is formed, it cannot be hydrolyzed by methanol.[27]

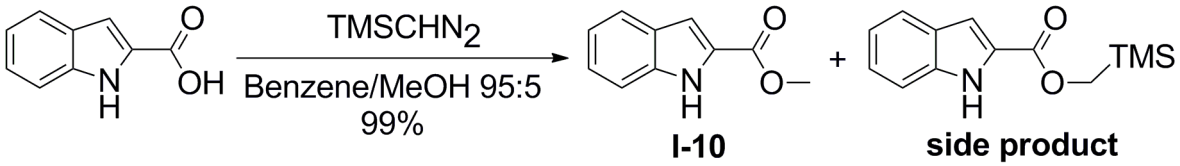

I-10 **side product**

Scheme I-2. Conversion to methyl ester **I-10** using (Trimethylsilyl)diazomethane.

In preparation for the intramolecular Dieckmann condensation, compound **I-10** must be acylated in the C-3 position of the indole ring. The acylation will allow for the introduction of a second ester group which contains acidic α protons that will generate the enolate anion necessary for the Dieckmann condensation. Compound **I-10** is readily acylated to aldehyde **I-11** via a Vilsmeier-Haack reaction with oxalyl chloride and DMF (Scheme I-3). During the reaction, **I-11** precipitates out of the solution as a chloride salt facilitating purification. By filtering and collecting the precipitate, any remaining starting material may be eliminated by rinsing with dichloromethane. The precipitate is an ionic salt and is not converted to the aldehyde (compound **I-11**) until quenched with water.

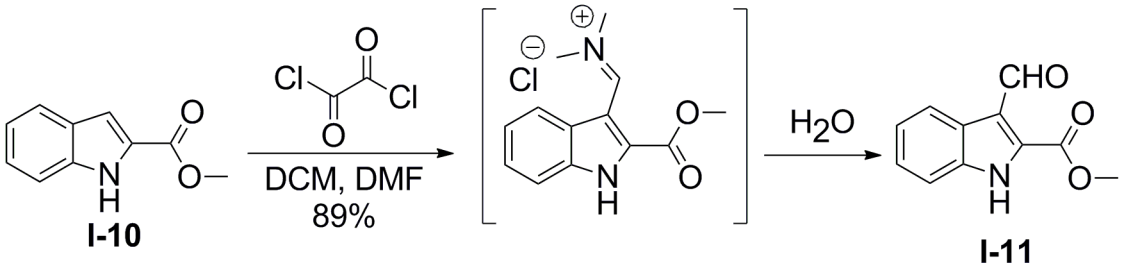

Scheme I-3. Vilsmeier-Haack reaction affording aldehyde **I-11.**

A series of oxidizing agents were used in an attempt to oxidize **I-11** to the corresponding carboxylic acid, which turned out to be problematic (Scheme I-4). $NaClO_2$, as well as the Jones reagent, did not oxidize the unprotected aldehyde **I-11** to the corresponding acid.[28,29] The carboxylic acid derivative of **I-11** was desired so an amide bond could be formed that would introduce the nitrogen for the 7-membered *iso*-indoloaldisine ring. This newly formed amide would also contain the necessary α-protons to generate an ester enolate for the Dieckmann condensation (Scheme I-5).

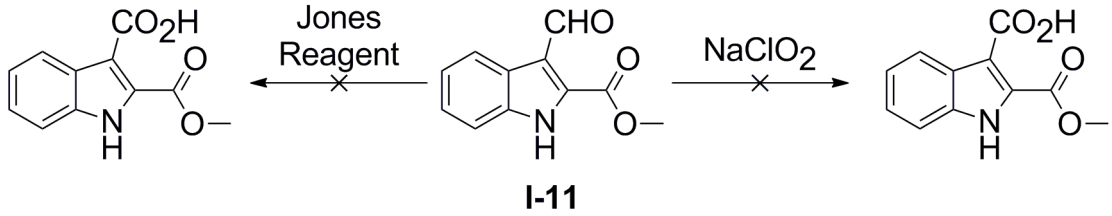

Scheme I-4. Unsuccessful oxidation conditions for compound **I-11**.

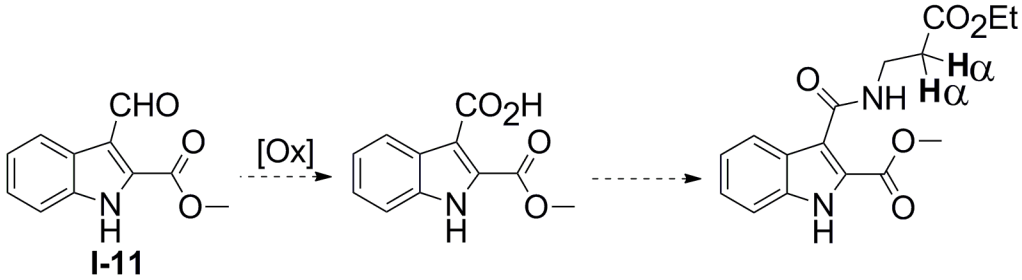

Scheme I-5. Proposed transformation of compound **I-11** to introduce α protons for Dieckmann condensation.

In order to promote oxidation, several reactions were investigated for protecting the indole nitrogen on **I-11** (Scheme I-6). Protecting compound **I-11** is eventually

necessary for the basic conditions of the Dieckmann condensation. Tosylation of **I-11** using TsCl, DMAP and DIPEA was unsuccessful.[30] NaH was used as a stronger base, but even with the addition of crown ether and refluxing temperatures in THF, only a trace amount of product was observed. Treating **I-11** with NaH and TsCl in DMF was also unsuccessful. Tosylation is likely prevented as a result of a strong $Na^+ N^-$ complex that is not readily dissociated in order to react with TsCl. Using K_2CO_3 did yield the desired product but in poor yield.

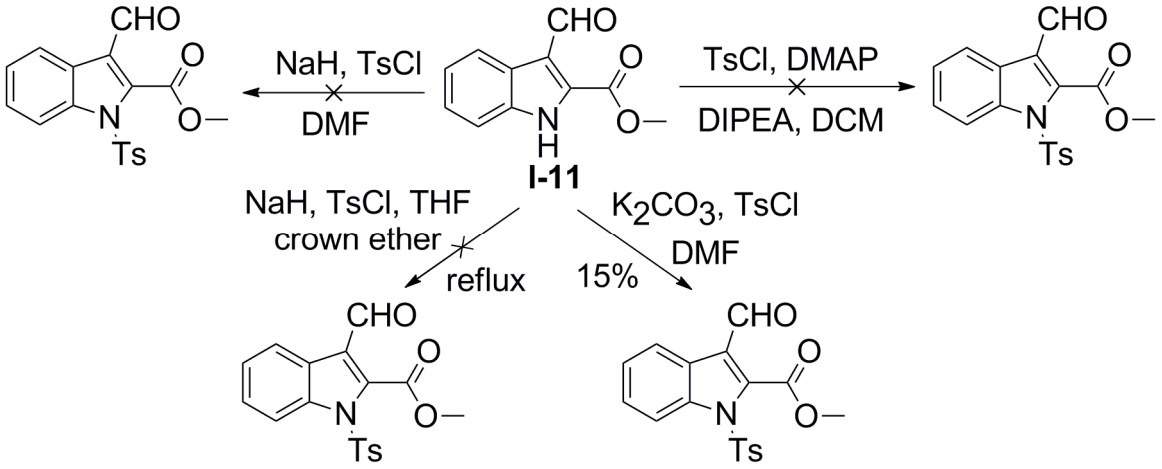

Scheme I-6. Difficultly in tosylating compound **I-11**.

Therefore, attempting to tosylate the precursor **I-10** was the next logical step (Scheme I-7). Using p-TsCl, DMAP and DIPEA, compound **I-12** was afforded in 30% yield. Although the desired product was obtained, purification was difficult due to close R_f values for silica column chromatography. Surprisingly, the unprotected compound **I-10** precedes compound **I-12** travelling through a silica column. The compounds were distinguished and separated by distinct colors under long wave UV radiation. The reported ^{13}C NMR contains additional peaks because of trace compound **I-10** that was inseparable using flash column chromatography.

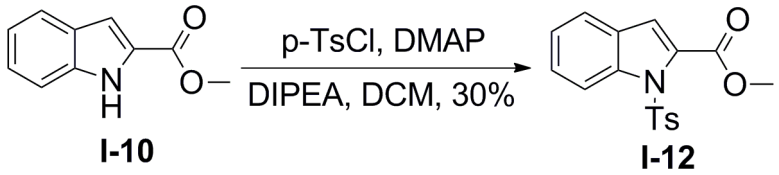

I-10 **I-12**

Scheme I-7. Tosylation of compound **I-10**.

Due to low yield, as well as the difficult purification of compound **I-12** from starting material, it was desirable to try a different protecting group for aldehyde **I-11** (which had proven to be difficult to tosylate). A better route was found by protecting **I-11** with Boc. As shown in Scheme I-8, Boc protected **I-13** is produced in much higher yield than the tosylated equivalent (78% compared to 15%).

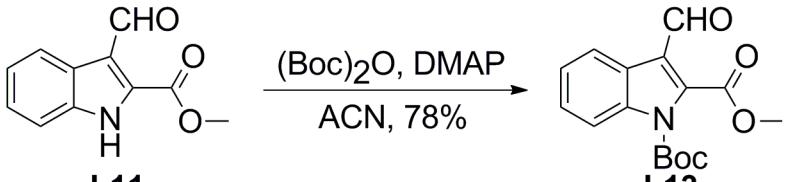

I-11 **I-13**

Scheme I-8. Protection of compound **I-11** with di-*tert*-butyl dicarbonate.

Following the protection of the indole nitrogen with Boc, **I-13** was successfully oxidized to carboxylic acid **I-14** using $NaClO_2$ in a mixture of *tert*-butanol, 2-methyl-2-butene and H_2O (Scheme I-9).[31] In the reaction, 2-methyl-2-butene was used as a chlorine trap. Note that the analogous oxidizing conditions were unsuccessful when the indole nitrogen was not protected (Scheme I-4). The carboxylic acid proton was not

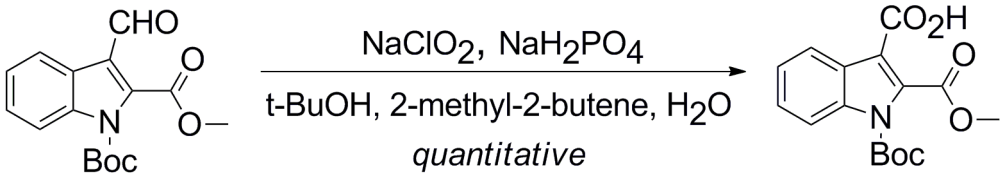

I-13 **I-14**

Scheme I-9. Compound **I-13** is successfully oxidized by conditions that do not oxidize **I-11**.

observed via ^{1}H NMR in $CDCl_3$, but mass spectrometry and ^{13}C NMR indicated that decarboxylation had not occurred. Mass spectrometry indicated that the sodium salt of **I-14** was present.

Carboxylic acid **I-14** allows for the formation of an amide bond that is found in the 7-membered ring of *iso*-indoloaldisine. Therefore, an EDCI-mediated coupling reaction of **I-14** with β-alanine ethyl ester hydrochloride afforded **I-15** in near quantitative yield (95%, Scheme I-10).[32] Following the coupling reaction, the amide nitrogen of **I-15** was protected with Boc (Scheme I-10), which is necessary for the basic conditions of the Dieckmann condensation. The resulting ester **I-16** (containing α protons) when treated with strong base should undergo a Dieckmann condensation to form the desired *iso*-indoloaldisine ring.[33]

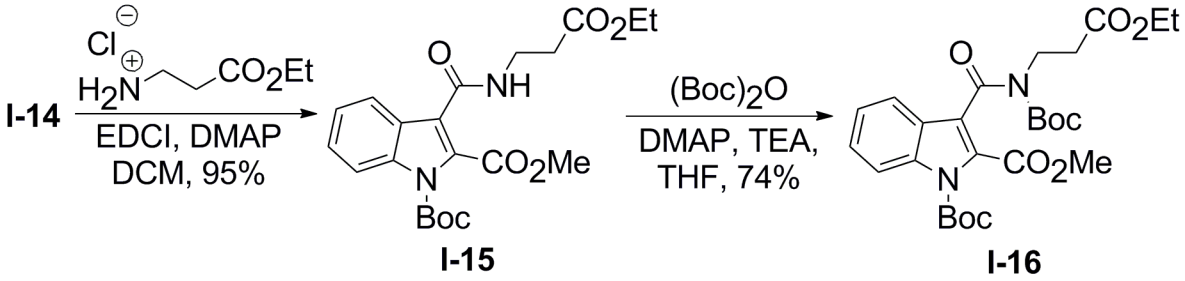

Scheme I-10. EDCI mediated coupling reaction to afford **I-15** and subsequent Boc protection to afford **I-16**.

The Dieckmann condensation was attempted using sodium hydride as outlined in Scheme I-11. The desired *iso*-indoloaldisine product was not obtained and approximately ten side products were observed by TLC. Two of these side products were identified and can be explained mechanistically by β-elimination resulting in the formation of ethyl acrylate (Scheme I-11).

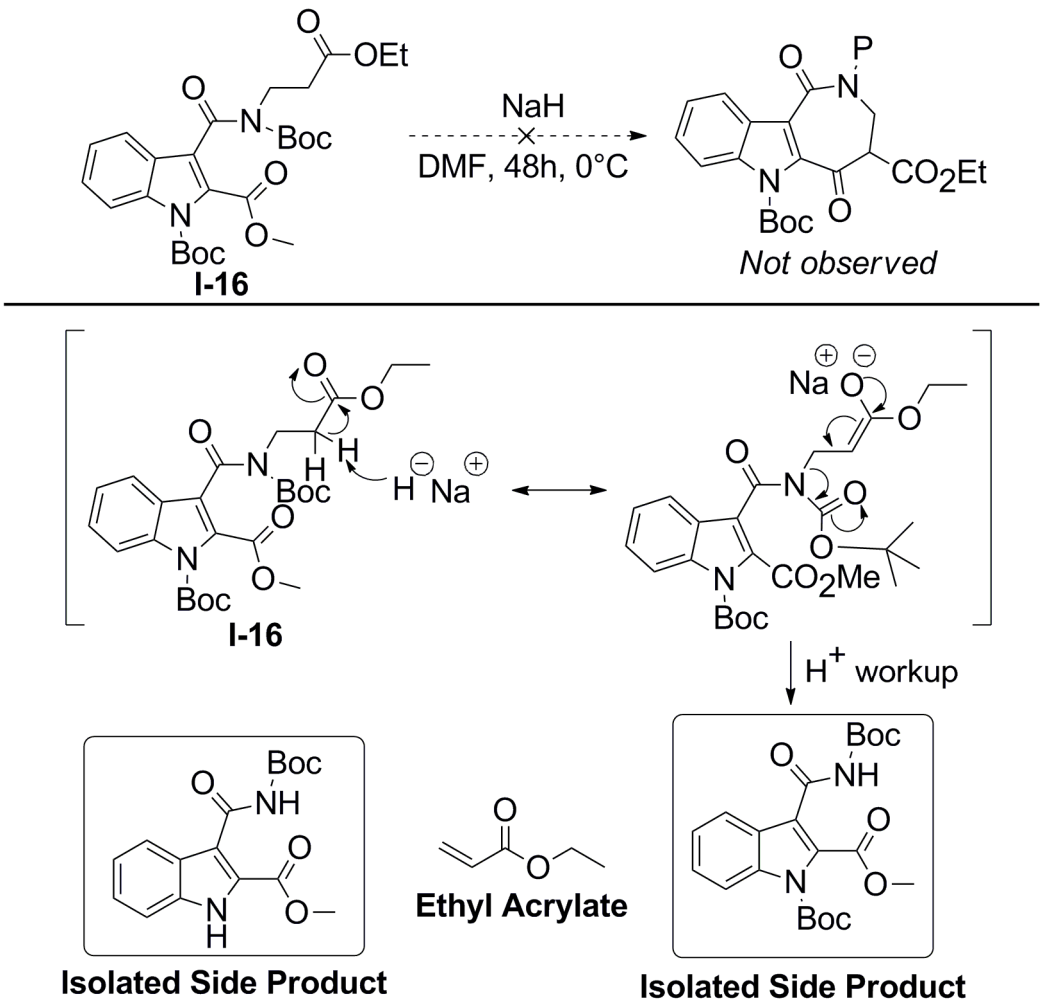

Scheme I-11. Side products result of acrylate formation during Dieckmann reaction with **I-16**.

Formation of the acrylate is a result of E2 elimination. Using ChemBioDraw3D, the starting material was modeled with a minimal potential energy. The configuration along the bond containing the acidic proton showed this proton was not in an anti configuration with respect to the indole leaving group. This is promising because the undesired E2 elimination will be slower than if the proton was in an anti configuration. Also, modeling indicated that the acidic α protons and the methyl ester of **I-16** are in closer proximity to react when Boc is replaced with a PMB group. The desired reaction

is an E conjugate base reaction, in order for the anion to attack the methyl ester carbonyl of compound **I-16.**

In order to prevent undesired acrylate formation, the protective group will be modified to make the indole a poorer leaving group. PMB (4-methoxybenzyl) was chosen since it is electron donating. Unlike the electron withdrawing Boc group, the electron donating PMB group should make the indole a poorer leaving group, thus disfavoring acrylate formation. However, protection of **I-15** with 4-methoxybenzaldehdye followed by $NaCNBH_3$ was unsuccessful and only starting material was recovered (Scheme I-12).[34]

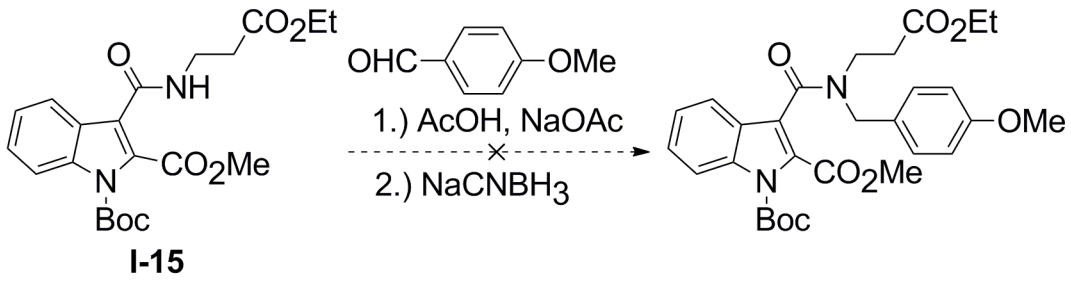

Scheme I-12. Unsuccessful protection of amide nitrogen of compound **I-15**.

Since protecting the amide nitrogen of compound **I-15** could be difficult due to delocalization of the lone pair into the carbonyl (thus lowering the nucleophilicity of the amide nitrogen), the synthetic route was redesigned to protect the free amine of β-alanine ethyl ester hydrochloride with PMB, and this protected amine would then be coupled to carboxylic acid **I-14.** Scheme I-13 details the proposed alternative synthetic pathway.

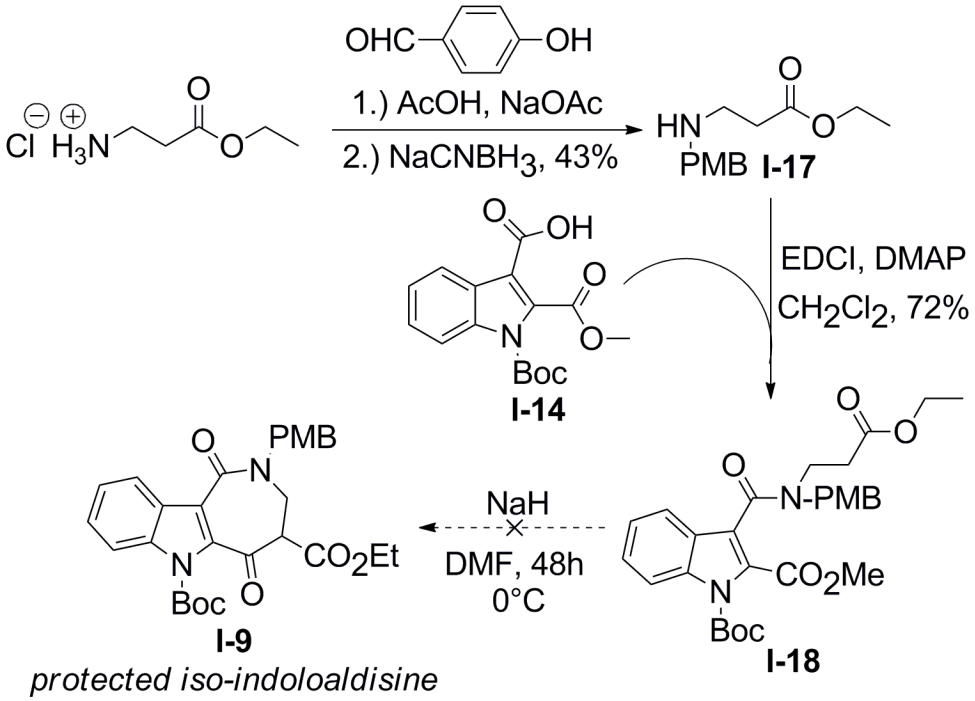

Scheme I-13. Proposed synthetic pathway for forming *iso*-indoloaldisine **I-9** with PMB protected amine **I-17**.

The PMB protected amine **I-17** was readily synthesized using 4-methoxybenzaldehyde followed by reduction with $NaCNBH_3$.[34] Compound **I-17** was coupled to carboxylic acid **I-14** and the product was validated by HRMS. Even after column chromatography, the NMR of **I-18** was difficult to interpret, possibly contributed to rotamers (due to the limited rotation of the amide bond due to delocalization of the nitrogen lone pair into the carbonyl). Thereafter the attempted Dieckmann reaction with **I-18** did not yield the protected *iso*-Indoloaldisine (Scheme I-13).

At this point the intramolecular Dieckmann reaction to yield the desired *iso*-indoloaldisine intermediate seemed difficult. In addition, finding a route that did not require protecting both the indole and amide nitrogens would be desirable. Therefore new synthetic efforts would focus on selectively functionalizing the C-2 position of indole.

G. Selective Acylation of the Indole C-2 Position

Since the modified Dieckmann route was unsuccessful, the next alternative strategy attempted was selectively acylating the C-2 position of indole. Such a chemical transformation presents a challenge for synthetic chemists since the indole C-3 position is substantially more nucleophilic than the C-2 position. This is exemplified by the Vilsmeier-Haack reaction of indole with $POCl_3$ and DMF affording exclusively Indole-3-carboxaldehyde (Scheme I-14).[35]

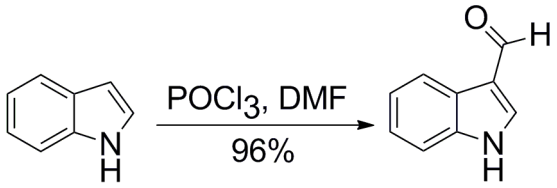

Scheme I-14. Vilsmeier-Haack reaction illustrating the more nucleophilic C-3 position of indole.

Additionally, the greater nucleophilicity of the C-3 position can be explained by the delocalization of electrons when indole reacts with a generic electrophile E^+ (Scheme I-15). This scheme illustrates that in order for the C-2 position to attack an electrophile, the aromaticity of the benzene ring must be broken. However, indole can readily react with an electrophile at the C-3 position because this aromaticity is not broken.

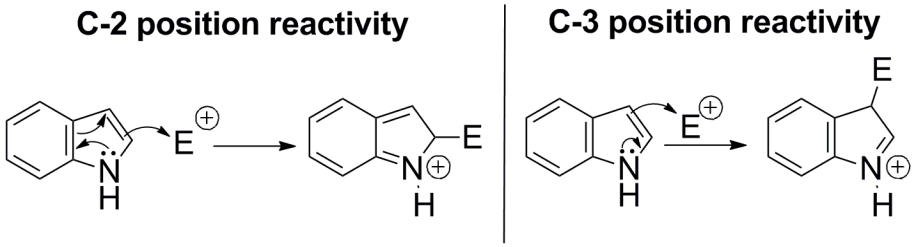

Scheme I-15. Comparsion of indole C-2 versus C-3 position reactivity with a generic electrophile (E^+).

Although classic reactions like the Vilsmeier-Haack indicate that selectively acylating the C-2 position of indole does not seem feasible, several examples of selective C-2 acylations have been reported in the literature.[36,37] These methodologies require a directing group on the indole nitrogen to direct selective deprotonation of the indole C-2 proton with a strong base. Protecting the indole nitrogen with carbon dioxide has been shown to direct deprotonation at the C-2 position of indole with t-butyl lithium.[36] Katritzky and Akutagawa propose the mechanism found in Scheme I-16 indicating the directing effects of CO_2 for deprotonation. In this mechanism, a nitrogen anion is generated using n-butyl lithium, followed by addition of CO_2 to generate the carboxylate protected indole. The resulting lithium carboxylate is believed to coordinate to a second equivalent of a lithium reagent (*t*-butyl lithium) and thus direct deprotonation of the proximal C-2 position instead of the more acidic C-3 proton. Thereafter, addition of the desired electrophile will generate the desired acylation at the C-2 position. This methodology has afforded C-2 acylated indoles using electrophiles such as benzoyl chloride and methyl benzoate with 59% and 52% yields, respectively. Additionally, the

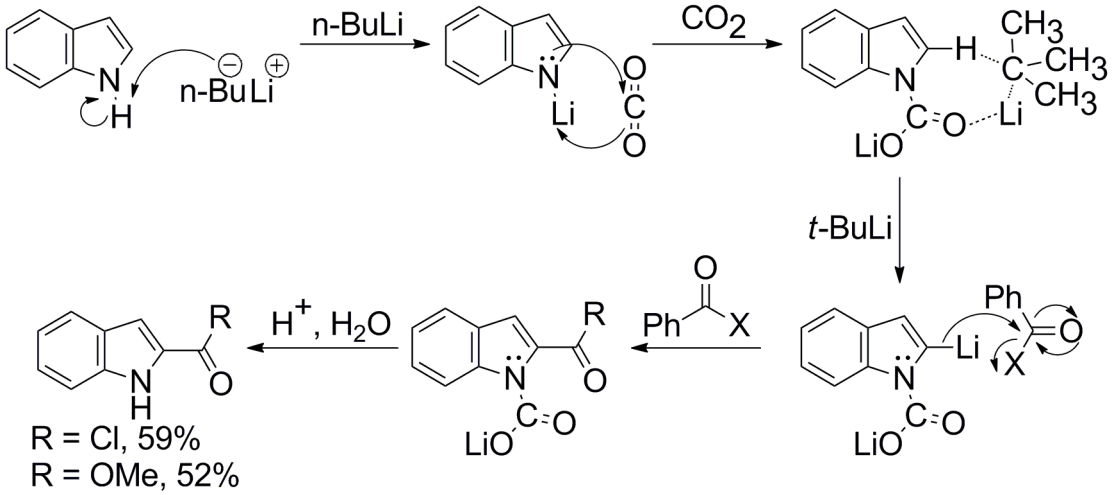

Scheme I-16. Mechanism of carbon dioxide directing C-2 acylation of indole.

CO_2 group is cleaved during work up and does not typically require pyrolysis.

Alternatively, Mahboobi *et al* have shown protecting the indole nitrogen with a phenylsulfonyl group will direct deprotonation at the C-2 position (Scheme I-17).[37] This methodology has afforded 2-acylated indole derivatives from various alkyl and aryl acyl chlorides in good yields. This methodology is perhaps preferred because n-butyl lithium is sufficient for the deprotonation and avoids use of the extremely flammable *t*-butyl lithium. Therefore this methodology was considered for continuing the synthesis towards *iso*-indoloaldisine.

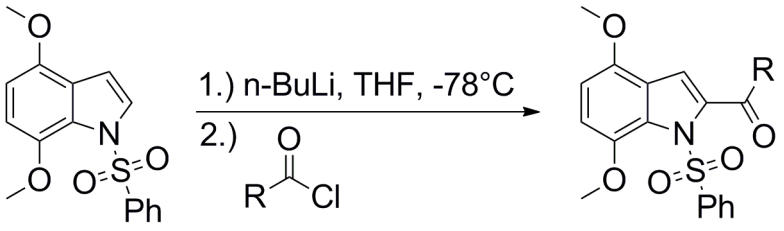

Scheme I-17. Selective 2-acylation of indole using phenylsulfonyl directing group.

It was desirable to devise a synthesis that would utilize 1-(phenylsulfonyl)indole and the respective acyl chloride. However, the necessary amino acyl chloride that would be required for the synthesis of *iso*-indoloaldisine would not be a stable molecule having both an acyl chloride and amine functional group (Scheme I-18). Therefore, a Troc protected 2-azetidinone (β-lactam) **I-19** would be the synthon equivalent for the selective C-2 acylation of indole. Ring opening of the Troc protected β-lactam by indole **I-20** would afford a protected amine intermediate (Scheme I-18). This intermediate could then be converted to the corresponding carboxylic acid by a Vilsmeier-Haack

reaction and subsequent oxidation. A final intramolecular coupling reaction utilizing EDCI and DMAP would yield *iso*-indoloaldisine.

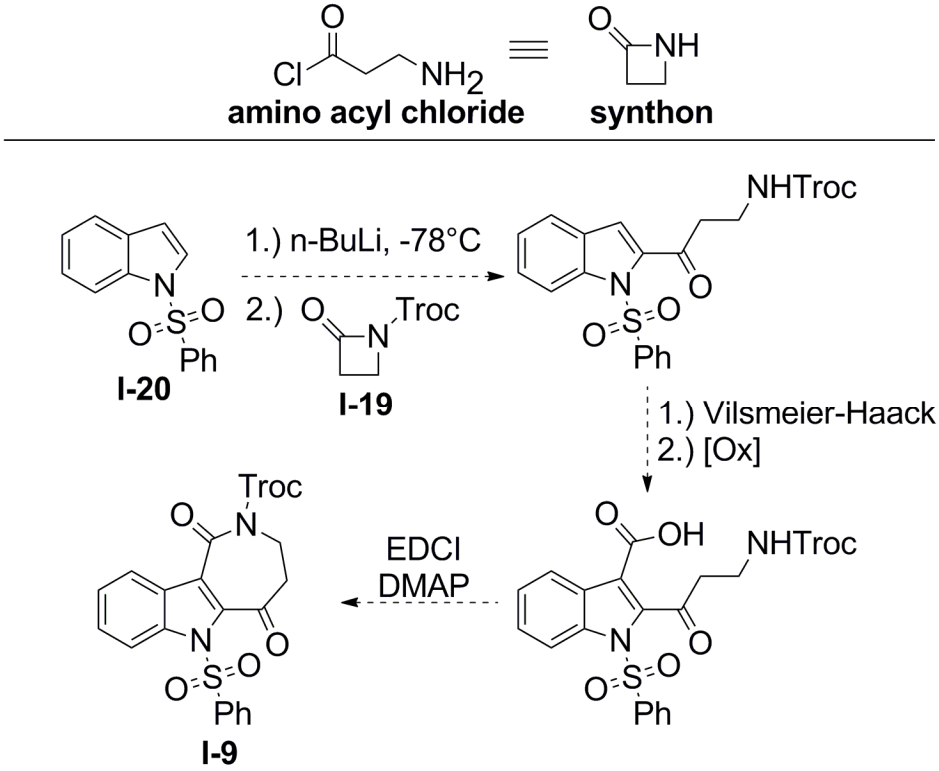

Scheme I-18. Proposed selective C-2 acylation with β-lactam **I-19** for synthesis of *iso*-indoloaldisine **I-9**.

Alternatively, if the selective C-2 acylation reaction with β-lactam **I-19** was successful, the resulting Troc-protected amine (also could be considered a carbamate) could readily undergo a Bischler-Napieralski cyclization which would yield *iso*-indoloaldisine in fewer synthetic steps. Treatment of this carbamate with trifilic anhydride (Scheme I-19) will result in a 7-*endo*-*dig* cyclization that is favored according to Baldwin's rules.[38] Subsequent aqueous workup should hydrolyze the Troc protecting group resulting in *iso*-indoloaldisine. This mechanism is outlined in Scheme I-19.

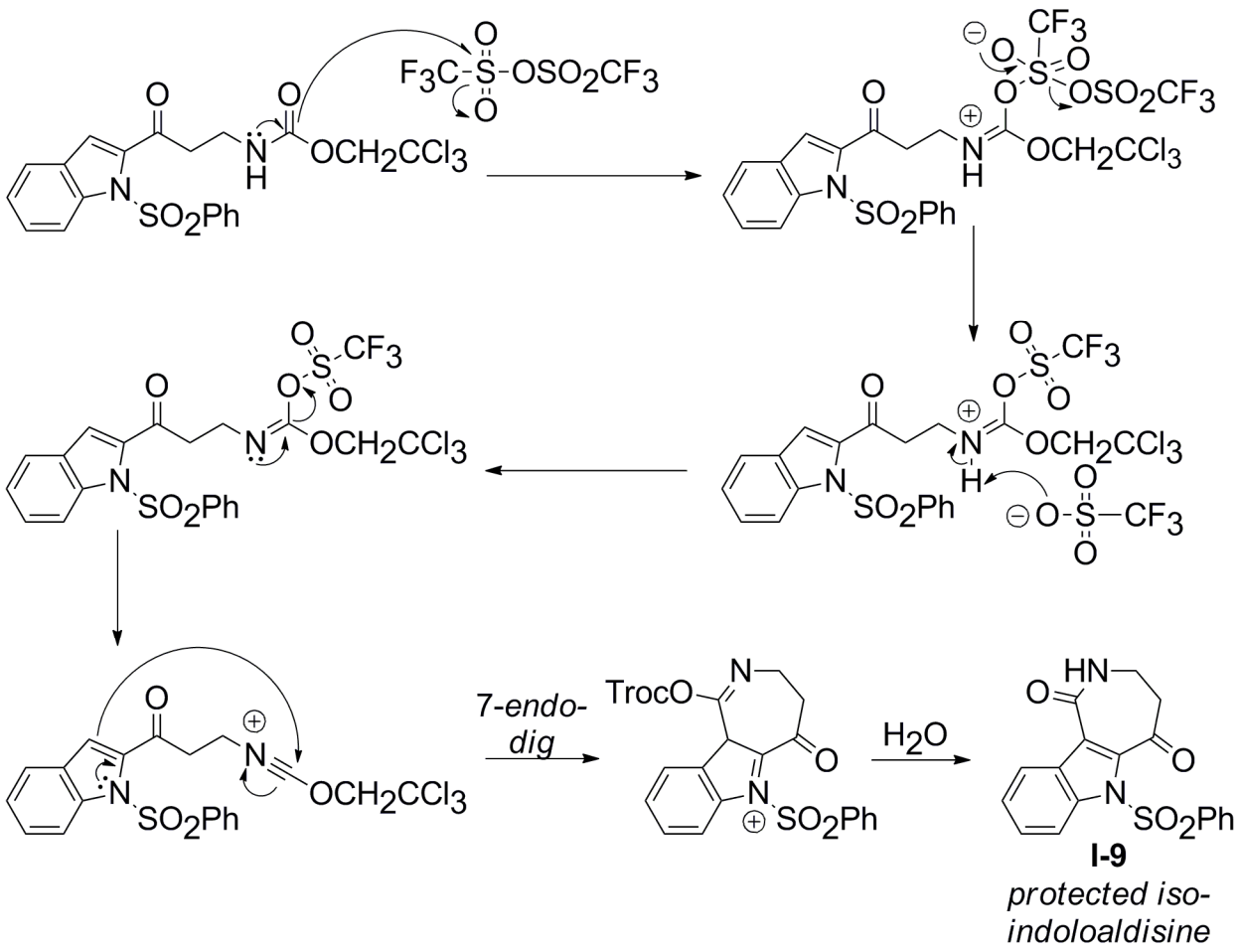

Scheme I-19. Proposed Bischler-Napieralski 7-*endo-dig* cyclization to afford *iso*-indoloaldisine **I-9**.

To start the newly proposed synthesis, both β-lactam **I-19** and 1-(phenylsulfonyl)indole **I-20** were prepared. The Troc-protected β-lactam **I-19** is quantitatively synthesized from 2-azetidinone, n-butyl lithium and 2,2,2-trichloroethyl chloroformate according to previous work done by Kevin Anderson.[39] Previously synthesized 1-(phenylsulfonyl)indole **I-20** was prepared quantitatively with benzenesulfonyl chloride and NaOH in DCM using tetrabutylammonium hydrogensulfate (TBAHS) as a phase-transfer catalyst.[40] The syntheses of compounds **I-19** and **I-20** are summarized in Scheme I-20.

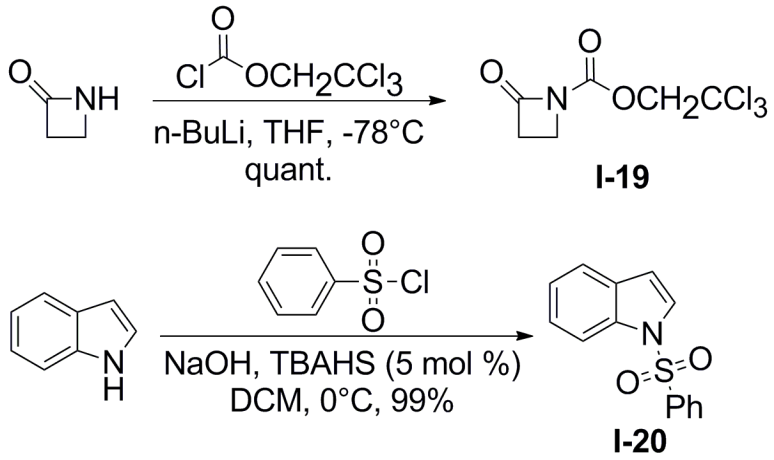

Scheme I-20. Synthesis of β-lactam **I-19** and 1-(phenylsulfonyl)indole **I-20**.[39,40]

Scheme 21 outlines the initial reaction performed with compounds **I-19** and **I-20**. As displayed in Scheme 21, the ring opening of β-lactam **I-19** by **I-20** did not yield the desired Troc-protected amine. Instead, 2 molecules of indole **I-20** reacted with the β-lactam and resulted in a dimer-like indole side product. This product is likely the result of isocyanate formation after 1 molecule of **I-20** reacts with **I-19**. A proposed mechanism for this transformation is outlined in Scheme I-21.

Once β-lactam **I-19** is opened by indole, a negative charge resides on the nitrogen (Scheme I-21). Being rather electron withdrawing and a decent leaving group, the isocyanate can form as a result of displacing OCH_2CCl_3. Since β-lactam **I-19** was added dropwise to the indole solution, this means that once the isocyanate forms it is readily surrounded by deprotonated **I-20**. Therefore a second molecule of indole **I-20** will react with the isocyanate affording the observed dimer-like side product. This mechanism can account for the formation of the observed side product that was confirmed by ^1H NMR and HRMS. Additionally, 44% of unreacted indole **I-20** was

recovered. Perhaps a base stronger than n-butyl lithium is needed for complete conversion.

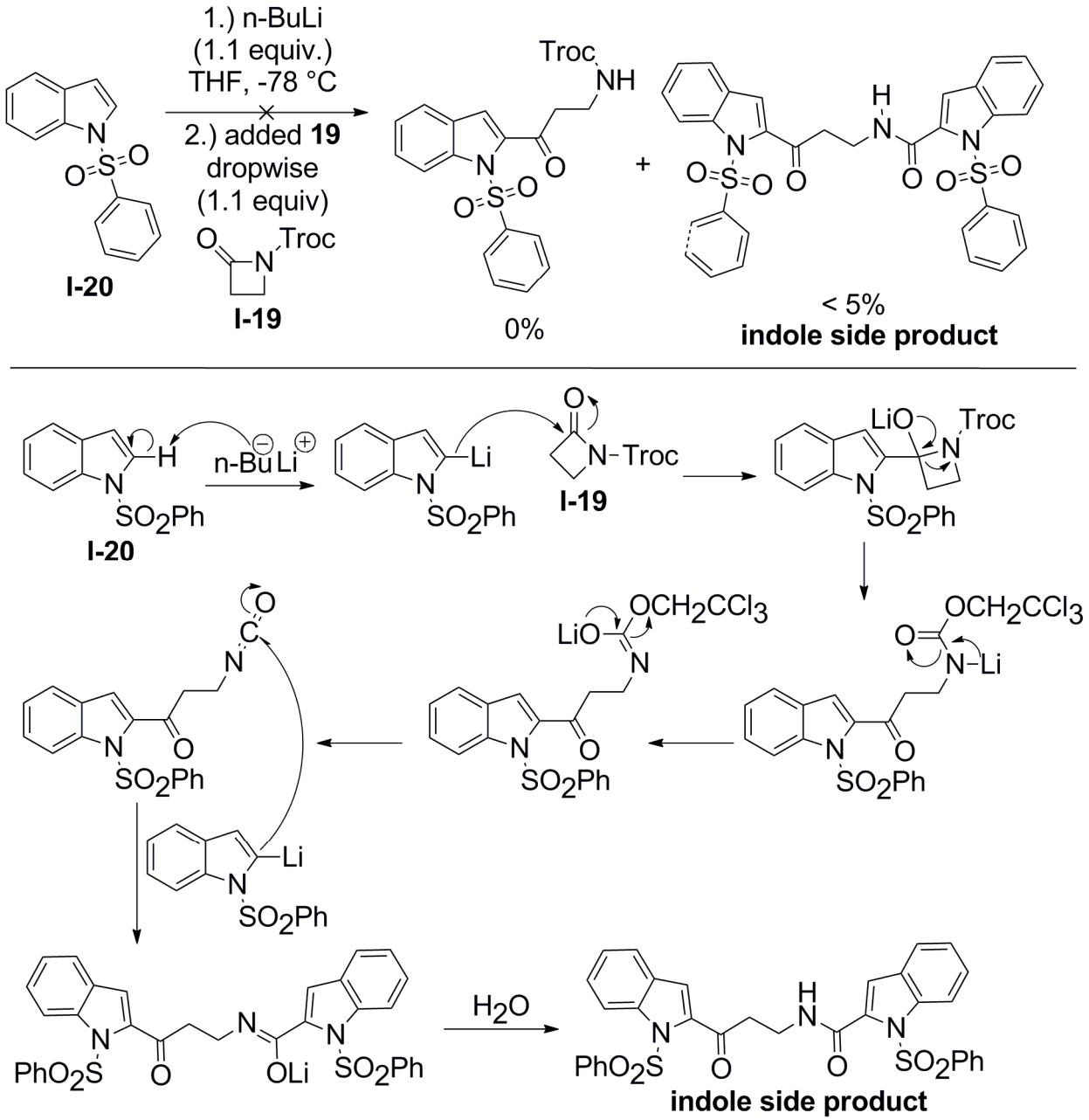

Scheme I-21. Mechanism of isocyanate formation explaining side product obtained from ring opening of **I-19** by indole **I-20**.

In order to prevent the formation of the undesired indole side product, several modifications were made to the methodology (Scheme I-22). First, the order of addition

was changed so that a solution of indole **I-20** was added dropwise to the β-lactam. Second, the equivalents of the β-lactam **I-19** were increased from 1.1 to 2. Both of these changes would increase the probability that indole **I-20** would react with the β-lactam and not with an additional molecule of **I-20**. Despite these modifications no product was observed from the reaction, nor was the product detected by MS.

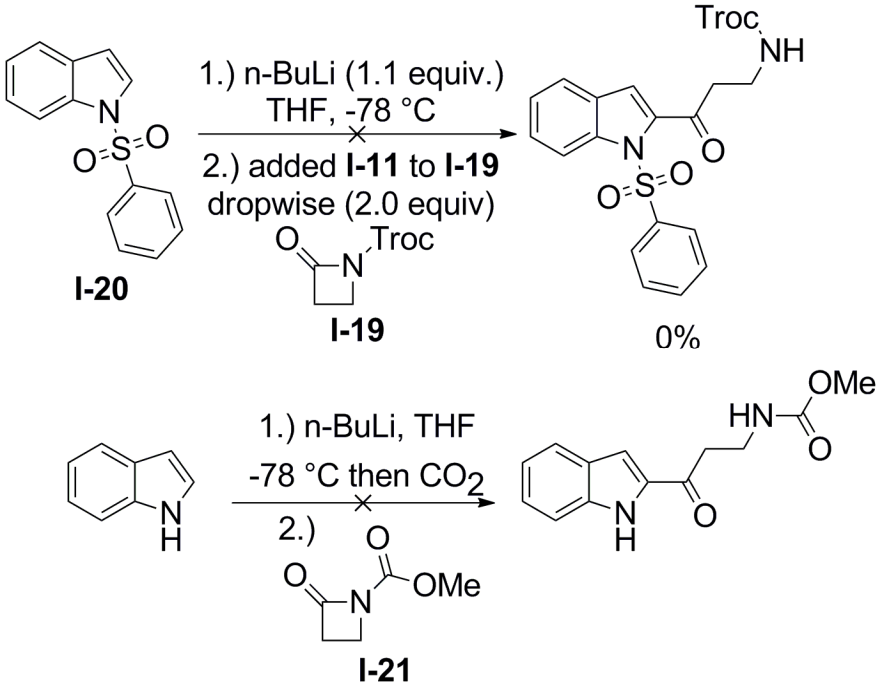

Scheme I-22. Additional unsuccessful reaction conditions for affording C-2 acylated product.

Additionally, β-lactam **I-21** was synthesized from 2-azetidinone and methyl chloroformate.[39] This β-lactam was used with CO_2 as the directing group for acylation, but no reaction was observed (Scheme I-22).[36] No observed product formation was likely the result of not using *t*-butyl lithium.

In summary, the selective acylation of the C-2 indole position proved difficult with the β-lactam substrates. The difficultly in reactivity may be a result of the fact that the acyl chlorides (used in the literature) are more electrophilic compared to a β-lactam. The

carbonyl of an acyl chloride has significant more positive character compared to an amide in which there is donation of electrons into the carbonyl from nitrogen. Additionally, one can envision that the tetrahedral transition state before displacement of the leaving group is more sterically hindered for the 4-membered ring compared to a simple acyclic acyl chloride. Therefore new methodology was explored that would utilize a new indole substrate.

H. Synthesis of *Iso*-indoloaldisine from Indole-3-carboxylic Acid

Since both modification of the indole-2-carboxylic acid core (Dieckmann condensation route, section F) and selective C-2 acylation methodology (section G) proved troublesome, the commercially available indole-3-carboxylic acid was investigated as an alternative starting material for the synthesis of *iso*-indoloaldisine **I-9**. Indole 3-carboxylic acid was successfully coupled to β-alanine ethyl ester using EDCI and DMAP yielding ester **I-22** in excellent yields (Scheme I-23). The subsequent hydrolysis with lithium hydroxide in ethanol afforded carboxylic acid **I-23**, the precursor to *iso*-indoloaldisine, in near quantitative yields.

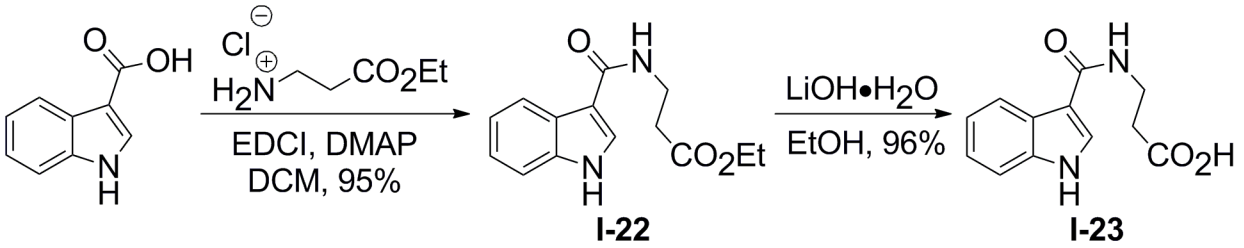

Scheme I-23. Syntheis of *iso*-indoloaldisine precursor **I-23** from indole-3-carboxylic acid.

Although acid **I-23** was readily synthesized, cyclization to the 7-membered ring *iso*-indoloaldisine **I-9** proved more difficult. The synthetic design was to use a Friedel-Crafts ring closure with P_2O_5 (phosphorous pentoxide). The cyclization step to generate

iso-indoloaldisine is likely difficult because the indole C-2 position is not very nucleophilic (see section G). In order for cyclization to occur, electrons must resonate and break the aromaticity of the indole ring.

The P_2O_5 Friedel-Crafts cyclization was successful although initially it was problematic. Table I-2 illustrates the optimization of the cyclization to afford *iso*-indoloaldisine **I-9** in a final optimum yield of 81%. Initially, the cyclization reaction was performed using methanesulfonic acid (CH_3SO_3H) and P_2O_5 (1.1 equiv) for 1.5 hours at 110℃ (Table I-2, entry 1). Even though the reac tion was performed on a 1 gram scale, only a trace amount (< 1%) of **I-9** was isolated. Therefore, the reaction time was increased to 18 hours (entry 2) but no product was observed. Considering that the longer reaction time did not increase the yield, this suggests that decomposition may be a factor. Therefore, the reaction temperature was lowered to 80℃ (entry 3) but still only

Table I-2. Optimization of Friedel-Crafts cyclization to afford *iso*-indoloaldisine **I-9**.

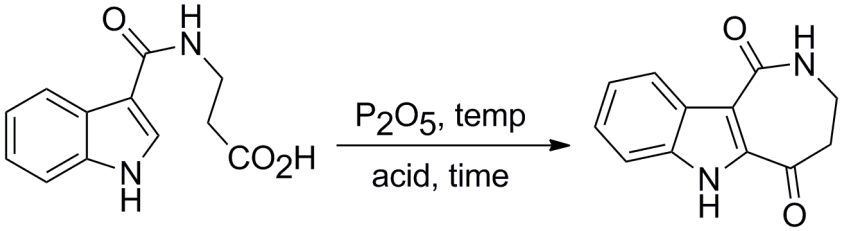

I-23 **I-9** *iso*-indoloaldisine

Entry	Acid	P_2O_5 (Equiv.)	Time (h)	Temp (°C)	Yield (%)
1	CH_3SO_3H	1.1	1.5	110	trace
2	CH_3SO_3H	1.1	18	110	0
3	CH_3SO_3H	1.1	1.5	80	trace
4	CH_3SO_3H	3	24	110	20
5	CH_3SO_3H	3	48	110	26
6	PPA	3	20	110	37
7	PPA	3	65	110	39
8	PPA	3.4	2	110	81

trace **I-9** was observed. Thereafter, increasing the number of equivalents of P_2O_5 from 1.1 to 3 (entry 4) and the reaction time to 24 hours afforded **I-9** in 20% yield. Doubling the reaction time only provided a 6% increase in yield (entry 5).

Since the reactions in methanesulfonic acid were low yielding, the acid was changed to PPA (polyphosphoric acid). Due to the high viscosity of PPA, these reactions required a mechanical stirrer. Initially this modification seemed promising as the yield of **I-9** increased to 37% (Table I-2, entry 6). Extending the reaction time did not offer a significant increase in yield (entry 7, 39% yield), but lowering the reaction time to 2 hours with a slight increase in P_2O_5 equivalents afforded **I-9** in 81% yield (entry 8). It is interesting to note that both entries 1 and 8 were reactions performed on a 1.0 or 3.9 gram scale respectively (Table I-2). Part of the drastic increase in yield found in entry 8 likely has to do with the workup procedure. Compound **I-9** will precipitate out of an ice/water mixture that is added to the PPA mixture (entry 8). However, even on a comparable scale, no precipitate is readily collected when methanesulfonic acid is used (Table I-2, entry 1). Precipitation is highly desirable during the workup due to the polar nature of **I-9**. *Iso*-indoloaldisine **I-9** can be further purified by stirring in boiling acetone and then filtering while hot. This illustrates the polar nature of this compound, and some of the low yields in other reactions may be attributed to the fact that solvent extractions were unsuccessful and **I-9** was being lost to the aqueous phase. Additionally, purification of **I-9** by column chromatography is possible but results in significant loss of material due to low solubility in organic solvents.

Over three synthetic steps, *Iso*-indoloaldisine **I-9** is prepared in an overall yield of 75%. Additionally, this synthesis is much more desirable than the previous routes

attempted (sections F and G). Both the Dieckmann condensation route and the selective C-2 acylation of indole required protecting groups. However, the current synthesis to *iso*-indoloaldisine is very desirable since no protecting groups are required.

I. Titanium (IV) Chloride Mediated Coupling Reactions with *Iso*-indoloaldisine.

Having now developed a scalable synthesis for the key intermediate *iso*-indoloaldisine **I-9**, several chemical transformations can potentially yield the target compound *iso*-indoloazepine. The most challenging synthetic modification that remains is introduction of the 5-membered glycocyamidine ring found in *iso*-indoloazepine **I-6**. Several proposed synthetic routes for affording *iso*-indoloazepine are delineated in Scheme I-24. Both proposed syntheses utilize a Titanium (IV) chloride mediated aldol condensation to introduce the precursor for the glycocyamidine ring found in *iso*-

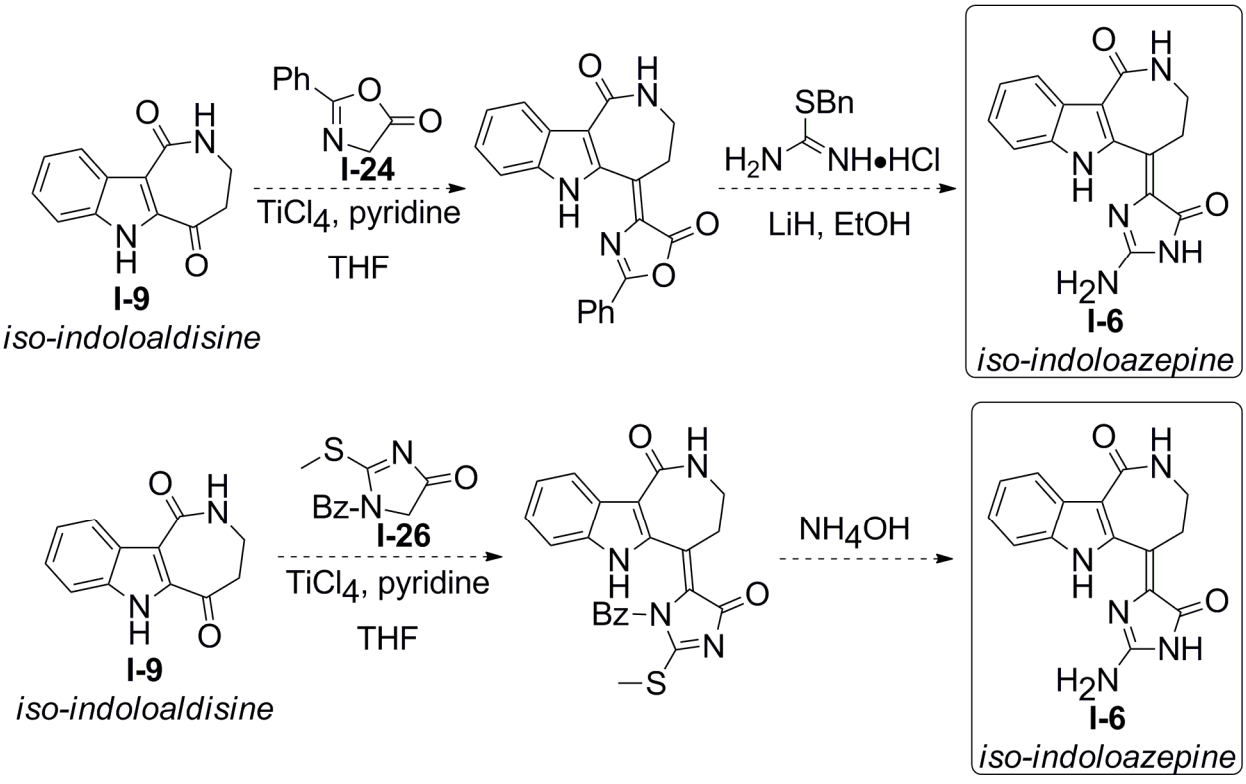

Scheme I-24. Proposed final syntheses for **I-6** from *iso*-indoloaldisine **I-9**.

indoloazepine. Fortunately, there are several precedents in the literature for the coupling reactions proposed.[26,41]

Previously, Sharma and Tepe have reported the $TiCl_4$ mediated coupling reaction between phenylazlactone **I-24** and indoloaldisine (constitutional isomer of **I-9**) in 55% yield (Scheme I-25).[26] Subsequent treatment of the coupled product with benzylthiourea under basic conditions afforded indoloazepine (constitutional isomer of target compound *iso*-indoloazepine) in 28% yield.[26] Additionally, Papeo et al have reported analogous $TiCl_4$ coupling conditions between imidazolinone **I-26** and aldisine for synthesizing marine sponge alkaloids hymenialdisine and debromohymenialdisine (Scheme I-25).[41] The resulting coupled intermediate was found to be unstable to

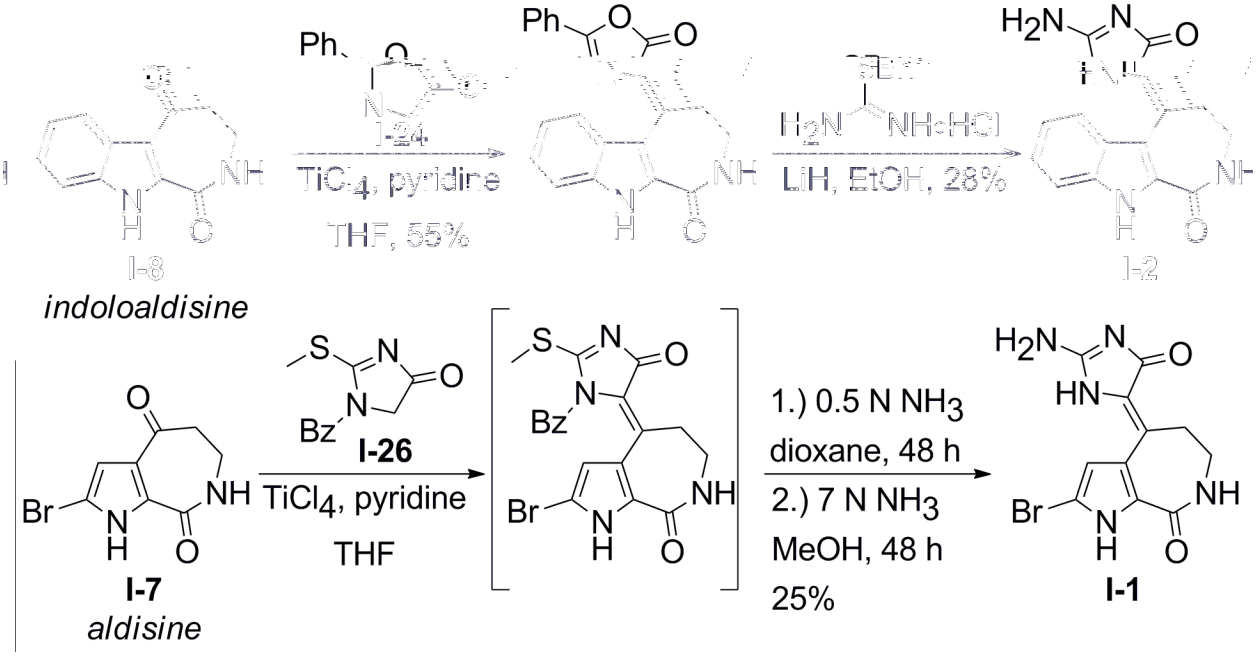

Scheme I-25. Previously reported $TiCl_4$ mediated coupling reactions for synthesis of indoloazepine **I-2** and hymenialdisine **I-1**.[26,41]

chromatography and was converted to the glycocyamidine ring (hymenialdisine) in 25% overall yield without isolation.

Therefore, the aforementioned heterocycles **I-24** and **I-26** were synthesized to use in the proposed final steps to afford *iso*-indoloazepine (Scheme I-26). Phenylazlactone **I-24** is prepared in 85% yield from an intramolecular dehydrative cyclization from *N*-benzoylglycine (hippuric acid) and TFAA in DCM.[26] The synthesis of imidazolinone **I-26** is achieved in two steps (Scheme I-26).[41] A finely ground mixture of hippuric acid and ammonium thiocyanate is treated with acetic acid and acetic anhydride, resulting in a benzoylated thiohydantoin **I-25**. Compound **I-25** is then treated with methyl iodide, DMAP and DIPEA in DCM to afford **I-26** in 76% yield. This methylation procedure was superior to the previously reported methodology of using methyl iodide, NaH and DMF which afforded **I-26** in 52% yield.[41]

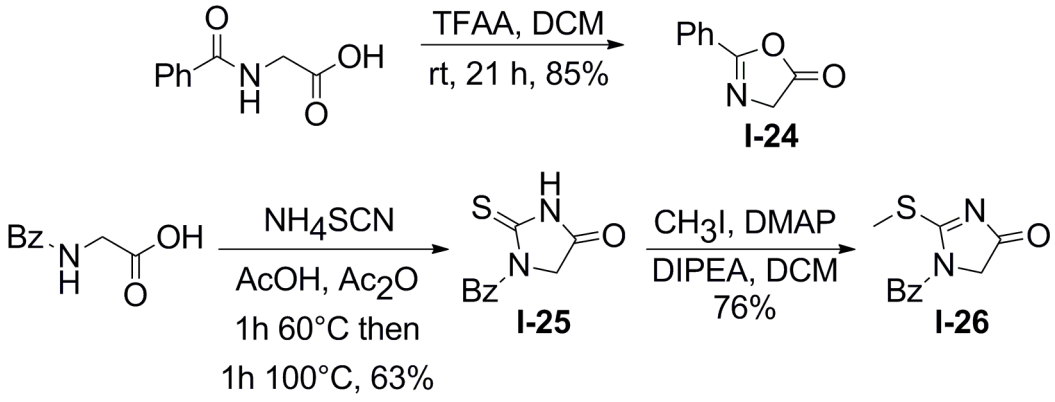

Scheme I-26. Synthesis of phenylazlactone **I-24** and imidazolinone **I-26**.

After completing these syntheses, phenylazlactone **I-24** and imidazolinone **I-26** were used in $TiCl_4$ aldol condensation reactions with *iso*-indoloaldisine. Scheme I-27 summarizes these reactions. The coupling conditions with phenylazlactone **I-24** were analogous to the conditions previously reported by Sharma and Tepe (2 equivalents **I-**

24, 4 equivalents $TiCl_4$, and 8 equivalents of pyridine added portion-wise).[26] No starting material was recovered and only decomposition was observed. Analogous coupling conditions utilizing imidazolinone **I-26** were also unsuccessful. In an attempt to prevent decomposition that may be occurring at 0℃, the reactio n with **I-26** was repeated at -78℃ but no product was observed.

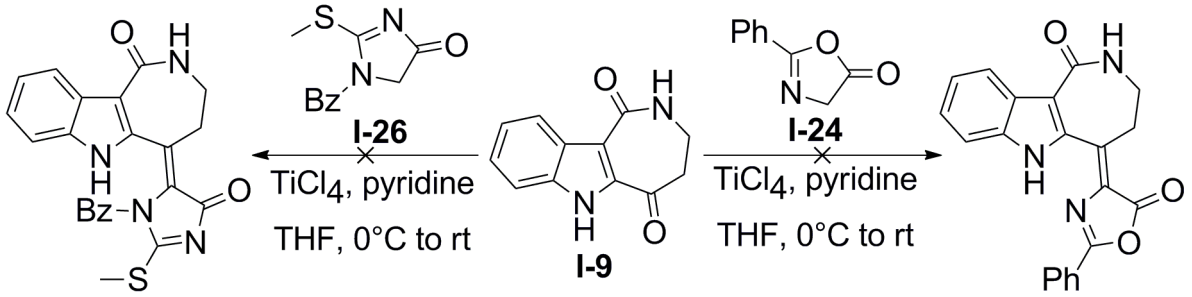

Scheme I-27. Unsuccessful $TiCl_4$ coupling reactions with *iso*-indoloaldisine **I-9**.

It is interesting that analogous coupling conditions between *iso*-indoloaldisine **I-9** and phenylazlactone **I-24** yield no product (Scheme I-27), whereas **I-24** is coupled successfully to indoloaldisine **I-8** (the constitutional isomer of **I-9**) in 55% yield (Scheme I-25). In order to account for this difference in reactivity, the ^{13}C NMR chemical shifts of both compounds in d_6-DMSO were compared (Figure I-11). Although counterintuitive, the ketone carbonyl in indoloaldisine is more deshielded at 195.0 ppm compared to the ketone carbonyl of 192.6 ppm in **I-9**.[26] Considering that the ketone of indoloaldisine is in conjugation with the indole nitrogen, one would predict that the carbonyl would be more shielded compared to the ketone in **I-9**. However, NMR verifies that indoloaldisine has the more electrophilic carbonyl compared to **I-9**. Therefore, the lower electrophilic nature of the ketone in **I-9** may explain why there was no reactivity in the $TiCl_4$ coupling reactions.

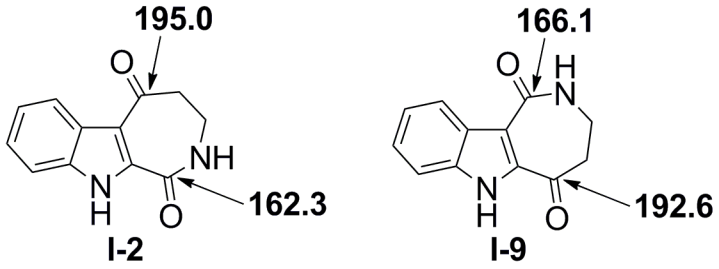

Figure I-11. ^{13}C NMR chemical shift comparison between indoloaldisine **I-2** and *iso*-indoloaldisine **I-9** in d_6-DMSO.

Interestingly, the same trend in shielding effects is also observed when comparing the chemical shifts of the amide carbonyls (Figure I-11). The amide carbon of indoloaldisine is at 162.3 ppm, which is more shielded than the amide of *iso*-indoloaldisine at 166.1 ppm. Once again, the carbonyl that is in conjugation with the indole nitrogen is more deshielded than one would predict.

At this point it was clear the current coupling conditions were problematic. Perhaps the nitrogen atoms of **I-9** form a complex with $TiCl_4$ that complicate the desired reaction. Although initially it would not be desirable for the synthesis, the next synthetic efforts would consist of protecting the nitrogen atoms on **I-9** and repeating the previous $TiCl_4$ coupling conditions.

J. Protection of Nitrogen Atoms in *Iso*-indoloaldisine

A precedent for protecting compounds similar to *iso*-indoloaldisine **I-9** is found by Annoura et al in the total synthesis of debromohymenialdisine.[24] In the reported total synthesis, aldisine (Figure I-10) was protected with SEMCl (2-(Trimethylsilyl)ethoxymethyl chloride), NaH and DMF at 0℃. Therefore, these conditions were chosen in an attempt to protect **I-9**. Additionally, if the protection was

successful, this could potentially yield an alternative route to *iso*-indoloazepine. Although previously only Lewis acidic conditions were being attempted, protection of the nitrogen atoms on **I-9** would permit the basic conditions of the Horner-Wadsworth-Emmons reaction utilized in Annoura's total synthesis of debromohymenialdisine (Scheme I-28).

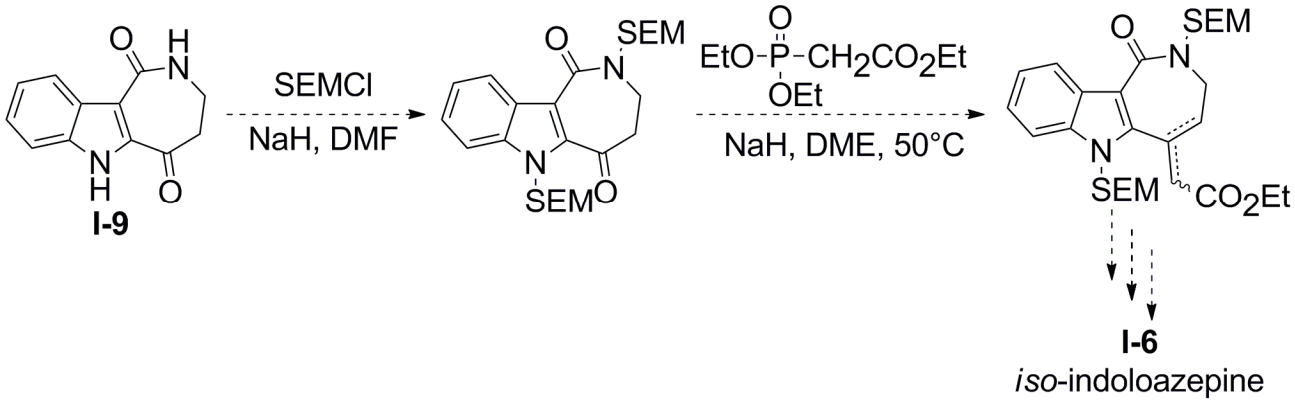

Scheme I-28. Proposed protection of compound **I-9** followed by HWE reaction.

Both the nitrogen atoms of compound **I-9** were attempted to be protected using SEMCl (Scheme I-29). Reaction of **I-9** with SEMCl (2 equiv.) and NaH (2 equiv.) did not yield the di-protected derivative **I-9**. Instead, the SEM protected enolate and mono-protected indole side products were observed in 29% and 15% yields respectively (Scheme I-29). The SEM protected enolate side product was identified by the appearance of a vinylic triplet at 5.7 ppm on the ^{1}H NMR. For the mono-protected side

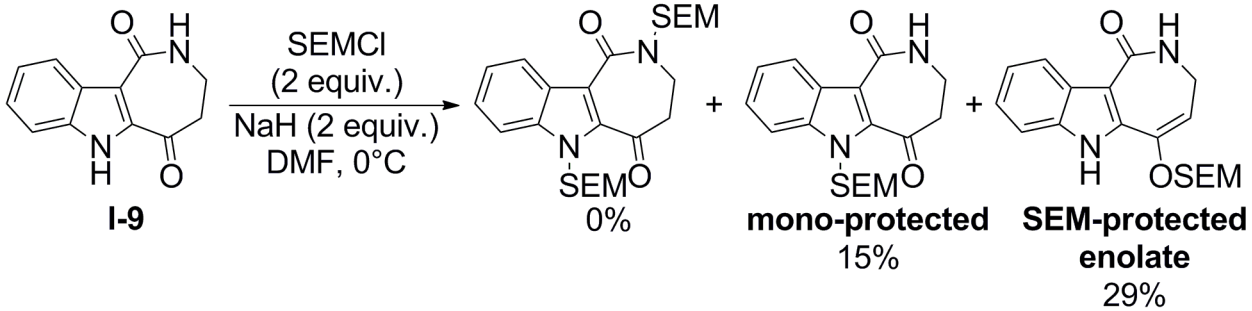

Scheme I-29. Identified side products during the SEM protection of *iso*-indoloaldisine **I-9.**

product, it was clear that the amide nitrogen had not been protected because of a broad triplet at 6.9 ppm which corresponds to the amide proton being split by the adjacent CH_2 in the 7-membered ring of **I-9**. Protection of compound **I-9** using BOC was also unsuccessful.

Since protecting **I-9** appeared to be problematic, the synthetic precursor ethyl ester **I-22** would be protected first (Scheme I-30). Subsequent cyclization with P_2O_5 and PPA would yield the SEM-protected derivative of **I-9**. Therefore ethyl ester **I-22** was treated with 2 equivalents of NaH and SEMCl in DMF at 0℃ (Scheme I-30). In the above reaction, no desired product was obtained when using 2 equivalents of SEMCl. Instead, a mono-protected indole **I-27** (13% yield) and an SEM protected ester (32% yield) were the two isolated side products (Scheme I-30). The surprising ethyl ester hydrolysis was later explained by water present in the DMF. The presence of water allowed the generation of sodium hydroxide, which likely hydrolyzed the ester to the

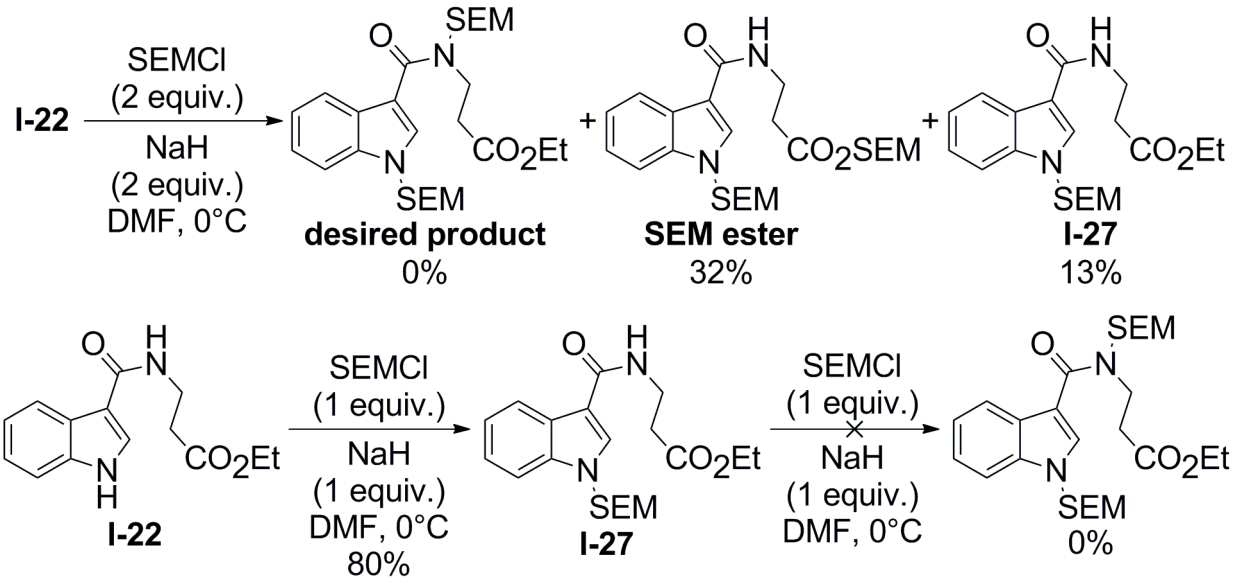

Scheme I-30. Protection of acyclic precursor ethyl ester **I-22** of *iso*-indoloaldisine

carboxylic acid. The resulting acid was then deprotonated and protected with SEMCl. When the above reaction was repeated with anhydrous DMF and SEMCl (2 equiv.), indole mono-protected **I-27** was obtained in 25% yield, while the SEM protected ester was obtained in 10% yield. Both side products were confirmed with HRMS, and no desired double SEM-protected product was observed.

The protection of **I-22** was repeated, but only one equivalent of SEMCl and NaH was used (Scheme I-30). The desired mono-protected compound **I-27** was obtained in 80% yield. This was the expected result since only 1 equivalent of NaH was used; the more acidic indole nitrogen was deprotonated preferentially over the amide nitrogen. Compound **I-27** was then reacted with a second equivalent of SEMCl (Scheme I-30). Only starting material was recovered after reacting for 16 hours, thus indicating the difficulty of protecting the amide nitrogen. Considering that the lone pair on nitrogen is delocalized in the carbonyl of an amide, this could explain the decrease in nucleophilicity that is observed.

Efforts to protect *iso*-indoloaldisine **I-9** proved more difficult than the structurally similar aldisine used in the total synthesis of **DBQ**.[24] Since protecting steps are not ideal for any synthesis, the synthetic strategy was altered so the $TiCl_4$ coupling reaction would precede the Friedel-Crafts cyclization step that affords **I-9**. To probe this newly proposed synthetic strategy, 2-acetylindole was adopted as a model system for the $TiCl_4$ coupling reactions.

K. Use of 2-acetylindole as a Model System for Developing $TiCl_4$ Aldol Reactions

Since the SEM protection of the amide group of **I-9** proved difficult, a new synthetic strategy was employed. Previous $TiCl_4$ coupling reactions with **I-9** proved to be a road block to the synthetic goal. Rather than attempt the $TiCl_4$ coupling reaction on the cyclic *iso*-indoloaldisine **I-9**, the coupling reaction would be attempted before the Friedel-Crafts cyclization step with P_2O_5 and PPA (Scheme I-31). If the coupling was successful, conversion of the amine into an iso-cyanate could yield the desired 7-membered ring. In order to synthesize the C-2 acylated indole starting material, previously described selective C-2 acylation procedures would be investigated further (section G).

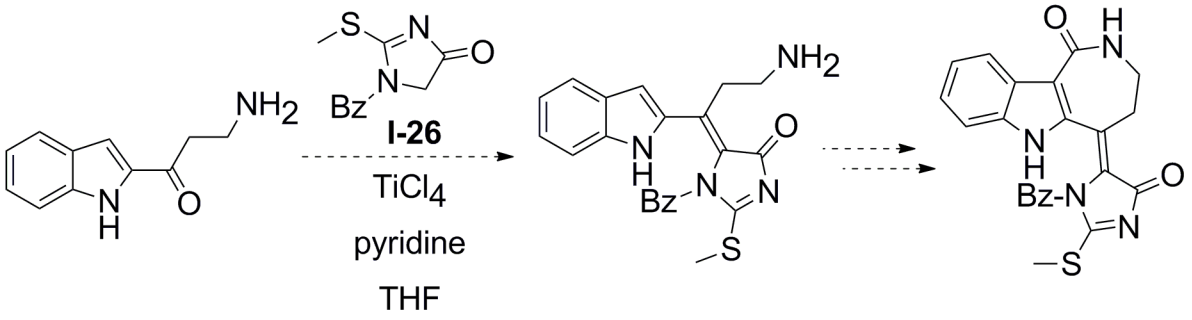

Scheme I-31. Proposed $TiCl_4$ coupling reaction prior to Friedel-Crafts cyclization.

As a proof of principle that this synthetic strategy could be utilized for completing the synthesis of *iso*-indoloazepine, synthesis would begin by working with a simpler model compound, 2-acetylindole **I-28**. Compound **I-28** was prepared in quantitative yields from indole-2-carboxylic acid treated with 6.2 equivalents of methyl lithium (Scheme I-32).[42]

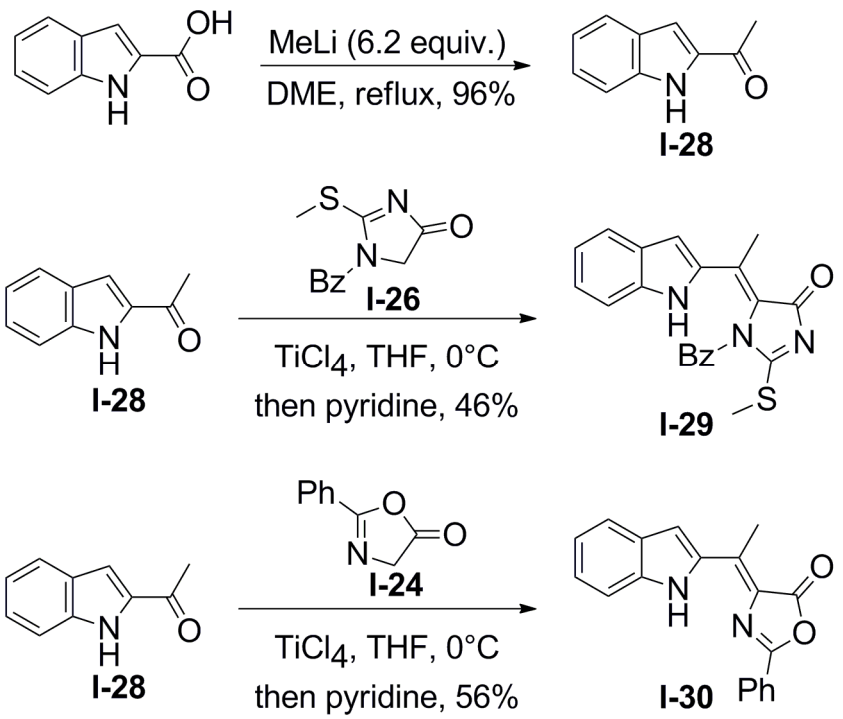

Scheme I-32. Successful aldol condensation reactions on model 2-acetylindole **I-28** system.

After having prepared **I-28**, $TiCl_4$ coupling reactions with phenylazlactone **I-24** and imidazolinone **I-26** were investigated. Analogous reaction conditions were used that had been problematic with *iso*-indoloaldisine **I-9**. Coupling with imidazolinone **I-26** yielded compound **I-29** in 46% yield, whereas coupling with phenylazlactone **I-24** yielded compound **I-30** in 56% yield. Despite previously reported degradation of structurally related compounds, these compounds were stable to flash chromatography.[41]

Despite identical reaction conditions, the $TiCl_4$ coupling reactions were unsuccessful with *iso*-indoloaldisine **I-9** but worked moderately well with **I-28** without further optimization. In order to account for these differences in reactivity, one can consider the different conformations of the ketone between compounds **I-9** and **I-28**

(Figure I-12). Compound **I-9** has a ketone that is part of a 7-membered ring which restricts its rotation. Additionally, nearly five of the seven atoms in the 7-membered ring are sp^2 hybridized (considering the lone pair on the amide nitrogen will donate electron density into the carbonyl). This indicates the ketone in **I-9** is restricted to rotate freely in a relatively planar molecule. Therefore, an incoming nucleophile such as **I-24** or **I-26** must approach the carbonyl from either the top or bottom face of **I-9**. Nucleophiles **I-24** and **I-26** are rather sterically bulky considering they have a phenyl or benzoyl group that can interact adversely with the indole ring of **I-9**. The limited rotation of the ketone does not allow for the incoming nucleophile to approach at an optimal trajectory that minimizes steric repulsion.

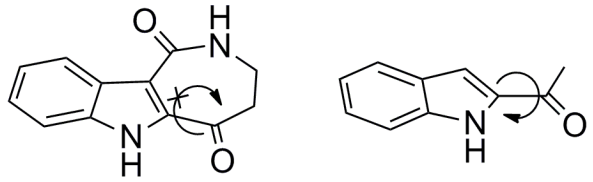

I-9 **I-28**

Figure I-12. Rotational barrier comparison of *iso*-indoloaldisine **I-9** ketone compared to 2-acetylindole **I-28** ketone.

Conversely, the ketone in compound **I-28** is able to rotate freely (Figure I-12). The ketone is not restricted to rotation since it is part of an acyclic system. Therefore, the incoming nucleophiles **I-24** or **I-26** are unable to approach the ketone at an angle that minimizes steric repulsion between the indole ring and the bulky phenyl or benzoyl substituents found in **I-24** and **I-26** respectively.

Now having synthesized the coupled product **I-29**, deprotection of the benzoyl group was investigated since this would be necessary in the synthesis of *iso*-indoloazepine. When **I-29** was treated with 5 equivalents of NaOH in THF/H_2O (1:1), an

interesting novel γ-carboline **I-31** was isolated (Scheme I-33). Scheme I-33 outlines a proposed mechanism for the formation of **I-31**. Deprotonation of the indole proton of **I-29** by NaOH allowed for the 3-position of indole to undergo a 6-*exo*-*trig* cyclization. Thereafter, elimination of hydroxide is driven by the formation of the aromatic γ-carboline system. The resulting positive charge on nitrogen makes the γ-carboline an excellent leaving group for the nucleophilic attack by hydroxide. The resulting thio-

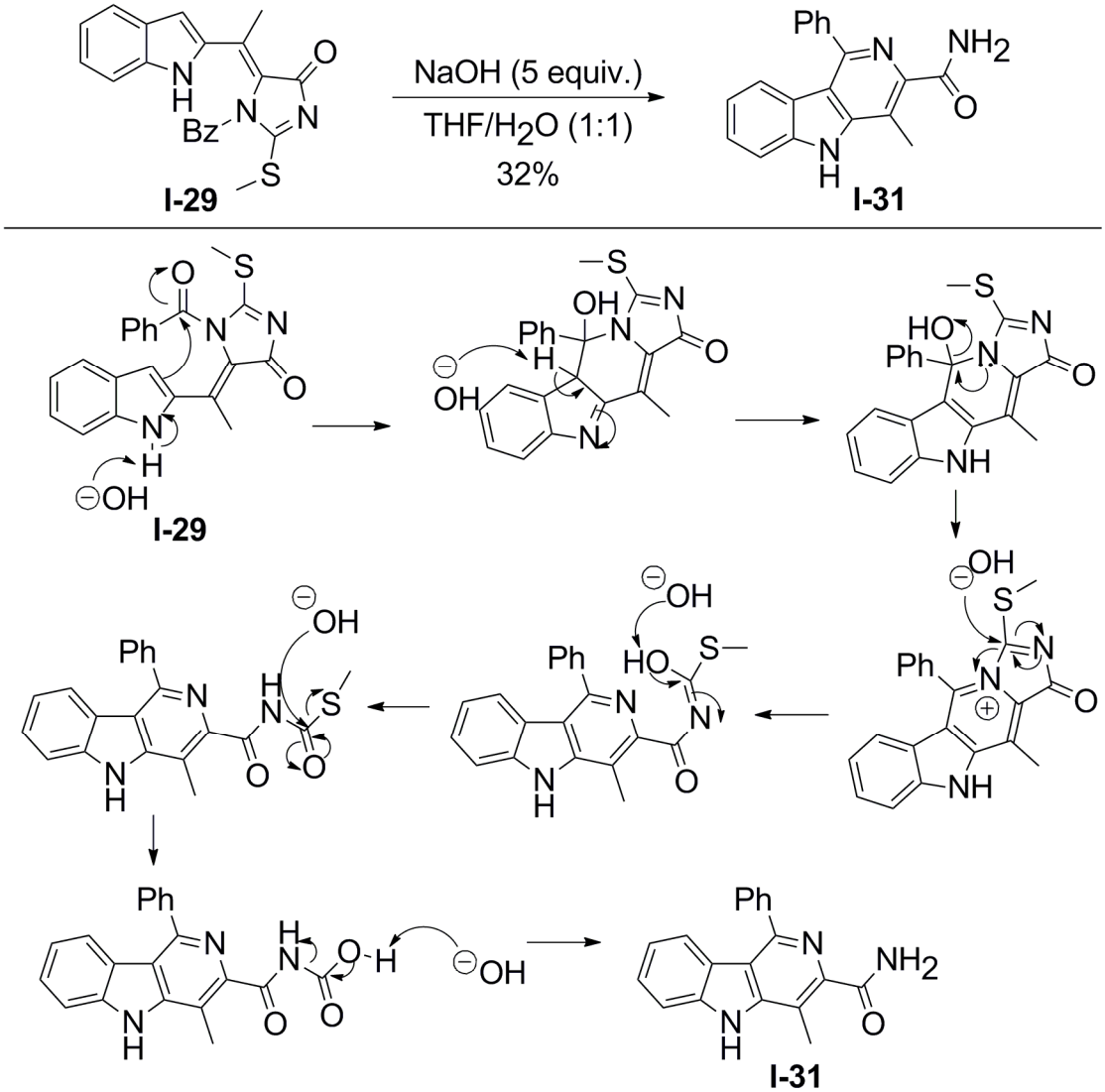

Scheme I-33. Proposed mechanism for the formation of γ-carboline **I-31**.

carbamate is hydrolyzed to the free amide seen in **I-31** under the basic conditions. Coupled product **I-30** was also treated to analogous reaction conditions but the carboxylic acid derivative of **I-31** was not observed.

Since the aldol coupling reactions with 2-acetylindole **I-28** worked smoothly, the proposed synthetic route in Scheme I-31 was investigated further. The difficulty is synthesis of the C-2 acylated indole starting material. Using a directing group such as phenylsulfonyl on the indole ring, selective acylation of the C-2 position of **I-20** with acryloyl chloride can be attempted as shown in Scheme I-34.[37] Subsequent 1,4 Michael addition with a Troc-protected amine followed by the $TiCl_4$ mediated aldol condensation should yield the desired acyclic coupled product. Thereafter, treatment of this intermediate with triflic anhydride and DMAP (Bischler-Napieralski conditions) can

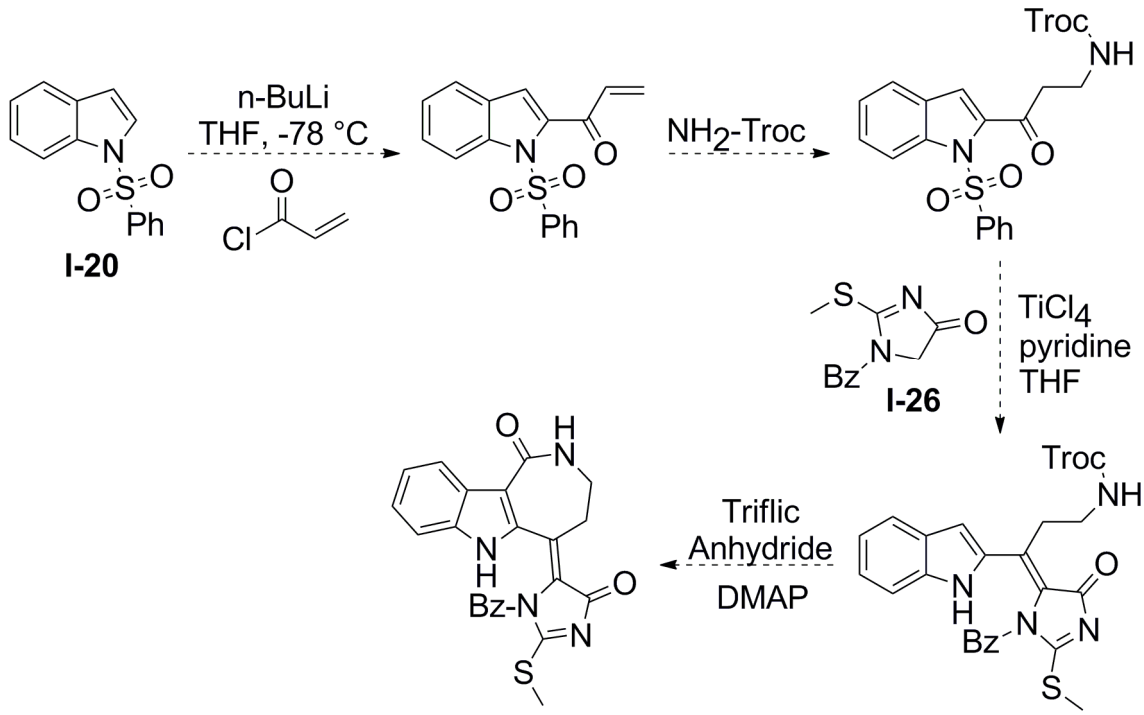

Scheme I-34. Proposed synthesis to *iso*-indoloazepine **I-6** precursor by performing $TiCl_4$ coupling reaction before Friedel-Crafts cyclization.

perform the desired cyclization to the 7-membered ring via generation of an isocyanate (mechanism illustrated in Scheme I-19).

Previous reactions with indole **I-20** and Troc-protected β-lactam **I-19** did not yield the desired C-2 acylated product (section G), so a simpler electrophile was used. Treatment of **I-20** with n-butyl lithium, followed by addition of acetic anhydride generated the desired C-2 acylated product **I-32** in 32% yield (previously reported by Mahboobi et al, Scheme I-35).[37] The analogous reaction conditions with acryloyl chloride and **I-20** (Scheme I-35) were unsuccessful and did not yield the desired starting material needed for the subsequent Michael addition reaction proposed in Scheme I-34.

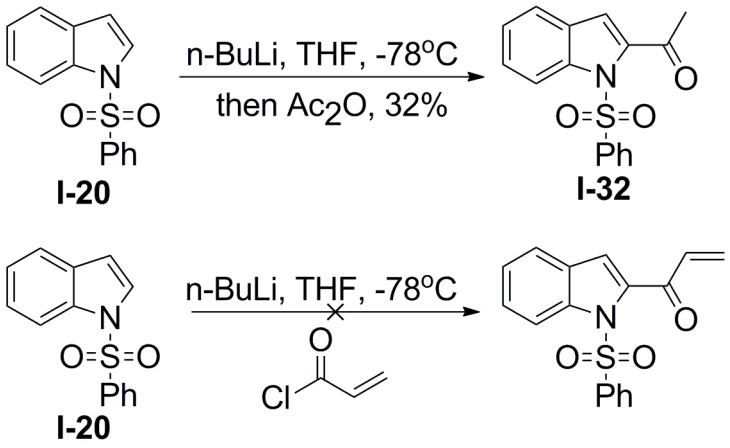

Scheme I-35. Synthesis of C-2 acylated indole **I-32** from acetic anhydride, but acryloyl chloride was not successful.

Since the selective C-2 acylation procedures proved difficult for the complex electrophiles that would be needed for the synthesis of *iso*-indoloazepine **I-6**, the previous $TiCl_4$ coupling reactions with *iso*-indoloaldisine **I-9** were reinvestigated. Although initially these coupling reactions were problematic, they were revisited due to the successful coupling reactions with the model 2-acetylindole system.

L. Completing the Synthesis of *Iso*-indoloazepine.

After difficulties with the selective C-2 acylations of **I-20** with β-lactam **I-19** or acryloyl chloride, a prior synthetic route with indole-3-carboxlic acid (section H) was reinvestigated. Since the key 7-membered ring *iso*-indoloaldisine **I-9** has been synthesized in good yield (section H, Table I-2) modifying the problematic coupling reaction between **I-9** and imidazolinone **I-26** was desirable (Scheme I-27).

Since it was postulated that the coupling reaction was problematic to aversive steric interactions between the indole ring and the rather bulky benzoyl group of **I-26** (section K, Figure I-12), a less bulky heterocycle was needed. Treatment of 2-thiohydantoin with methyl iodide, DMAP and DIPEA afforded **I-33** in 64% yield, which is the debenzoylated derivative of **I-26** (Scheme I-36).

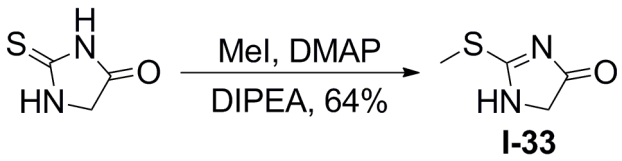

I-33

Scheme I-36. Synthesis of **I-33**, the debenzoylated equivalent of **I-26**.

Obtaining the debenzoylated **I-33** allowed for completing the synthesis of *iso*-indoloazepine. The total synthesis of *iso*-indoloazepine **I-6** is outlined in Scheme I-37. Treatment of *iso*-indoloaldisine **I-9** with $TiCl_4$ and **I-33** yielded the desired coupled product **I-34** is 64% yield. Interestingly, the analogous reaction conditions with imidazolinone **I-26** (*N*-benzoylated derivative of **I-33**) resulted in no product formation. This suggests that the sterically less bulky nucleophile **I-33** was more suitable for attacking the ketone of **I-9**. Due to the limited rotation of the ketone in the 7-membered ring (see Figure I-12), compound **I-33** is able to approach the ketone without the steric repulsion that would exist between the indole ring and the benzoyl group found on **I-26**.

Coupled product **I-34** was readily converted to *iso*-indoloazepine **I-6** by treatment with aqueous NH_4OH heated to 110℃ in a sealed tube (Scheme I-37). *Iso*-indoloazepine **I-6** was purified by column chromatography and recrystallized from methanol affording a vibrant yellow compound. The structure of *iso*-indoloazepine **I-6** was confirmed by X-ray crystallography (Figure I-13).

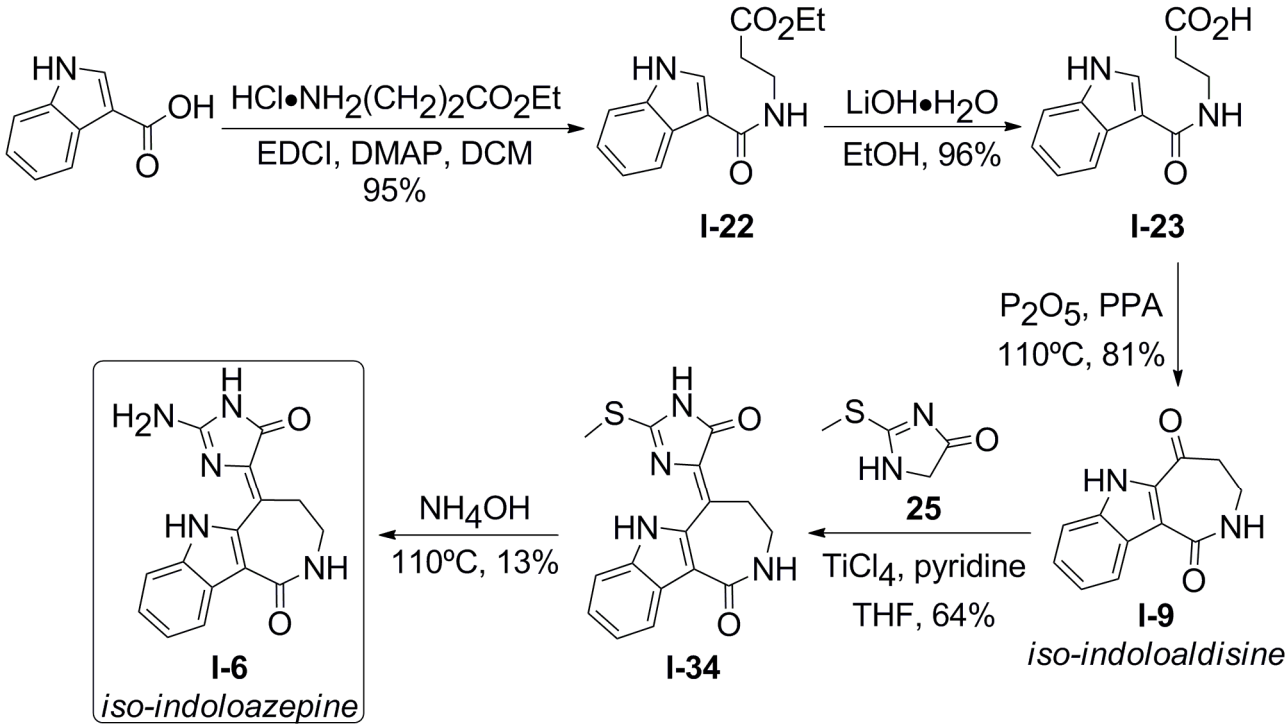

Scheme I-37. Total synthesis of *iso*-indoloazepine **I-6** from indole-3-carboxylic acid.

The synthesis of *iso*-indoloazepine **I-6** was completed in five synthetic steps with an overall yield of 6.1%. The yield associated with the final step is quiet low (13%), which can be the result of several factors. First, the low yield is likely a result of the decrease in conjugation of the double bond with the carbonyl in the glycocyamidine ring. The crystal structure of **I-6** indicates the preferred tautomer of the glycocyamidine ring has the amide nitrogen protonated (N-2 of crystal structure in Figure I-13). This is

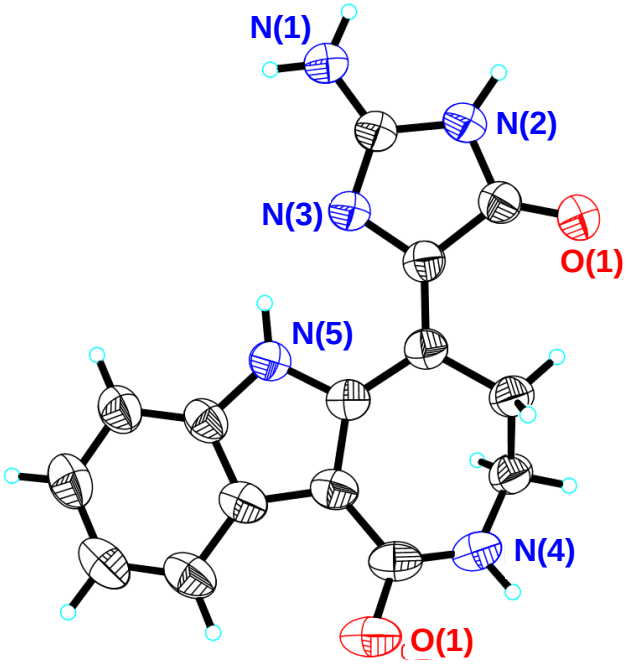

Figure I-13. Crystal structure of *iso*-indoloazepine **I-6** in methanol.

postulated to be the result of an intramolecular hydrogen bonding interaction between the N-3 nitrogen of the glycocyamidine ring and the indole proton within an acceptable distance of 2.66 Å. In turn, this results in a less electrophilic C-2 carbon and a preference of the double bond between the C-2 and N-3 positions.

Using similar reasoning, it is likely that the preferred tautomer of **I-34** also has the glycocyamidine ring N-3 atom protonated, indicating that the double bond in **I-34** is not in conjugation with the carbonyl within the glycocyamidine ring. Therefore, the C-2 carbon is not as electrophilic, thereby making the nucleophilic displacement of methanethiol by ammonia more difficult attributing to the low yields. Additionally, *iso*-indoloazepine **I-6** is an extremely polar compound. If more than approximately 4 mg of **I-6** were used to collect a ^{1}H NMR, one would observe precipitation of **I-6** out of d_6-DMSO. Since **I-6** is purified with column chromatography, it is probable that some mass is lost during the purification.

After completing the synthesis of *iso*-indoloazepine, synthetic efforts were focused on synthesizing several analogs of **I-6.**

M. Synthesis of *iso*-indoloazepine derivatives

After completing the synthesis of *iso*-indoloazepine, several derivatives were readily prepared from the precursor **I-34** (Scheme I-38). Treatment of **I-34** with 4-methoxybenzylamine afforded **I-35** in 16% yield. Treatment of **I-34** with ethylene diamine afforded **I-36** in 13% yield, while treating **I-34** with benzylamine afforded **I-37** in 37% yield. The benzyl derivative **I-37** was easily purified as it crashed out of ethanol during the reaction.

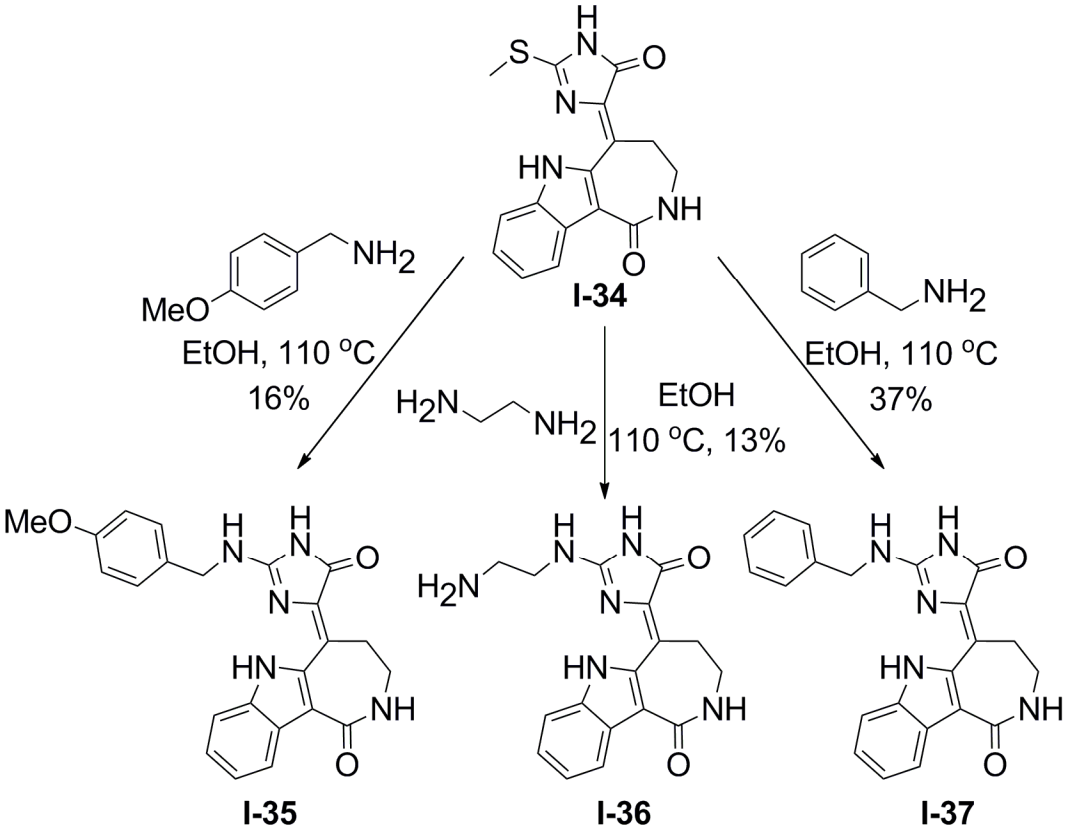

Scheme I-38. Synthesis of *iso*-indoloazepine **I-6** derivatives **I-35**, **I-36** and **I-37**.

N. Biological Evaluation of *Iso*-indoloazepine and Derivatives to Determine Efficacy as Chk2 Inhibitors.

After completing the synthesis, *iso*-indoloazepine **I-6** was evaluated for its efficacy of inhibiting Chk1 and Chk2 by Dr. Thu N.T. Nguyen. This was accomplished by using a radioactive-based filter assay *in vitro* with purified Chk1 and Chk2 enzymes. The results of the assay and the corresponding IC_{50} values are found in Figure I-14. It was determined that *iso*-indoloazepine **I-6** has an IC_{50} = 65.9 nM for Chk2 (Figure I-14b) and an IC_{50} = 581.4 nM for Chk1 (Figure I-14a). Therefore **I-6** is selective for Chk2 over Chk1 approximately 9:1 which is desirable since Chk1 has antagonistic effects compared to inhibiting Chk2. It also shows increased selectivity compared to the natural product debromohymenialdisine (4:1).

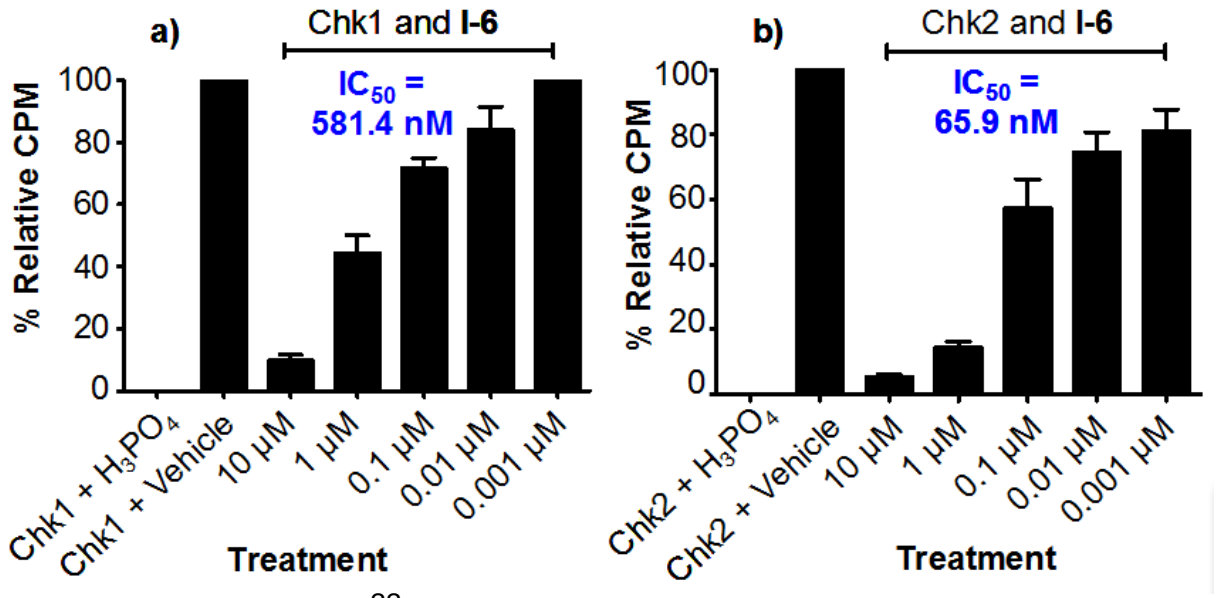

Figure I-14. Inhibition of [γ-^{33}P]-ATP phosphorylation by purified active Chk1 or Chk2. H_3PO_4 was used as a negative or untreated control. a) Inhibition of [γ-^{33}P]-ATP phosphorylation of Chk1 by *iso*-indoloazepine **I-6**. b) Inhibition of [γ-^{33}P]-ATP phosphorylation of Chk2 by *iso*-indoloazepine **I-6**. The data were expressed as mean ± SEM from 3 independent experiments**.**

To further elucidate how *iso*-indoloazepine was inhibiting Chk2, western blot analysis of **I-6** was performed by Dr. Thu N.T. Nguyen to determine if **I-6** inhibited autophosphorylation of Chk2 at Ser516 (Figure I-15). Both *iso*-indoloazepine **I-6** and Indoloazepine **I-2** demonstrated a dose dependent effect on inhibition of Chk2 Ser516, supporting cellular inhibition.

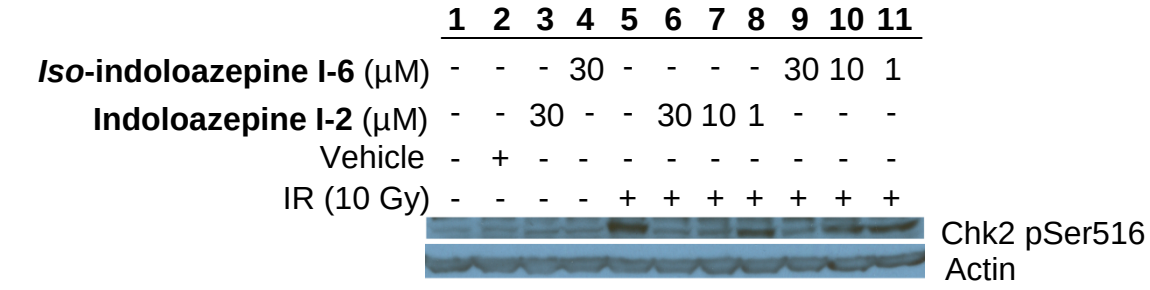

Figure I-15. Western blot analysis of 184B5 whole cells untreated (control) or treated with vehicle or with compounds **I-6** and **I-2** for 2 hours prior to IR (10 Gy). Cells were incubated for 4 hours after IR when extracts were collected. The western blot was evaluated with Chk2 antibodies. These blots are representative of 3 independent experiments.

In addition to *iso*-indoloazepine **I-6**, the various structural analogs **I-35**, **I-36** and **I-37** were evaluated for Chk2 activity by Teri Lansdell (Figure I-16). The 4-methoxy and ethylene diamine analogs **I-35** and **I-36** were determined to be micromolar inhibitors of Chk2 (IC_{50} = 2217 nM and 3203 nM, respectively). However, the benzyl analog **I-37**

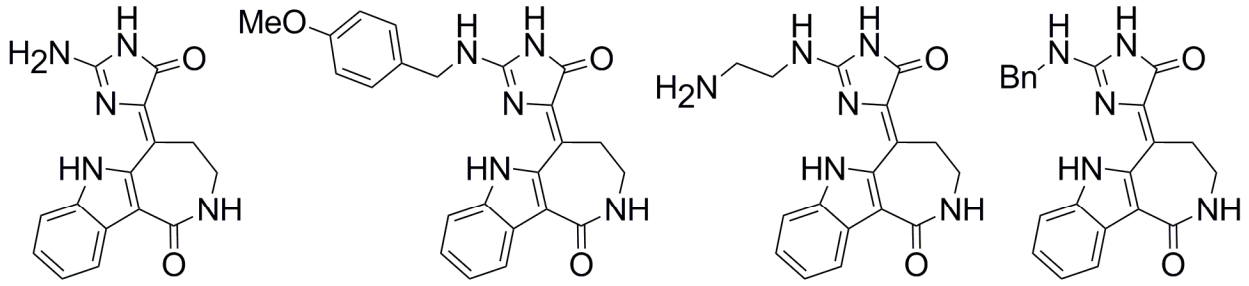

Figure I-16. Chk2 IC_{50} values for *iso*-indoloazepine **I-6** analogs.

was determined to be an effective inhibitor of Chk2 (IC_{50} = 405.6 nM). Both **I-35** and **I-37** contain a bulky benzyl substituent. Aversive steric interactions in the Chk2 binding pocket likely could contribute to the decrease in activity of these compounds compared to **I-6**.

At this point it is clear that **I-6** and some of its derivatives are potent Chk2 inhibitors. Within the Tepe group, several indole derivatives of **DBQ** have been prepared which can provide some insight into a structure-activity relationship for these Chk2 inhibitors. These inhibitors and there associated IC_{50} values are compared in Figure I-17. Both indoloazepine **I-2** (synthesized Dr. Thu N.T. Nguyen, Chk2 IC_{50} = 13.5 nM) and the phenyl pyrrole analog **I-38** (synthesized by Dr. Rahman S.Z. Saleem, Chk2 IC_{50} = 53.9 nM) are slightly more potent inhibitors of Chk2 compared to indoloazepine **I-6** (Chk2 IC_{50} = 65.9 nM). However, all three of these inhibitors are very potent inhibitors of Chk2 and show selectivity for Chk2 over Chk1 (ranging from approximately 9:1 selectivity for **I-6** to 16:1 selectivity for indoloazepine).

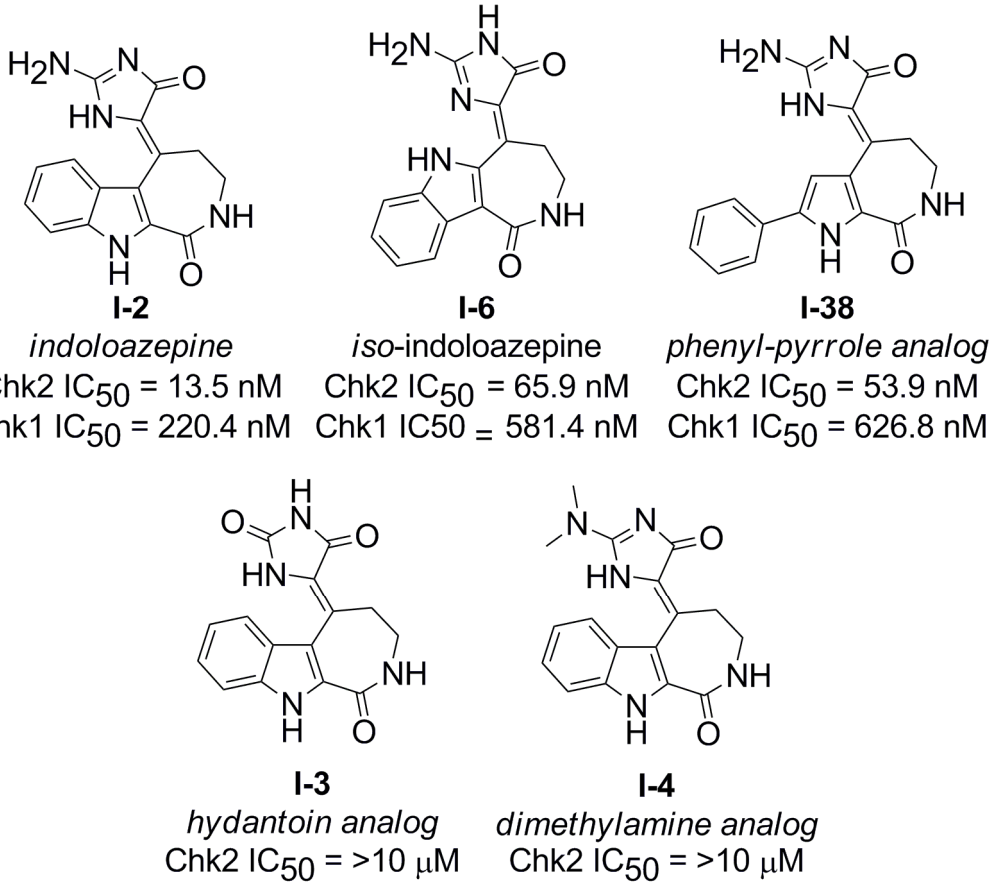

Figure I-17. Chk2 and Chk1 IC_{50} values for indoloazepine, *iso*-indoloazepine **I-6** and the phenyl-pyrrole analog of DBQ. Both the dimethylamine and hydantoin analogs of indoloazepine are inactive for Chk2.

In order to understand the trend in potency, it is first important to recognize why indoloazepine **I-2**, *iso*-indoloazepine **I-6** and the phenyl-pyrrole analog **I-38** are all active inhibitors. All three of these inhibitors possess a primary exocyclic amine from the glycocyamidine ring. Therefore, all of these inhibitors are capable of making a hydrogen bond contact with ASN352. This is the same hydrogen bonding interaction that is found with the exocyclic free amine of DBQ (section E, Figure I-6). Furthermore, the hydantoin and dimethylamine analogs of indoloazepine (**I-3** and **I-4**, Figure I-17) further indicate the importance of this hydrogen bonding interaction. In the dimethylamine analog **I-4**, there are no longer protons available on the exocyclic amine to participate in hydrogen

bonding with ASN352. Additionally, there may be an aversive steric interaction that impedes this analog from fitting properly in the Chk2 binding pocket. The hydantoin analog **I-3** has replaced the exocyclic amine (hydrogen bond donor) with a carbonyl (hydrogen bond acceptor). Once again, this analog is not capable of making the hydrogen bonding interaction with ASN352. Since neither the dimethylamine nor hydantoin analogs are capable of hydrogen bonding with ASN352, neither of these analogs are active inhibitors (IC_{50} > 10 μM).

The final interesting trend in the active inhibitors of Chk2 is describing why *iso*-indoloazepine **I-6** is not as potent of an inhibitor as either **I-2** or **I-38**. The crystal structure of *iso*-indoloazepine **I-6** can help elucidate this observed trend (Figure I-13). In the crystal structure of **I-6**, the preferred tautomer has N-2 protonated in the glycocyamidine ring (essentially an amide proton). This is believed to be the preferred tautomer as a result of intramolecular hydrogen bonding. Intramolecular hydrogen bonding is possible between the indole proton (N(5)-H) and N(3) at distance of 2.656 Å (Figure I-18). This intramolecular hydrogen bonding may compete with GLU308 in Chk2 catalytic site resulting in lower activity compared to the parent compound indoloazepine. Normally N(3) of the glycocyamidine ring could hydrogen bond with GLU308, but this

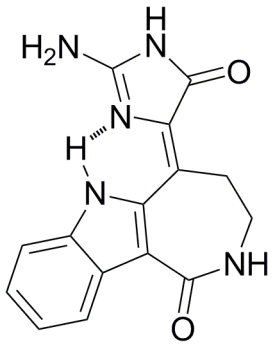

Figure I-18. Intramolecular hydrogen bonding between indole proton and glycocyamidine ring in **I-6** (2.656 Å).

interaction is compromised due to the intramolecular hydrogen bonding. Since both indoloazepine and the phenyl pyrrole analog do not have the potential for this hydrogen bonding, they are able to more effectively bind to Chk2.

O. Conclusion

The synthesis of *iso*-indoloaldisine was completed and proved to be a potent inhibitor of Chk2. Prior synthetic efforts utilizing a Dieckmann condensation reaction proved difficult, as well as utilizing selective acylation procedures for the indole C-2 position. The major synthetic breakthrough was use of the debenzoylated imidazolinone **I-33** during the $TiCl_4$ mediated coupling reactions. *Iso*-indoloazepine has shown to be a potent inhibitor of Chk2 and further studies *in vitro* would be the next step to determine its efficacy as a therapeutic. It is the hope that *iso*-indoloazepine or another novel Chk2 inhibitor can help mitigate the aversive effects of radiation treatments in the future.

P. Experimental Section

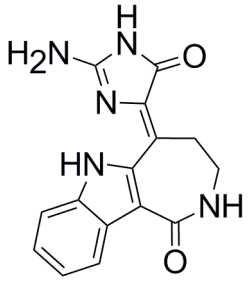

I-6
iso-indoloazepine

(Z)-5-(2-amino-5-oxo-1H-imidazol-4(5H)-ylidene)-2,3,4,5-tetrahydroazepino[4,3-b]indol-1(6H)-one (I-6). To a sealed tube was added **I-34** (0.92 g, 2.8 mmol) and aqueous NH_4OH (100 mL) which was stirred for 24 h at 110℃ (behin d a blast shield).

The reaction mixture was concentrated *in vacuo* before methanol (200 mL) was added to the crude residue and heated until boiling. Insoluble impurities were removed by filtration, and the filtrate was concentrated and purified by flash chromatography (silica, gradient solvent system,10:90 MeOH/CH_2Cl_2 to 15:85 MeOH/CH_2Cl_2). The collected fractions were concentrated *in vacuo* and recrystallized from boiling methanol to afford *iso*-indoloazepine **I-6** (yellow solid, 0.107 g, 13% yield from **I-34**). *Notebook reference: ML-II-29.*

^{1}H NMR (500 MHz) (DMSO-d_6) δ: 3.23-3.26 (m, 2H), 3.39-3.40 (m, 2H), 7.06-7.09 (m, 1H), 7.19 (ddd, J = 1.0 Hz, J = 7.0 Hz, J = 8.5 Hz, 1H), 7.36 (d, J = 8.1 Hz, 1H), 7.43 (bs, 2 N-H), 7.74 (t, J = 5.4 Hz, 1 N-H), 8.25 (t, J = 8.1 Hz, 1H), 11.05 (bs, 1 N-H), 13.10 (bs, 1 N-H). ^{13}C NMR (125 MHz) (DMSO-d_6) δ: 28.7, 39.4 109.9, 110.8, 119.2, 120.4, 122.4, 123.4, 128.4, 135.2, 137.0, 138.6, 157.2, 167.1, 170.3. IR (KBr, pellet): 3546, 3407, 3291, 3221, 3142, 1699, 1677, 1636, 1605, 1559 cm^{-1}. HRMS (ESI): m/z calcd for $C_{15}H_{14}N_5O_2$ [M+H], 296.1147; found, 296.1154. m.p. decomposed over 275 ℃.

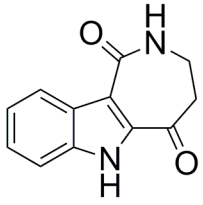

I-9

iso-indoloaldisine

3,4-dihydroazepino[4,3-b]indole-1,5(2H,6H)-dione (I-9). To a flame dried 3-neck flask at room temperature was added polyphosphoric acid (86 g) and P_2O_5 (8.12 g, 57.2 mmol) under N_2. The mixture was mechanically stirred and heated to 85℃ whereupon

carboxylic acid **I-23** (3.90 g, 16.8 mmol) was added. The mixture was then heated to 110℃ and stirred for 2 h before cooling to room tem perature. After cooling, the mixture was added to an ice/water mixture (800 mL) and stirred for 30 minutes. A purple precipitate was collected by filtration, which was then stirred in boiling acetone (300 mL) and filtered. The resulting filtrate was concentrated *in vacuo*, treated with boiling acetone, and additional precipitate was collected. The combined precipitates were washed with water (300 mL) and dried affording **I-9** (light gray solid, 2.92 g, 81% yield from **I-23**) which was used without further purification.

^{1}H NMR (500 MHz) (DMSO-d_6) δ: 2.88-2.90 (m, 2H), 3.43 (q, J = 5.2 Hz, 2H), 7.16-7.19 (m, 1H), 7.32-7.35 (m, 1H), 7.50 (d, J = 8.2 Hz, 1H), 8.16 (bt, J = 5.0 Hz, 1 N-H), 8.28 (d, J = 8.2 Hz, 1H), 12.23 (bs, 1 N-H). ^{13}C NMR (125 MHz) (DMSO-d_6) δ: 36.1, 43.4, 112.7, 113.0, 121.7, 123.8, 126.0, 127.2, 133.0, 136.6, 166.1, 192.6. IR (KBr pellet, neat): 3300, 1660, 1630 cm^{-1}. HRMS (ESI): m/z calcd for $C_{12}H_{11}N_2O_2$ $[M+H]^+$, 215.0821; found, 215.0846. m.p. decomposes over 292-294℃.

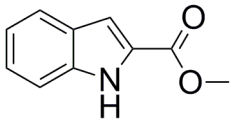

I-10

Methyl 1H-indole-2-carboxylate (I-10). To a flame dried flask under N_2, Indole-2-carboxylic acid (1.008 g, 6.25 mmol) was dissolved in a 95:5 benzene/methanol mixture (55 mL). A 2M (Trimethylsilyl)diazomethane solution in diethyl ether (6.2 mL, 12.41 mmol) was added to the solution and stirred for 50 minutes under Argon at 0°C. Thereafter the solvent was evaporated *in vacuo* and the crude mixture was dissolved in

DCM (25 mL). The DCM layer was washed with $NaHCO_3$ (1 x 40 mL) and the aqueous layer was extracted with additional DCM (1 x 20 mL). The combined organic layers were dried with Na_2SO_4 and concentrated to dryness *in vacuo* affording **I-10** (brown solid, 1.09 g, 99% yield from indole-2-carboxlyic acid). Also is possible to use thionyl chloride and methanol. *Notebook reference: ML-I-13.*

^{1}H NMR (500 MHz) ($CDCl_3$) δ: 3.88 (s, 3H), 7.14 (dt, J = 0.7 Hz, J = 7.8 Hz, 1H), 7.21-7.22 (m, 1H), 7.31 (dt, J = 1.0 Hz, J = 8.3 Hz, 1H), 7.41 (d, J = 7.3 Hz, 1H), 7.67 (d, J = 7.3 Hz, 1H), 8.99 (bs, 1 N-H). ^{13}C NMR (125 MHz) ($CDCl_3$) δ: 52.2, 109.1, 112.1, 121.1, 122.9, 125.7, 127.4, 127.8, 137.2, 162.8. IR (NaCl, neat): 3321, 1690, 1642, 1620, 1574, 1549, 1528, 1503, 1441, 1381, 1342, 1314, 1254, 1210, 1142 cm^{-1}. MS (direct probe), calcd for $C_{10}H_9NO_2$ (MII^+): 175.18. Found: 175.3. mp 142-144°C.

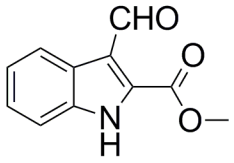

I-11

Methyl 3-formyl-1H-indole-2-carboxylate (I-11). To a flame dried flask under N_2, dry DCM (250 mL) and anhydrous DMF (34 mL) were combined and stirred for 10 minutes at 0°C. A 98% grade oxalyl chloride solution (5.42 mL, 62.11 mmol) was added dropwise at 0℃ and the mixture stirred for 30 minute s. Thereafter methyl ester **I-10** (9.89 g, 56.46 mmol) was added and the mixture was taken off ice after 5 minutes and allowed to reach room temperature. After reacting for 21 h, the resulting yellow

precipitate was collected by filtration, rinsed with DCM, and then dissolved in H_2O (400 mL). The aqueous mixture stirred for 10 minutes and then was extracted with EtOAc (3 x 300 mL). The combined organics were washed with $NaHCO_3$ (1 x 100 mL) and then brine (1 x 100 mL). The organic layers were dried with Na_2SO_4 and concentrated to dryness *in vacuo* affording **I-11** (white solid, 10.6 g, 89% yield from **I-10**). *Notebook reference: ML-I-55.*

^{1}H NMR (500 MHz) (d_6-DMSO) δ: 3.97 (s, 3H), 7.29 (dt, J = 7.1 Hz, J = 0.9 Hz, 1H), 7.38 (dt, J = 7.1 Hz, J = 1.1 Hz, 1H), 7.55 (d, J = 8.2 Hz, 1H), 8.24 (d, J = 8.0 Hz, 1H), 10.59 (s, 1H), 12.86 (bs, 1 N-H). ^{13}C NMR (125 MHz) (d_6-DMSO) δ: 52.7, 113.1, 118.5, 122.4, 123.5, 124.7, 125.9, 132.4, 135.8, 160.6, 187.6. IR (NaCl, neat): 3848, 3811, 3684, 3146, 1715, 1642, 1578, 1536, 1453, 1433, 1370, 1258, 1206, 1179, 1136, 1100 cm^{-1}. MS (direct probe), calcd for $C_{11}H_9NO_3$ (MII^+): 203.19. Found: 203.3. mp 212-214°C.

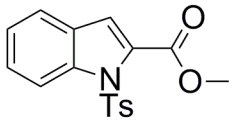

I-12

Methyl 1-tosyl-1H-indole-2-carboxylate (I-12)., In a flamed dried flask under N_2, methyl ester **I-10** (0.23 g, 1.31 mmol) was dissolved in dry DCM (10 mL) at room temperature. Thereafter recrystallized tosyl chloride (0.501 g, 2.63 mmol), DMAP (0.400 g, 3.28 mmol), and DIPEA (0.57 mL, 3.28 mmol) were subsequently added. After reacting for 26 h the mixture was quenched with a 5% HCl solution (v/v 25 mL). The

aqueous mixture was extracted with DCM (3 x 25 mL). The combined organics were washed with $NaHCO_3$ (1 x 25 mL), then brine (1 x 25 mL), and dried with Na_2SO_4, and concentrated to dryness *in vacuo.* The crude material was purified by flash chromatography (silica, 8:2 hexanes/EtOAc). Note that the column was loaded using minimal DCM. The purified product was concentrated *in vacuo* affording compound **I-12** (solid, 0.129 g, 30% yield from compound **I-10**). *Notebook reference: ML-I-34.*

^{1}H NMR (500 MHz) ($CDCl_3$) δ: 2.35 (s, 3H), 3.92 (s, 3H), 7.14 (d, J = 0.7 Hz, 1H), 7.23-7.26 (m, 3H), 7.40-7.43 (m, 1H), 7.53-7.55 (m, 1H), 7.88-7.90 (m, 2H), 8.09-8.12 (m, 1H). ^{13}C NMR (125 MHz) ($CDCl_3$) δ: 21.9, 52.9, 109.0, 112.1, 115.7, 117.0, 121.1, 122.7, 122.9, 124.3, 125.7, 127.3, 127.6, 128.4, 129.8, 131.7, 136.0, 138.5, 145.2, 162.0 (note that extra carbon peaks correspond to starting material). IR (NaCl, neat): 1730, 1433, 1373, 1343, 1307, 1264, 1202, 1179, 1150, 1126, 1090, 1042 cm^{-1}. MS (direct probe), calcd for $C_{17}H_{15}NO_4S$ (MII^{+}): 329.37. Found: 328.7. mp 70-72°C.

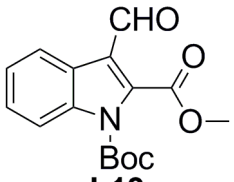

I-13

1-tert-butyl 2-methyl 3-formyl-1H-indole-1,2-dicarboxylate (I-13). To a flame dried flask, aldehyde **I-11** (0.5 g, 2.46 mmol), di-*tert*-butyl dicarbonate (0.645 g, 2.96 mmol) and DMAP (0.458 g, 3.74 mmol) were subsequently added to anhydrous acetonitrile (50 mL) at room temperature under N_2. After 18 h the reaction mixture was concentrated *in vacuo*. The crude material was dissolved in diethyl ether (50 mL),

washed with $NaHCO_3$ (1 x 25 mL) and dried with Na_2SO_4. The compound was dissolved in EtOAc and dry loaded onto a column. Purification via flash chromatography (silica, 7:3 hexanes/EtOAc) afforded **I-13** (white solid, 0.581 g, 78% yield from **I-11**). *Notebook reference: ML-I-35*.

^{1}H NMR (500 MHz) ($CDCl_3$) δ: 1.65 (s, 9H), 4.02 (s, 3H), 7.36-7.39 (m, 1H), 7.44-7.47 (m, 1H), 8.07 (d, J = 8.3 Hz, 1H), 8.33 (d, J = 8.1 Hz, 1H), 10.19 (s, 1H). ^{13}C NMR (125 MHz) ($CDCl_3$) δ: 28.1, 53.4, 86.9, 115.1, 121.3, 123.1, 125.0, 125.4, 127.7, 136.0, 137.8, 148.5, 161.8, 186.2. IR (NaCl, neat): 1742, 1667 cm^{-1}. HRMS (ESI): m/z calcd for $C_{16}H_{17}NO_5Na$ $[M+Na]^+$, 326.1004; found 326.1020. mp 94-96°C.

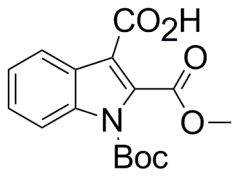

I-14

1-(tert-butoxycarbonyl)-2-(methoxycarbonyl)-1H-indole-3-carboxylic acid (I-14).[31] Aldehyde **I-13** (1.995 g, 6.58 mmol) and $Na_2HPO_4 \bullet 7H_2O$ (1.780 g, 6.58 mmol) were subsequently added to a mixture of *t*-butanol (53 mL), H_2O (14.5 mL) and 2-methyl-2-butene (3 mL, 28.88 mmol) at room temperature. Thereafter 80% technical grade $NaClO_2$ (2.982 g, 32.89 mmol) was added. After reacting for 24 h, the reaction mixture was cooled to 0℃ and 1M HCl (30 mL) was added to pH = 3. The aqueous mixture was extracted with DCM (3 x 100 mL), and the combined organics were dried

with Na_2SO_4. The organic layers were concentrated *in vacuo* affording **I-14** (flaky yellow solid, 2.41 g, quantitative yield from **I-13**). *Notebook reference: ML-I-39*

^{1}H NMR (500 MHz) ($CDCl_3$) δ: 1.66 (s, 9H), 4.02 (s, 3H), 7.36-7.44 (m, 2H), 8.14 (d, J = 9.3 Hz, 1H), 8.22 (d, J = 9.2 Hz, 1H). ^{13}C NMR (125 MHz) ($CDCl_3$) δ: 28.2, 53.6, 87.0, 111.0, 115.7, 122.6, 125.0, 126.3, 126.6, 135.1, 136.8, 148.5, 163.2, 168.8. IR (NaCl, neat): 3500-2800 (broad), 1752, 1684 cm^{-1}. HRMS (ESI): m/z calcd for $C_{16}H_{17}NO_6Na$ $[M+Na]^+$, 342.0954; found 342.0947. mp 248-250°C (decomposition).

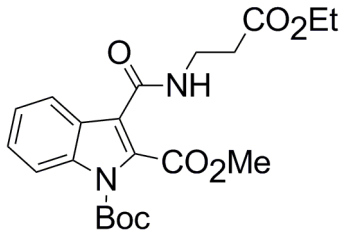

I-15

1-tert-butyl 2-methyl 3-(3-ethoxy-3-oxopropylcarbamoyl)-1H-indole-1,2-dicarboxylate (I-6). To a flamed dried flask under N_2, carboxylic acid **I-14** (0.051 g, 0.16 mmol) was dissolved in dry DCM (4 mL) at 0℃. Thereafter DMAP (0.032 g, 0.25 mmol) was added. After stirring for 15 minutes, EDCI•HCl (0.034 g, 0.17 mmol) and β-alanine ethylester hydrochloride (0.027 g, 0.17 mmol) were added subsequently to the mixture. The mixture reacted for 4 h at 0°C and then 20 h at room temperature. The reaction was quenched with H_2O (2 mL) and 10% HCl solution (v/v 2 mL) and allowed to stir for 15 minutes. The aqueous mixture was extracted with DCM (3 x 10 mL) and the combined organics were dried with Na_2SO_4. Organics were concentrated *in vacuo*

yielding **I-15** (viscous brown oil, 0.0625 g, 95% yield from **I-14**). *Notebook reference: ML-I-37*

^{1}H NMR (500 MHz) ($CDCl_3$) δ: 1.26 (t, J = 7.1 Hz, 3H), 1.63 (s, 9H), 2.63 (t, J = 6.1 Hz, 2H), 3.72 (q, J = 6.2 Hz, 2H), 3.96 (s, 3H), 4.17 (q, J = 7.1 Hz, 2H), 7.29-7.34 (m, contains N-H, 2H), 7.40 (ddd, J = 1.3 Hz, J= 7.1 Hz, J = 8.4 Hz, 1H), 8.06 (t, J = 7.4 Hz, 2H). ^{13}C NMR (125 MHz) ($CDCl_3$) δ: 14.4, 28.2, 34.5, 35.3, 53.5, 61.0, 86.2, 115.3, 118.3, 122.3, 124.5, 126.6, 127.0, 130.2, 135.5, 149.0, 162.9, 164.0, 172.6. IR (NaCl, neat): 3378 (broad), 1757, 1665 cm^{-1}. HRMS (ESI): m/z calcd for $C_{21}H_{27}N_2O_7$ $[M+H]^+$, 419.1818; found 419.1835.

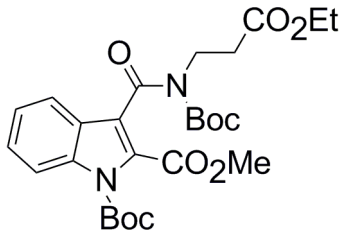

I-16

1-tert-butyl 2-methyl 3-(tert-butoxycarbonyl(3-ethoxy-3-oxopropyl)carbamoyl)-1H-indole-1,2-dicarboxylate (I-16). To a flame dried flask under N_2, amide **I-15** (1.012 g, 2.39 mmol), di-*tert*-butyl dicarbonate (0.641 g, 2.87 mmol), DMAP (0.268 g, 2.15 mmol), and TEA (0.29 mL, 2.39 mmol) were subsequently added to dry THF (100 mL) at room temperature. After reacting for 24 h, additional di-*tert*-butyl dicarbonate (0.414 g, 1.90 mmol) was added and the mixture refluxed for 2 h. The mixture was then cooled and reacted an additional 18 h at room temperature. The crude mixture was concentrated *in vacuo* and placed on a vacuum pump for 3 h. The crude material was dissolved in DCM (100 mL), and then was washed with 1 N HCl (1 x 20 mL). The

separated organic layer was subsequently washed with saturated Na_2CO_3 (1 x 20 mL) and Brine (1 x 50 mL). The crude product was dried with Na_2SO_4 and purified via flash chromatography (silica, 85:15 hexanes/EtOAc then 8:2 hexanes/EtOAc) affording **I-16** (white solid, 0.882 g, 71% from **I-15**). *Notebook reference: ML-I-44.*

^{1}H NMR (500 MHz) ($CDCl_3$) δ: 1.03 (s, 9H), 1.24 (t, J = 7.1 Hz, 3H), 1.59 (s, 9H), 2.75 (t, J = 7.6 Hz, 2H), 3.88 (s, 3H), 4.11-4.16 (m, 4H), 7.26-7.29 (m, 1H), 7.40 (ddd, J = 1.2 Hz, J = 7.3 Hz, J = 8.5 Hz, 1H), 7.50-7.52 (m, 1H), 8.08-8.09 (m, 1H). ^{13}C NMR (125 MHz) ($CDCl_3$) δ: 14.3, 27.4, 27.9, 33.7, 41.0, 52.8, 60.8, 83.9, 85.6, 115.3, 120.7, 123.5, 124.1, 126.0, 127.2, 128.2, 136.2, 149.0, 152.2, 161.6, 166.0, 171.4. IR (NaCl, neat): 1740, 1674 cm^{-1}. HRMS (ESI): m/z calcd for $C_{26}H_{35}N_2O_9$ $[M+H]^+$, 519.2343; found 519.2391. mp 98-100°C.

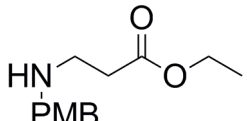

I-17

Ethyl 3-(4-methoxybenzylamino)propanoate (I-17). β-alanine ethyl ester hydrochloride (1.004 g, 6.51 mmol), NaOAc (1.061 g, 13.02 mmol) and 4-methoxybenzaldehyde (0.80 mL, 6.58 mmol) were added to acetic acid (10 mL) at room temperature under N_2. The white thick suspension stirred for 1 h, followed by portion-wise addition of $NaCNBH_3$ (0.44 g, 6.9 mmol) over a 10 minute period. After 2 h, additional $NaCNBH_3$ (0.214 g, 3.405 mmol) was added and the reaction stirred overnight. The reaction was stopped after 19 total h, and the acetic acid was removed

under high vacuum. The crude mixture was dissolved in DCM (100 mL) and washed with $NaHCO_3$ (3 x 50 mL). The organic layer was washed with Brine (1 x 50 mL), dried with Na_2SO_4 and concentrated *in vacuo* to yield a clear oil. Purification via flash chromatography (silica, 7:3 EtOAc/hexanes) yielded amine **I-17** (yellow oil, 0.668 g, 43% yield from β-alanine ethyl ester hydrochloride). *Notebook reference: ML-I-49*.

^{1}H NMR (500 MHz) ($CDCl_3$) δ: 1.24 (t, J = 7.1 Hz, 3H), 1.67 (bs, 1 N-H), 2.51 (t, J = 6.6 Hz, 2H), 2.88 (t, J = 6.6 Hz, 2H), 3.73 (s, 2H), 3.78 (s, 3H), 4.13 (q, J = 7.1 Hz, 2H), 6.84-6.86 (m, 2H), 7.21-7.24 (m, 2H). ^{13}C NMR (125 MHz) ($CDCl_3$) δ: 14.3, 34.9, 44.5, 53.3, 55.4, 60.5, 113.9, 129.3, 132.4, 158.8, 172.9. HRMS (ESI): m/z calcd for $C_{13}H_{20}NO_3$ $[M+H]^+$, 238.1443; found 238.1432.

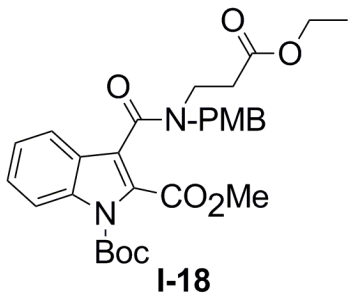

I-18

1-tert-butyl 2-methyl 3-((3-ethoxy-3-oxopropyl)(4-methoxybenzyl)carbamoyl)-1H-indole-1,2-dicarboxylate (I-18). Carboxylic acid **I-14** (0.200 g, 0.63 mmol) and DMAP (0.123 g, 1.00 mmol) were subsequently added to dry DCM (10 mL) in a flame dried flask under N_2. The mixture chilled at 0°C for 15 minutes and then EDCI hydrochloride (0.133 g, 0.69 mmol) and amine **I-17** (0.151 g, 0.63 mmol) were added subsequently. After 24 h the reaction was quenched with 10% aqueous HCl solution (v/v 6 mL) until pH = 1. The organic layer was collected and the aqueous layer was

extracted an additional time with DCM (1 x 20 mL). The combined organics were washed with $NaHCO_3$ (1 x 30 mL) and Brine (1 x 30 mL), dried with Na_2SO_4 and concentrated *in vacuo*. The crude material was purified using flash chromatography (silica, 35:65 EtOAc/hexanes) yielding compound **I-18** (0.243 g, 72% yield from **I-14**). *Notebook reference: ML-I-51*.

The ^{1}H NMR and ^{13}C NMR spectra were not clear. ^{1}H NMR contained broad splitting patterns and ^{13}C NMR contained extra peaks. Formation of product based solely on mass spectrometry. HRMS (ESI): m/z calcd for $C_{29}H_{35}N_2O_8$ $[M+H]^+$, 539.2393; found 539.2396.

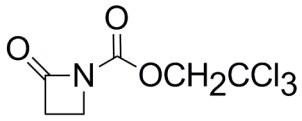

I-19

2,2,2-trichloroethyl 2-oxoazetidine-1-carboxylate (I-19).[39] In a flame dried flask under N_2, 2-azetidinone (0.300 g, 4.22 mmol) was dissolved in anhydrous THF (14 mL) and cooled to -78°C in an acetone/dry ice bath. Then n-butyl lithium (2.5 M in hexanes, 1.9 mL, 4.64 mmol) was added dropwise to the solution. After stirring for 30 minutes a solution of 2,2,2-trichloroethyl chloroformate (0.64 mL, 4.64 mmol) in anhydrous THF (4 mL) was added dropwise. The reaction stirred at -78℃ for 1.5 h and then 1 h at room temperature. The reaction was quenched with NH_4Cl (1 x 15 mL), and the aqueous mixture was extracted with diethyl ether (3 x 20 mL). The combined organic layers were

dried with Na_2SO_4 and concentrated *in vacuo* affording β-lactam **I-19** (white solid, 0.923 g, 89% yield from 2-azetidinone). *Notebook reference: ML-I-59.*

^{1}H NMR (500 MHz) ($CDCl_3$) δ: 3.14 (t, J = 5.3 Hz, 2H), 3.73 (t, J = 5.3 Hz, 2H), 4.84 (s, 2H). ^{13}C NMR (125 MHz) ($CDCl_3$) δ: 37.6, 38.6, 75.2, 94.7, 147.5, 164.3. IR (NaCl, neat): 1792, 1732 cm^{-1}. HRMS (ESI): m/z calcd for $C_6H_7NO_3Cl_3$ $[M+H]^+$, 245.9492; found 245.9468. mp 88-92°C.

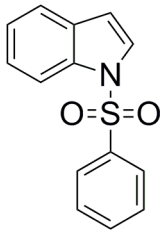

I-20

1-(phenylsulfonyl)-1H-indole (**I-20**).[40] To a flame dried flask under N_2 was added crushed NaOH (fine powder, 0.401 g, 10 mmol) and tetrabutylammonium hydrogensulfate (0.034 g, 0.1 mmol) subsequently to dry DCM (15 mL). The mixture was stirred for 10 minutes at 0°C in an ice bath whereupon indole (0.387 g, 3.30 mmol) was added. After stirring for 5 minutes, benzenesulfonyl chloride (0.43 mL, 3.30 mmol) dissolved in dichloromethane (10 mL) was added dropwise over a 30 minute period to the reaction mixture at 0℃. The ice was allowed to m elt and the mixture reacted for 14 h. The mixture was filtered and the crude solid was rinsed with dichloromethane (10 mL). The DCM filtrate was concentrated and purified via flash chromatography (silica, 15:85 EtOAc/Hexanes). The column was loaded with 100% EtOAc. Column afforded indole **I-20** (solid, 0.844 g, 99% yield from indole). *Notebook reference: ML-I-145.*

^{1}H NMR (500 MHz) ($CDCl_3$) δ: 6.67 (dd, J = 3.7 Hz, J = 0.7 Hz, 1H), 7.22-7.25 (m, 1H), 7.31-7.34 (m, 1H), 7.41-7.45 (m, 2H), 7.50-7.54 (m, 2H), 7.58 (d, J = 3.7 Hz, 1H), 7.88-7.90 (m, 2H), 8.01 (d, J = 8.4 Hz, 1H). ^{13}C NMR (125 MHz) ($CDCl_3$) δ: 109.4, 113.7, 121.5, 123.5, 124.8, 126.4, 126.9, 129.4, 130.9, 133.9, 135.0, 138.4. IR (KBr, pellet): 1446, 1372, 1261, 1186, 1177, 1129, 1092 cm^{-1}. HRMS (ESI): m/z calcd for $C_{14}H_{12}NO_2S$ $[M+H]^+$, 258.0580; found 258.0589. mp 72-74°C.

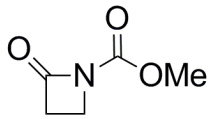

I-21

methyl 2-oxoazetidine-1-carboxylate (I-21).[39] To a flame dried flask under N_2 was added 2-azetidinone (0.514 g, 7.03 mmol) to dry THF (23 mL). The solution was cooled to -78°C, and 2.5 M n-BuLi (3.14 mL, 7.73 mmol) was added dropwise over 35 minutes. After stirring 25 minutes, a solution of methyl chloroformate (0.60 ml, 7.73 mmol) and THF (7 mL) was added dropwise over an hour. The mixture was allowed to react for 1 h at -78°C, and then an additional hour at room temperature. The reaction was then quenched with NH_4Cl (20 ml). The aqueous layer was extracted with diethyl ether (3 x 20 ml) and dried with Na_2SO_4. The crude material was purified using flash chromatography (silica, 99:1 dichloromethane/ethanol) affording **I-21** (white solid, 0.504 g, 55% yield from 2-azetidinone). *Notebook Reference: ML-I-98.*

^{1}H NMR (500 MHz) ($CDCl_3$) δ: 3.01 (t, J = 5.3 Hz, 2H), 3.59 (t, J = 5.1 Hz, 2H), 3.81 (s, 3H). ^{13}C NMR (125 MHz) ($CDCl_3$) δ: 36.6, 37.8, 53.5, 149.8, 164.3. IR (NaCl, neat): 1792, 1716 cm^{-1}. mp 60-62°C.

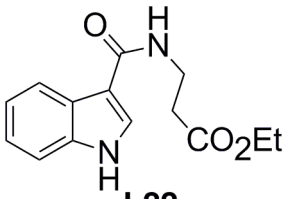

I-22

Ethyl 3-(1H-indole-3-carboxamido)propanoate (I-22). To a flame dried flask under N_2, indole-3-carboxylic acid (7.00 g, 43.4 mmol) was dissolved in dry CH_2Cl_2 (250 mL) at 25℃. Thereafter, β-alanine ethylester hydrochloride (7.35 g, 47.8 mmol) and DMAP (9.02 g, 73.9 mmol) were subsequently added. The mixture was cooled to 0℃ for 20 minutes at which point EDCI hydrochloride (10.01 g, 52.1 mmol) was added. Thereafter, the mixture was stirred for 4 h at 0℃ and then 20 h at room temperature. The reaction mixture was acidified to pH 1 with 10% aqueous HCl (*v*/*v*, 100 mL) and stirred for 15 minutes. Additional H_2O (100 mL) was added and the organic layer was separated. The aqueous layer was extracted with additional CH_2Cl_2 (2 x 100 mL). The combined organics were then washed with sat. $NaHCO_3$ (1 x 100 mL) and brine (1 x 100 mL). The organics were dried with Na_2SO_4 and the mixture was concentrated *in vacuo* yielding ethyl ester **I-22** (light brown solid, 10.7 g, 95% yield from indole-2-carboxylic acid) which was used without further purification.

^{1}H NMR (500 MHz) ($CDCl_3$) δ: 1.29 (t, J = 6.7 Hz, 3H), 2.70 (t, J = 5.8 Hz, 2H), 3.82 (q, J = 5.3 Hz, 2H), 4.21 (q, J = 7.2 Hz, 2H), 6.79 (bt, J = 5.6 Hz, 1 N-H), 7.24-7.28 (m, 2H), 7.43-7.45 (m, 1H), 7.75 (d, J = 2.8 Hz, 1H), 7.96-7.98 (m, 1H), 9.35 (bs, 1 N-H). ^{13}C NMR (125 MHz) ($CDCl_3$) δ: 14.3, 34.5, 35.0, 61.0, 112.21, 112.25, 119.9, 121.8, 123.0, 124.7, 128.6, 136.6, 165.6, 173.2. IR (NaCl, neat): 3500-3000 (broad), 1719, 1624, 1543 cm^{-1}. HRMS (ESI): m/z calcd for $C_{14}H_{17}N_2O_3$ [M+H], 261.1239; found, 261.1237. m.p. 122-124℃.

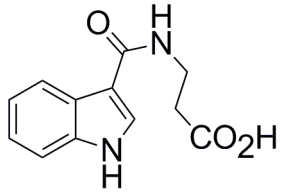

I-23

3-(1H-indole-3-carboxamido)propanoic acid (I-23). Ethyl ester **I-22** (15.2 g, 58.4 mmol) was dissolved in ethanol (400 mL) and LiOH monohydrate (7.35 g, 175.2 mmol) was added at 25℃. After 39 h, the solvent was evaporated *in vacuo* and the resulting carboxylate salt was dissolved in H_2O (400 mL). The mixture was cooled to 0℃ and concentrated HCl was added until pH 1. After stirring for 1 h at 0℃, the precipitate was collected, dissolved in methanol (300 mL), dried with Na_2SO_4 and concentrated affording carboxylic acid **I-23** (light brown solid, 13.0 g, 96% yield from **I-22**) which was used without further purification.

^{1}H NMR (500 MHz) (Acetone-d_6) δ: 2.67 (t, J = 6.7 Hz, 2H), 3.67 (q, J = 6.0 Hz, 2H), 7.12-7.19 (m, 2H), 7.37 (bs, 1 N-H), 7.46-7.48 (m, 1H) 7.99 (d, J = 2.9 Hz, 1H), 8.21-8.23 (m, 1H), 10.72 (bs, 1 N-H). ^{13}C NMR (125 MHz) (Acetone-d_6) δ: 35.0, 35.9, 112.5,

112.6, 121.5, 121.9, 123.0, 127.0, 128.5, 137.6, 166.0, 173.7. δ: IR (NaCl, neat): 3500-3000 (broad, O-H), 1724, 1557 cm^{-1}. HRMS (ESI): m/z calcd for $C_{12}H_{13}N_2O_3$ $[M+H]^+$, 233.0926; found, 233.0932. m.p. 178-180 ℃.

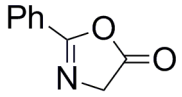

I-24

2-phenyloxazol-5(4H)-one (I-24).[26] To a flame dried flask under N_2, *N*-benzoylglycine (2.002 g, 11.1 mmol) and trifluoroacetic anhydride (1.9 mL, 13.4 mmol) were subsequently added to dry DCM (150 mL). The reaction mixture stirred overnight at room temperature. After 20 h the reaction was quenched with saturated $NaHCO_3$ (100 mL) and was allowed to stir for an additional 30 minutes. The organic layer was separated and washed an additional time with saturated $NaHCO_3$ (1 x 100 mL). This aqueous layer was extracted with additional DCM (1 x 100 mL). The combined organics were washed with Brine (1 x 80 mL) and dried with Na_2SO_4. The organics were concentrated *in vacuo* yielding phenylazlactone **I-24** (brown solid, 1.524 g, 85% yield from *N*-benzoylglycine). *Notebook reference: ML-I-78.*

^1H NMR (500 MHz) ($CDCl_3$) δ: 4.42 (s, 2H), 7.47-7.50 (m, 2H), 7.58 (tt, J = 7.3 Hz, J = 1.2 Hz, 1H), 7.98-8.00 (m, 2H). ^{13}C NMR (125 MHz) ($CDCl_3$) δ: 55.2, 126.0, 128.0, 129.0, 133.0, 163.6, 176.1. IR (NaCl, neat): 1815, 1659 cm^{-1}. HRMS (ESI): m/z calcd for $C_9H_8NO_2$ $[M+H]^+$, 162.0555; found 162.0562. m.p. 76-78°C.

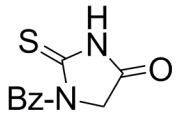

I-25

1-benzoyl-2-thioxoimidazolidin-4-one (I-25).[41] A mixture of hippuric acid (4.00 g, 22.32 mmol) and ammonium thiocyanate (4.00 g, 52.55 mmol) were thoroughly ground together in a mortar. The mixture was then suspended in a mixture of glacial acetic acid (2 mL) and acetic anhydride (18 mL). The reaction was heated for 1 h at 60°C and for an additional hour at 100°C. The red solution was then cooled and diluted with cold water (100 mL) and stirred overnight to decompose the acetic anhydride. The resulting precipitate was collected by filtration and recrystallized from ethanol (30 mL) yielding thiohydantoin **I-25** (brown solid, 3.097 g, 63% yield from hippuric acid). *Notebook Reference: ML-I-94*

^{1}H NMR (500 MHz) (d_6-DMSO) δ: 4.60 (s, 2H), 7.42-7.45 (m, 2H), 7.53-7.56 (m, 1H), 7.64-7.66 (m, 2H), 12.53 (bs, 1 N-H). ^{13}C NMR (125 MHz) (d_6-DMSO) δ: 52.9, 127.9, 128.5, 131.8, 134.4, 169.0, 170.8, 182.6. IR (NaCl, neat): 3183, 1759, 1686 cm^{-1}. m.p. 158-161°C.

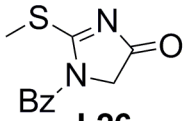

I-26

1-benzoyl-2-(methylthio)-1H-imidazol-4(5H)-one (I-26).[41] In a flame dried flask under N_2, thiohydantoin **I-25** (1.00 g, 4.54 mmol), iodomethane (0.85 mL, 13.62 mmol), DMAP (0.057 g, 0.45 mmol) and DIPEA (0.40 ml, 2.27 mmol) were subsequently added

to dry DCM (50 mL) at room temperature. The reaction was monitored by TLC (silica, 3:7 EtOAc/Hexanes) until starting material was consumed or formation of the N-methylated side product was observed (approximately 4 hours reaction time). The reaction was quenched with 1% HCl (50 mL) and stirred briefly. The aqueous layer was extracted with DCM (3 x 50 mL). The combined organics were dried with Na_2SO_4 and concentrated *in vacuo* leaving a goopy residue. The residue was heated in boiling EtOAc until everything dissolved and then a few drops of hexanes were added to induce crystallization. The beige crystals were filtered and washed with cold EtOAc, yielding **I-26** (beige solid, 0.812 g, 76% yield from **I-25**). A few non polar impurities remained, possibly DIPEA. *Notebook Reference: ML-I-95*

^{1}H NMR (500 MHz) (d_6-DMSO) δ: 2.54 (s, 3H), 4.48 (s, 2H), 7.50-7.54 (m, 2H), 7.59-7.63 (m, 1H), 7.71-7.73 (m, 2H). ^{13}C NMR (125 MHz) (d_6-DMSO) δ: 16.0, 54.9, 127.6, 128.5, 131.9, 133.5, 166.6, 182.3, 186.0. IR (NaCl, neat): 1755, 1732 cm^{-1}. m.p. 130-133 °C.

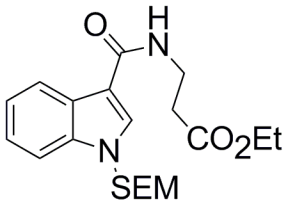

I-27

Ethyl 3-(1-((2-(trimethylsilyl)ethoxy)methyl)-1H-indole-3-carboxamido)propanoate (I-27). To a flame dried flask under N_2 was added dry DMF (3 mL) followed by 60% NaH (0.016 g, 0.384 mmol). The mixture was cooled to 0°C, and ethyl ester **I-22** (0.100 g, 0.38 mmol) was added. After stirring for 20 minutes,

SEMCl (68 µL, 0.384 mmol) was added dropwise. Thereafter the reaction was allowed to warm to room temperature. After 19 h the reaction was quenched with cold $NaHCO_3$ (3 mL). Additional water was added (5 mL) to improve separation. The aqueous layer was extracted with diethyl ether (3 x 10 mL) and the combined organics were dried with Na_2SO_4. The organics were concentrated *in vacuo* and purified using flash chromatography (silica, 1:1 EtOAc/hexanes) affording **I-27** (0.120 g, 80% yield from **I-22**). *Notebook reference: ML-I-118*.

^{1}H NMR (500 MHz) ($CDCl_3$) δ: -0.08 (s, 9H), 0.87 (dd, J = 8.2 Hz, J = 8.2 Hz, 2H), 1.27 (t, J = 7.1 Hz, 3H), 2.66 (dd, J = 5.9 Hz, J = 5.9 Hz, 2H), 3.45 (dd, J = 8.1 Hz, J = 8.1 Hz, 2H), 3.76 (bs, 2H), 4.17 (q, J = 7.1 Hz, 2H), 5.47 (s, 2H), 6.72 (broad s, 1H), 7.25-7.31 (m, 2H), 7.49-7.54 (m, 1H), 7.76 (s, 1H), 7.94-7.97 (m, 1H). ^{13}C NMR (125 MHz) ($CDCl_3$) δ: -1.3, 14.3, 17.8, 34.4, 34.8, 60.9, 66.4, 76.3, 111.0, 112.1, 120.3, 122.2, 123.1, 125.8, 131.5, 136.8, 164.9, 173.2. IR (NaCl, neat): 3312, 3103, 2953, 2896, 1737, 1625, 1551, 1525, 1465, 1371, 1278, 1231, 1185, 1084 cm^{-1}. HRMS(ESI): m/z calcd for $C_{20}H_{31}N_2O_4Si$ $[M+H]^+$, 391.2053; found 391.2062. m.p. 70-72 °C.

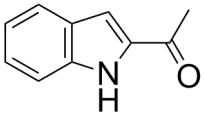

I-28

2-acetylindole (**I-28**).[42] In a flame dried flask under N_2, indole-2-carboxylic acid (2.00 g, 12.4 mmol) was dissolved in anhydrous dimethoxyethane (150 mL) and cooled to -78°C. Then 2.59 M methyl lithium in diethoxymethane (4.8 mL, 12.4 mmol) was

added dropwise to the solution and was subsequently allowed to warm to room temperature (45 minutes). Thereafter the solution was cooled to 0°C and additional 2.59 M methyl lithium (10 mL, 25.9 mmol) was added dropwise. The mixture was then refluxed for 1 h, cooled back to room temperature, and additional 2.59 M methyl lithium (15 mL, 38.9 mmol) was added at room temperature. This mixture was allowed to reflux for 21 h, and then was quenched by saturated NH_4Cl solution (100 mL) whereupon the solution turned clear orange. This aqueous mixture was extracted with diethyl ether (3 x 100 mL), and the combined organics were washed with H_2O (1 x 100 mL), dried with Na_2SO_4 and concentrated *in vacuo* affording 2-acetylindole **I-28** (1.90 g, 96% yield from indole-2-carboxylic acid). This particular reaction was not purified further, but further purification can be accomplished using flash chromatography (silica, 100% dichloromethane). *Notebook reference: ML-I-138*

^{1}H NMR (500 MHz) ($CDCl_3$) δ: 2.62 (s, 3H), 7.17 (ddd, J = 0.9, J = 7.0 Hz, J = 7.9 Hz, 1H), 7.21-7.22 (m, 1H), 7.36 (ddd, J = 1.0 Hz, J = 6.9 Hz, J = 8.1 Hz, 1H), 7.45-7.47 (m, 1H), 7.71-7.73 (m, 1H), 9.49 (bs, 1H). ^{13}C NMR (125 MHz) ($CDCl_3$) δ: 26.0, 110.1, 112.4, 121.0, 123.1, 126.5, 127.7, 135.5, 137.6, 190.8. m.p. 138-140 °C.

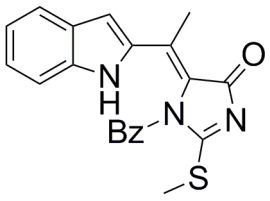

I-29

(Z)-5-(1-(1H-indol-2-yl)ethylidene)-1-benzoyl-2-(methylthio)-1H-imidazol-4(5H)-one (**I-29**). To a flame dried flask under N_2 was added anhydrous THF (15 mL) followed

by 1 M $TiCl_4$ in dichloromethane (5 mL, 5.02 mmol) at -5°C (ice and NaCl bath). Thereafter 2-acetylindole **I-28** (0.200 g, 1.26 mmol) and imidazolinone **I-26** (0.588 g, 2.51 mmol) were subsequently added and stirred at 0°C for 40 minutes. Thereafter pyridine (0.82 mL, 10.05 mmol) was added portion-wise over a 30 minute period. The reaction was kept at 0℃ for 2 h and then reacted at ro om temperature for an additional 26 h. The reaction was quenched with saturated NH_4Cl (30 mL) and the aqueous layer was extracted with EtOAc (3 x 50 mL). The combined organics were washed with H_2O (1 x 100 mL) and Brine (1 x 100 mL). The organics were dried with Na_2SO_4 and concentrated *in vacuo*. The crude mixture was purified via flash chromatography (silica, 100% dichloromethane) affording compound **I-29** (solid, 0.215 g, 46% yield from **I-28**). *Notebook reference: ML-I-129*

^{1}H NMR (500 MHz) ($CDCl_3$) δ: 2.36 (s, 3H), 2.99 (s, 3H), 6.66 (d, J = 8.9 Hz, 1H), 7.06 (ddd, J = 1.3 Hz, J = 7.1 Hz, J = 8.6 Hz, 1H), 7.18 (s, 1H), 7.36 (t, J = 7.5 Hz, 1H), 7.60-7.65 (m, 4H), 7.68-7.72 (m, 1H), 7.82 (d, J = 8.1 Hz, 1H), 10.75 (bs, 1 N-H). ^{13}C NMR (125 MHz) ($CDCl_3$) δ: 12.5, 14.5, 99.5, 115.3, 121.2, 122.6, 124.4, 128.15, 128.19, 129.2, 129.3, 130.72, 130.78, 130.81, 134.6, 137.9, 147.2, 164.2, 170.4 (note some carbon chemical shifts are nearly overlapping). IR (NaCl, neat): 3297, 1700, 1655, 1549, 1448 cm^{-1}. TOF MS ES+ m/z 376.2. m.p. decomposed at 238 °C.

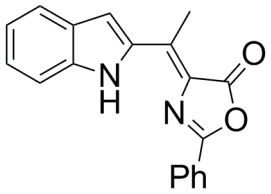

I-30

(Z)-4-(1-(1H-indol-2-yl)ethylidene)-2-phenyloxazol-5(4H)-one (**I-30**). To a flame dried flask under N_2, 1 M $TiCl_4$ in dichloromethane (1.5 mL, 1.5 mmol) was added to dry THF (5 mL) at -10°C. A yellow complex formed and 2-acetylindole **I-28** (0.060 g, 0.38 mmol) and phenylazlactone **I-24** (0.120 g, 0.75 mmol) were subsequently added. After reacting for 2.5 h, pyridine (0.25 mL, 3.02 mmol) was added dropwise over a 30 minute period. The mixture was allowed to warm to room temperature and reacted for an additional 16 h. The reaction was quenched with NH_4Cl solution (5 mL) and allowed to stir for 1 h. The aqueous mixture was then extracted with EtOAc (3 x 15 mL). The combined organics were washed with Brine (1 x 20 mL), dried with Na_2SO_4 and concentrated *in vacuo*. The crude mixture was purified using flash chromatography (silica, 4:6 DCM/hexanes) affording compound **I-30** (0.064 g, 56% yield from **I-28**). *Notebook reference: ML-I-139*

^{1}H NMR (500 MHz) ($CDCl_3$) δ: 2.76 (s, 3H), 7.11-7.16 (m, 2H), 7.32 (ddd, J = 1.0 Hz, J = 7.0 Hz, J = 8.0 Hz, 1H), 7.46-7.47 (m, 1H), 7.54-7.67 (m, 4H), 8.09-8.11 (m, 2H), 11.33 (bs, 1 N-H). ^{13}C NMR (125 MHz) ($CDCl_3$) δ: 14.7, 110.7, 111.9, 120.7, 122.2, 125.6, 125.9, 127.4, 127.7, 127.9, 129.1, 133.0, 136.8, 137.3, 138.9, 159.6, 166.1. IR (NaCl, neat): 3338, 3056, 2954, 2922, 2851, 1792, 1755, 1635, 1328, 1262

cm^{-1}. HRMS (ESI): m/z calcd for $C_{19}H_{15}N_2O_2$ $[M+H]^+$, 303.1134; found 303.1145. m.p. 170-173 °C.

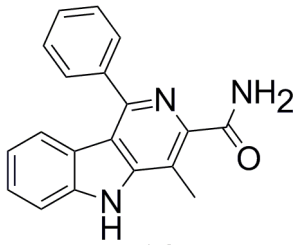

I-31

4-methyl-1-phenyl-5H-pyrido[4,3-b]indole-3-carboxamide (**I-31**). Crushed NaOH pellets (0.080 g, 2.00 mmol) were added to a THF/H_2O 1:1 mixture (v/v, 10 mL). Compound **I-29** (0.150 g, 0.40 mmol) was added at room temperature and stirred for 18 h. Thereafter the reaction was neutralized to pH = 7 using a 10% HCl solution (v/v, ~2 mL). The aqueous layer was extracted with EtOAc (3 x 20 mL), and the combined organics were dried with Na_2SO_4. The organics were concentrated *in vacuo* and the crude mixture was purified using flash chromatography (silica, 5:95 methanol/DCM; dry loaded) affording γ-carboline **I-31** (0.0383 g, 32% yield from **I-29**). *Notebook reference: ML-I-130.* Alternative workup by acidifying to pH = 1 will isolate the HCl salt of **I-31** (see *ML-I-137*).

^{1}H NMR (500 MHz) (DMSO-d_6) δ: 2.89 (s, 3H), 7.09-7.12 (m, 1H), 7.42-7.50 (m, 2H, contains 1 N-H), 7.55-7.66 (m, 5H), 7.84-7.86 (m, 2H), 8.02 (bs, 1 N-H), 12.05 (bs, 1 N-H). ^{13}C NMR and DEPT (125 MHz) (DMSO-d_6) δ: 13.2 (CH_3), 111.9 (CH), 115.8 (quaternary C), 116.6 (quaternary C), 119.9 (CH), 120.6 (quaternary C), 121.7 (CH), 126.9 (CH), 128.4 (CH), 128.7 (CH), 129.0 (CH), 140.0 (quaternary C), 140.8

(quaternary C), 143.0 (quaternary C), 145.8 (quaternary C), 149.8 (quaternary C), 169.1 (quaternary C). IR (NaCl, neat): 3420, 3256, 1691, 1670, 1574 cm^{-1}. HRMS (ESI): m/z calcd for $C_{19}H_{16}N_3O$ $[M+H]^+$, 302.1293; found 302.1303. m.p. 255-258 °C.

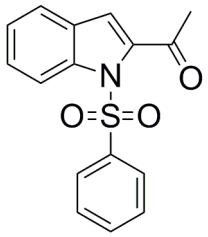

I-32

1-(1-(phenylsulfonyl)-1H-indol-2-yl)ethanone (I-32).[40] To a flame dried flask under N_2, 1-(phenylsulfonyl)indole **I-20** (0.301 g, 1.17 mmol) was added to dry THF (10 mL). The mixture was cooled to -78 °C whereupon 1.53 M n-BuLi (0.84 mL, 1.29 mmol) was added dropwise turning the solution orange. Thereafter a separate solution of acetic anhydride (120 µL, 1.29 mmol) and dry THF (1 mL) was cooled to -78 °C. The acetic anhydride solution was then added via a cannula to the indole mixture at -78 °C. After 2 h the mixture was allowed to warm to room temperature and reacted for an additional 1.5 h. Then the reaction was quenched with Na_2CO_3 solution (0.200 g Na_2CO_3 in 10 mL H_2O). The aqueous mixture was extracted with EtOAc (3 x 15 mL); approximately 5 mL of H_2O was added to improve the slow separation. The combined organics were concentrated *in vacuo* and the crude mixture was purified via flash chromatography (silica, 1:9 methanol/DCM). When dissolving this mixture to load onto the column, a precipitate crashed out which was not loaded. The column afforded purified compound **I-32** (solid, 0.111 g, 32% yield from **I-20**). *Notebook Reference: ML-I-146.*

^{1}H NMR (500 MHz) ($CDCl_3$) δ: 2.65 (s, 3H), 7.146-7.153 (m, 1H), 7.28-7.32 (m, 1H), 7.44-7.50 (m, 3H), 7.53-7.59 (m, 2H), 7.96-7.99 (m, 2H), 8.17-8.20 (m, 1H). ^{13}C NMR (125 MHz) ($CDCl_3$) δ: 29.6, 115.9, 117.7, 123.0, 124.5, 127.4, 127.8, 128.5, 128.9, 133.9, 138.4, 139.0, 140.0, 191.6. IR (KBr, pellet): 1678, 1448, 1364, 1184, 1143 cm^{-1}. HRMS (ESI): m/z calcd for $C_{16}H_{14}NO_3S$ $[M+H]^+$, 300.0694; found 300.0682. m.p. 68-72 °C.

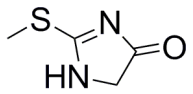

I-33

2-(methylthio)-1H-imidazol-4(5H)-one (I-33). Procedure adopted from Dr. Rahman Saleem (Tepe lab). To a flame dried flask was added 2-Thiohydantoin (3.00 g, 25.83 mmol), iodomethane (6.4 mL, 103 mmol), DIPEA (9.0 mL, 52 mmol) and DMAP (0.31g, 2.58 mmol) to dry CH_2Cl_2 (20 mL). After 2.5 h the reaction mixture was concentrated, purified on silica (100% EtOAc) affording compound **I-33** (solid, 3.57 g, 94%).

^{1}H NMR spectrum shows multiple peaks due to resonance forms. ^{1}H NMR (500 MHz) (CD_3OD) δ: 2.84 (s, 3H), 4.51 (s, 2H), 6.63 (broad N-H, 1H). ^{13}C NMR (125 MHz) (CD_3OD) δ: 14.3, 52.6, 172.9, 178.3. IR (KBr, pellet): 3091, 2915, 1754, 1669, 1511, 1444, 1389, 1330, 1291, 1251, 1230, 1173 cm^{-1}. HRMS (ESI): m/z calcd for $C_4H_7N_2OS$ $[M+H]^+$, 131.0279; found, 131.0284. m.p. decomposed over 160℃.

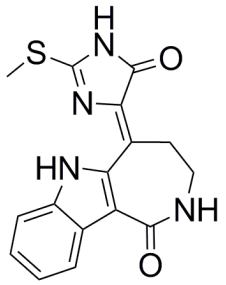

I-34

(Z)-5-(2-(methylthio)-5-oxo-1H-imidazol-4(5H)-ylidene)-2,3,4,5-tetrahydroazepino[4,3-b]indol-1(6H)-one (I-34). To a flame dried flask under N_2, a 1 M $TiCl_4$ in CH_2Cl_2 solution (23 mL, 23.0 mmol) was added to dry THF (100 mL) at 0℃. Thereafter *iso*-indoloaldisine **I-9** (1.20 g, 5.6 mmol) and **I-33** (1.46 g, 11.2 mmol) were consecutively added to the reaction flask at 0℃ and sti rred for 3 h. Thereafter, pyridine (3.6 mL, 44.8 mmol) was added portion-wise over a period of 2.5 h, and during this time the reaction was allowed to warm to room temperature. After an additional 24 h, the reaction was quenched with sat. NH_4Cl (100 mL) and stirred briefly. The mixture was filtered and the precipitate was isolated as product **I-34**. The remaining filtrate was subsequently extracted with EtOAc (3 x 150 mL). The combined organics were washed with brine (1 x 100 mL), H_2O (1 x 100 mL) and then dried with Na_2SO_4. The organic solvent was then removed *in vacuo*, leaving a solid which was rinsed with methanol, hexanes and ethyl acetate. The initial precipitate and washed solid were combined to afford compound **I-34** (brown solid, 1.17 g, 64% yield from **I-9**) which was used without further purification. *Notebook reference: ML-II-28.*

^{1}H NMR (500 MHz) (DMSO-d_6) δ: 2.76 (s, 3H), 3.27-3.30 (m, 2H), 3.44-3.46 (m, 2H), 7.09-7.15 (m, 1H), 7.23-7.26 (m, 1H), 7.57 (d, J = 8.2 Hz, 1H), 7.95 (bt, J = 5.1 Hz,

1 N-H), 8.23 (d, J = 8.2 Hz, 1H), 12.13 (bs, 1 N-H), 12.43 (bs, 1 N-H). ^{13}C NMR (125 MHz) (DMSO-d_6) δ: 12.5, 29.7, 38.7, 112.0, 113.1, 121.0, 122.7, 124.5, 127.9, 129.3, 134.6, 135.5, 136.3, 162.6, 166.5, 169.5. IR (KBr, pellet): 3418, 3194, 3056, 1691, 1621, 1587, 1508 cm^{-1}. HRMS (ESI): m/z calcd for $C_{16}H_{15}N_4O_2S$ $[M+H]^+$, 327.0916; found, 327.0923. m.p. decomposed over 250 ℃.

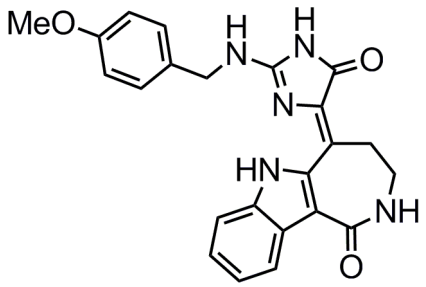

I-35

(Z)-5-(2-((4-methoxybenzyl)amino)-5-oxo-1H-imidazol-4(5H)-ylidene)-2,3,4,5-tetrahydroazepino[4,3-b]indol-1(6H)-one (I-35). To an oven dried 35 mL sealed tube was added **I-34** (0.106 g, 0.33 mmol), 4-methoxybenzylamine (1.06 mL, 8.12 mmol) and ethanol (10 mL) subsequently. The sealed tube reacted for 24 h at 110 ℃ (behind a blast shield). The mixture was allowed to cool and was concentrated *in vacuo*. The crude material was purified via flash chromatography (silica, 5:95 methanol/DCM to 1:9 methanol//DCM). The fractions were crystallized from 1:9 methanol/DCM affording **I-35** (yellow solid, 0.022 g, 16% yield from **I-34**). *Notebook reference: ML-II-33*

^{1}H NMR (500 MHz) (DMSO-d_6) δ: 3.21-3.24 (m, 2H), 3.38 (bs, 2H), 3.68 (s, 3H), 4.54 (bs, 2H), 6.90-6.92 (m, 2H), 7.07 (ddd, J = 1.0 Hz, J = 7.0 Hz, J = 8.1 Hz, 1H), 7.20 (ddd, J = 1.2 Hz, J =7.0 Hz, J = 8.1 Hz, 1H), 7.38-7.47 (m, 3H), 7.72 (t, J = 5.5 Hz, 1H), 8.23 (d, J = 7.9 Hz, 2H), 11.17 (N-H), 12.91 (N-H). ^{13}C NMR (150 MHz) (DMSO-d_6) δ:

31.8, 43.2, 47.3, 58.1, 113.1, 114.3, 116.9, 123.0, 123.6, 125.4, 126.5, 131.4, 131.7, 134.0, 138.4, 139.5, 141.3, 159.0, 161.5, 170.1, 173.1. IR (KBr, pellet): 3277, 3220, 3177, 3057, 2961, 2836, 1721, 1648, 1610, 1569, 1511, 1484, 1420, 1247 cm^{-1}. HRMS (ESI): m/z calcd for $C_{23}H_{22}N_5O_3$ $[M+H]^+$, 416.1723; found, 416.1705. m.p. decomposed 280-282 °C.

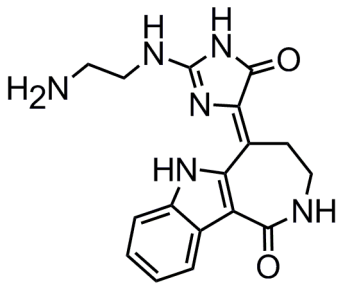

I-36

(Z)-5-(2-((2-aminoethyl)amino)-5-oxo-1H-imidazol-4(5H)-ylidene)-2,3,4,5-tetrahydroazepino[4,3-b]indol-1(6H)-one (I-36). To a flame dried sealed tube and stir bar containing ethanol (10 mL) was added **I-34** (0.150 g, 0.460 mmol) and ethylenediamine (0.77 mL, 11.50 mmol) subsequently. The sealed tube was heated to 115 °C (behind a blast shield) and reacted for 20 h. Thereafter the mixture was cooled to room temperature and the resulting precipitate was filtered off (an impurity). The filtrate was concentrated *in vacuo*, and to the crude mixture was added ethanol (20 mL). This mixture was heated to boiling and placed in the freezer. The fine yellow precipitate collected was **I-36**. A second batch of precipitate was collected affording **I-36** (yellow solid, 0.021 g, 13% yield from **I-34**). *Notebook reference: ML-II-37*

^{1}H NMR (500 MHz) (DMSO-d_6) δ: 2.47 (bs, 3 N-H), 2.71 (t, J = 6.1 Hz, 2H), 3.23-3.26 (m, 2H), 3.41-3.44 (m, 2H), 3.55 (t, J = 6.2 Hz, 2H), 7.08 (ddd, J = 1.1 Hz, J = 7.0

Hz, J = 8.1 Hz, 1H), 7.20 (ddd, J = 1.2 Hz, J = 7.0 Hz, J = 8.2 Hz, 1H), 7.38 (d, J = 8.1 Hz, 1H), 7.75 (bt, J = 5.6 Hz, 1 N-H), 8.25 (d, J = 8.1 Hz, 1H), 13.12 (bs, 1 N-H). ^{13}C NMR (125 MHz) (DMSO-d_6) δ: 29.0, 40.3, 42.2, 44.8, 110.1, 110.8, 119.8, 120.5, 122.4, 123.5, 128.4, 135.3, 136.1, 138.4, 157.9, 167.0, 168.2. IR (KBr, pellet): 3362, 3295, 3142, 2862, 1700, 1675, 1605, 1556, 1484, 1448, 1333, 1249, 1170 cm^{-1}. HRMS (ESI): m/z calcd for $C_{17}H_{19}N_6O_2$ $[M+H]^+$, 339.1569; found, 339.1584. m.p. decomposed 258-260 °C.

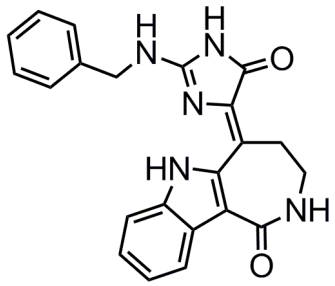

I-37

(Z)-5-(2-(benzylamino)-4-oxo-1H-imidazol-5(4H)-ylidene)-2,3,4,5-tetrahydroazepino[4,3-b]indol-1(6H)-one (I-37).[15] To a 35 mL oven-dried tube and stir bar was added **I-34** (0.244 g, 0.778 mmol), benzylamine (2.2 mL, 19.45 mmol) and ethanol (20 mL) subsequently. The tube was sealed and reacted at 120 °C for 22 h (behind a blast shield). The reaction mixture was allowed to cool and the reaction precipitate was collected and washed with ethanol affording benzylated *iso*-indoloazepine **I-37** (solid, 0.106 g, 37% yield from **I-34**). *Notebook reference: ML-II-30*

^{1}H NMR (500 MHz) (DMSO-d_6) δ: 3.21-3.23 (m, 2H), 3.35-3.40 (m, 2H), 4.62 (s, 2H), 7.06 (t, J = 7.6 Hz, 1H), 7.18-7.25 (m, 2H), 7.36 (t, J = 7.7 Hz, 2H), 7.43-7.47 (m,

3H (contains 2 broad N-H)), 7.75 (t, J = 5.4 Hz, 1H), 8.22 (d, J = 8.1 Hz, 1H), 8.36 (bs, 1 N-H), 11.20 (bs, 1 N-H), 12.90 (bs, 1 N-H). ^{13}C NMR (150 MHz) (DMSO-d_6) at 85°C δ: 28.5, 39.1, 44.6, 109.9, 110.5, 119.8, 120.0, 122.1, 122.8, 126.6, 126.8, 128.0, 128.1, 135.1, 136.0, 137.8, 138.5, 156.1, 166.6, 169.5. IR (KBr, pellet): 3392, 3275, 1714, 1650, 1607, 1581, 1543, 1509, 1478 cm^{-1}. HRMS (ESI): m/z calcd for $C_{22}H_{20}N_5O_2$ $[M+H]^+$, 386.1617; found 386.1604. m.p. decomposed 275-280 $^{\circ}$C.

Q. Spectra

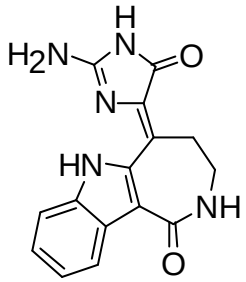
H
N
H_2N
O
N
HN
NH
O

I-6

13.0
11.5
10.0
8.5
7.0
5.5
4.0
2.5
1.0
190
170
150
130
110
90
80
70
60
50
40
30
20
10
0

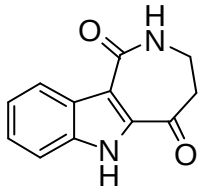
O
H
N
N
H
O

I-9

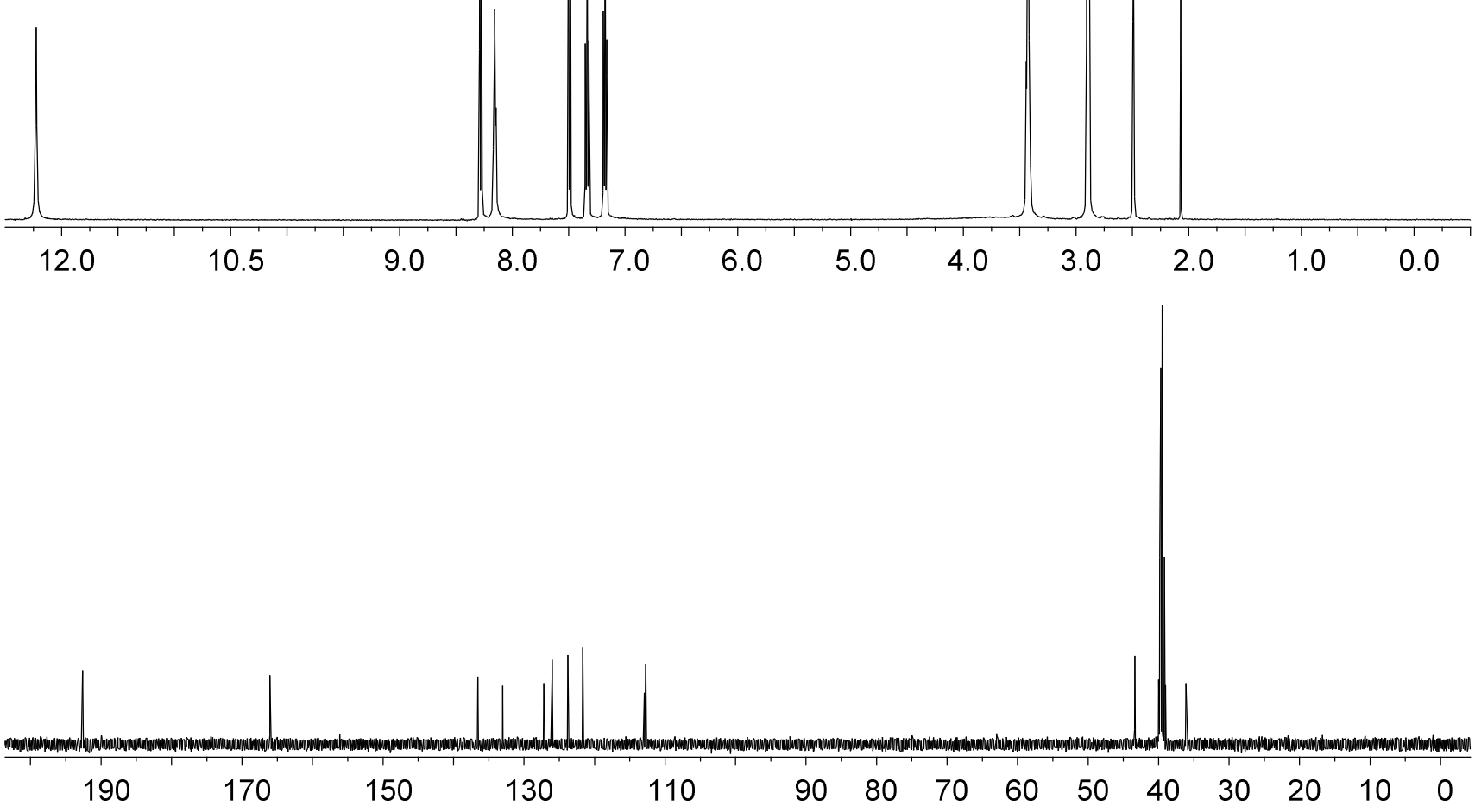
12.0
10.5
9.0
8.0
7.0
6.0
5.0
4.0
3.0
2.0
1.0
0.0
190
170
150
130
110
90
80
70
60
50
40
30
20
10
0

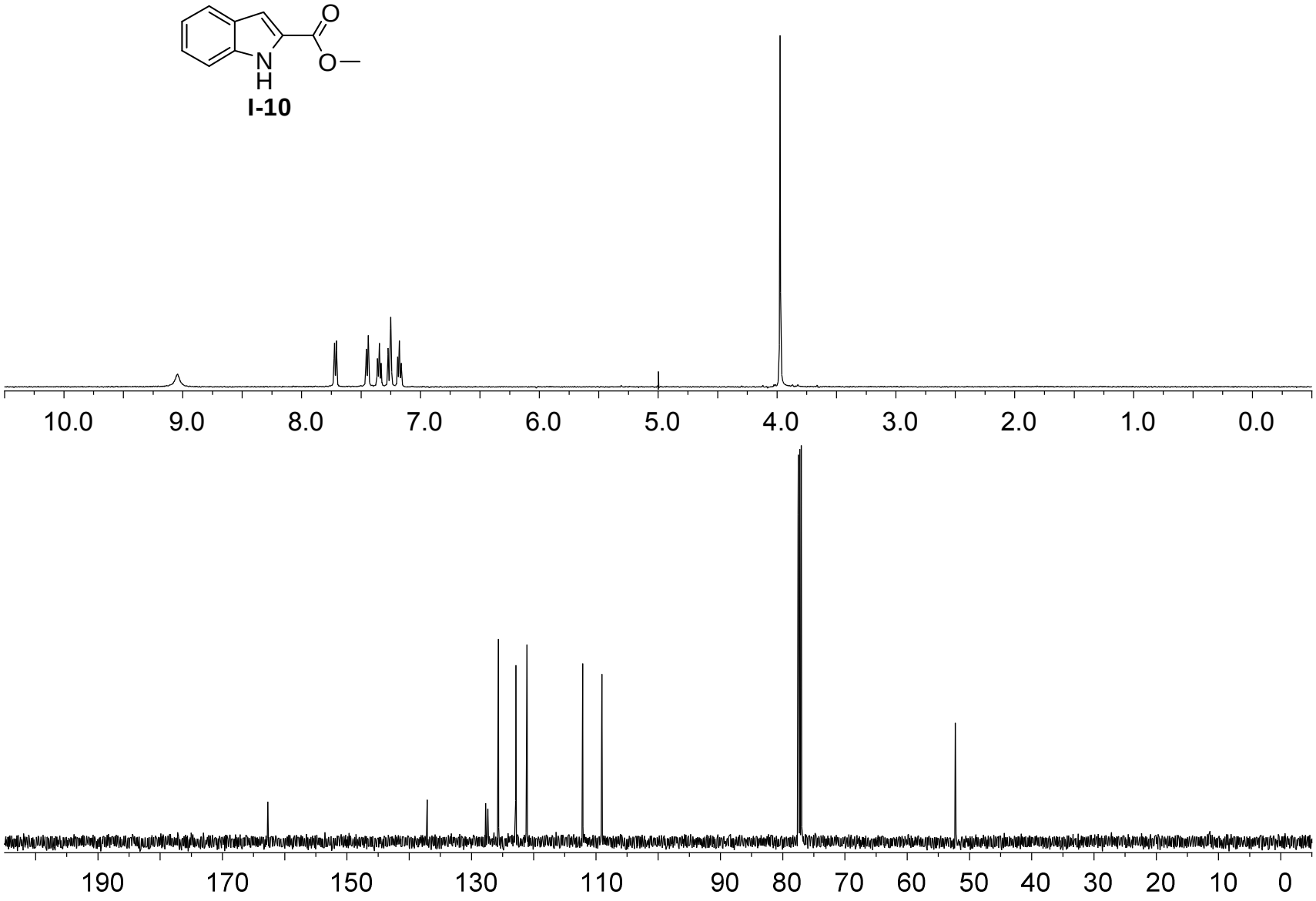
O
O
N
H
10.0
9.0
8.0
7.0
6.0
5.0
4.0
3.0
2.0
1.0
0.0
190
170
150
130
110
90
80
70
60
50
40
30
20
10
0

I-10

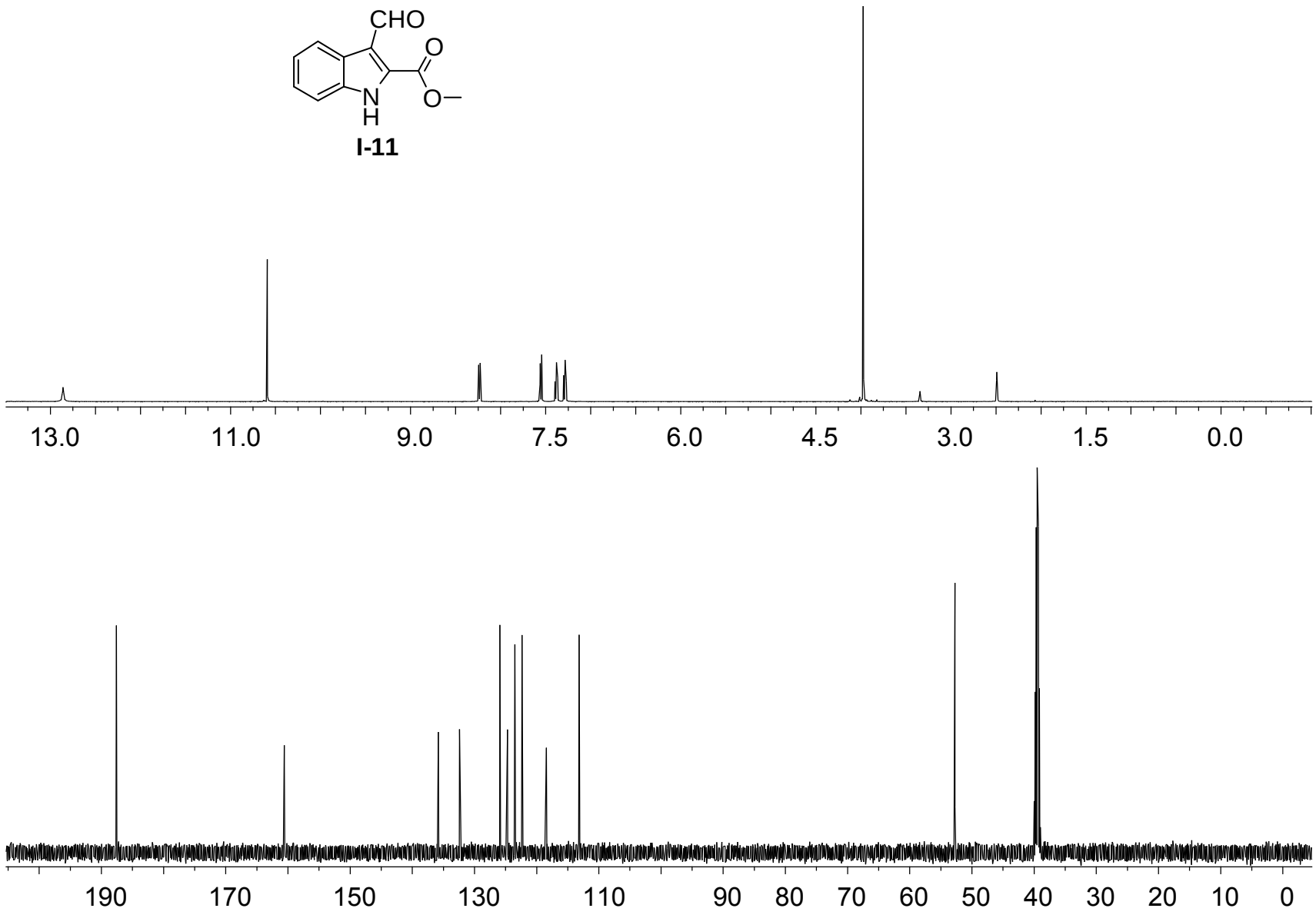
CHO
O
O—
N
H
13.0
11.0
9.0
7.5
6.0
4.5
3.0
1.5
0.0
190
170
150
130
110
90
80
70
60
50
40
30
20
10
0

I-11

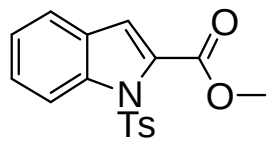
O
N
O
Ts

I-12

10.0
9.0
8.0
7.0
6.0
5.0
4.0
3.0
2.0
1.0
0.0

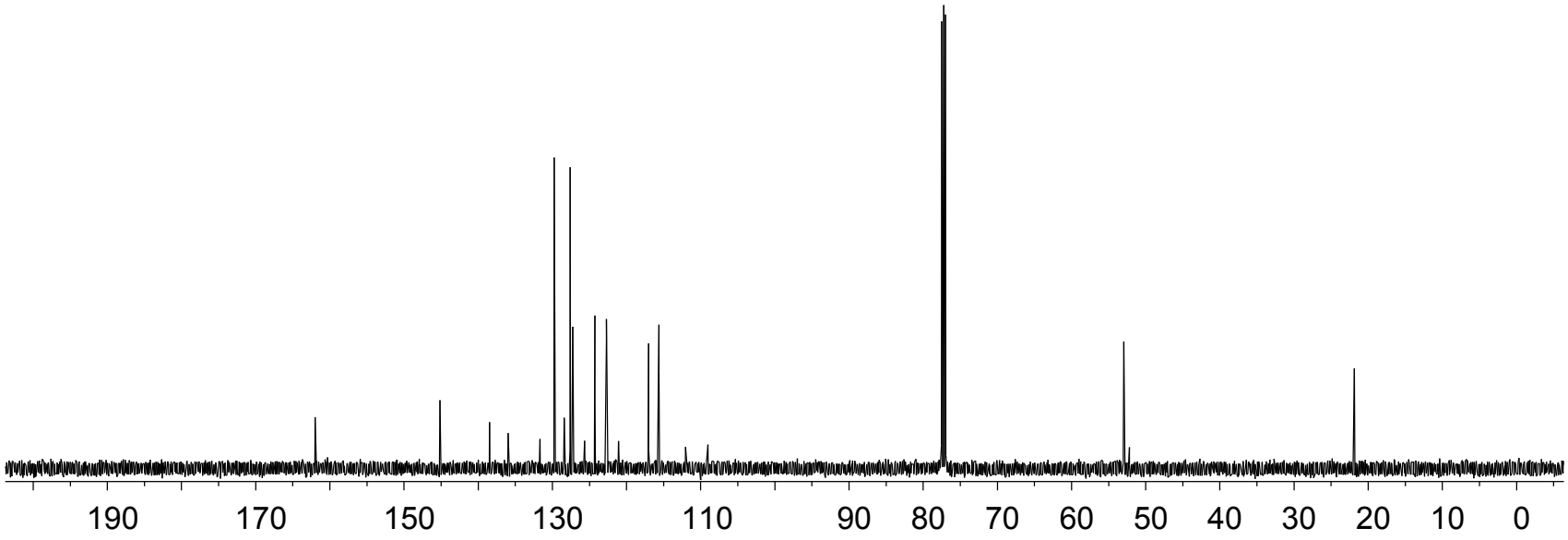
190
170
150
130
110
90
80
70
60
50
40
30
20
10
0

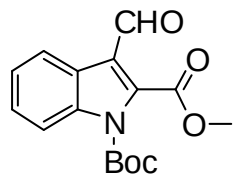
CHO
O
N
O
Boc

I-13

11.0
10.0
9.0
8.0
7.0
6.0
5.0
4.0
3.0
2.0
1.0
0.0

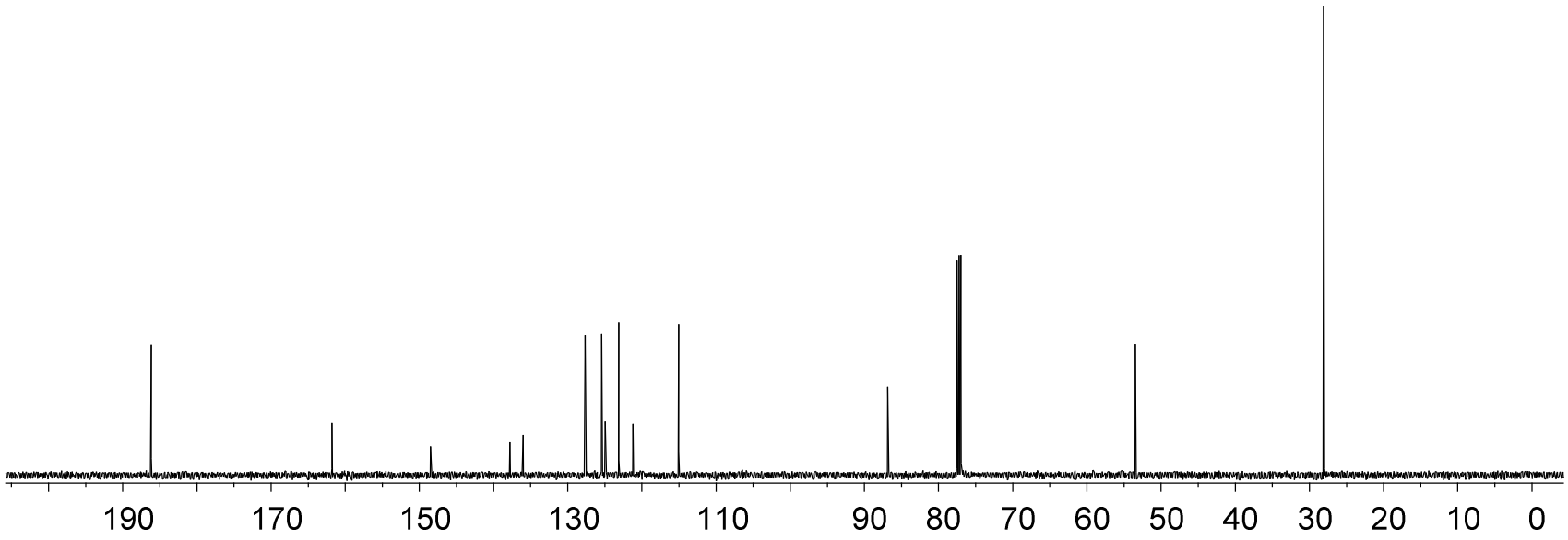
190
170
150
130
110
90
80
70
60
50
40
30
20
10
0

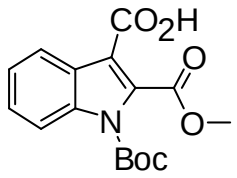
CO2H
O
O—
N
Boc

I-14

10.0
9.0
8.0
7.0
6.0
5.0
4.0
3.0
2.0
1.0
0.0
190
170
150
130
110
90
80
70
60
50
40
30
20
10
0

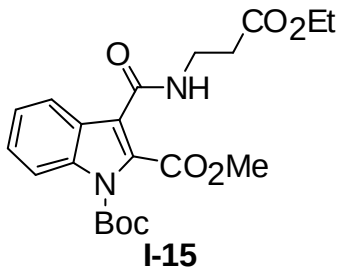
CO2Et
O
NH
CO2Me
N
Boc

I-15

10.0
9.0
8.0
7.0
6.0
5.0
4.0
3.0
2.0
1.0
0.0
190
170
150
130
110
90
80
70
60
50
40
30
20
10
0

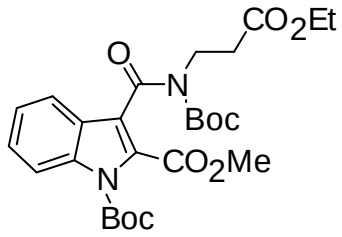
CO2Et
O
N
Boc
CO2Me
N
Boc

I-16

10.0
9.0
8.0
7.0
6.0
5.0
4.0
3.0
2.0
1.0
0.0

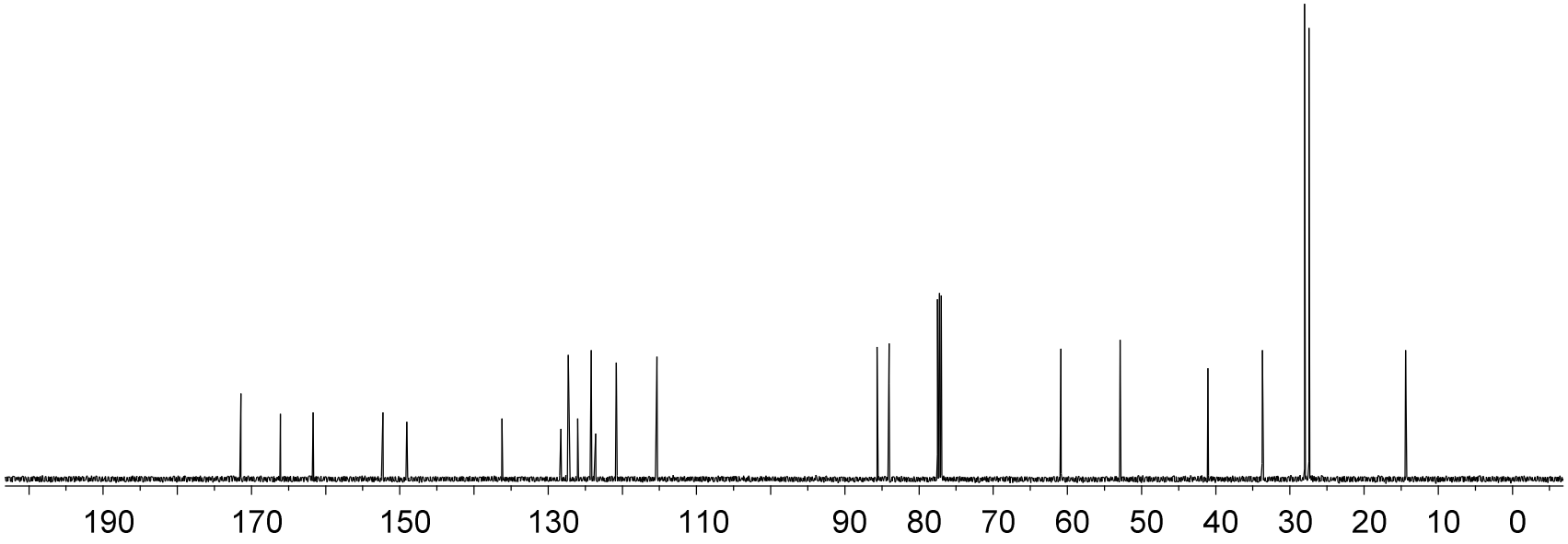
190
170
150
130
110
90
80
70
60
50
40
30
20
10
0

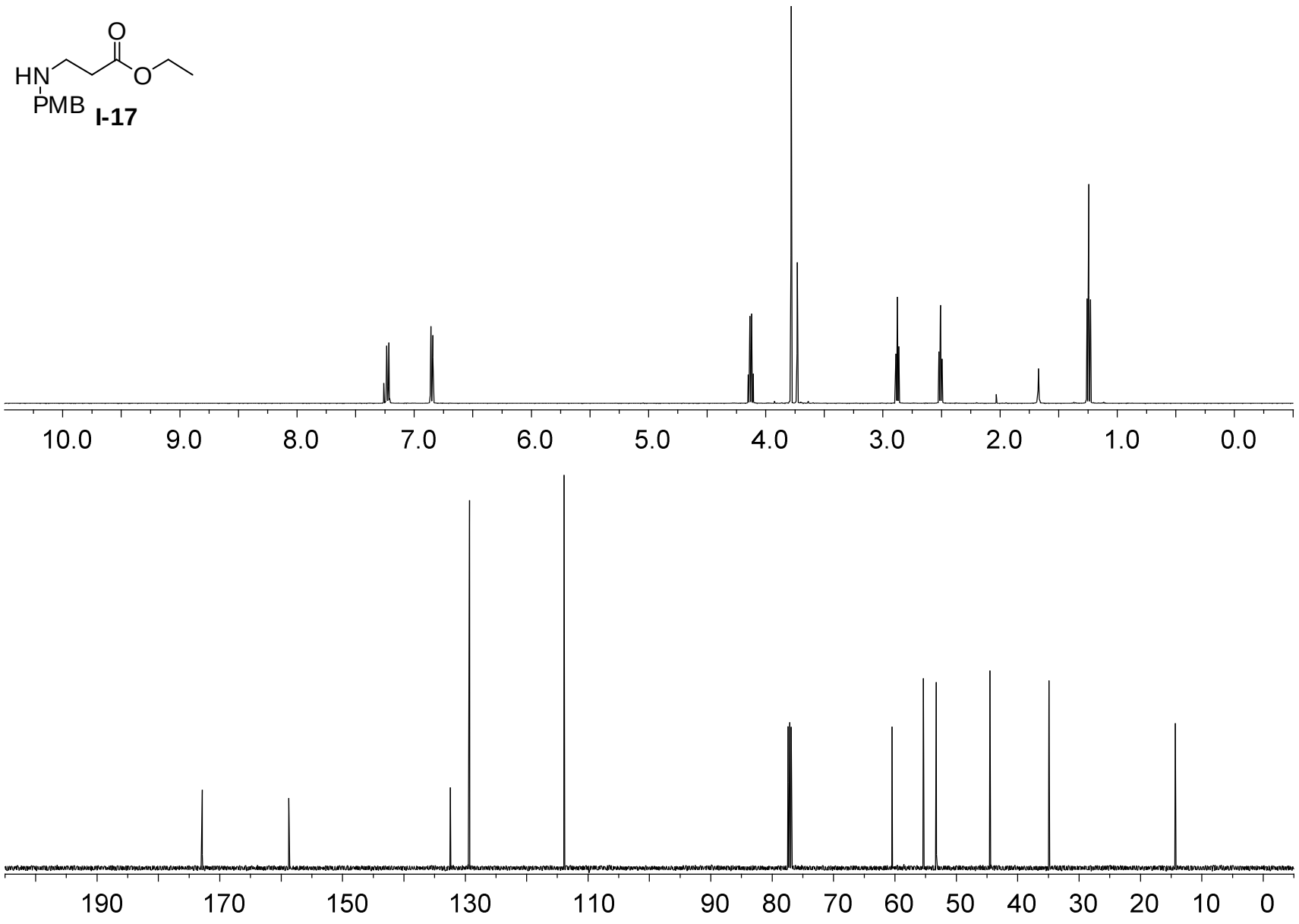
O
HN
PMB
O
10.0
9.0
8.0
7.0
6.0
5.0
4.0
3.0
2.0
1.0
0.0
190
170
150
130
110
90
80
70
60
50
40
30
20
10
0

I-17

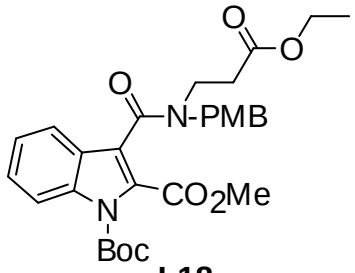
O
O
O
N-PMB
CO2Me
N
Boc

I-18

10.0
9.0
8.0
7.0
6.0
5.0
4.0
3.0
2.0
1.0
0.0
190
170
150
130
110
90
80
70
60
50
40
30
20
10
0

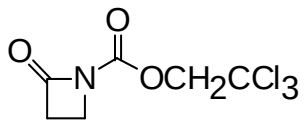
O
O
N
OCH2CCl3

I-19

10.0
9.0
8.0
7.0
6.0
5.0
4.0
3.0
2.0
1.0
0.0
190
170
150
130
110
90
80
70
60
50
40
30
20
10
0

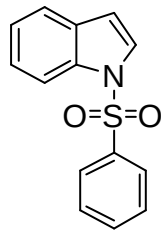
N
O=S=O

I-20

10.0
9.0
8.0
7.0
6.0
5.0
4.0
3.0
2.0
1.0
0.0
190
170
150
130
110
90
80
70
60
50
40
30
20
10
0

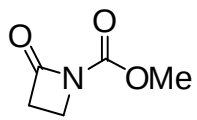
O
O
N
OMe

I-21

10.0
9.0
8.0
7.0
6.0
5.0
4.0
3.0
2.0
1.0
0.0

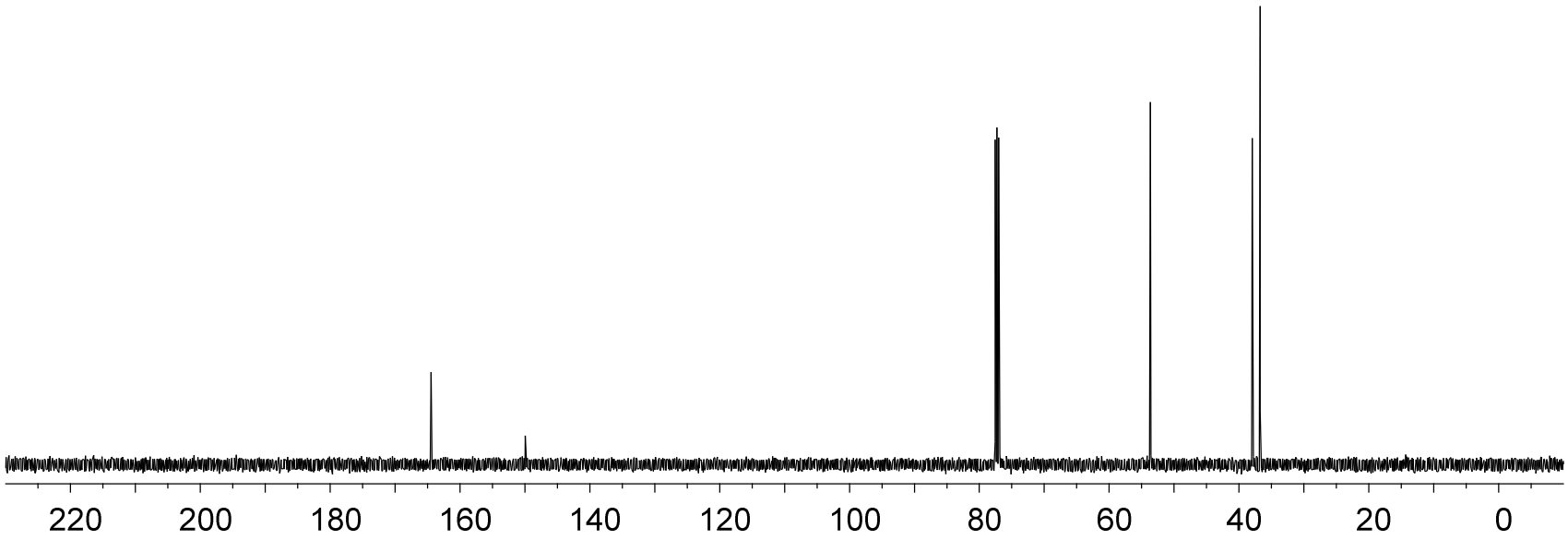
220
200
180
160
140
120
100
80
60
40
20
0

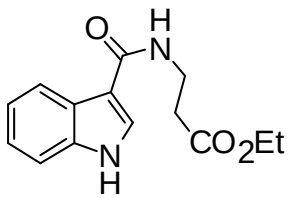
O
H
N
CO2Et
N
H

I-22

10.0
9.0
8.0
7.0
6.0
5.0
4.0
3.0
2.0
1.0

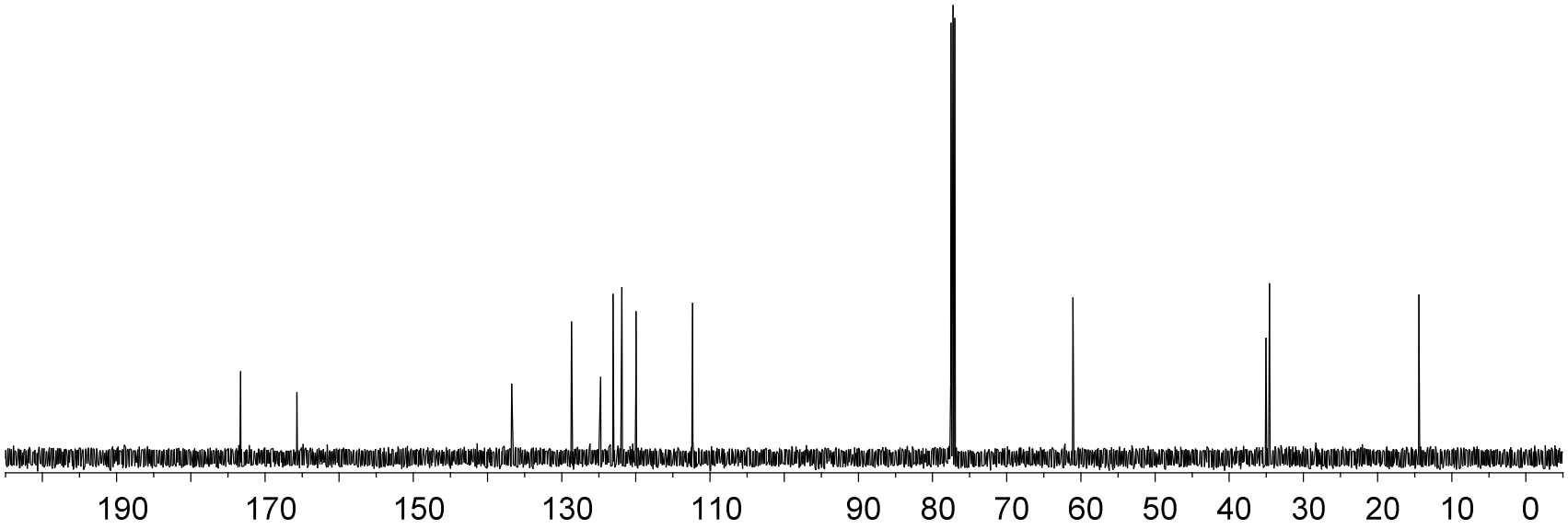
190
170
150
130
110
90
80
70
60
50
40
30
20
10
0

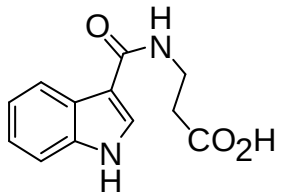
O
H
N
CO2H
N
H

I-23

11.0
10.0
9.0
8.0
7.0
6.0
5.0
4.0
3.0
2.0
1.0
0.0
210
190
170
150
130
110
90
80
70
60
50
40
30
20
10
0

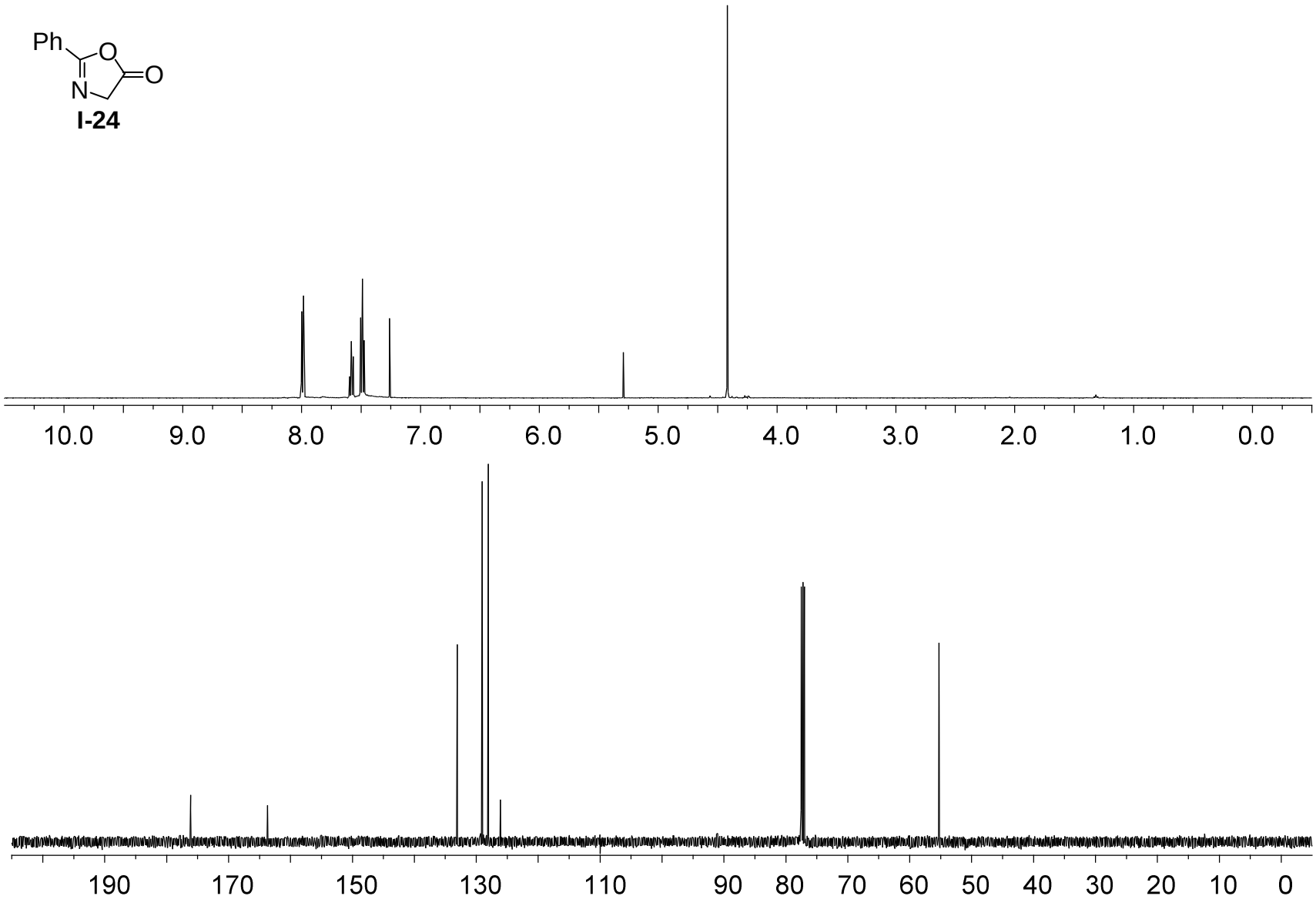
Ph
O
N
O
10.0
9.0
8.0
7.0
6.0
5.0
4.0
3.0
2.0
1.0
0.0
190
170
150
130
110
90
80
70
60
50
40
30
20
10
0

I-24

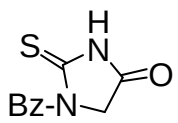
H
N
S
O
Bz-N

I-25

12.5
11.0
9.5
8.5
7.5
6.5
5.5
4.5
3.5
2.5
1.5
0.5
190
170
150
130
110
90
80
70
60
50
40
30
20
10
0

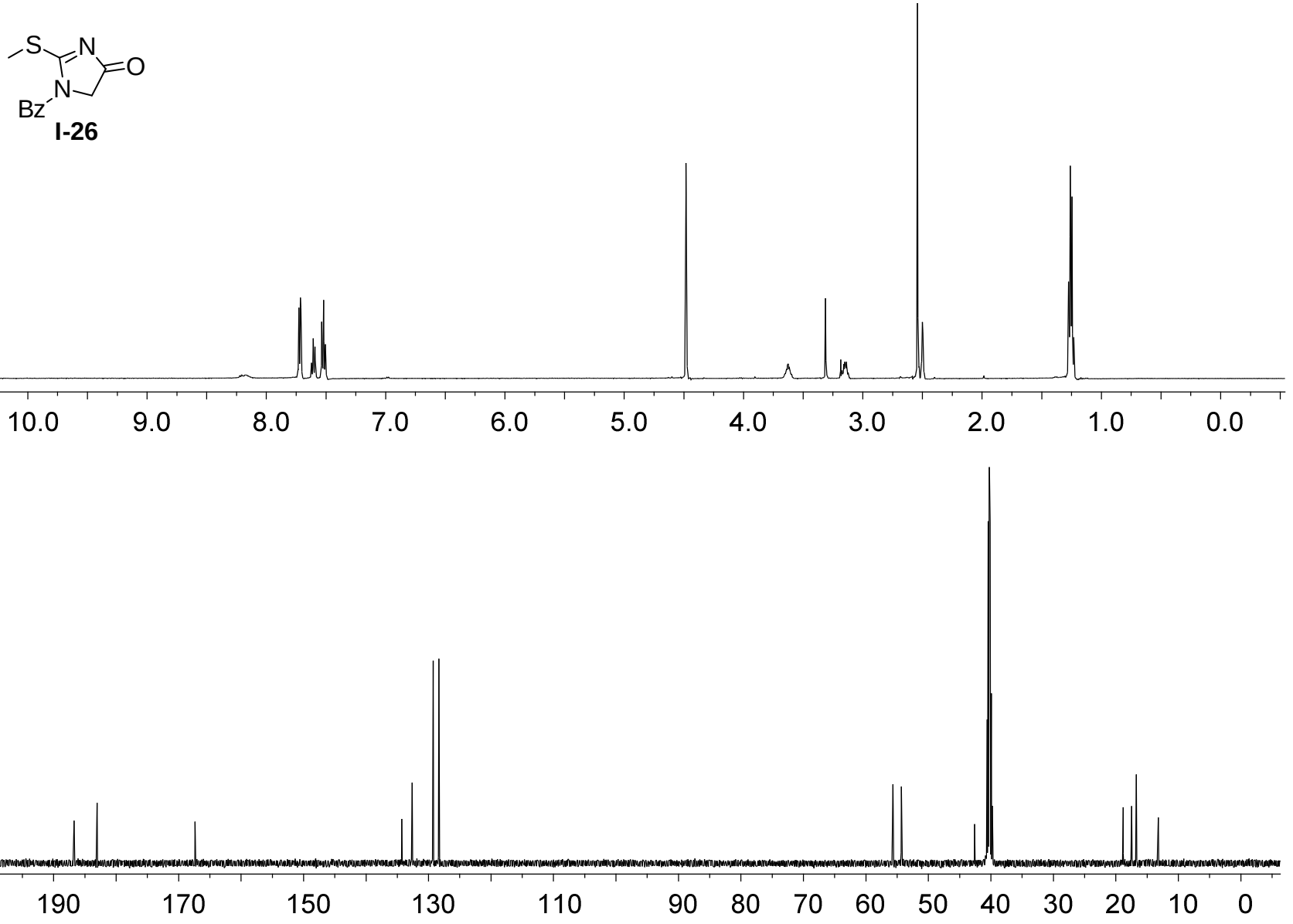
S
N
O
N
Bz
10.0
9.0
8.0
7.0
6.0
5.0
4.0
3.0
2.0
1.0
0.0
190
170
150
130
110
90
80
70
60
50
40
30
20
10
0

I-26

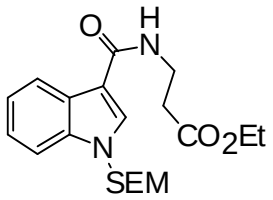
O
H
N
CO2Et
N
SEM

I-27

10.0
9.0
8.0
7.0
6.0
5.0
4.0
3.0
2.0
1.0
0.0
190
170
150
130
110
90
80
70
60
50
40
30
20
10
0

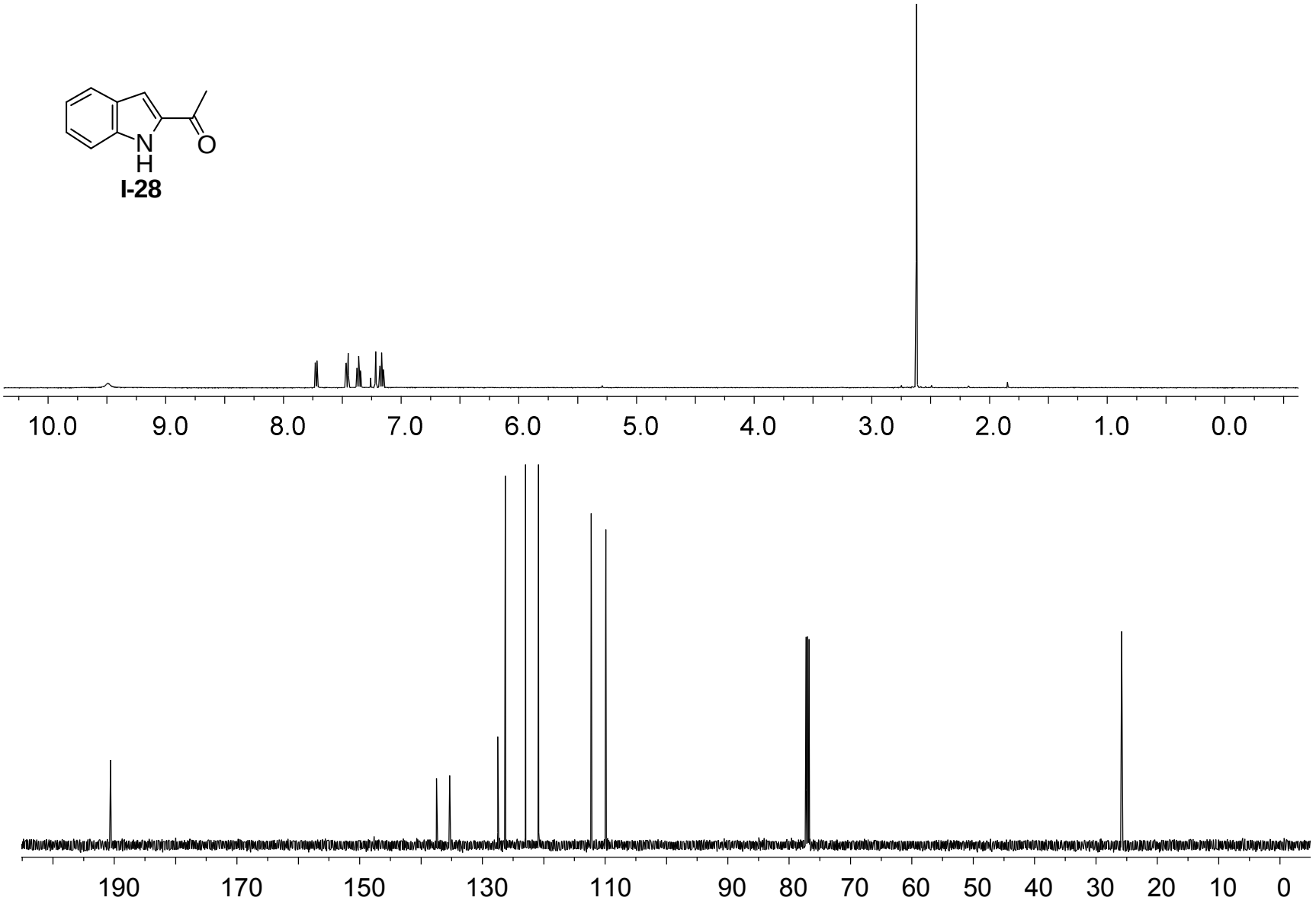
N
H
O
10.0
9.0
8.0
7.0
6.0
5.0
4.0
3.0
2.0
1.0
0.0
190
170
150
130
110
90
80
70
60
50
40
30
20
10
0

I-28

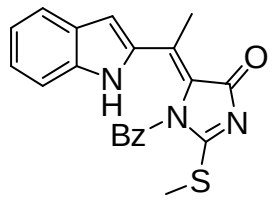
O
N
H
Bz
N
N
S

I-29

11.0
10.0
9.0
8.0
7.0
6.0
5.0
4.0
3.0
2.0
1.0
0.0

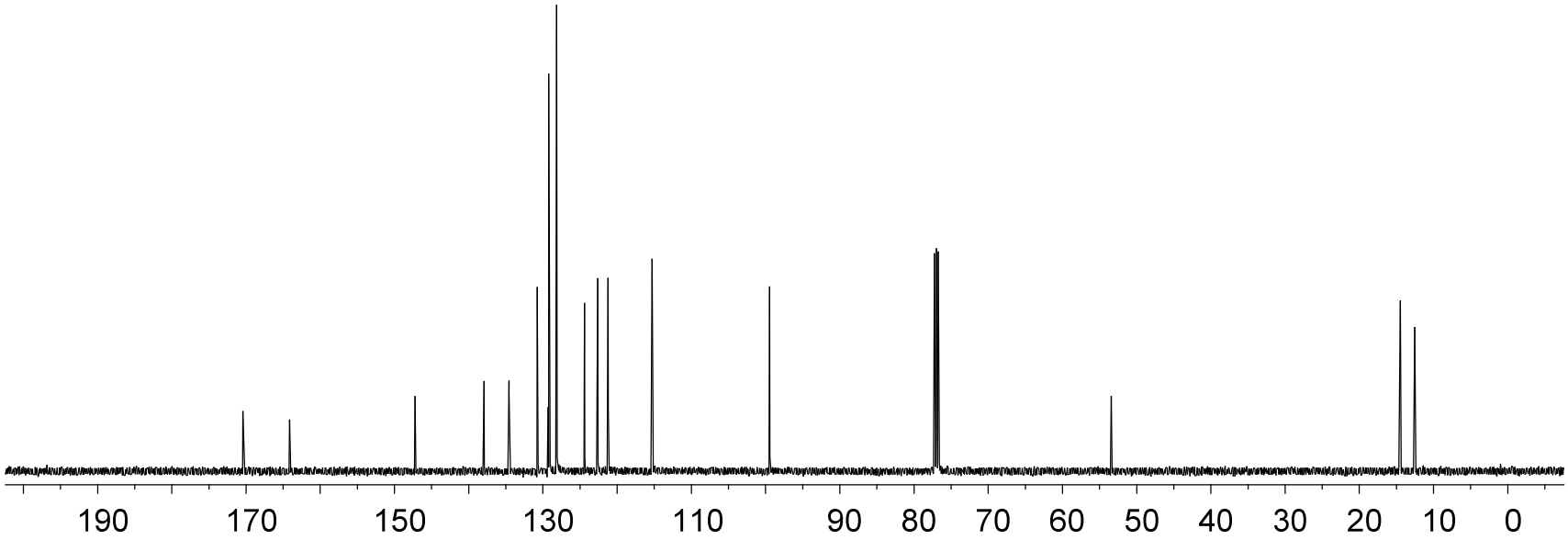
190
170
150
130
110
90
80
70
60
50
40
30
20
10
0

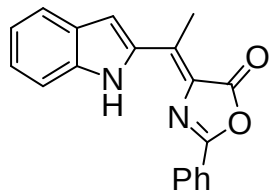
O
N
H
N
O
Ph

I-30

12.0
10.5
9.0
8.0
7.0
6.0
5.0
4.0
3.0
2.0
1.0
0.0
190
170
150
130
110
90
80
70
60
50
40
30
20
10
0

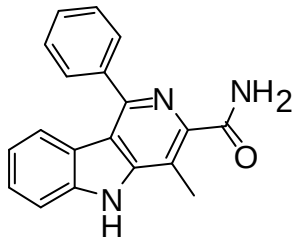
N
NH2
O
N
H

I-31

12.0
10.5
9.0
8.0
7.0
6.0
5.0
4.0
3.0
2.0
1.0
0.0
190
170
150
130
110
90
80
70
60
50
40
30
20
10
0

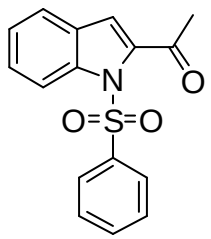
N
O
O=S=O

I-32

10.0
9.0
8.0
7.0
6.0
5.0
4.0
3.0
2.0
1.0
0.0

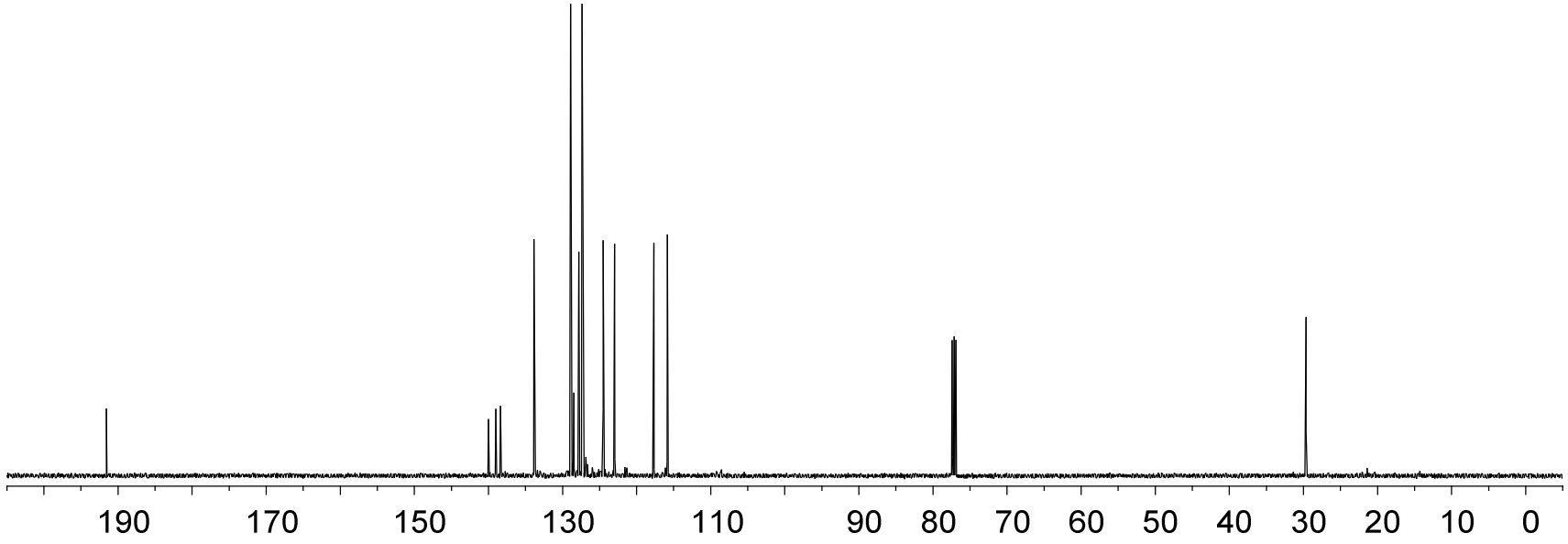
190
170
150
130
110
90
80
70
60
50
40
30
20
10
0

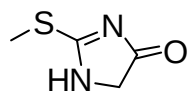
S
N
O
HN

I-33

9.5
9.0
8.5
8.0
7.5
7.0
6.5
6.0
5.5
5.0
4.5
4.0
3.5
3.0
2.5
2.0
1.5
1.0
0.5
0.0

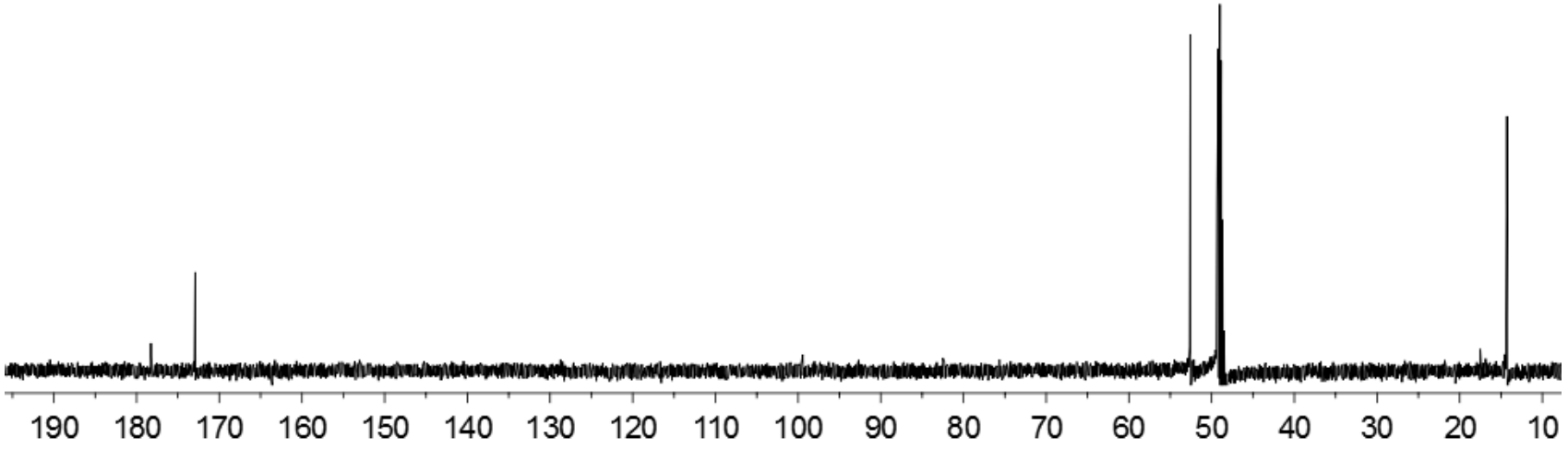
190
180
170
160
150
140
130
120
110
100
90
80
70
60
50
40
30
20
10

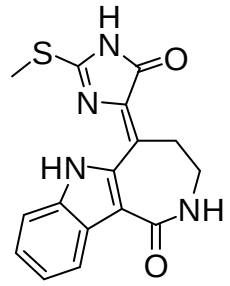
H
N
S
O
N
HN
NH
O

I-34

12.0
10.5
9.0
8.0
7.0
6.0
5.0
4.0
3.0
2.0
1.0
0.0
190
170
150
130
110
90
80
70
60
50
40
30
20
10
0

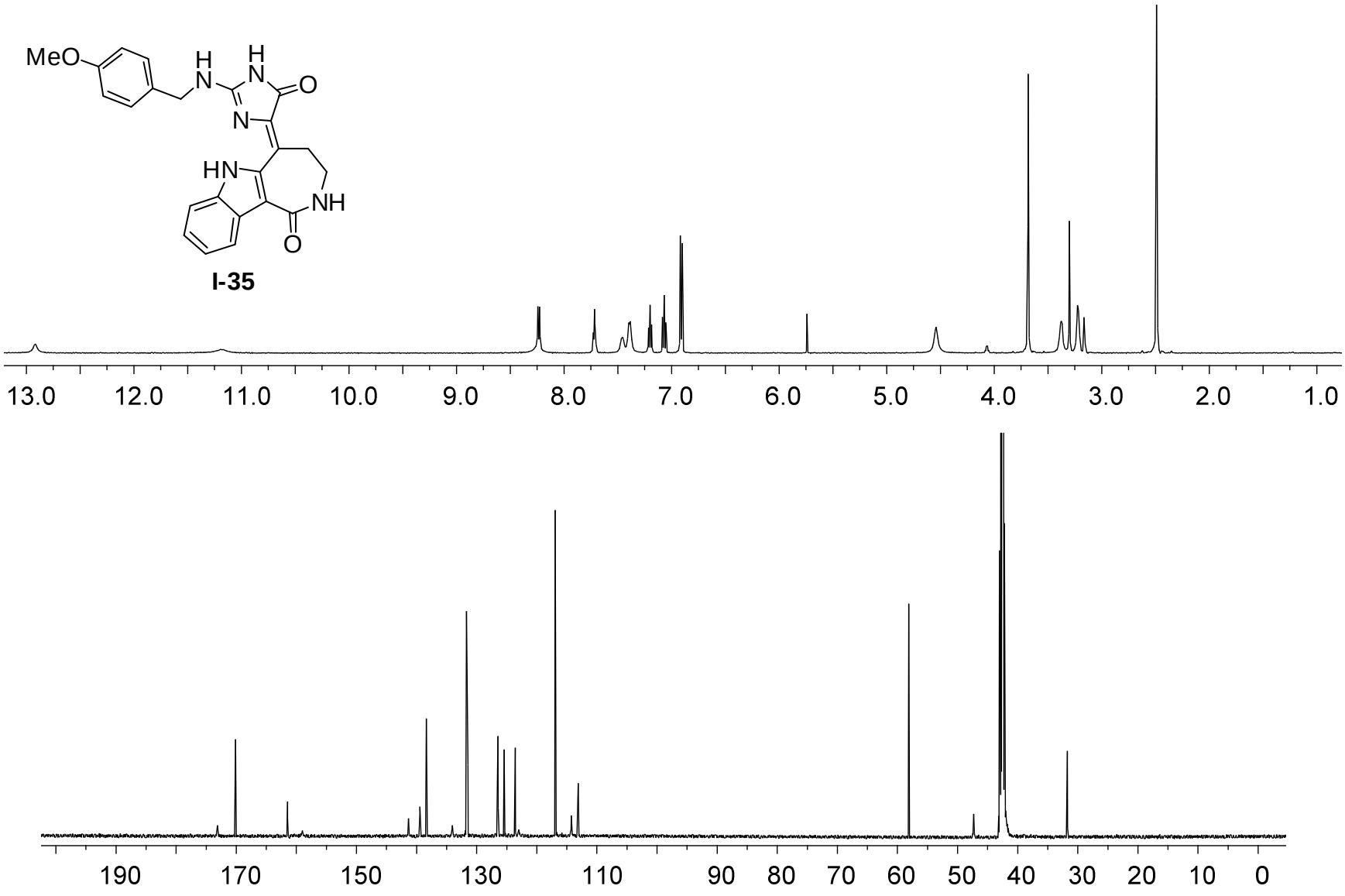
MeO
H
N
H
N
O
N
HN
NH
O
13.0
12.0
11.0
10.0
9.0
8.0
7.0
6.0
5.0
4.0
3.0
2.0
1.0
190
170
150
130
110
90
80
70
60
50
40
30
20
10
0

I-35

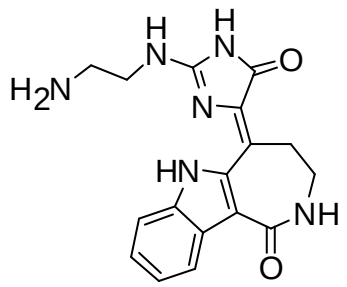
H
N
H
N
O
H_2N
N
HN
NH
O

I-36

12.5
11.0
9.5
8.0
6.5
5.0
3.5
2.0
0.5

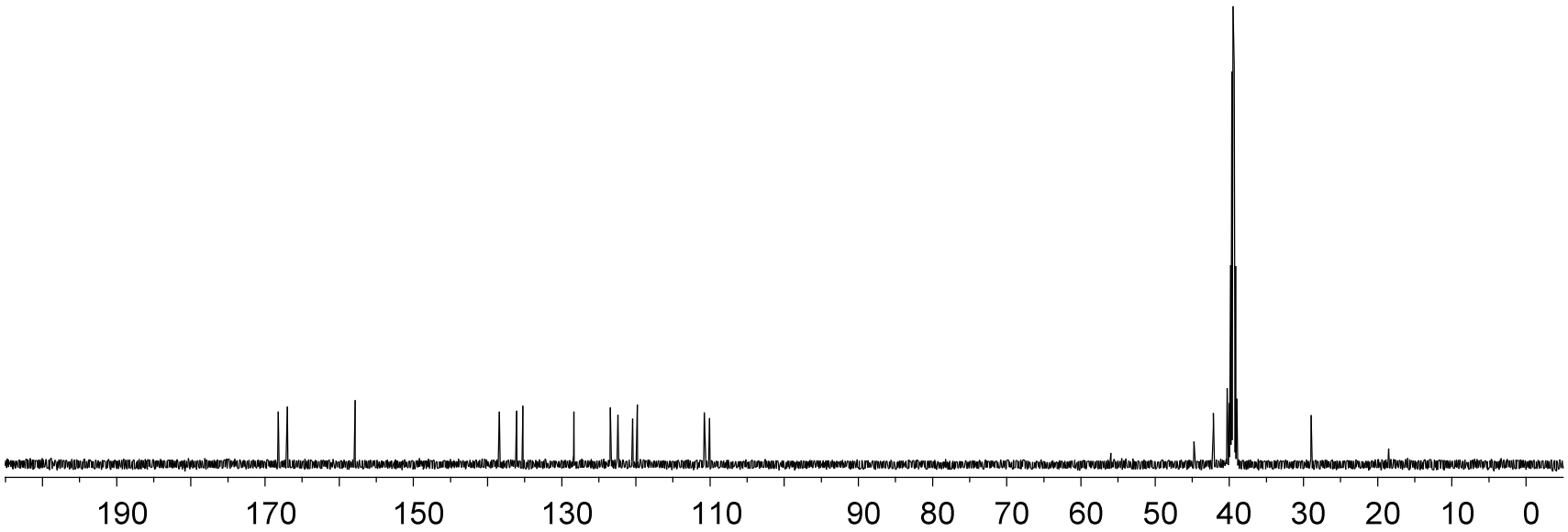
190
170
150
130
110
90
80
70
60
50
40
30
20
10
0

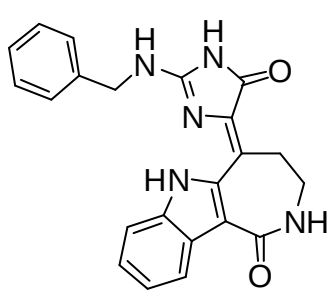
H
N
H
N
O
N
HN
NH
O

I-37

190
170
150
130
110
90
80
70
60
50
40
30
20
10
0
13.0
11.5
10.0
8.5
7.0
5.5
4.0
2.5
1.0

R. References

References

(1) Weinberg, R. A. *Scientific American* **1996**, *275*, 62-70.

(2) Tejada-Vera., J. X. K. D. K. S. L. M. a. B. In *National Vital Statistics Reports*; Statistics, D. o. V., Ed. 2010; Vol. 58, p 1-135.

(3) Group, U. S. C. S. W.; Atlanta: U.S. Department of Health and Human Services, Centers for Disease Control and Prevention and National Cancer Institute: 2010.

(4) Society, A. C.; Atlanta: American Cancer Society: 2010.

(5) Statistical Research and Applications Branch, N. C. I. **2009**.

(6) Institute, N. C. 2011.

(7) DiVall, M. V.; Cersosimo, R. J. *Formulary* **2007**, *42*, 378.

(8) Institute, N. C. 2010.

(9) Balosso, J. *Radiotherapy and Oncology* **2004**, *73*, S141-S143.

(10) Smith, J.; Tho, L. M.; Xu, N. H.; Gillespie, D. A. In *Advances in Cancer Research, Vol 108*; Elsevier Academic Press Inc: San Diego, 2010; Vol. 108, p 73-112.

(11) Sancar, A.; Lindsey-Boltz, L. A.; Unsal-Kacmaz, K.; Linn, S. *Annual Review of Biochemistry* **2004**, *73*, 39-85.

(12) Sharma, V.; Hupp, C. D.; Tepe, J. J. *Current Medicinal Chemistry* **2007**, *14*, 1061-1074.

(13) Abraham, R. T. *Genes & Development* **2001**, *15*, 2177-2196.

(14) Ahn, J. Y.; Schwarz, J. K.; Piwnica-Worms, H.; Canman, C. E. *Cancer Research* **2000**, *60*, 5934-5936.

(15) Oliver, A. W.; Paul, A.; Boxall, K. J.; Barrie, S. E.; Aherne, G. W.; Garrett, M. D.; Mittnacht, S.; Pearl, L. H. *Embo Journal* **2006**, *25*, 3179-3190.

(16) Ahn, J. Y.; Li, X. H.; Davis, H. L.; Canman, C. E. *Journal of Biological Chemistry* **2002**, *277*, 19389-19395.

(17) Takai, H.; Naka, K.; Okada, Y.; Watanabe, M.; Harada, N.; Saito, S.; Anderson, C. W.; Appella, E.; Nakanishi, M.; Suzuki, H.; Nagashima, K.; Sawa, H.; Ikeda, K.; Motoyama, N. *Embo Journal* **2002**, *21*, 5195-5205.

(18) Arienti, K. L.; Brunmark, A.; Axe, F. U.; McClure, K.; Lee, A.; Blevitt, J.; Neff, D. K.; Huang, L.; Crawford, S.; Pandit, C. R.; Karlsson, L.; Breitenbucher, J. G. *Journal of Medicinal Chemistry* **2004**, *48*, 1873-1885.

(19) Sausville, E. A.; Arbuck, S. G.; Messmann, R.; Headlee, D.; Bauer, K. S.; Lush, R. M.; Murgo, A.; Figg, W. D.; Lahusen, T.; Jaken, S.; Jing, X. X.; Roberge, M.; Fuse, E.; Kuwabara, T.; Senderowicz, A. M. *Journal of Clinical Oncology* **2001**, *19*, 2319-2333.

(20) Yu, Q.; La Rose, J.; Zhang, H.; Takemura, H.; Kohn, K. W.; Pommier, Y. *Cancer Research* **2002**, *62*, 5743-5748.

(21) Sharma, V.; Tepe, J. J. *Bioorganic & Medicinal Chemistry Letters* **2004**, *14*, 4319-4321.

(22) Sharma, G. M.; Buyer, J. S.; Pomerantz, M. W. *Journal of the Chemical Society-Chemical Communications* **1980**, 435-436.

(23) Curman, D.; Cinel, B.; Williams, D. E.; Rundle, N.; Block, W. D.; Goodarzi, A. A.; Hutchins, J. R.; Clarke, P. R.; Zhou, B. B.; Lees-Miller, S. P.; Andersen, R. J.; Roberge, M. *Journal of Biological Chemistry* **2001**, *276*, 17914-17919.

(24) Annoura, H.; Tatsuoka, T. *Tetrahedron Letters* **1995**, *36*, 413-416.

(25) Sosa, A. C. B.; Yakushijin, K.; Horne, D. A. *Journal of Organic Chemistry* **2000**, *65*, 610-611.

(26) Sharma, V.; Lansdell, T. A.; Jin, G.; Tepe, J. J. *Journal of Medicinal Chemistry* **2004**, *47*, 3700-3703.

(27) Kuhnel, E.; Laffan, D. D. P.; Lloyd-Jones, G. C.; Martinez Del Campo, T.; Shepperson, I. R.; Slaughter, J. L. *Angew Chem Int Ed Engl* **2007**, *46*, 7075-8.

(28) Yamada, F.; Makita, Y.; Somei, M. *Heterocycles* **2007**, *72*, 599-620.

(29) Covarrubias-Zuniga, A.; Avila-Zarraga, J. G.; Salas, D. A. *Synthetic Communications* **2003**, *33*, 3173-3181.

(30) Baron, B. M.; Cregge, R. J.; Farr, R. A.; Friedrich, D.; Gross, R. S.; Harrison, B. L.; Janowick, D. A.; Matthews, D.; McCloskey, T. C.; Meikrantz, S.; Nyce, P. L.; Vaz, R.; Metz, W. A. *Journal of Medicinal Chemistry* **2005**, *48*, 995-1018.

(31) Kainuma, M.; Makishima, M.; Hashimoto, Y.; Miyachi, H. *Bioorganic & Medicinal Chemistry* **2007**, *15*, 2587-2600.

(32) Chacun-Lefèvre, L.; Bénéteau, V.; Joseph, B.; Mérour, J.-Y. *Tetrahedron* **2002**, *58*, 10181-10188.

(33) Bit, R. A.; Davis, P. D.; Hill, C. H.; Keech, E.; Vesey, D. R. *Tetrahedron* **1991**, *47*, 4645-4664.

(34) Adediran, S. A.; Cabaret, D.; Flavell, R. R.; Sammons, J. A.; Wakselman, M.; Pratt, R. F. *Bioorganic & Medicinal Chemistry* **2006**, *14*, 7023-7033.

(35) Smith, G. F. *Journal of the Chemical Society (Resumed)* **1954**, 3842-3846.

(36) Katritzky, A. R.; Akutagawa, K. *Tetrahedron Letters* **1985**, *26*, 5935-5938.

(37) Mahboobi, S.; Sellmer, A.; Eichhorn, E.; Beckers, T.; Fiebig, H.-H.; Kelter, G. *European Journal of Medicinal Chemistry* **2005**, *40*, 85-92.

(38) Baldwin, J. E. *Journal of the Chemical Society, Chemical Communications* **1976**, 734-736.

(39) Anderson, K. W.; Tepe, J. J. *Organic Letters* **2002**, *4*, 459-461.

(40) Ramalingan, C.; Lee, I. S.; Kwak, Y. W. *Chemical & Pharmaceutical Bulletin* **2009**, *57*, 591-596.

(41) Papeo, G.; Posteri, H.; Borghi, D.; Varasi, M. *Organic Letters* **2005**, *7*, 5641-5644.

(42) Bennasar, M. L. s.; Vidal, B.; Bosch, J. *The Journal of Organic Chemistry* **1997**, *62*, 3597-3609.

CHAPTER II: Synthesis of novel imidazolines as inhibitors of the NF-κB pathway.

A. Introduction to the NF-κB pathway

If a cell is subjected to chemotherapy or ionizing radiation, DNA damage results. Ultimately, the cell may undergo one of two pathways: apoptosis or cell survival (Figure II-1).[1] As described in Chapter I, the Chk2 pathway is a known apoptotic pathway that is activated in response to DNA damage, such as double strand breaks.[2] In contrast, the NF-κB pathway essentially has the opposite effect on the fate of a cell when DNA damage occurs. Whereas the Chk2 pathway responds to DNA damage and activates cellular apoptosis, the NF-κB pathway promotes cellular survival.[1] Due to this fact, activation of the NF-κB pathway by chemotherapeutics is believed to be a contributor to chemoresistance.[3] Therefore, if the NF-κB pathway could be inhibited in cancerous tissue, the NF-κB pathway becomes an attractive target for cancer therapeutics. For

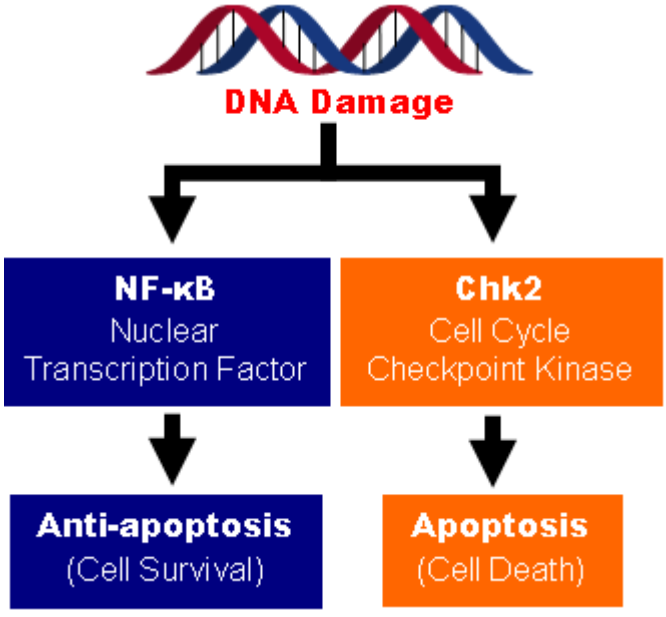

Figure II-1. DNA damage activates NF-κB and Chk2 pathways [1].

more information on cancer statistics and treatment, refer to Chapter I (section A and B).

It is well known that the NF-κB pathway is involved in inflammatory and immune responses.[3] Figure II-2 illustrates the NF-κB pathway adopted from reference [1]. NF-κB

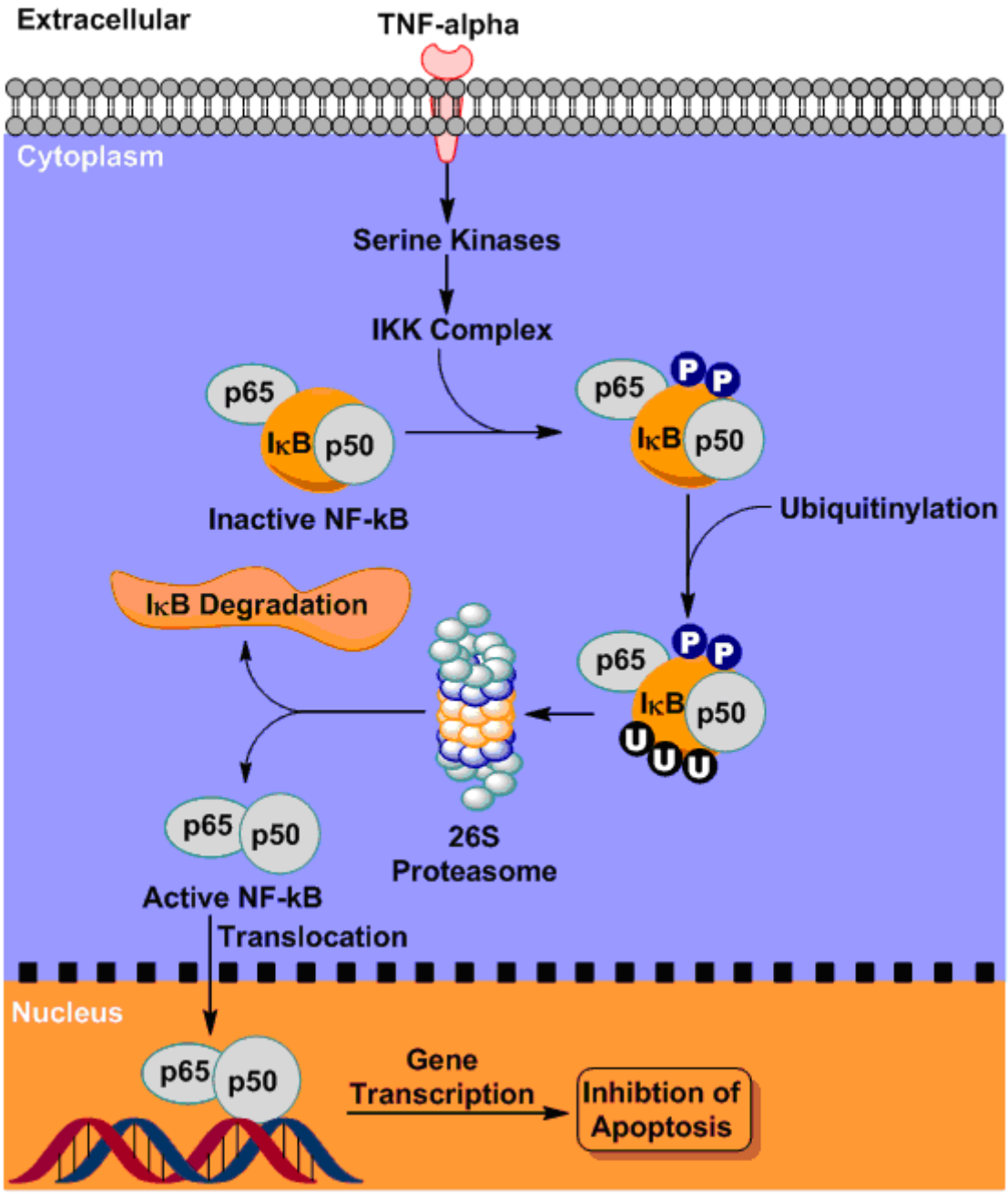

Figure II-2. The NF-κB pathway.

is a nuclear transcription factor, and in the mammalian cell NF-kB exists in an inactive form. NF-kB commonly exists as a heterodimer consisting of p50 and p65.[1] When these subunits are bound to the inhibitory protein IκB, NF-κB is inactive and remains in the cytoplasm.[4] Activation of NF-κB begins with phosphorylation of IκB by IKK (IκB kinase complex). Phosphorylation occurs at Ser 32 and Ser 36 on IκB; mutations at these residues are known to create a "super repressor" in which NF-κB remains bound to IκB rendering it inactive.[3,5] After phosphorylation, this complex is ubiquitinylated thereby tagging this complex for degradation by the 26S proteasome.

The 26S proteasome consists of a 20S core and two 19S regulatory subunits.[6] A diagram of the 26S proteasome is found in Figure II-3 adopted from reference [7]. The 26S proteasome is comprised of a 20S core and two 19S caps. The 20S core is composed of 14 α and 14 β subunits that are arranged to form a cylindrical structure.[7] The 20S core serves as the catalytic site and is responsible for degradation of the tagged proteins.[6] The proteolytic function of the 20S core is known to display

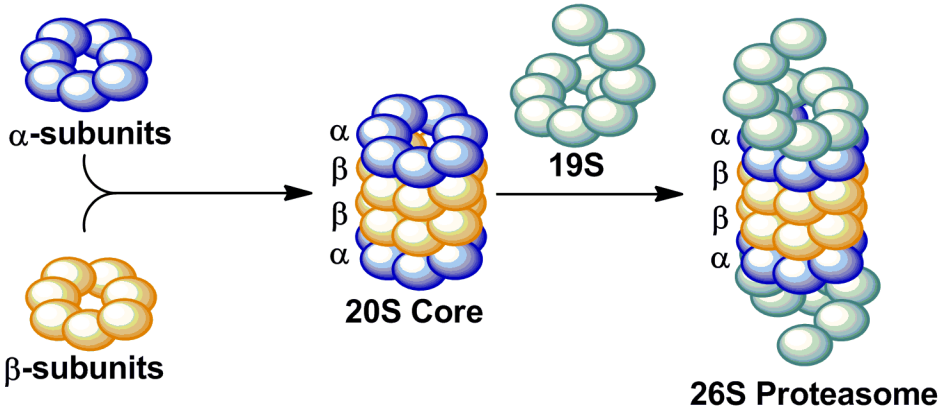

Figure II-3. The 26S proteasome.

chymotryptic, tryptic and peptidylglutamyl-like activities.[6] The 19S subunits function to recognize the ubiquitin-tagged proteins and regulate proteins entering the 20S core.[6]

Once the inactive form NF-κB has been phosphorylated and ubiquitinylated, this complex is degraded by the 26S proteasome (Figure II-2). The degradation of IκB by the proteasome releases the active form of NF-κB, the p50/p65 complex. Subsequently, this active form of NF-κB is translocated into the nucleus where it is able to bind to DNA. Upon binding, NF-κB modulates gene transcription and promotes the expression of many survival, or anti-apoptotic genes. Genes activated via NF-κB translocation include TNF-α, IL-6 and IL-8 among others.[5] The overall effect is increased cellular survival.

With this detailed understanding of the NF-κB pathway, there are numerous therapeutic targets conceivable found within Figure II-2. For instance, inhibition of the IKK complex will prevent phosphorylation of IκB thereby keeping NF-κB in its inactive form. Additionally, inhibition of the 26S proteasome is another therapeutic target. Inhibiting the 26S proteasome will prevent degradation of IκB, and therefore it will remain associated with the p50/p65 complex rendering NF-κB inactive. Inhibition of these mentioned therapeutic targets by small molecules has been developed and is outlined in the following section.

Inhibition of the NF-κB pathway has therapeutic potential for fighting rheumatoid arthritis and cancer among other diseases. The NF-κB pathway is often activated by TNF-α (tumor necrosis factor alpha, Figure II-2), a cytokine. It is known that elevated levels of TNF-α are a contributor to the inflammatory effects associated with rheumatoid arthritis, thereby making inhibition of NF-κB potentially useful for fighting this disease.[8]

In the case of multiple myeloma, NF-κB is also found in elevated levels inducing cell growth and survival.[6] Due to this principle, NF-κB pathway inhibitors such as Bortezomib have proven effective and have been approved for multiple myeloma treatment by the FDA.

B. Current inhibitors of the NF-κB pathway

As mentioned in the previous section, the NF-κB pathway contains multiple therapeutic targets for small molecule inhibitors. One class of inhibitors target inhibition of the IKK complex which is responsible for phosphorylating IκB (section A, Figure II-2).[1] If IκB is not phosphorylated, then NF-κB will not be ubiquitinylated and it will remain as an inactive complex with IκB. A few of the existing IKK complex inhibitors are shown in Figure II-4 .

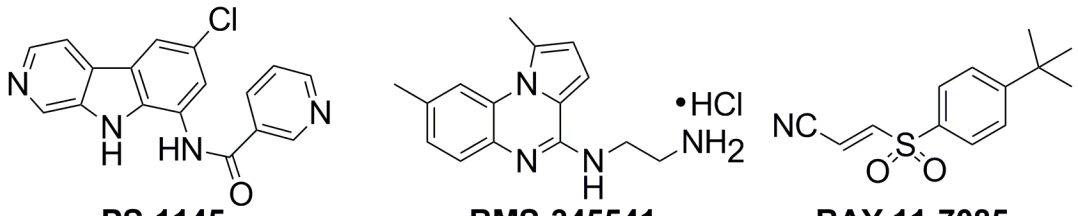

PS-1145 *Millennium Pharmaceuticals* **BMS-345541** *Bristol-Meyer Squibb* **BAY 11-7085** *Bayer*

Figure II-4. Some current IKK complex inhibitors.

A current IKK complex inhibitor **BMS-345541** was synthesized by Bristol-Meyer Squibb (Figure II-4).[5] **BMS-345541** is a selective allosteric inhibitor of the catalytic subunits of the IKK complex (IKK-2 IC_{50} = 0.3 μM, IKK-1 IC_{50} = 4 μM), thereby preventing phosphorylation of IκB. Another IKK complex inhibitor is Bayer compound **BAY 11-7085** (Figure II-4).[9] **BAY 11-7085** is an irreversible inhibitor (IC_{50}

approximately 10 μM) that functions by inhibiting TNF-α induced phosphorylation of IκB.[9] A final inhibitor, **PS-1145** (IC_{50} < 0.1 μM), was prepared by Millennium Pharmaceuticals.[10] If prostate carcinoma cells were treated with **PS-1145**, these cells demonstrated sensitization to apoptosis.[1,9] These and other IKK complex inhibitors hold therapeutic potential for fighting cancer.

Interest in developing proteasome inhibitors is also a rapidly expanding focus for inhibiting NF-κB. One of the leading proteasome inhibitors is Bortezomib (Velcade®) which was developed by Millenium Pharmaceuticals (Figure II-5).[4] Approval of Bortezomib by the FDA for treatment of multiple myeloma and mantle cell lymphoma has validated NF-κB as a therapeutic target.[6] Whereas Bortezomib is an example of a boronic acid that is a proteasome inhibitor, Salinosporamide A is a β-lactone developed by Nereus Pharmaceuticals that is also an effective proteasome inhibitor (Figure II-5).[6] In addition to some of these notable proteasome inhibitors, the Tepe lab has identified imidazolines as a distinct structural core that is an effective proteasome inhibitor (Figure II-5).[11,12] The lead imidazoline **TCH 013** contains an ethyl ester and is found in

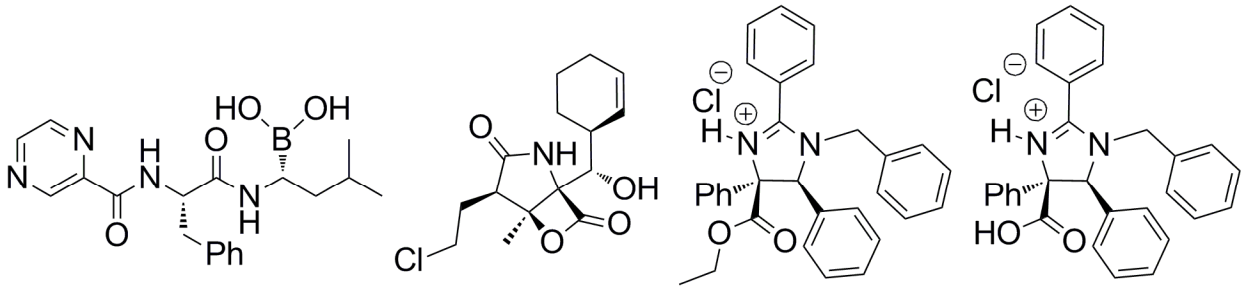

Figure II-5. Some current examples of proteasome inhibitors.

Figure II-5. In addition, these imidazolines have proven to not induce significant cell cytotoxicity.[12]

The **TCH** imidazoline library originated with **TCH 001** containing a carboxylic acid (Figure II-5). Pre-treatment of CEM (acute leukemia) cells with carboxylic acid **TCH 001** has shown a 76-fold enhancement of the efficacy of camptothecin, a DNA damaging agent.[12] In addition to this success as a chemotherapeutic additive, **TCH 001** is a potent inhibitor of the 20S proteasome (IC_{50} = 950 nM). However, chemical and metabolic instability of this imidazoline has limited further study.[8] Esterification of **TCH 001** to the more stable ethyl ester **TCH 013** (Figure II-5) yielded an imidazoline with a potency in the low micromolar range (IC_{50} = 2.8 μM). It is believed that the instability of **TCH 001** is caused in part by decarboxylation to generate an ylide intermediate

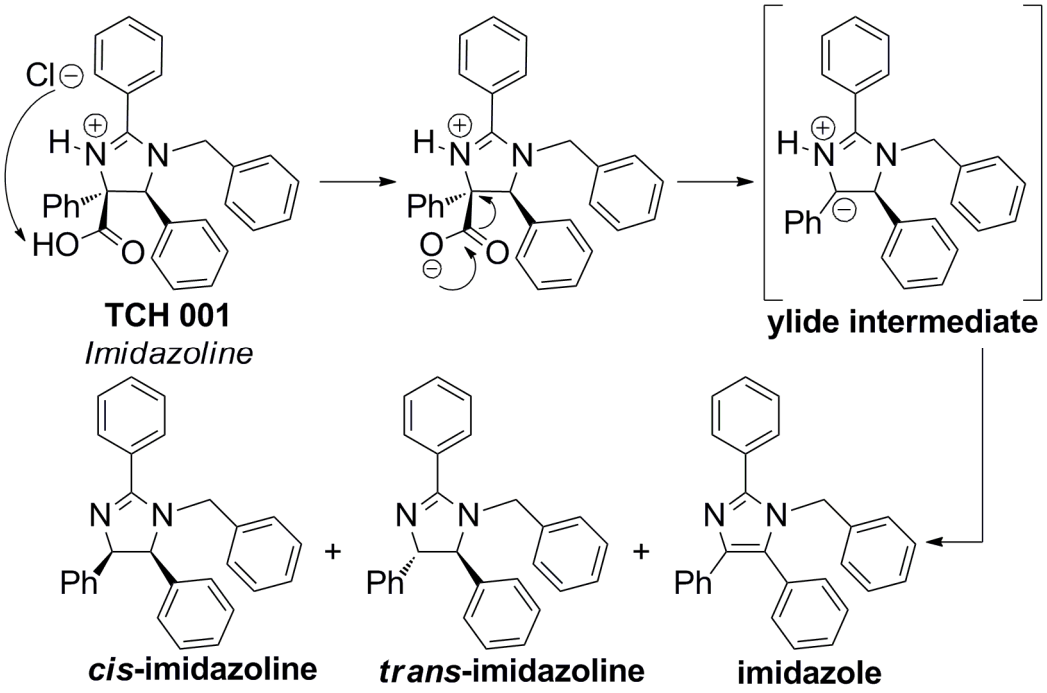

Figure II-6. Decomposition of **TCH 001** via ylide formation.

(Figure II-6).[8] Generation of the corresponding ylide can then lead to generation of the corresponding *cis*- and *trans*- imidazolines as well as the fully aromatized imidazole. This decomposition is likely a contributor to the decrease in activity observed with **TCH 001**.

As the **TCH** library expanded due to synthetic efforts of Dr. Jason Fisk and Dr. Robert Mosey, **TCH 165** has emerged as a nanomolar inhibitor of the 20S proteasome (IC_{50} = 291 nM, Figure II-7). Compared to parent compound **TCH 013**, introduction of a benzylamine group has contributed to increased activity from the micromolar to nanomolar range (Figure II-7). Additionally, **TCH 013** also contains an ethyl ester, thereby preventing decarboxylation and ylide formation described previously (Figure II-6).

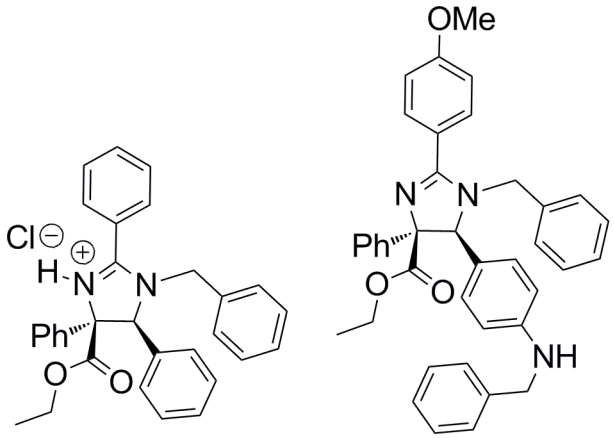

TCH 013 IC_{50} = 2.8 μM

TCH 165 IC_{50} = 291 nM

Figure II-7. Structure of imidazolines **TCH 165** and **TCH 013** and corresponding 20S proteasome inhibition.

C. Synthesis of imidazoline TCH 165

Currently, **TCH 165** is the most potent proteasome inhibitor contained within the **TCH** imidazoline library. Imidazoline **TCH 165** was first synthesized by Dr. Robert

Mosey from the Tepe lab.[13] Scheme II-1 outlines the synthesis of **TCH 165**; the reported yields and experimental procedures found in Scheme II-1 reflect my own repetition of his work.[13] To begin the synthesis, commercially available 2-phenylglycine is readily acylated with 4-methoxybenzoyl chloride affording amide **II-1.** Treatment of amide **II-1** with trifluoroacetic anhydride will undergo a dehydrative cyclization yielding phenylazlactone **II-2** in 88% yield. Thereafter, phenylazlactone **II-2** undergoes a [3+2] cyclization with imine **II-3** and TMSCl to afford the carboxylic acid imidazoline **II-4** as the HCl salt. The necessary imine **II-3** is readily prepared in quantitative yield by reacting benzylamine and 4-nitrobenzaldehyde in the presence of a Dean-Stark trap.

Having synthesized imidazoline **II-4**, the carboxylic acid is converted to the acyl chloride, which then reacts with anhydrous ethanol to generate the desired ethyl ester **TCH 152** (Scheme II-1). After the esterification, the nitro group found in **TCH 152** is reduced to amine **TCH 157** by excess Zinc and glacial acetic acid in excellent yield. The final step utilizes a reductive benzylation with benzaldehyde and $NaBH(OAc)_3$ to ensure mono benzylation affording **TCH 165** in 78% yield. Overall the synthesis of **TCH 165** consists of 6 steps with an overall yield of 6.6%.

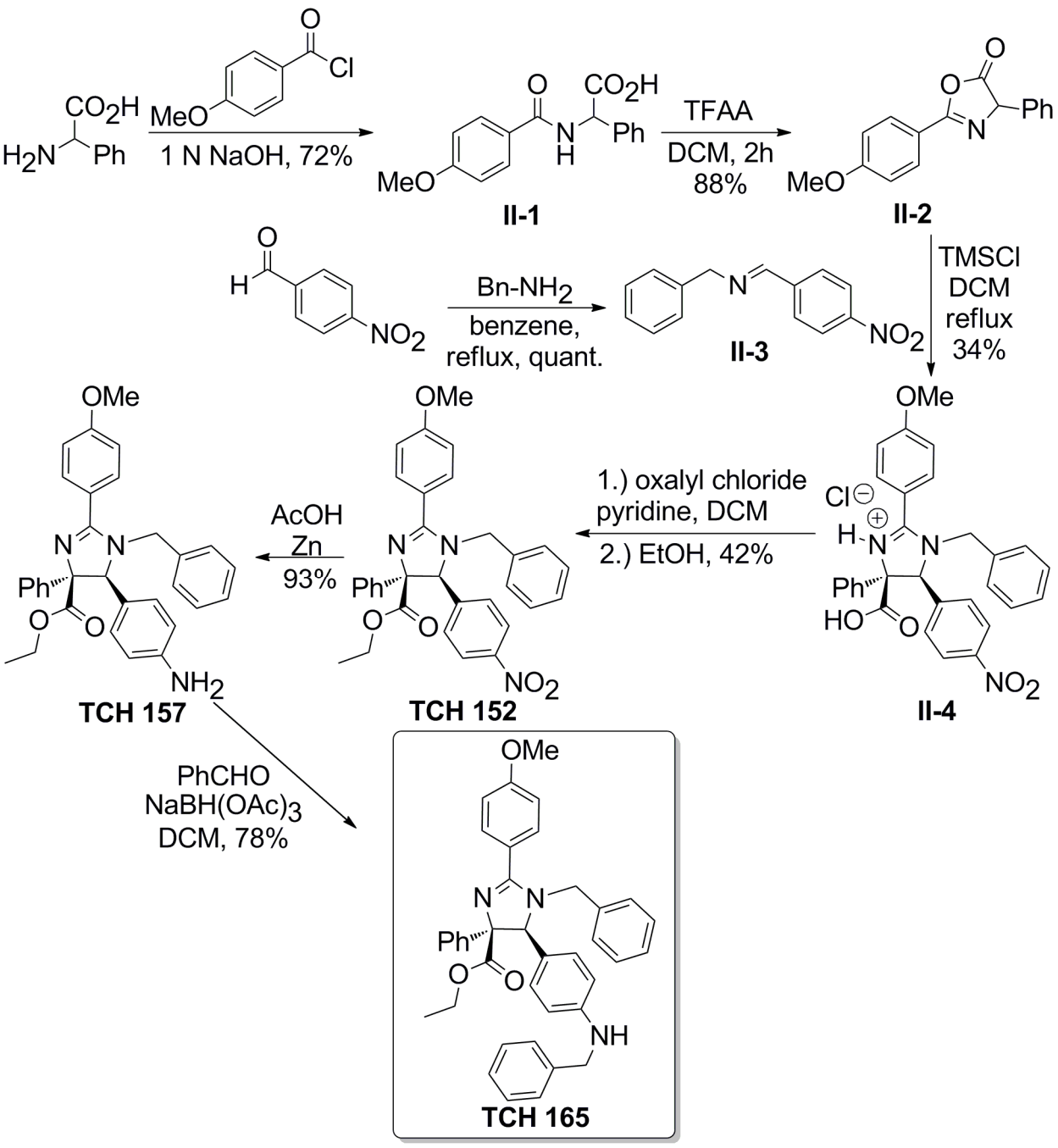

Scheme II-1. Synthesis of **TCH 165** from 2-phenylglycine.

In the synthesis of **TCH 165**, the yield limiting step is the [3+2] cyclization to generate imidazoline **II-4**. Although these reactions are typically not high yielding, the low yield can partially be attributed to the formation of β-lactam **TCH 172**. In the [3+2] cyclization reaction that generates imidazoline **II-4** in 34% yield, β-lactam **TCH 172** is

isolated in 20% yield as a side product. A proposed mechanism for the generation **TCH 172** is found in Scheme II-2. The β-lactam is formed as a result of the competing [2+2] cyclization reaction. During the reaction, phenylazlactone **II-2** can generate a ketene intermediate that can account for the formation of **TCH 172** (Scheme II-2).

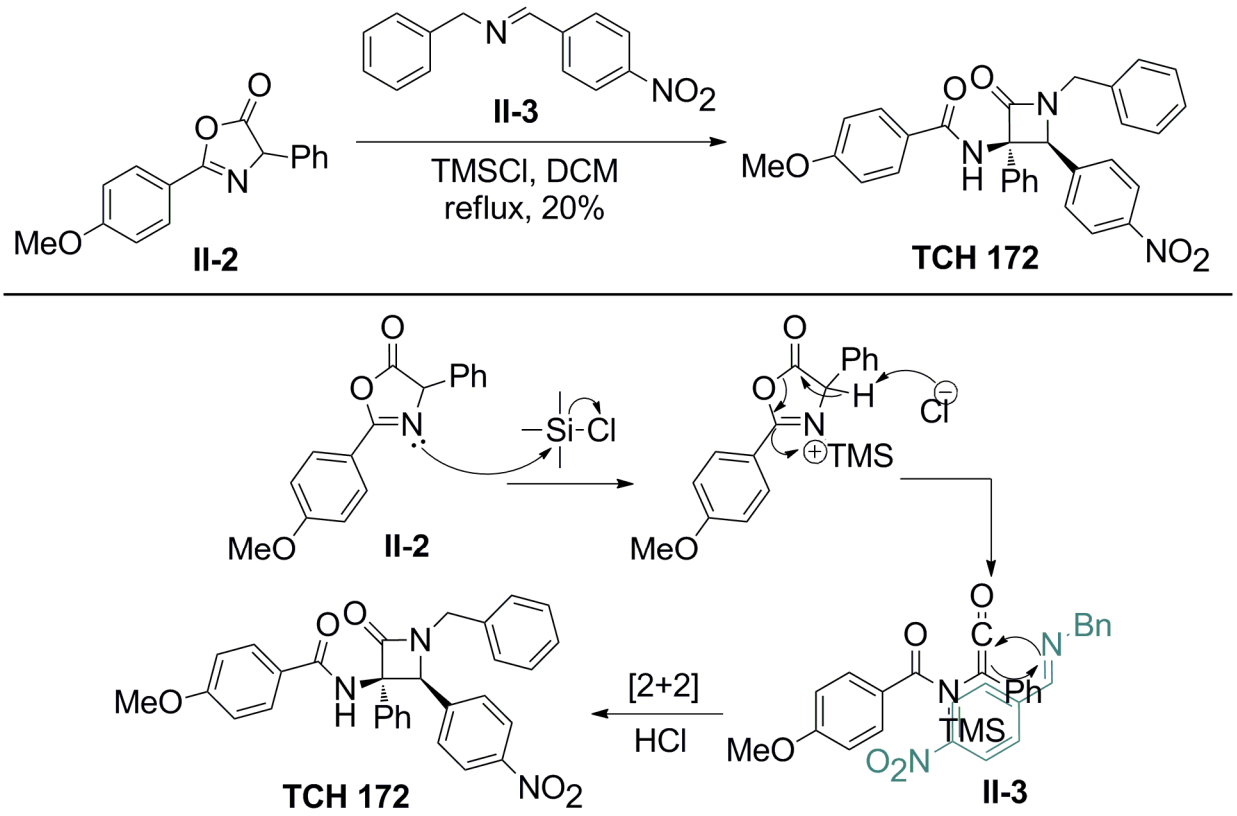

Scheme II-2. Proposed mechanism for β-lactam **TCH 172** formation.

Additionally, upon workup of the aforementioned cyclization reaction, the crude mixture contains both imidazoline **II-4** and β-lactam **TCH 172**. As expected, these compounds are difficult to distinguish by ^{1}H and ^{13}C NMR. The most distinguishing peak for the β-lactam is the amide peak that occurs at 9 ppm in ^{1}H NMR. Fortunately, these compounds are readily separated by heating the crude mixture in boiling ethyl acetate followed by filtration. The imidazoline HCl salt **II-4** is not soluble in ethyl acetate

whereas **TCH 172** dissolves. The structure of **TCH 172** was further validated by X-ray crystallography (performed by Dr. Richard Staples) as shown in Figure II-8.

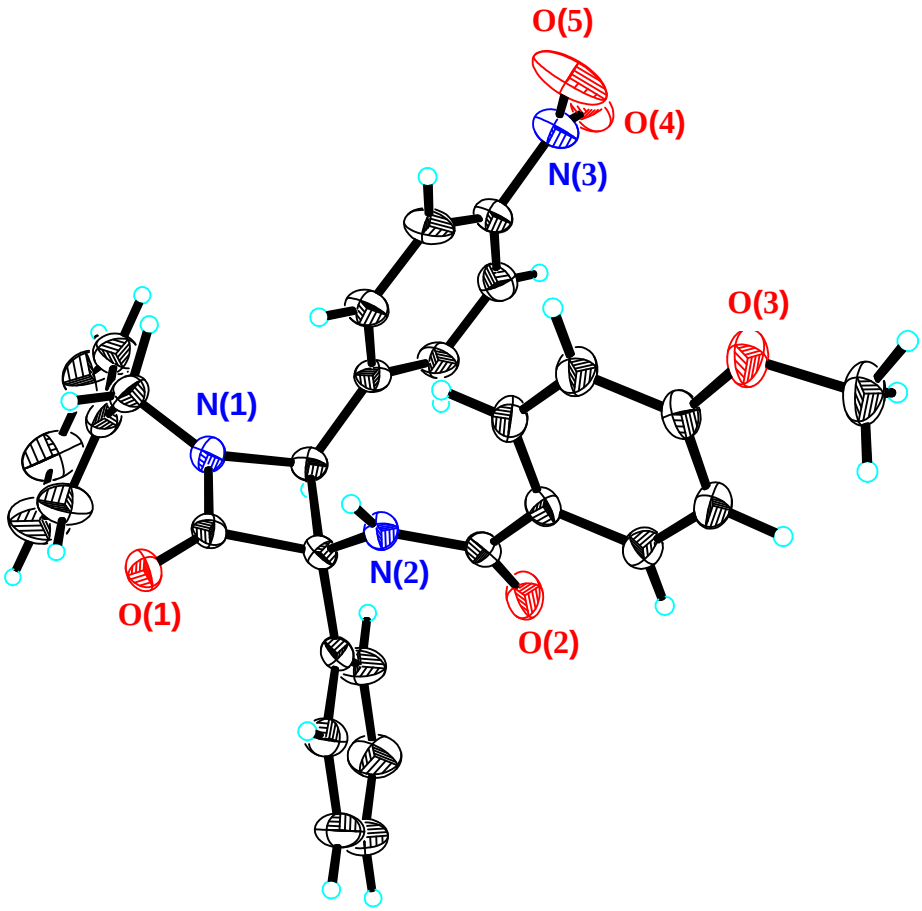

Figure II-8. X-ray crystal structure of β-lactam **TCH 172**.

After completing the synthesis of **TCH 165**, it was desirable to separate the compound into its enantiomers to further evaluate proteasome inhibition.

D. Attempted resolution of TCH 165 via chiral HPLC

Due to the amazing specificity of the human body, drugs must be administered as an enantiopure substance. If a drug were to be approved by the FDA as a racemate, both enantiomers must undergo the same cytotoxicity studies and subsequent clinical trials. It is estimated that the cost for developing a novel drug is 1 billion dollars from

bench side to market. Therefore, approval of a racemate would double this cost. For this reason, it is highly desirable to devise enantioselective syntheses. Alternatively, chiral resolution techniques may also be employed. This may include separating enantiomers via chiral HPLC or converting the enantiomers into a resolvable pair of diastereomers.

In the **TCH** imidazoline library, **TCH 013** is one of the lead imidazolines. Previously, **TCH 013** has been successfully resolved by chiral HPLC into its (*S,S*) enantiomer **TCH 017** and (*R,R*) enantiomer **TCH 018** (Figure II-9). Since this resolution of **TCH 013**, imidazoline **TCH 165** has emerged as a more potent inhibitor of the 26S proteasome. Therefore, it was desirable to separate **TCH 165** into its enantiomers and evaluate the corresponding biological activity. Since **TCH 013** was successfully resolved using chiral HPLC, this was chosen as the first methodology for resolving **TCH 165**.

Conditions for resolving **TCH 013** had previously been optimized by Dr. Robert Mosey in the Tepe lab. Using an analytical CHIRALPAK® AD-H column, **TCH 013** was successfully resolved and this chromatogram is found in Figure II-9. The optimal solvent system was 20:80 isopropanol/hexanes with a flow rate of 1.0 mL/min. **TCH 013** enantiomer peaks **TCH 017** (*S,S)* and **TCH 018** (*R,R*) have retention times of 6.47 and 11.33 min respectively (Figure II-9). The corresponding peak areas for enantiomers #1 and #2 were 50.52% and 49.29% respectively. This 1:1 peak area ratio is expected for a racemic mixture of **TCH 013**.

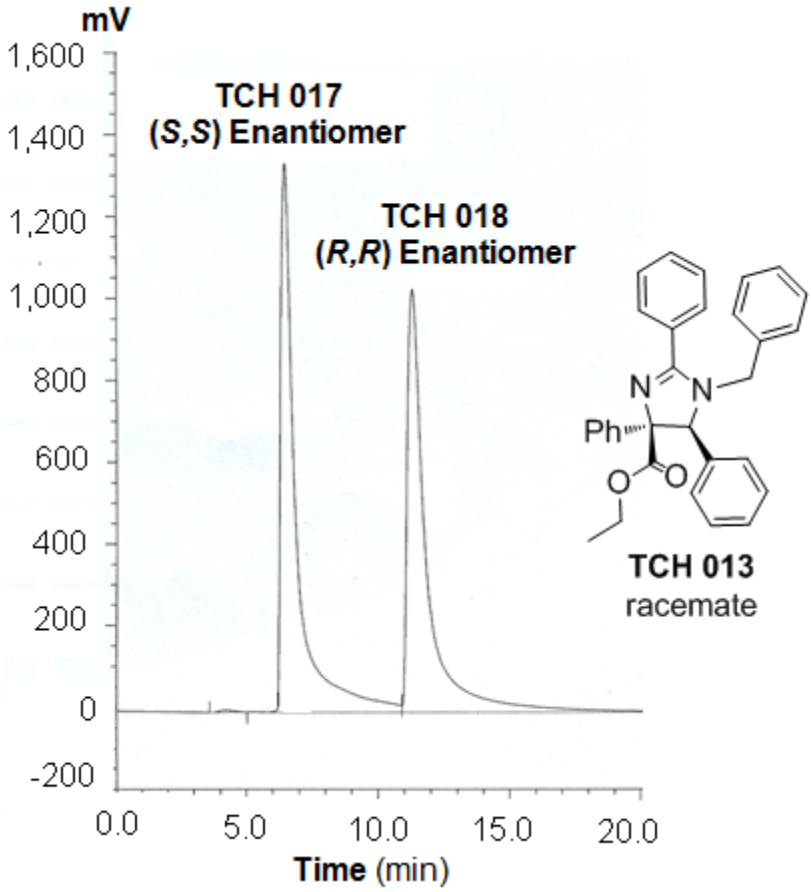

Figure II-9. Chiral resolution of **TCH 013** using CHIRALPAK® AD-H column.

Given this precedent, it was desirable to attempt to resolve **TCH 165** by chiral HPLC (Figure II-10). Analogous conditions (20:80 isopropanol/hexanes, flow rate 1.0 mL/min) used for **TCH 013** did not show any separation for **TCH 165**. Varying the solvent system polarity, column temperature (25 ℃ or 37 ℃), as well as altering the flow rate did not indicate any potential for resolving the enantiomers. Imidazolines **TCH 148** and **TCH 163** were also unsuccessfully resolved with the CHIRALPACK® AD-H column. Use of a CHIRALCEL OD-H column afforded no apparent separation of **TCH 013**, **TCH 165**, **TCH 163** and **TCH 148**.

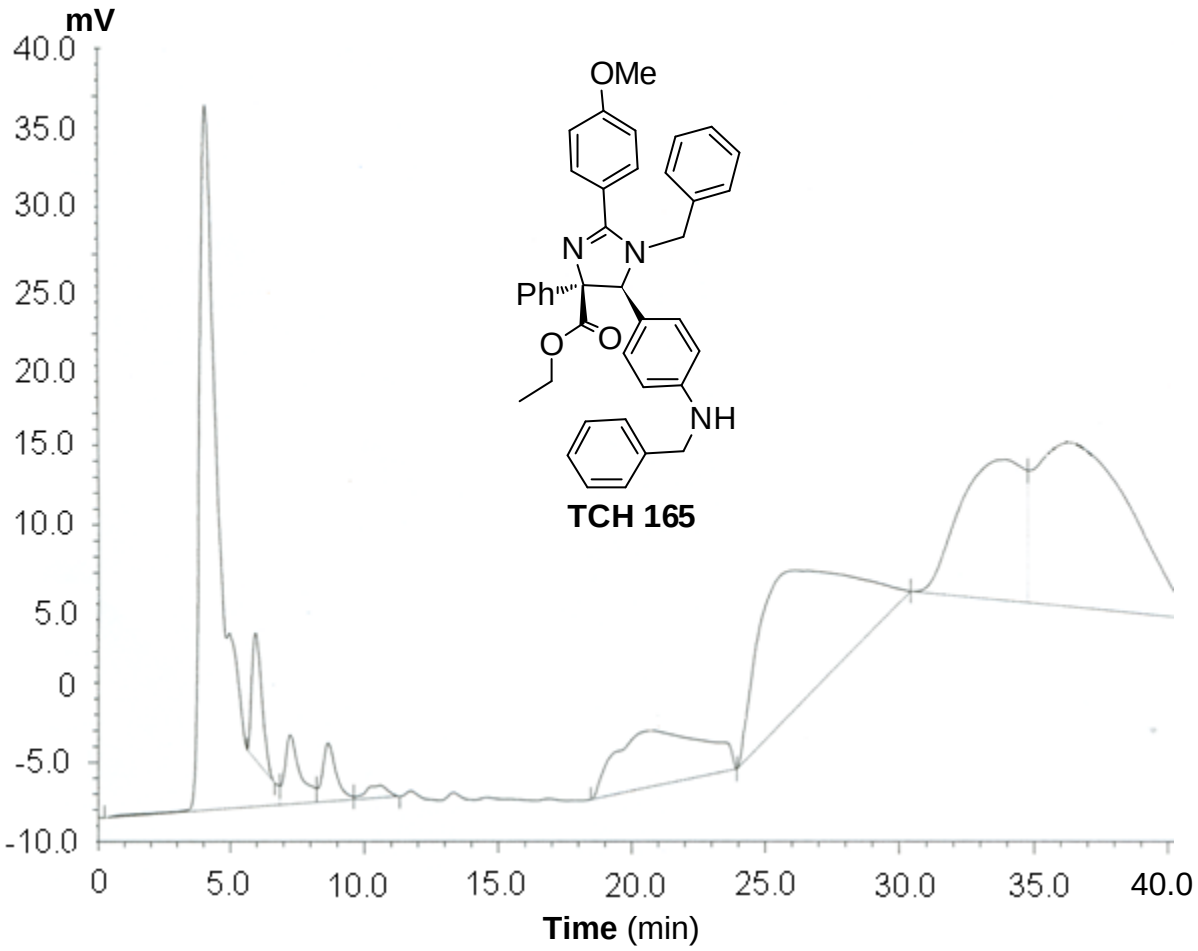

Figure II-10. Unsuccessful chiral resolution of **TCH 165** using CHIRALPAK® AD-H column.

Since chiral HPLC initially was troublesome, it was desirable to investigate resolving the enantiomers of **TCH 165** by finding a diastereomeric mixture that could be separated.

E. Resolution of TCH 165 via diastereomer formation

Initially it was desirable to form diastereomers with amine **TCH 157** since this was the precursor of **TCH 165** (Scheme II-1). By resolving the enantiomers of **TCH 157** via diastereomers, it would then be possible to remove the chiral auxiliary and convert these enantiomers into the enantiomers of **TCH 165**. In order to generate

diastereomers, (1*S*)-(+)-camphor-10-sulfonylchloride was used in an attempt to generate diastereomeric sulfonamides (Scheme II-3). Upon treating **TCH 157** with 1.2 equivalents of (1*S*)-(+)-camphor-10-sulfonylchloride and TEA, the desired mono-sulfonated product was not formed after reacting for 24 hours.[14] However, the product was observed by HRMS but was not isolated in sufficient quantity for NMR. Therefore, mono-sulfonated product was not isolated, but instead the double-sulfonated imidazoline **II-5** was isolated and validated by HRMS (Scheme II-3). The diastereomers

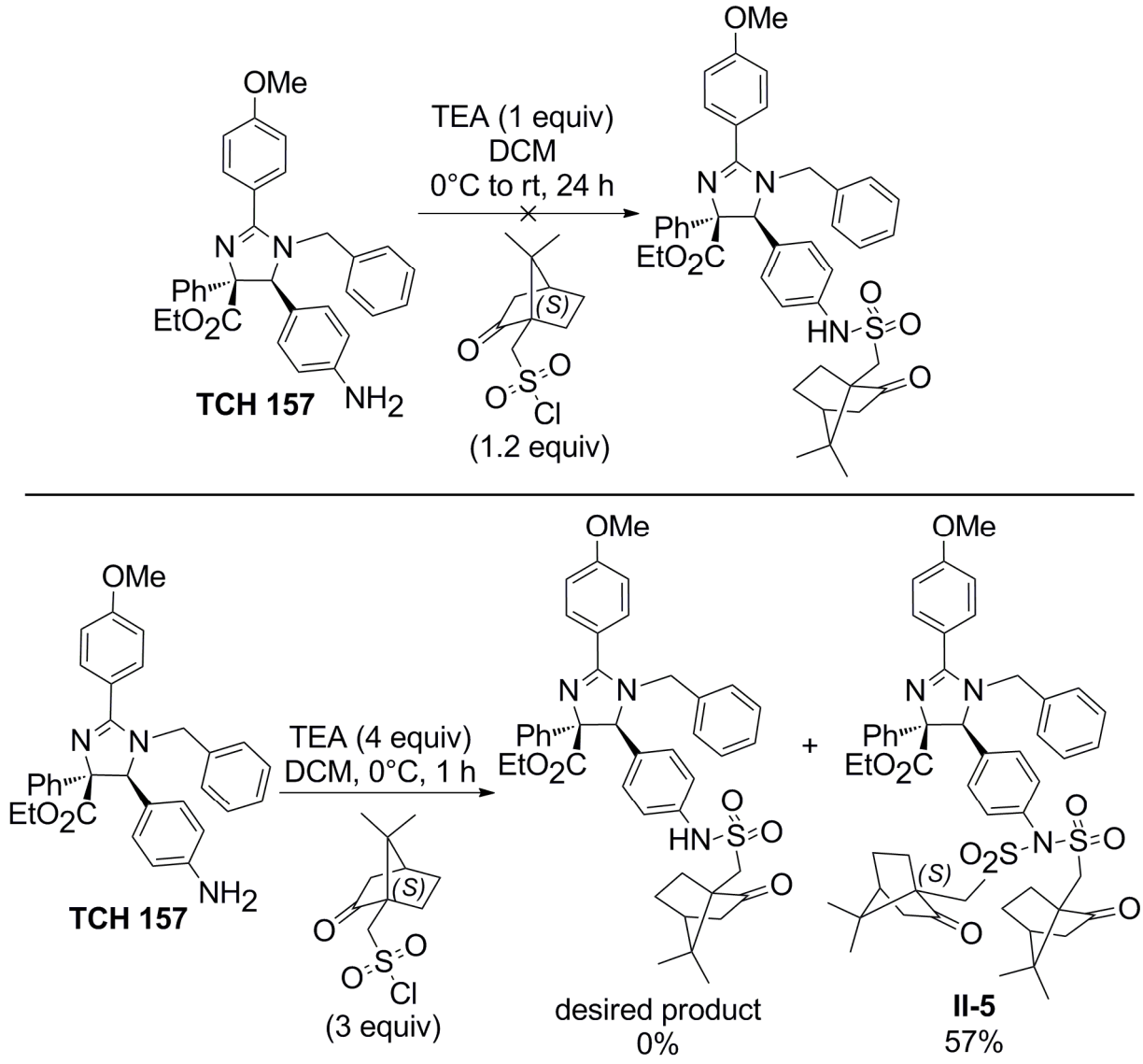

Scheme II-3. Attempted diastereomeric sulfonamide formation with **TCH 157.**

of **II-5** were not separable by column chromatography and were not readily distinguished by ^{1}H NMR.

After unsuccessfully resolving **TCH 157** via sulfonamides, it was desirable to form diastereomers from carboxylic acid **II-4**. Specifically, it could be envisioned that starting from a chiral alcohol, diastereomeric esters could be generated and separated by chromatography (Scheme II-4). The first attempt to form the diastereomeric esters was modifying the reaction conditions that previously yielded ethyl ester **TCH 152**. First, the acyl chloride was generated with oxalyl chloride, and subsequently DCM and (*R*)-2-butanol (3 equiv.) was added (Scheme II-4). The *sec*-butyl ester diastereomers **TCH**

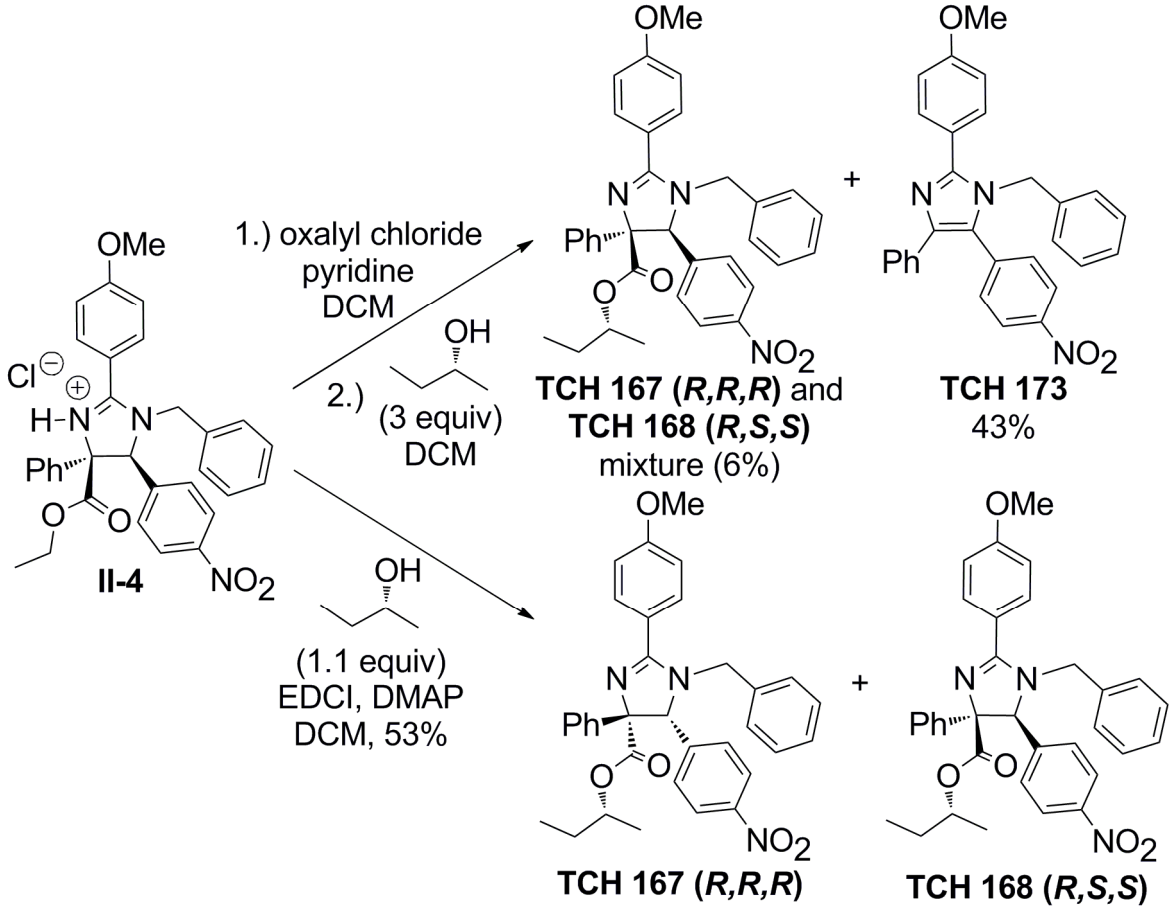

Scheme II-4. Synthesis of diastereomers **TCH 167 (*R,R,R*)** and **TCH 168 (*R,S,S*)**.

167 (*R,R,R*) and **TCH 168 (*R,S,S*)** were observed as a mixture in 6% yield. However, the major product isolated from these conditions was the undesired imidazole **TCH 173** (Scheme II-4).

Since generating the acyl chloride proved problematic due to the undesired formation of imidazole **TCH 173**, carboxylic acid **II-4** was treated with EDCI, DMAP and (*R*)-2-butanol. This methodology afforded diastereomers **TCH 167 (*R,R,R*)** and **TCH 168 (*R,S,S*)** in 53% combined yield (Scheme II-4). As an added benefit, only 1 equivalent of the expensive chiral alcohol is necessary for this procedure. The absolute stereochemistry of these diastereomers has been assigned according to an X-ray crystal structure of **TCH 168 (*R,S,S*)** provided by Dr. Richard Staples (Figure II-11). Absolute stereochemistry determination is possible since the chirality of the *sec*-butyl

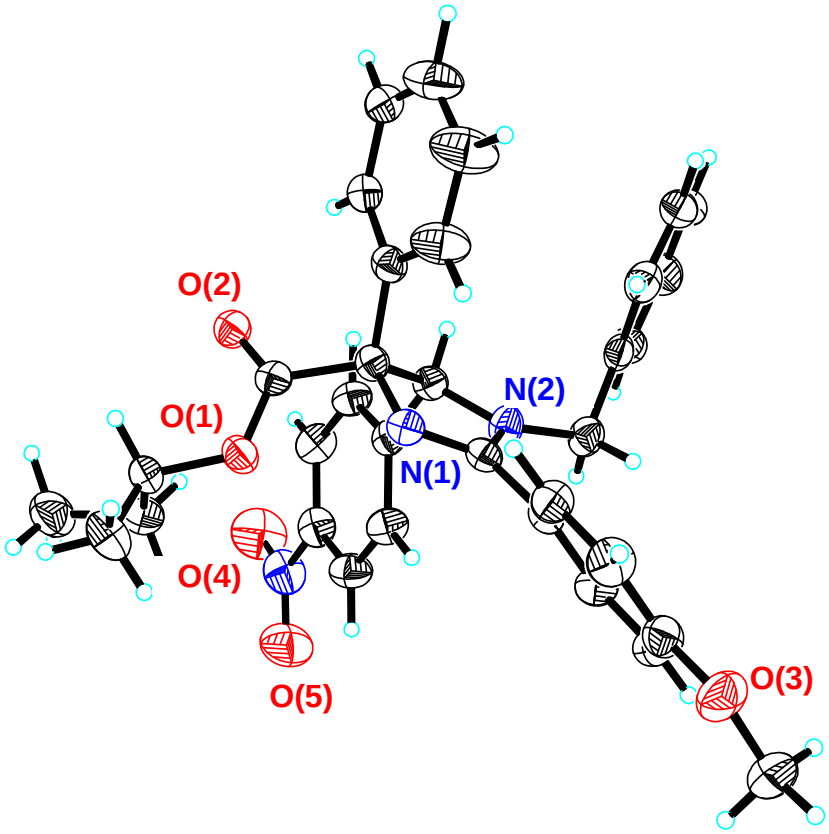

Figure II-11. X-ray crystal structure of **TCH 168 (*R,S,S*).**

stereocenter (*R*) is known. Note that diastereomer **TCH 167 (*R,R,R*)** elutes through a silica column (4:6 EtOAc/Hexanes) prior to **TCH 168 (*S,S,S*)**.

Additionally, these diastereomers are easily distinguished by ^{1}H NMR. In $CDCl_3$, **TCH 167 (*R,R,R*)** has a distinct doublet (0.84 ppm, peak **A** in Figure II-12) and a triplet (0.51 ppm, peak **B**) corresponding to the terminal methyl groups of the *sec*-butyl ester. In contrast, **TCH 168 (*R,S,S*)** does not have this distinction between the terminal methyl groups of its *sec*-butyl ester in $CDCl_3$. Peak **C** (Figure II-12) integrates to 6 protons and represents both methyl groups belonging to the *sec*-butyl ester. Both spectra also illustrate a slight difference in chemical shifts of their methylene protons in the *sec*-butyl ester; 1.08 ppm for **TCH 167 *(R,R,R)*** and 1.25 ppm for **TCH 168 (*R,S,S*)**.

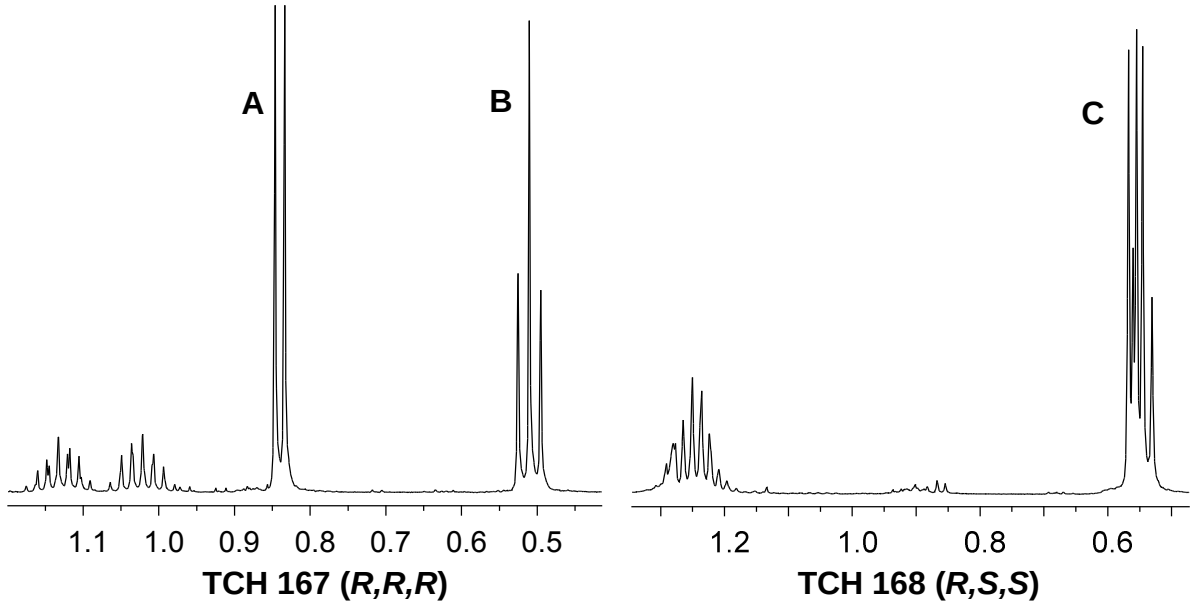

Figure II-12. Comparsion of *sec*-butyl ester chemical shifts of **TCH 167 *(R,R,R)*** and **TCH 168 (*R,S,S*)**.

Now having resolved **TCH 167 (*R,R,R*)** and **TCH 168 (*R,S,S*)** by column chromatography, these diastereomers can be converted to the diastereomeric analogs of **TCH 165** (Scheme II-5). Although these derivatives will not be the true enantiomers

of **TCH 165**, the substitution of the ethyl ester (found in **TCH 165**) with the *sec*-butyl ester found within **TCH 167 (*R,R,R*)** and **TCH 168 (*R,S,S*)** is expected to have a negligible effect on proteasome activity. Therefore, using the reaction conditions found in Scheme II-1, **TCH 167 (*R,R,R*)** and **TCH 168 (*R,S,S*)** were converted to the diastereomeric analogs of **TCH 165** (Scheme II-5).

First, the nitro group of **TCH 167 (*R,R,R*)** and **TCH 168 (*R,S,S*)** was reduced with zinc in glacial acetic acid to afford enantiopure amines **II-6 (*R,R,R*)** and **II-7 (*R,S,S*)** respectively. Subsequent reductive benzylation with benzaldehyde and $NaBH(OAc)_3$

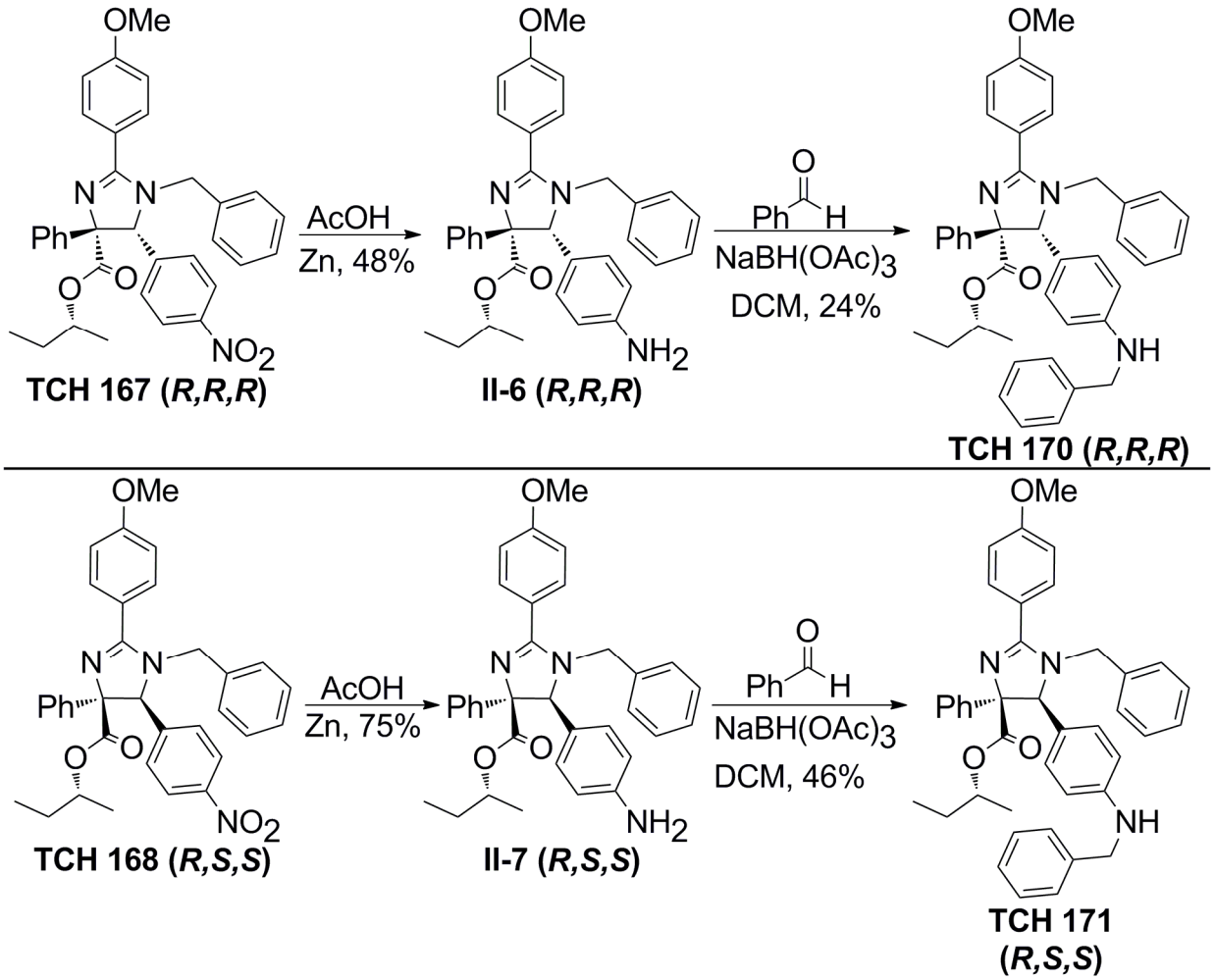

Scheme II-5. Synthesis of **TCH 165** diastereomeric analogs **TCH 170 (*R,R,R*)** and **TCH 171 (*R,S,S*)**.

afforded **TCH 170 (*R,R,R*)** and **TCH 171 (*R,S,S*)**. Imidazolines **TCH 170 (*R,R,R*)** and **TCH 171 (*R,S,S*)** are considered to be enantiopure analogs of **TCH 165** since their syntheses began with diastereopure starting materials **TCH 167 (*R,R,R*)** or **TCH 168 (*R,S,S*)**.

Now having synthesized the diastereomer analogs of **TCH 165**, it was desirable to convert **TCH 167 (*R,R,R*)** and **TCH 168 (*R,S,S*)** back into their respective ethyl esters. This would generate both enantiomers of ethyl ester **TCH 152** used in the original **TCH 165** synthesis (Scheme II-1). Having the resolved enantiomers of **TCH 152** would allow for the actual enantiomers of **TCH 165** to be readily synthesized.

F. Synthesis of TCH 165 Enantiomers

In order to synthesize the enantiomers of **TCH 165**, **TCH 167 (*R,R,R*)** and **TCH 168 (*R,S,S*)** must be converted from their *sec*-butyl esters back into ethyl esters. The most desirable transformation to accomplish this is transesterification, although oftentimes this requires rather harsh conditions. The first attempt of transesterification involved a diastereomeric mixture of **TCH 167 (*R,R,R*)** and **TCH 168 (*R,S,S*)** with p-toluenesulfonic acid (p-TsOH) in anhydrous ethanol (Scheme II-6). Even with 5 equivalents of p-TsOH and refluxing conditions no ethyl ester was observed. It is possible that in the acidic conditions, the imine nitrogen of the imidazoline is protonated preferentially, thereby making it difficult to activate the ester carbonyl since this intermediate would have two positive charges in close proximity.

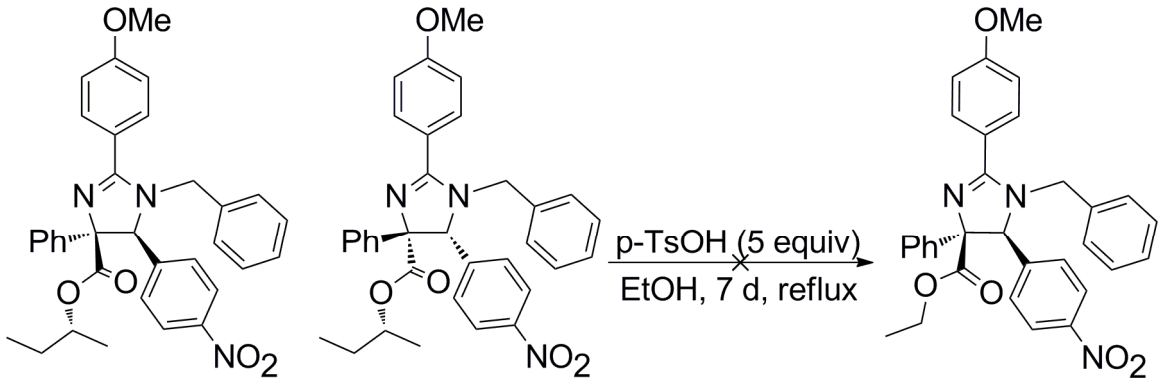

TCH 167 (*R,R,R*) and **TCH 168 (*R,S,S*)** mixture

Scheme II-6. Unsuccessful transesterification conditions.

Since acidic transesterification conditions were unsuccessful, basic conditions were also investigated (Scheme II-7). Treatment of **TCH 167 (*R,R,R*)** at room temperature with NaOEt (40 equiv.) in anhydrous ethanol lead to decomposition. Alternatively, if NaOEt was generated *in situ* (NaH in anhydrous ethanol), only trace product was observed. Refluxing temperatures led to decomposition and no detection of the desired ethyl ester.

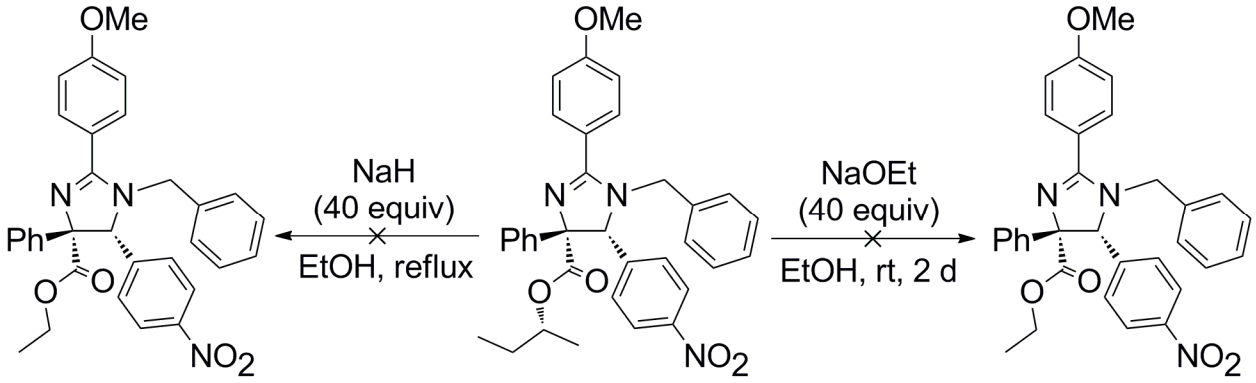

TCH 177 (*R,R*) **TCH 167 (*R,R,R*)** **TCH 177 (*R,R*)**

Scheme II-7. Unsucessful basic transesterifcaiton conditions.

Since transesterification proved troublesome, hydrolysis of the *sec*-butyl ester back to carboxylic acid **II-4** was investigated. To test this methodology, ethyl ester **TCH 152** was refluxed in 2 N NaOH/ethanol mixture for 3 hours. Subsequent acidification

with concentrated HCl afforded carboxylic acid **II-4** in 57% yield (Scheme II-8). For this reaction, ethanol is important due to the limited solubility of **TCH 152** in water.

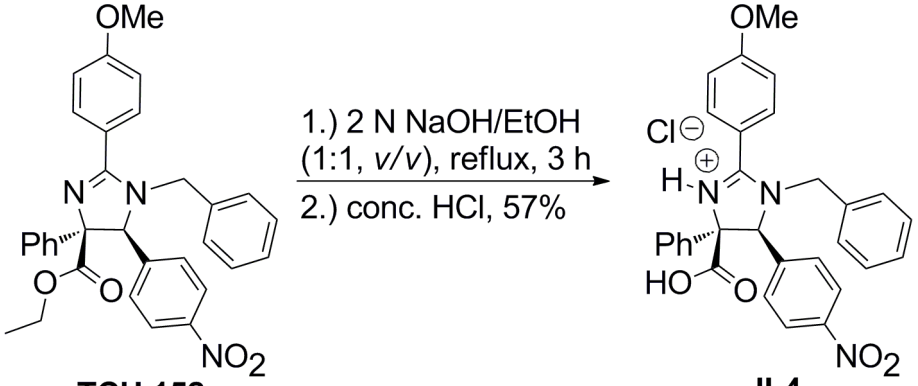

TCH 152 **II-4**

Scheme II-8. Successful hydrolysis of **TCH 152.**

Having illustrated the successful hydrolysis of ethyl ester **TCH 152**, this methodology was used to convert *sec*-butyl ester **TCH 167 (*R,R,R*)** to its corresponding ethyl ester **TCH 177 (*R,R*)** (Scheme II-9). Treatment of **TCH 167 (*R,R,R*)** with 2 N NaOH formed the corresponding carboxylic acid. The crude material was then treated with EDCI, DMAP and ethanol affording enantiopure ethyl ester **TCH 177 (*R,R*)** in 14% yield (over 2 steps). Subsequent zinc reduction of the nitro group afforded amine **II-8 (*R,R*)** in 82% yield. Finally, reductive benzylation with benzaldehyde and $NaBH(OAc)_3$ yields enantiopure **TCH 178 (*R,R*)** in 53% yield. **TCH 178 (*R,R*)** is the (*R,R*) enantiomer of **TCH 165**. The assignment of absolute stereochemistry is rationalized by the X-ray crystal structure of **TCH 168 (*R,S,S*)** (refer to Figure II-11). By default, **TCH 167 (*R,R,R*)** is the (*R,R,R*) *sec*-butyl diastereomer.

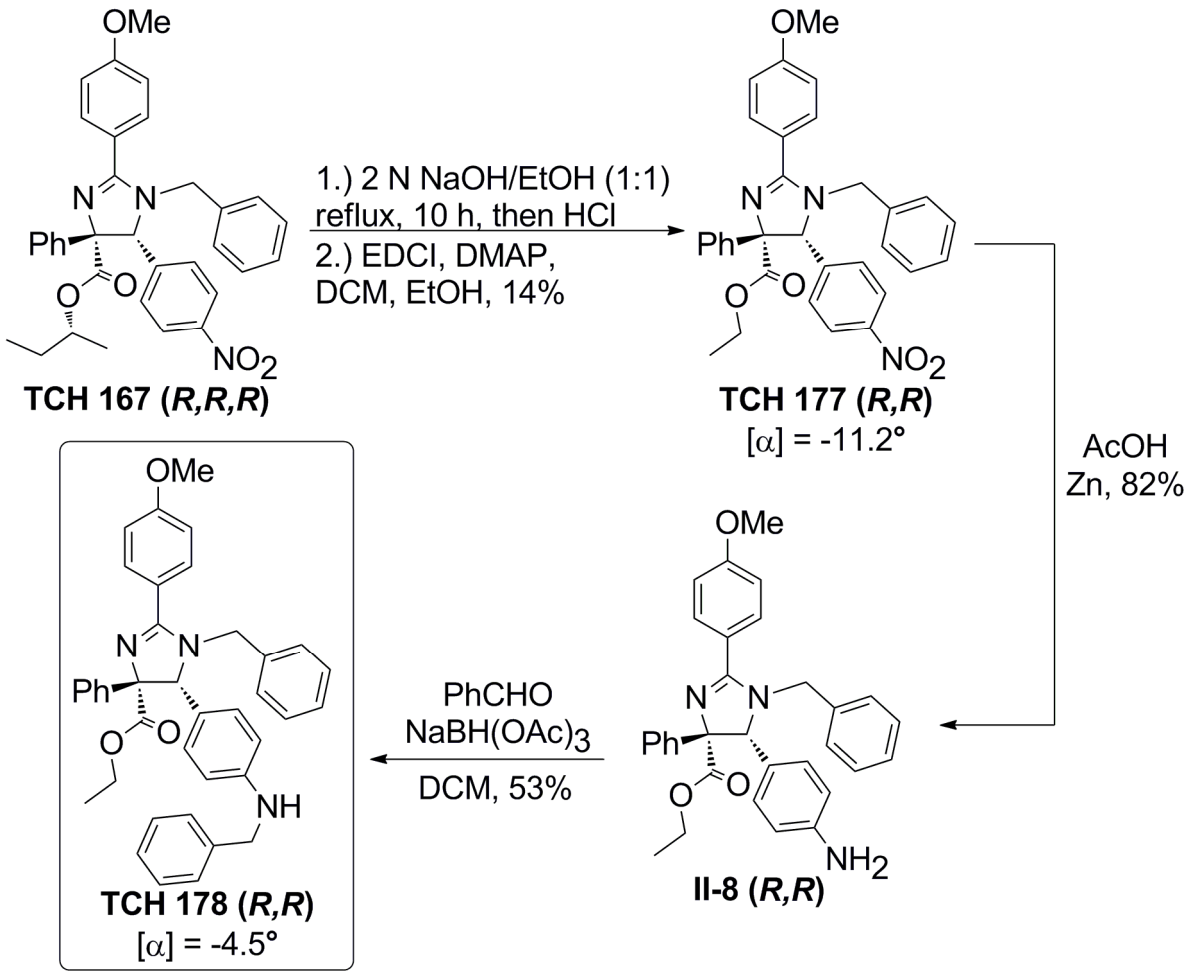

Scheme II-9. Synthesis of enantiopure **TCH 178 (*R,R*).**

The remaining *sec*-butyl ester **TCH 168 (*R,S,S*)** was converted to the corresponding ethyl ester **TCH 179 (*S,S*)** in 11% yield over 2 steps (Scheme II-10). The same hydrolysis/esterification procedure described for **TCH 177 (*R,R*)** was used. Subsequently, ethyl ester **TCH 179 (*S,S*)** was reduced to amine **II-9 (*S,S*)** in 87% yield. Thereafter, amine **II-9 (*S,S*)** was benzylated to afford **TCH 180 (*S,S*)** in 50% yield. **TCH 180 (*S,S*)** is the (*S,S*) enantiomer of **TCH 165**. This is further validated since the absolute stereochemistry of **TCH 168 (*R,S,S*)** has been determined from its X-ray crystal structure (Figure II-11).

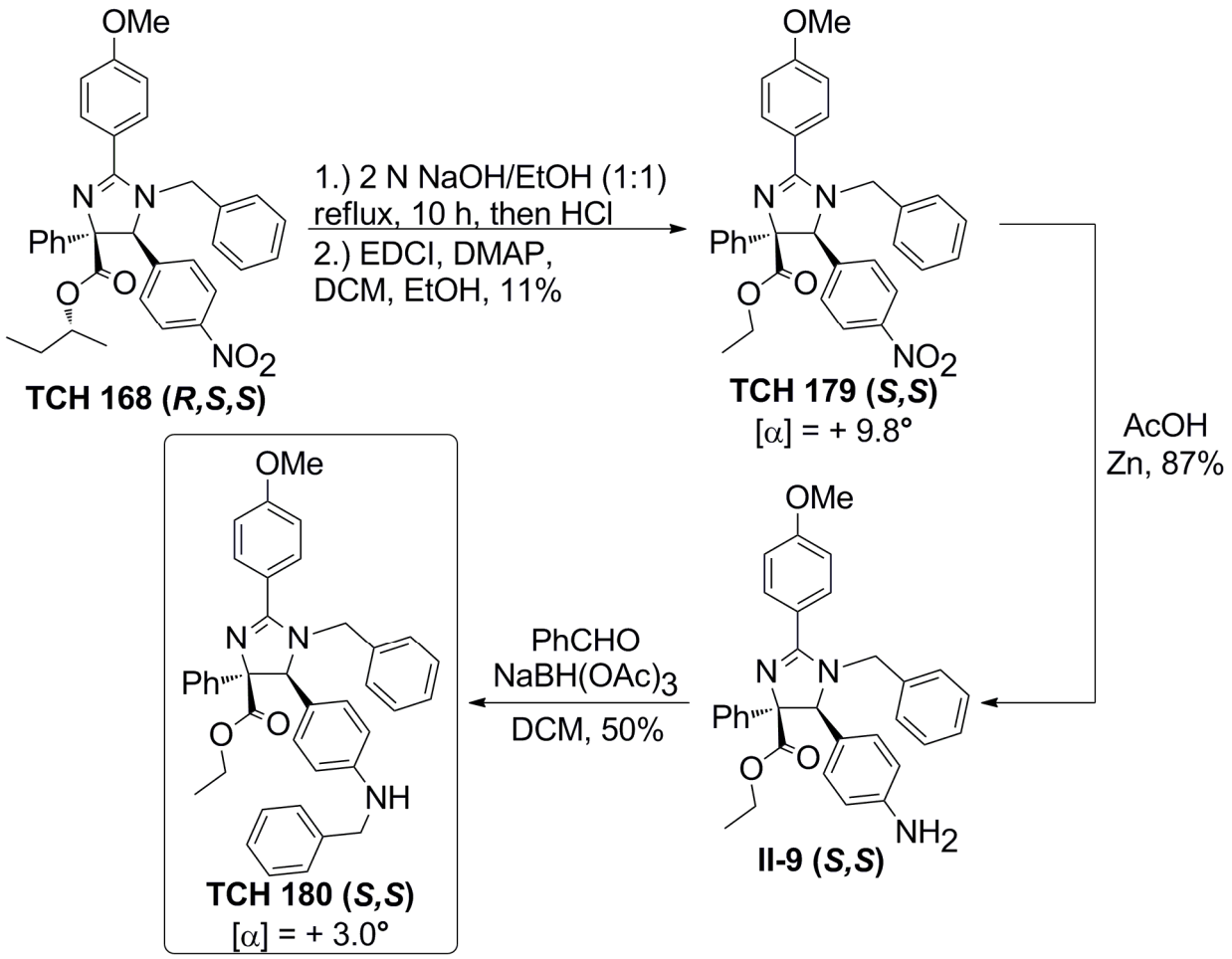

Scheme II-10. Synthesis of enantiopure **TCH 180 (*S,S*)**.

In order to insure that **TCH 178 (*R,R*)** and **TCH 180 (*S,S*)** are indeed enantiopure compounds, their corresponding optical rotations were measured (Table II-1). For all optical rotations found in Table II-1, a concentration of 1 mg/mL was used. The nitro intermediates **TCH 177 (*R,R*)** and **TCH 179 (*S,S*)** have corresponding optical rotations of $[\alpha]_D^{20}$ = -11.2° and +9.8° respectively. The enantiomers of **TCH 165**, **TCH 178 (*R,R*)** and **TCH 180 (*S,S*)** have optical rotations of $[\alpha]_D^{20}$ = -4.5° and +3.0° respectively. In both sets of measurements, the optical rotations are opposite in sign as expected for enantiomers. The small differences in optical rotation values observed are likely a result of small variations in solution concentration.

Table II-1. Measured optical rotations of **TCH 178 (*R,R*)**, **TCH 180 (*S,S*)** and their nitro derivatives.*

Compound	Optical Rotation $[\alpha]_D^{20}$
TCH 177 (*R,R*)	- 11.2 °
TCH 178 (*R,R)*	- 4.5 °
TCH 179 (*S,S*)	+ 9.8 °
TCH 180(*S,S*)	+ 3.0 °

**All measurements were collected at 20℃ with a wavelengt h of 589 nm. All solution concentrations were 1 mg/mL.*

At this point **TCH 165** has been resolved into its enantiomers **TCH 178 (*R,R*)** and **TCH 180 (*S,S*).** Additionally, **TCH 165** diastereomeric analogs **TCH 170 (*R,R,R*)** and **TCH 171 (R,S,S)** have been synthesized (Scheme II-5). In addition to evaluating the biological activity of these chiral imidazolines, it was desirable to synthesize a few additional analogs of **TCH 165** for a terse structure activity relationship (SAR) study.

G. Synthesis of additional TCH 165 analogs

Starting with racemic ethyl ester **TCH 152**, several analogs were prepared to elucidate the importance of the ethyl ester moiety found in **TCH 165**. Reduction of **TCH 152** with 1 equivalent of $LiBH_4$ afforded alcohol **TCH 181** in 56% yield (Scheme II-11).

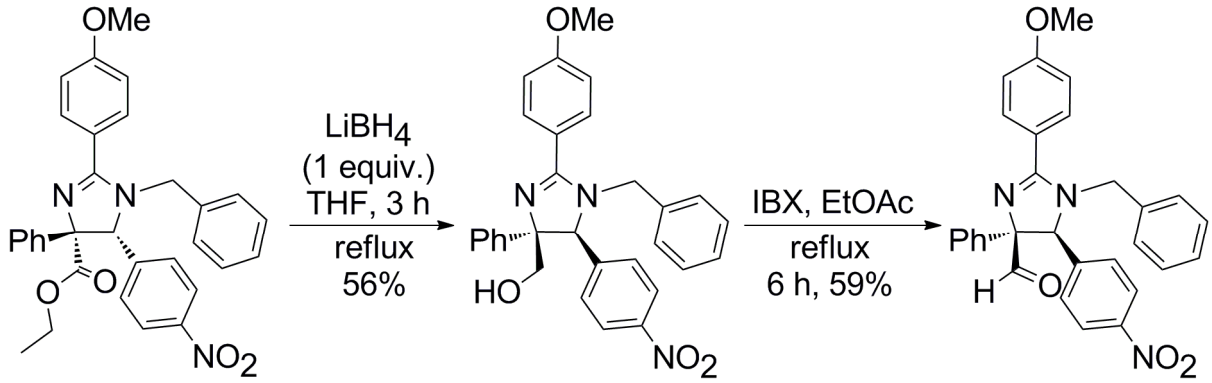

TCH 152 *racemic* **TCH 181** *racemic* **TCH 182** *racemic*

Scheme II-11. Analogs of **TCH 152.**

The use of 2 equivalents of $LiBH_4$ did not increase the yield (only 53% yield of **TCH 181**). Subsequent oxidation of **TCH 181** with IBX afforded aldehyde **TCH 182** in 59% yield.

A final synthetic effort was to prepare a derivative of **TCH 165** that would hopefully have greater solubility in water. Being a rather greasy molecule, **TCH 165** has limited solubility, even when administered as the HCl salt. Treatment of **TCH 165** HCl salt with BBr_3 afforded alcohol **TCH 183** in 19% yield (Scheme II-12). Although using an excess of BBr_3 (13 equiv.) seems extremely harsh, treatment with 3 equivalents of BBr_3 and refluxing conditions does not show any sign of reactivity (no decomposition nor product formation observed).

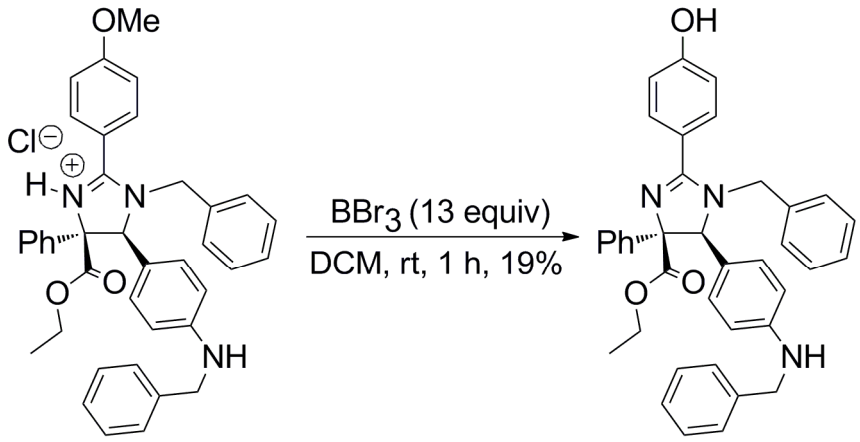

TCH 165 *racemic*

TCH 183 *racemic*

Scheme II-12. Demethylation of **TCH 165**.

At this point a handful of imidazolines have been synthesized for proteasome evaluation and expansion of the **TCH** imidazoline library. As a final synthetic effort, it was desirable to synthesize several imidazole and β-lactam derivatives to insure that the imidazoline core is critical for the observed biological activity.

H. β-lactam and imidazole derivatives as negative controls for proteasome inhibition

One of the interesting side products isolated during the synthesis of **TCH 165** is β-lactam **TCH 172**, which is the constitutional isomer of **II-4** (Scheme II-1). As described previously this β-lactam forms as a result of a competing [2+2] cyclization reaction (refer to Scheme II-2). **TCH 172** was reduced with zinc to afford amine **TCH 174** in 54% yield (Scheme II-13). Additionally, imidazole **TCH 173** was isolated during the initial (*R*)-2 butanol reactions as a side product when using oxalyl chloride instead of EDCI (refer to Scheme II-4). Imidazole **TCH 173** was reduced to amine **TCH 175** in 34% yield (Scheme II-13). Note that **TCH 173** and **TCH 175** are the imidazole analogs of **TCH 152** and **TCH 157** respectively (refer to Scheme II-1). Additionally, **TCH 172** and **TCH 174** are the β-lactam analogs of **TCH 152** and **TCH 157** respectively. These analogs will provide further insight into the importance of the imidazoline scaffold when evaluated for proteasome inhibition.

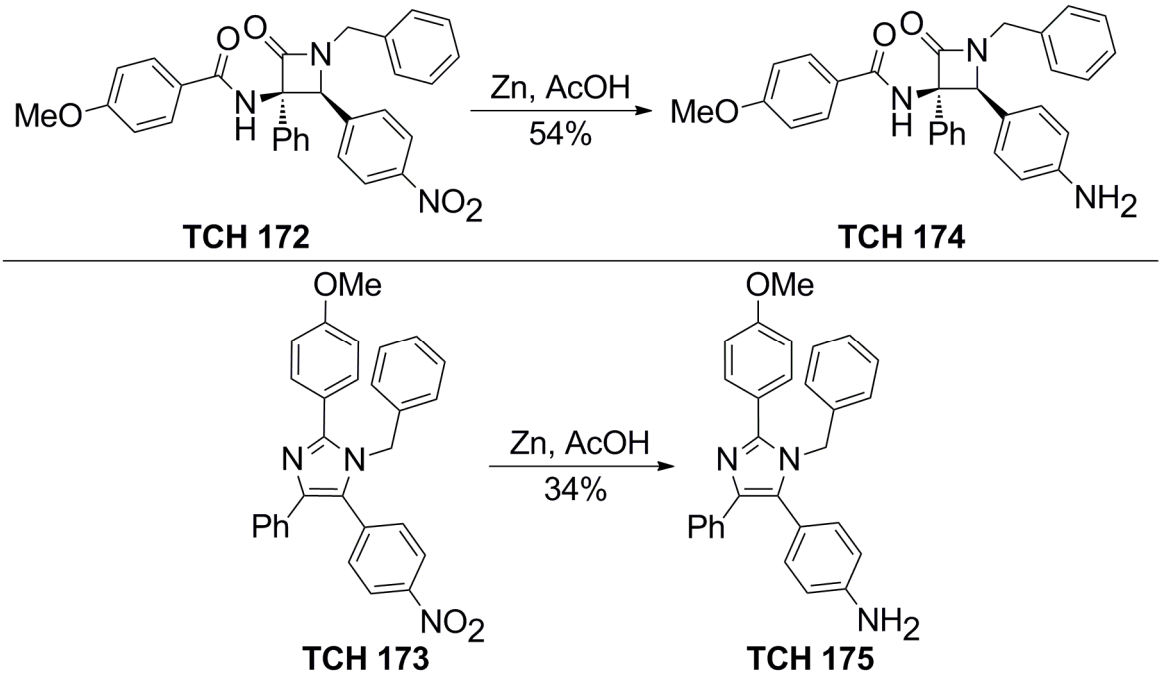

Scheme II-13. β-lactam and imidazole analogs of **TCH 152** and **TCH 157**.

I. Proteasome inhibition by novel TCH imidazolines

Having synthesized several novel imidazolines, these compounds were tested by Teri Lansdell for biological activity. The aforementioned imidazolines (with a designated **TCH** number) have been tested for CT-L inhibition of the h20S proteasome. Previously, racemic **TCH 013** has been resolved into enantiomers **TCH 017 (*S,S*)** and **TCH 018 (*R,R*)** (see Figure II-9). Surprisingly, the separated enantiomers do not show statistically significant differences in proteasome inhibition as shown in Figure II-13.

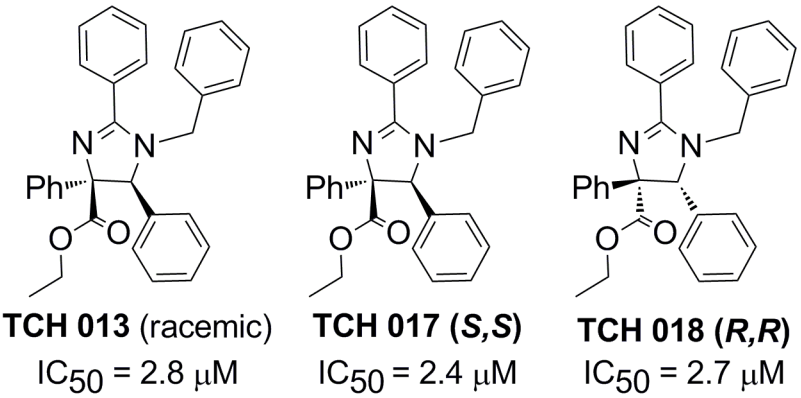

TCH 013 (racemic) IC_{50} = 2.8 μM

TCH 017 (*S,S*) IC_{50} = 2.4 μM

TCH 018 (*R,R*) IC_{50} = 2.7 μM

Figure II-13. h20S proteasome IC_{50} values for the separated enantiomers of **TCH 013**.

Having synthesized the *sec*-butyl ester diastereomer analogs of **TCH 165** (**TCH 170 (*R,R,R*)** and **TCH 171 (*R,S,S*)**) (Scheme II-5), it could now be determined if this apparent lack enantioselectivity found with **TCH 013** in the h20S proteasome was also conserved with the **TCH 165** diastereomers. Figure II-14 contains the h20S proteasome IC_{50} values for diastereomers **TCH 170 (*R,R,R*)** and **TCH 171 (*R,S,S*)**. Notably, there is no significant difference in proteasome inhibition between the separated diastereomers and racemic **TCH 165**. Imidazolines **TCH 170 (*R,R,R*)** and **TCH 171 (*R*,S,S)** have IC_{50} = 310 nM and 306 nM respectively. In comparison, racemic **TCH 165** has an IC_{50} = 291 nM (Figure II-14). This small difference in activity observed between **TCH 170 (*R,R,R*)**,

TCH 171 (*R,S,S*) and **TCH 165** indicates that substitution of the ethyl ester for a *sec*-butyl ester did not significantly affect proteasome activity. Thereby, this indicates that the trend observed for diastereomers **TCH 170 (*R,R,R*)** and **TCH 171 (R,S,S)** is probably indicative of the trend expected for the separated enantiomers of **TCH 165**.

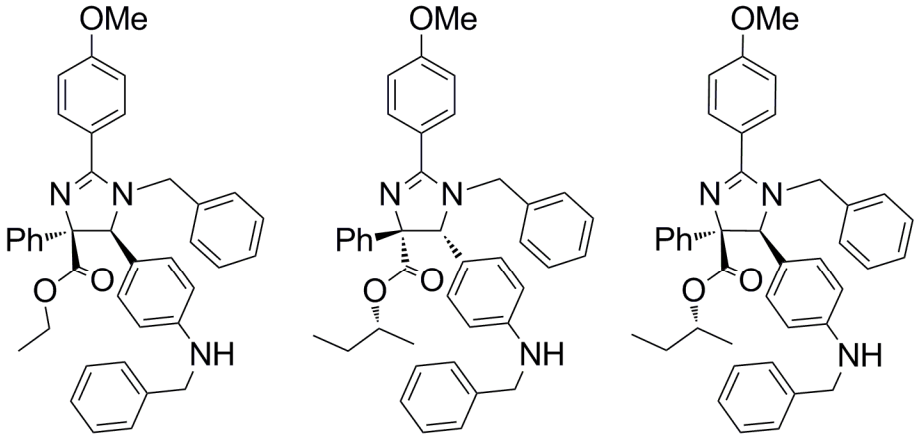

TCH 165 (racemic) IC_{50} = 291 nM

TCH 170 (*R,R,R*) IC_{50} = 310 nM

TCH 171(*R,S,S*) IC_{50} = 306 nM

Figure II-14. h20S proteasome IC_{50} values for *sec*-butyl ester diastereomer analogs of **TCH 165**.

Additionally, the diastereomeric intermediates from the syntheses of **TCH 170 (*R,R,R*)** and **TCH 171 (*R,S,S*)** (Scheme II-5) were also evaluated for proteasome inhibition as shown in Figure II-15. **TCH 167 (*R,R,R*)** and **TCH 168 (*R,S,S*)** are the diastereomeric analogs of **TCH 152** and have IC_{50} values of 1.6 and 2.3 μM respectively (Figure II-15). The corresponding racemic **TCH 152** has an IC_{50} = 2.3 μM, showing no significant difference in activity between the diastereomers.

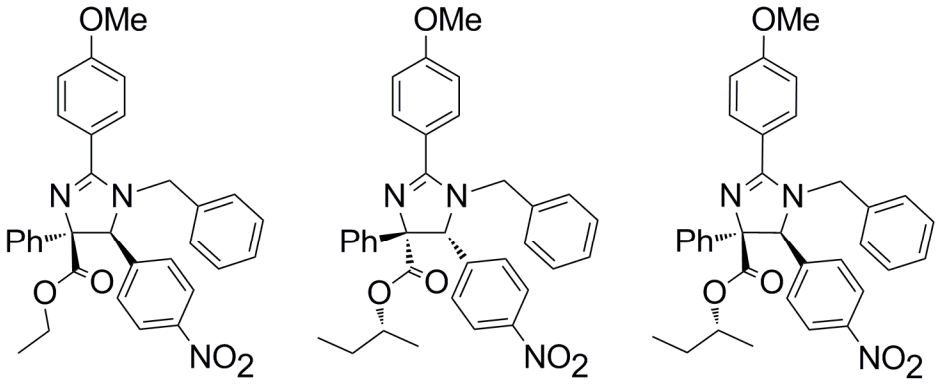

TCH 152 (racemic) IC_{50} = 2.3 μM

TCH 167 (*R,R,R*) IC_{50} = 1.6 μM

TCH 168 (*R,S,S*) IC_{50} = 2.3 μM

Figure II-15. h20S proteasome activity of *sec*-butyl ester analogs of **TCH 152**.

Although the aforementioned series of diastereomers showed no apparent enantioselectivity for proteasome inhibition, the actual enantiomers of **TCH 165** were also evaluated for biological activity. The proteasome IC_{50} values for the enantiomers of **TCH 165** and their corresponding enantiopure intermediates are found in Figure II-16. Nitro imidazoline **TCH 152** has an IC_{50} = 2.3 μM. The corresponding enantiopure analogs **TCH 177 (*R,R*)** and **TCH 179 (*S,S*)** have an IC_{50} = 3.3 μM (95% confidence interval: 3.0 to 3.7 μM) and 4.1 μM (95% confidence interval: 3.3 to 4.9 μM) respectively. This indicates no significant difference in activity between the enantiomers.

The actual enantiomers of **TCH 165** (IC_{50} = 225 nM; 95% confidence interval: 146 to 346 nM) were also evaluated for proteasome inhibition (Figure II-16). **TCH 178 (*R,R*)** has an IC_{50} = 297 nM (95% confidence interval: 287 to 307 nM), whereas **TCH 180 (*S,S*)** has an IC_{50} = 369 nM (95% confidence interval: 321 to 425 nM). As seen previously, there is no significant difference in activity between the enantiomers. The small decrease in potency observed with **TCH 178 (*R,R*)** and **TCH 180 (*S,S*)** compared

to racemic **TCH 165** can be attributed to having been synthesized by a slightly different synthetic route or a small difference in the stock solution concentrations. After testing both the diastereomer analogs of **TCH 165**, as well as the actual enantiomers of **TCH 165**, there is no apparent selectivity for one enantiomer over another by the h20S proteasome.

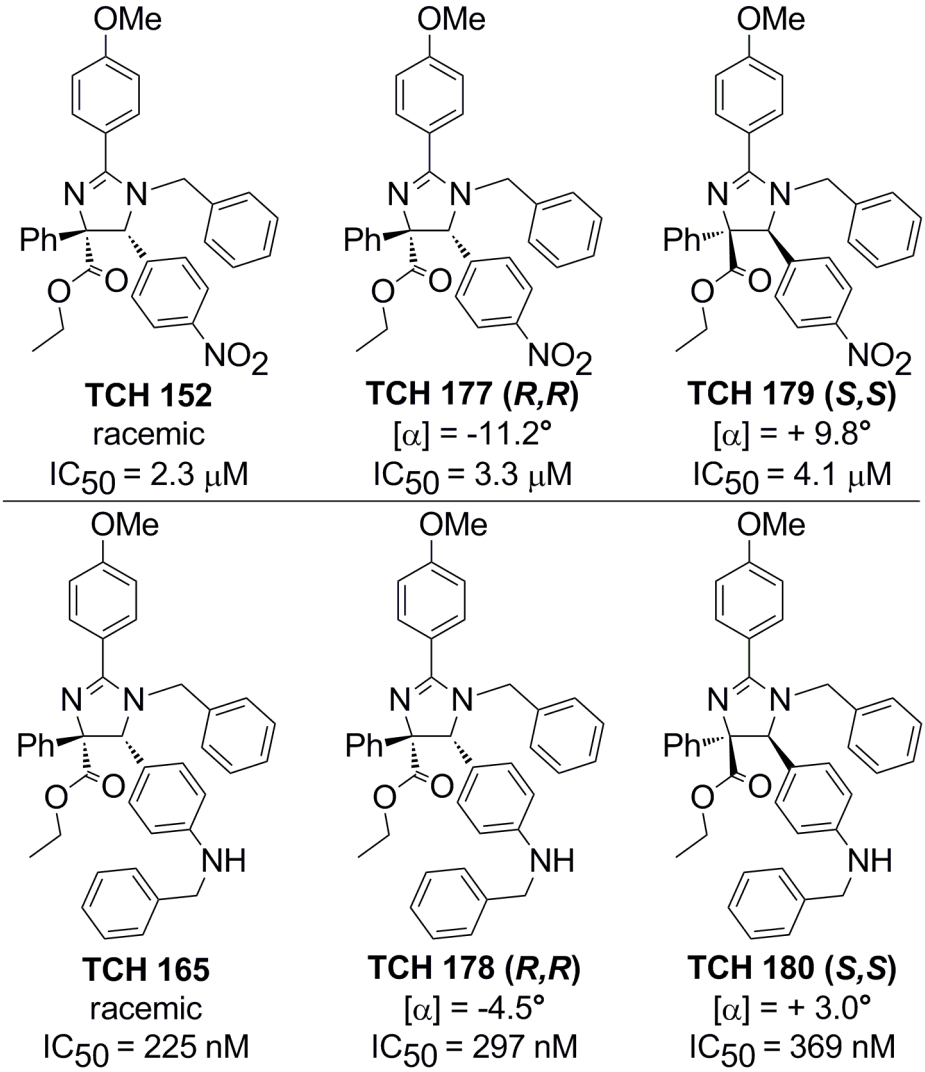

TCH 152
racemic
IC_{50} = 2.3 μM

TCH 177 (*R,R*)
[α] = -11.2°
IC_{50} = 3.3 μM

TCH 179 (*S,S*)
[α] = + 9.8°
IC_{50} = 4.1 μM

TCH 165
racemic
IC_{50} = 225 nM

TCH 178 (*R,R*)
[α] = -4.5°
IC_{50} = 297 nM

TCH 180 (*S,S*)
[α] = + 3.0°
IC_{50} = 369 nM

Figure II-16. h20S proteasome IC_{50} values for **TCH 178 (*R,R*)**, **TCH 180(*S,S*)** and their precursors.

To further understand the importance of the imidazoline scaffold for proteasome inhibition, several imidazole and β-lactam analogs were compared to a structurally

related imidazoline (Figure II-17). The nitro imidazoline **TCH 152** has an IC_{50} = 2.3 μM; however, imidazole analog **TCH 173** (IC_{50} > 10 μM) and β-lactam **TCH 172** (IC_{50} > 10 μM) are inactive compounds. Additionally, amine **TCH 157** (IC_{50} = 1.2 μM) is slightly more potent than its nitro precursor (**TCH 152**). However, the structurally similar amines **TCH 175** (IC_{50} > 10 μM) and **TCH 174** (IC_{50} > 10 μM) are also biologically inactive. These results indicate that the imidazoline scaffold is critical for the observed proteasome activity.

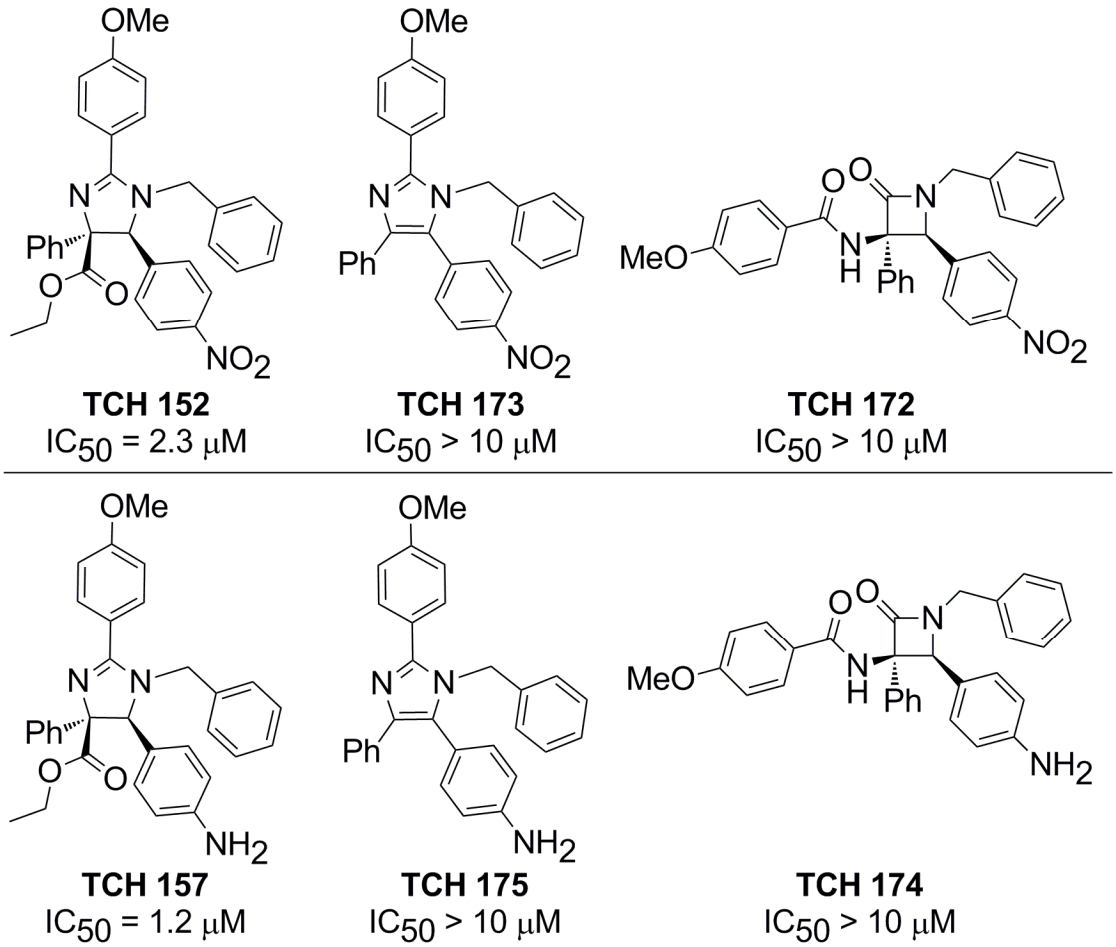

Figure II-17. Proteasome IC_{50} values for imidazole and β-lactam analogs of imidazolines **TCH 152** and **TCH 157**.

Several analogs of **TCH 152** were investigated to understand the importance of the ethyl ester moiety found within the imidazolines. Compared to **TCH 152** (IC_{50} = 2.3 μM), the alcohol derivative **TCH 181** is a more potent inhibitor (IC_{50} = 883 nM; 95% confidence interval: 829 to 943 nM). This indicates that the ethyl ester moiety is not entirely essential for the activity found in many of the imidazolines. Additionally, **TCH 181** is a promising candidate for further study because of its predicted better solubility in water (ClogP = 5.84). The aldehyde analog **TCH 182** is found not to be significantly more potent (IC_{50} = 1.4 μM; 95% confidence interval: 1.3 to 1.5 μM) than **TCH 152**.

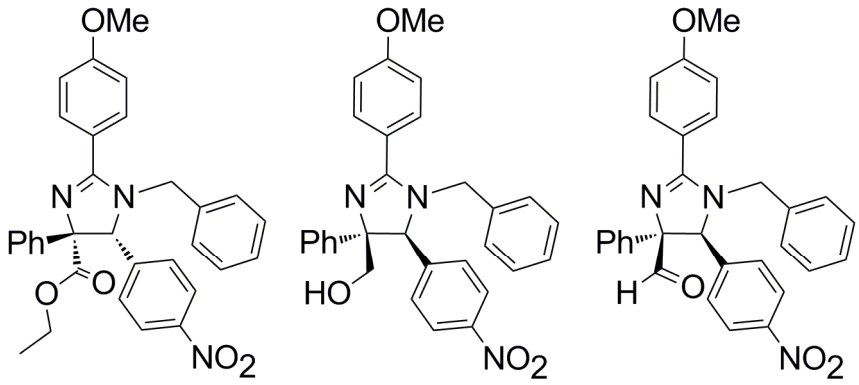

Figure II-18. Analysis of the ethyl ester moiety found in **TCH** imidazolines**.**

The final compound analyzed for proteasome inhibition is the free alcohol derivative of **TCH 165** (Figure II-19). **TCH 183** has an IC_{50} = 394 nM (95% confidence interval: 333 to 465 nM). Therefore, **TCH 183** appears to be a potent inhibitor of the h20S proteasome in comparison to **TCH 165** (IC_{50} = 225 nM; 95% confidence interval: 146 to 346 nM). Additionally, it is expected that **TCH 183** should have slightly better solubility in water due to the presence of the free hydroxyl group.

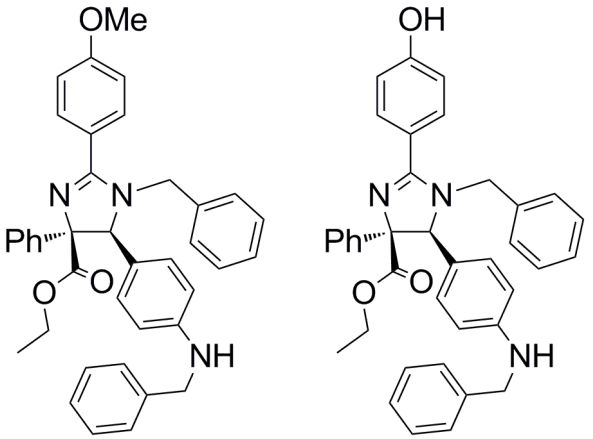

TCH 165 (racemic) IC_{50} = 225 nM

TCH 183 (racemic) IC_{50} = 394 nM

Figure II-19. Demethylated derivative of **TCH 165**.

J. Conclusion

Through the evaluation of a series of chiral imidazolines, no apparent enantioselectivity preference by the h20S proteasome has been observed. By the synthesis of imidazole and β-lactam analogs, it is apparent that the imidazoline core is essential for proteasome activity. The synthesis of several imidazolines possessing a free hydroxyl group has yielded imidazolines with comparable IC_{50} values. Additional investigation of these hydroxyl containing imidazolines is desirable in hopes of improving the solubility of these compounds in water.

K. Experimental Section

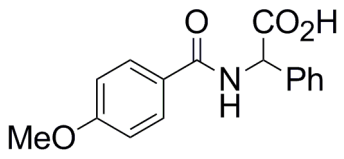

II-1

2-(4-methoxybenzamido)-2-phenylacetic acid (II-1).[13] DL-α-phenylglycine (6.00 g, 39.69 mmol) was added to a 1 N NaOH solution (100 mL) and cooled to 0℃.

Thereafter 4-methoxybenzoyl chloride (6.00 mL, 43.66 mmol) was added dropwise via an addition funnel under N_2. The mixture was allowed to warm to room temperature and react for 18 h. The reaction was quenched with 10% HCl solution (*v*/*v*, 50 mL) and Brine (200 mL) to improve separation. The aqueous layer was then extracted with EtOAc (3 x 250 mL). The combined organics were concentrated *in vacuo* and then dissolved in methanol (500 mL) and dried with Na_2SO_4. The organics were concentrated *in vacuo* and the crude mixture was dissolved in boiling EtOAc/Hexanes (1:1, 600 mL). The mixture was filtered while hot collecting a white precipitate **II-1**. The filtrate sat at room temperature and after several days additional precipitate **II-1** was collected. The combined precipitates afforded carboxylic acid **II-1** (7.99 g, 71% yield from DL-α-phenylglycine). *Notebook reference: ML-II-47.*

^{1}H NMR (500 MHz) (d_6-DMSO) δ: 3.80 (s, 3H), 5.58 (d, J = 7.5 Hz, 1H), 6.97-7.00 (m, 2H), 7.30-7.39 (m, 3H), 7.47-7.49 (m, 2H), 7.89-7.92 (m, 2H), 8.83 (d, J = 7.5 Hz, 1H), 12.85 (bs, 1H). ^{13}C NMR (125 MHz) (d_6-DMSO) δ: 55.3, 56.7, 113.3, 125.9, 127.8, 128.1, 128.3, 129.5, 137.3, 161.7, 165.6, 172.0. m.p. 186-188°C.

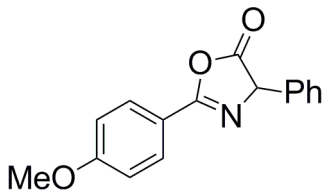

II-2

2-(4-methoxyphenyl)-4-phenyloxazol-5(4H)-one (II-2).[13] In a flame dried flask under N_2, carboxylic acid **II-1** (4.00 g, 14.02 mmol) was dissolved in dry DCM (50 mL). Thereafter trifluoroacetic anhydride (2.14 mL, 15.42 mmol) was added dropwise at room

temperature. After 18 h the reaction was quenched with $NaHCO_3$ (1 x 50 mL, added slowly). The organic layer was separated, and the remaining aqueous layer was extracted with additional DCM (2 x 50 mL). The combined organics were concentrated *in vacuo* affording phenylazlactone **II-2** (3.30 g, yellow solid, 88% yield from **II-1**). *Notebook reference*: *ML-II-41*.

^{1}H NMR (500 MHz) ($CDCl_3$) δ: 3.89 (s, 3H), 5.49 (s, 1H), 7.00-7.02 (m, 2H), 7.35-7.46 (m, 5H), 8.03-8.05 (m, 2H). ^{13}C NMR (125 MHz) ($CDCl_3$) δ: 55.7, 68.3, 114.5, 118.1, 127.0, 128.8, 129.1, 130.2, 134.0, 162.4, 163.6, 176.6. m.p. 113-116 °C.

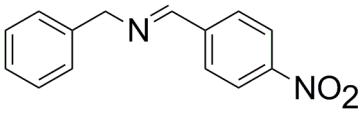

II-3

(E)-N-(4-nitrobenzylidene)-1-phenylmethanamine (II-3).[13] To a flame dried flask under N_2, 4-nitrobenzaldehyde (4.23 g, 28.00 mmol) was dissolved in dry benzene (275 mL). Thereafter benzylamine (3.06 mL, 28.00 mmol) was added. The flask was connected to a 10 mL Dean-Stark trap (containing Na_2SO_4) and reflux condenser. The reaction refluxed for 20 h. Thereafter the mixture was cooled and concentrated *in vacuo*. The brown oil was placed on the vacuum pump and solidified overnight affording imine **II-3** (6.73 g, brown oil, quantitative yield from benzylamine). *Notebook reference: ML-II-40*.

^{1}H NMR (500 MHz) ($CDCl_3$) δ: 4.89 (s, 2H), 7.28-7.39 (m, 5H), 7.95 (d, J = 8.8 Hz, 2H), 8.27 (d, J = 8.8 Hz, 2H), 8.47 (s, 1H). ^{13}C NMR (125 MHz) ($CDCl_3$) δ: 65.3, 124.0, 127.4, 128.2, 128.8, 129.1, 138.6, 141.7, 149.2, 159.5. m.p. 52-54 °C.

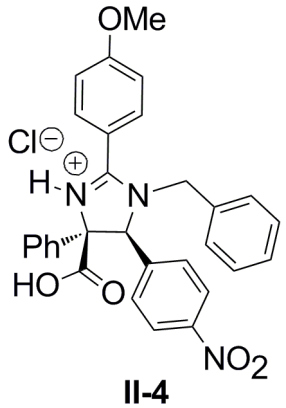

II-4

(4S,5S)-1-benzyl-4-carboxy-2-(4-methoxyphenyl)-5-(4-nitrophenyl)-4-phenyl-4,5-dihydro-1H-imidazol-3-ium chloride (II-4).[13] In a flame dried flask under N_2, phenylazlactone **II-2** (11.90 g, 44.52 mmol) was dissolved in dry DCM (200 mL) at room temperature. Thereafter imine **II-3** (12.84 g, 53.43 mmol) and freshly distilled TMSCl (6.8 mL, 53.43 mmol) were subsequently added. The mixture was allowed to reflux for 17 h and then was concentrated *in vacuo*. Additional DCM was added to the crude mixture and concentrated *in vacuo* a second time at 55 ℃ to help remove excess TMSCl. The resulting yellow/orange foam was placed on the vacuum line for 2.5 h. EtOAc (300 mL) was then added and allowed to stir for several hours. The resulting precipitate was collected by filtration and determined to be approximately a 2:1 ratio of **II-4** and β-lactam **TCH 172**. This precipitate was stirred in boiling ethyl acetate (500 mL) for 10 minutes and filtered while hot. The collected precipitate afforded the HCl salt **II-4** (8.23 g, off white solid, 34% yield from phenylazlactone **II-2**). The concentrated filtrate

contained β-lactam **TCH 172** (4.83 g, solid, 20% yield from phenylazlactone **II-2**) and the associated spectroscopy date is found in a separate entry. *Notebook reference: ML-II-75*.

^{1}H NMR (500 MHz) (d_6-DMSO) δ: 3.91 (s, 3H), 4.30 (d, J = 16.0 Hz, 1H), 4.95 (d, J = 16.0 Hz, 1H), 5.77 (s, 1H), 6.74 (d, J = 7.3 Hz, 2H), 7.08 (t, J = 7.7 Hz, 2H), 7.17 (t, J = 7.4 Hz, 1H), 7.27 (d, J = 8.8 Hz, 2H), 7.44-7.56 (m, 3H), 7.77 (d, J = 7.2 Hz, 2H), 7.88 (d, J = 8.8 Hz, 2H), 8.01-8.06 (m, 2H), 8.33 (d, J = 8.7 Hz, 2H), 12.70 (bs, 1H). ^{13}C NMR (125 MHz) (d_6-DMSO) δ: 49.3, 55.9, 72.4, 75.8, 112.8, 114.9, 123.8, 125.8, 127.3, 128.2, 128.6, 128.8, 129.0, 130.1, 132.2, 133.2, 139.0, 140.6, 148.2, 163.9, 165.6, 167.4. IR (NaCl, neat): 2637, 2510, 2397, 1719, 1610, 1522, 1505, 1349, 1262, 1219, 1180 cm^{-1}. HRMS (ESI): m/z calcd for $C_{30}H_{26}N_3O_5^+$ $[M+H]^+$ 508.1872; found, 508.1886. m.p. 190-192 °C.

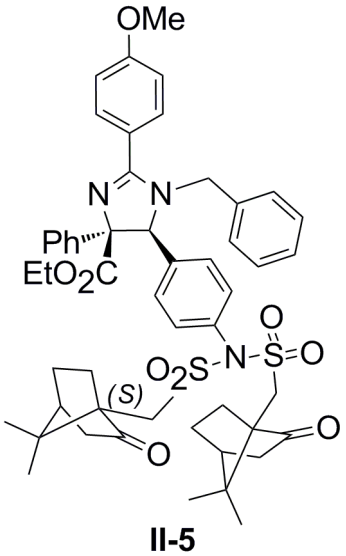

II-5

(4S,5S)-ethyl 1-benzyl-5-(4-(1-(7,7-dimethyl-2-oxobicyclo[2.2.1]heptan-1-yl)-N-((((1S,4S)-7,7-dimethyl-2-oxobicyclo[2.2.1]heptan-1-

yl)methyl)sulfonyl)methylsulfonamido)phenyl)-2-(4-methoxyphenyl)-4-phenyl-4,5-dihydro-1H-imidazole-4-carboxylate (II-5).

To dry DCM (5 mL), amine **TCH 157** (0.027 g, 0.053 mmol) and TEA (30 µL, 0.22 mmol) were subsequently added. This solution was cooled to 0 ℃ and cannulated over a 30 minute period to a solution of DCM (5 mL) and 1*S*-(+)-camphor-10-sulfonylchloride (0.040 g, 0.16 mmol) at 0 ℃. The mixture was allowed to react for 1 h. Thereafter the reaction was quenched at 0 ℃ with 0.5 M HCl (10 mL) and the organic layer was isolated. The aqueous layer was extracted with additional DCM (2 x 15 mL). The combined organic layers were washed with H_2O (1 x 20 mL), dried with Na_2SO_4 and concentrated *in vacuo*. Purified crude material via flash chromatography (TEA neutralized silica, 55:45 DCM/Hexanes, then 7:3 DCM/Hexanes, then 100 DCM; then 40:60 EtOAc/Hexane) affording **II-5** (0.022 g, solid, 57% yield from **TCH 157**). *Notebook reference: ML-II-54.*

^{1}H NMR (500 MHz) ($CDCl_3$) δ: 0.82 (t, *J* = 7.1 Hz, 3H), 0.96 (s, 6H), 1.19 (s, 6H), 1.37-1.51 (m, 2H), 1.55-1.69 (m, 2H), 1.91–2.21 (m, 6H), 2.36-2.58 (m, 4H), 3.43-3.73 (m, 2H), 3.75-3.85 (m, 2H), 3.88 (s, 3H), 3.91-4.03 (m, 3H), 4.68 (dd, *J* = 9.1, 15.8 Hz, 1H), 4.96 (s, 1H), 6.77-6.79 (m, 2H), 6.97-7.18 (m, 5H), 7.24-7.39 (m, 3H), 7.44-7.52 (m, 8H), 7.65-7.82 (m, 4H). ^{13}CNMR (125 MHz) ($CDCl_3$) δ: 13.63, 13.66, 19.7, 20.06, 20.08, 25.32, 26.9, 42.45, 42.46, 42.71, 42.72, 47.9, 49.4, 52.8, 55.4, 58.85, 58.88, 61.4, 73.04, 73.09, 114.0, 122.5, 126.84, 126.85, 127.26, 127.31, 127.4, 128.0, 128.36, 128.38, 130.57, 130.61, 131.0, 133.33, 133.38, 136.5, 141.2, 144.1, 161.3, 165.4, 170.53, 213.7, 213.8 (extra peaks likely due to diastereomers). IR (NaCl, neat): 2959,

2926, 1746, 1613, 1514, 1378, 1356, 1252, 1160 cm^{-1}. HRMS (ESI): m/z calcd for $C_{52}H_{60}N_3O_9S_2$ $[M+H]^+$ 934.3771; found, 934.3730.m.p. 102-104 °C.

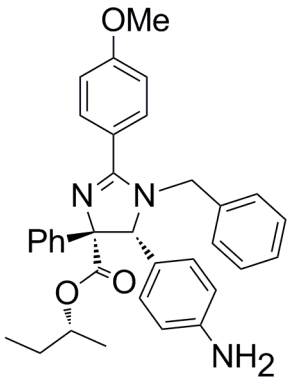

II-6 (*R,R,R*)

(4S,5S)-(R)-sec-butyl 5-(4-aminophenyl)-1-benzyl-2-(4-methoxyphenyl)-4-phenyl-4,5-dihydro-1H-imidazole-4-carboxylate (II-6 (*R,R,R*)). To a flame dried under N_2 **TCH 167 (*R,R,R*)** (0.103 g, 0.18 mmol) wad added to glacial acetic acid (5 mL). Thereafter zinc dust (0.430 g, 6.58 mmol) was added. After 40 minutes the reaction mixture was filtered, and the filtrate was neutralized with saturated $NaHCO_3$ (30 mL plus additional $NaHCO_3$ (s)). The aqueous mixture was extracted with DCM (3 x 10 mL). The combined organics were washed with saturated $NaHCO_3$ (1 x 30 mL), dried with Na_2SO_4 and concentrated *in vacuo*. The crude material was purified via flash chromatography (silica neutralized with TEA, 6:4 EtOAc/Hexanes) affording amine **II-6 (*R,R,R*)** (0.046 g, solid, 48% yield from **TCH 167 (*R,R,R*)**). *Notebook reference: ML-II-63*.

^1H NMR (500 MHz) ($CDCl_3$) δ: 0.60 (t, J = 7.5 Hz, 3H), 0.90 (d, J = 6.3 Hz, 3H), 1.08-1.30 (m, 2H), 3.71 (bs, 2H), 3.82 (d, J = 16.0 Hz, 1H), 3.86 (s, 3H), 4.45 (dd, J =

12.4, 6.2 Hz, 1H), 4.59 (d, J = 15.9 Hz, 1H), 4.81 (s, 1H), 6.67 (d, J = 7.9 Hz, 2H), 6.79 (d, J = 7.3 Hz, 2H), 6.97-7.00 (m, 2H), 7.09-7.19 (m, 6H), 7.26-7.34 (m, 4H), 7.68-7.70 (m, 2H), 7.75-7.77 (m, 2H). ^{13}C NMR (125 MHz) ($CDCl_3$) δ: 9.3, 18.5, 28.1, 48.5, 55.4, 73.2, 73.5, 82.5, 114.0, 115.1,123.4, 127.0, 127.18, 127.24, 127.26, 127.7, 127.9, 128.4, 129.6, 130.4, 137.3, 144.7, 146.6, 161.1, 165.1, 170.7. IR (NaCl, neat): 3456, 3371, 3208, 2968, 2928, 2853, 1724, 1614, 1515, 1447, 1423, 1252, 1175 cm^{-1}. HRMS (ESI): m/z calcd for $C_{34}H_{36}N_3O_3$ $[M+H]^+$ 534.2757; found, 534.2760. m.p. 52-54 °C.

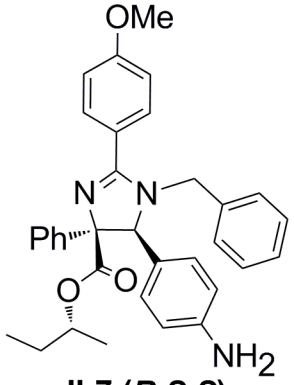

II-7 (*R,S,S*)

(4R,5R)-(R)-sec-butyl 5-(4-aminophenyl)-1-benzyl-2-(4-methoxyphenyl)-4-phenyl-4,5-dihydro-1H-imidazole-4-carboxylate (II-7 (*R,S,S*)). To a flame dried flask under N_2, **TCH 168 (*R,S,S*)** (0.096 g, 0.17 mmol) was dissolved in glacial acetic acid (2 mL). Thereafter zinc dust (0.430 g, 6.13 mmol) was added. After 30 minutes the mixture was filtered, and the filtrate was neutralized with saturated $NaHCO_3$ (30 mL and additional $NaHCO_3$ (s) until pH = 9). The aqueous mixture was extracted with DCM (3 x 15 mL), and brine was added to improve separation of the layers. The combined organics were washed with $NaHCO_3$ (1 x 30 mL), dried with Na_2SO_4 and concentrated

in vacuo affording amine **II-7 (R,S,S)** (0.068 g, solid, 75% yield from **TCH 168 (*R,S,S*)**). *Notebook reference: ML-II-65.*

^{1}H NMR (500 MHz) ($CDCl_3$) δ: 0.55 (t, J = 7.4 Hz, 3H), 0.61 (d, J = 6.2 Hz, 3H), 1.22-1.31 (m, 2H), 3.75 (bs, 2H), 3.79-3.83 (m, 4H), 4.44 (dd, J = 12.4, 6.2 Hz, 1H), 4.58 (d, J = 15.8 Hz, 1H), 4.83 (s, 1H), 6.65 (d, J = 7.9 Hz, 2H), 6.80 (d, J = 7.3 Hz, 2H), 6.96 (d, J = 8.3 Hz, 2H), 7.09-7.32 (m, 8H), 7.67 (d, J = 8.3 Hz, 2H), 7.74 (d, J = 7.3 Hz, 2H). ^{13}C NMR (125 MHz) ($CDCl_3$) δ: 9.3, 18.3, 28.5, 48.4, 55.4, 72.9, 73.0, 82.4, 113.9, 115.0, 123.3, 126.9, 127.17, 127.23, 127.25, 127.83, 127.87, 128.4, 129.5, 130.4, 137.4, 144.6, 146.7, 161.1, 164.8, 170.6. HRMS (ESI): m/z calcd for $C_{34}H_{36}N_3O_3$ $[M+H]^+$ 534.2757; found, 534.2758.

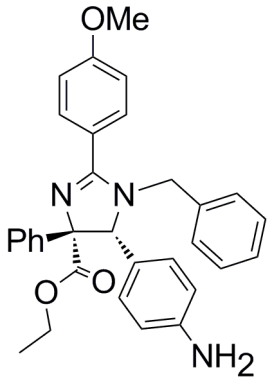

II-8 (*R,R*)

(4R,5R)-ethyl 5-(4-aminophenyl)-1-benzyl-2-(4-methoxyphenyl)-4-phenyl-4,5-dihydro-1H-imidazole-4-carboxylate (II-8 (*R,R*)). Followed procedure for **TCH 157** using enantiopure starting material **TCH 177 (*R,R*)**. ^{1}H and ^{13}C NMR spectra consistent with racemic **TCH 157**.

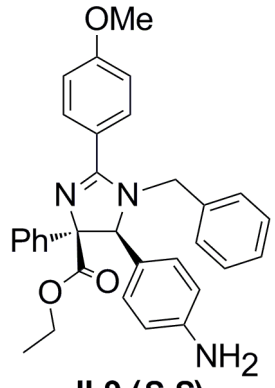

II-9 (*S,S*)

(4S,5S)-ethyl 5-(4-aminophenyl)-1-benzyl-2-(4-methoxyphenyl)-4-phenyl-4,5-dihydro-1H-imidazole-4-carboxylate (II-9 (*S,S*)). Followed procedure for **TCH 157** using enantiopure starting material **TCH 179 (*S,S*)**. ^{1}H and ^{13}C NMR spectra consistent with racemic **TCH 157**.

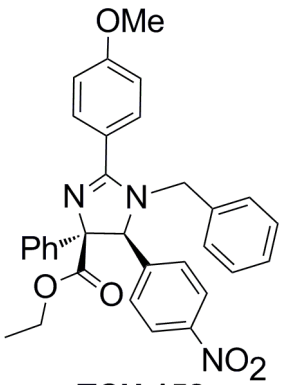

TCH 152

(4S,5S)-ethyl 1-benzyl-2-(4-methoxyphenyl)-5-(4-nitrophenyl)-4-phenyl-4,5-dihydro-1H-imidazole-4-carboxylate (TCH 152).[13] To a flame dried flask under N_2, HCl salt **II-4** (0.445 g, 0.82 mmol) was dissolved in dry DCM (25 mL) and cooled to 0 ℃. Thereafter oxalyl chloride (0.21 mL, 2.45 mmol) was added over 10 minutes followed by the addition of anhydrous pyridine (0.25 mL, 3.09 mmol). The reaction stirred for 2 h at 0 ℃ and then was concentrated *in vacuo*. The crude mixture was placed on the vacuum line for 20 minutes. Thereafter, this mixture was cooled to 0 ℃

and anhydrous ethanol (30 mL) was added. The mixture was warmed to room temperature and reacted for 16 h. This mixture was then concentrated *in vacuo* and the crude material was dissolved in dichloromethane (40 mL). The organic layer was washed with $NaHCO_3$ (1 x 40 mL) and H_2O (1 x 40 mL). The organic layer was dried with Na_2SO_4 and concentrated *in vacuo*. The crude material was purified via flash chromatography (silica, 1:1 EtOAc/Hexanes) affording ethyl ester **TCH 152** (0.183 g, solid, 42% yield from **II-4**). Additionally, **TCH 152** may be recrystallized from heating in a 1:1 EtOAc:Hexane mixture and placed in the freezer. *Notebook reference: ML-II-45*.

^{1}H NMR (500 MHz) (d_6-DMSO) δ: 0.70 (t, J = 7.1 Hz, 3H), 3.42-3.53 (m, 2H), 3.83 (s, 3H), 3.91 (d, J = 16.2 Hz, 1H), 4.56 (d, J = 16.2 Hz, 1H), 5.06 (s, 1H), 6.74 (d, J = 7.2 Hz, 2H), 7.01 (t, J = 7.4 Hz, 2H), 7.06-7.14 (m, 3H), 7.28-7.30 (m, 1H), 7.34-7.37 (m, 2H), 7.66 (t, J = 8.1 Hz, 4H), 7.75-7.77 (m, 2H), 8.23-8.25 (m, 2H). ^{13}C NMR (125 MHz) (d_6-DMSO) δ: 13.2, 49.0, 55.3, 60.5, 72.6, 83.0, 114.1, 122.0, 123.3, 126.6, 127.0, 127.2, 127.4, 128.0, 128.2, 129.3, 130.3, 136.4, 143.8, 146.3, 147.2, 161.0, 164.6, 170.0. IR (NaCl, neat): 1734, 1608, 1520, 1352, 1252 cm^{-1}. HRMS (ESI): m/z calcd for $C_{32}H_{30}N_3O_5$ $[M+H]^+$ 536.2185; found 536.2187. m.p. 154-156 °C.

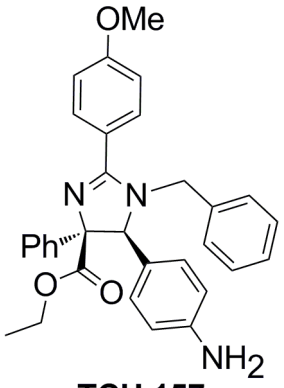

TCH 157

(4S,5S)-ethyl 5-(4-aminophenyl)-1-benzyl-2-(4-methoxyphenyl)-4-phenyl-4,5-dihydro-1H-imidazole-4-carboxylate (TCH 157).[13] To a flame dried flask under N_2, ethyl ester **TCH 152** (0.190 g, 0.35 mmol) was dissolved in glacial acetic acid (10 mL) at room temperature. Thereupon zinc dust (0.854 g, 13.06 mmol) was added. After 30 minutes the mixture was filtered and the filtrate was neutralized with saturated $NaHCO_3$ (40 mL plus additional $NaHCO_3$ (s) until pH = 6). The aqueous layer was extracted with DCM (3 x 20 mL) and the combined organics were concentrated *in vacuo.* The resulting brown oil was dissolved in DCM (20 mL) and stirred in saturated $NaHCO_3$ (20 mL) for 10 minutes to remove excess acetic acid. The organic layer was separated, dried with Na_2SO_4 and concentrated *in vacuo* affording amine **TCH 157** (0.166 g, yellow foam, 93% yield from **TCH 152**.) *Notebook reference: ML-II-59.*

^{1}H NMR (500 MHz) ($CDCl_3$) δ: 0.91 (t, J = 7.1 Hz, 3H), 3.67-3.82 (m, 4H), 3.85 (s, 3H), 3.88 (d, J = 16.0 Hz, 1H), 4.64 (d, J = 15.8 Hz, 1H), 4.84 (s, 1H), 6.67 (d, J = 8.6 Hz, 2H), 6.79 (d, J = 7.1 Hz, 2H), 6.99-7.02 (m, 2H), 7.07-7.19 (m, 5H), 7.26-7.30 (m, 1H), 7.32-7.36 (m, 2H), 7.71-7.80 (m, 4H). ^{13}C NMR (125 MHz) ($CDCl_3$) δ: 13.7, 48.5,

55.4, 60.9, 73.6, 82.5, 113.9, 114.9, 123.2, 126.9, 127.17, 127.21, 127.3, 127.9, 128.4, 129.2, 130.4, 137.1, 144.5, 146.6, 161.1, 165.1, 171.2. IR (NaCl, neat): 3462, 3370, 3218, 1737, 1617, 1513, 1252, 1179 cm^{-1}. HRMS (ESI): m/z calcd for $C_{32}H_{32}N_3O_3$ $[M+H]^+$ 506.2444; found 506.2449. m.p. 149-151°C.

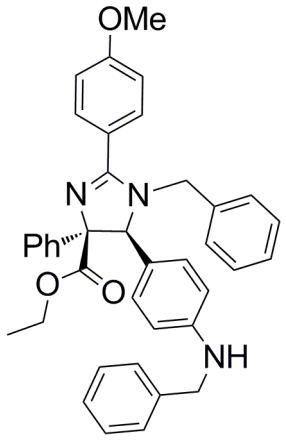

TCH 165

(4S,5S)-ethyl 1-benzyl-5-(4-(benzylamino)phenyl)-2-(4-methoxyphenyl)-4-phenyl-4,5-dihydro-1H-imidazole-4-carboxylate (TCH 165).[13] To a flame dried flask under N_2, amine **TCH 157** (0.084 g, 0.17 mmol) was dissolved in dry DCM (3 mL) at room temperature. Thereafter anhydrous benzaldehyde (21 µL, 0.17 mmol) and $NaBH(OAc)_3$ (0.082 g, 0.39 mmol) were subsequently added. After 24 h the reaction was quenched with saturated $NaHCO_3$ (1 x 10 mL). The organic layer was collected and the aqueous layer was extracted with additional DCM (2 x 10 mL). The combined organics were dried with Na_2SO_4 and concentrated *in vacuo*. The crude product was purified via flash chromatography (TEA neutralized silica, 3:7 EtOAc/Hexanes then 1:1

EtOAc/hexanes) affording the free base of **TCH 165** (0.077 g, beige foam, 78% yield from **TCH 157**). *Notebook reference: ML-II-64.*

Forming the HCl salt of **TCH 165**: The free base of **TCH 165** (3.5 grams) was dissolved in diethyl ether (150 mL); slight heating was used if necessary. Thereafter concentrated HCl (1 mL) was added dropwise while swirling the flask. Immediately following a white precipitate was collected via filtration (1 gram) affording the HCl salt of **TCH 165**. The remaining material persisted as a yellow goo that was stuck to the flask. The goo was neutralized with $NaHCO_3$, extracted into DCM, and concentrated *in vacuo*. Now having recovered the free base of **TCH 165** the above procedure may be repeated. *Note:* One may also try dissolving the free base in minimal isopropanol, adding concentrated HCl, followed by heating and recrystallization. However, this procedure did not yield as white of a precipitate. *Notebook reference: ML-II-88.*

Data for **TCH 165** free base: ^{1}H NMR (600 MHz) ($CDCl_3$) δ: 0.85 (t, *J* = 7.1 Hz, 3H), 3.57-3.77 (m, 2H), 3.82-3.90 (m, 4H), 4.14 (bs, 1 N-H), 4.35 (s, 2H), 4.61 (d, *J* = 15.9 Hz, 1H), 4.80 (s, 1H), 6.62 (d, *J* = 8.6 Hz, 2H), 6.76 (d, *J* = 7.3 Hz, 2H), 6.93-7.20 (m, 7H), 7.23-7.39 (m, 8H), 7.66 – 7.76 (m, 4H). ^{13}C NMR (600 MHz) ($CDCl_3$) δ: 13.6, 48.2, 48.4, 55.3, 60.9, 73.6, 82.4, 112.6, 113.9, 123.1, 126.3, 126.9, 127.09, 127.13, 127.14, 127.2, 127.4, 127.8, 128.3, 128.6, 129.2, 130.4, 137.1, 139.3, 144.5, 148.0, 161.0, 165.0, 171.1. IR (NaCl, neat): 3394, 3282, 1732, 1610, 1520, 1252, 1291, 1176 cm^{-1}. HRMS (ESI): m/z calcd for $C_{39}H_{38}N_3O_3$ $[M+H]^+$ 596.2913; found 596.2914. m.p. 56-58 °C.

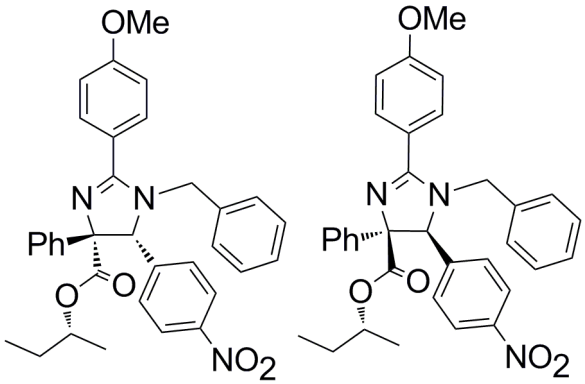

TCH 167 (*R,R,R*) **TCH 168 (*R,S,S*)**

(4R,5R)-(R)-sec-butyl 1-benzyl-2-(4-methoxyphenyl)-5-(4-nitrophenyl)-4-phenyl-4,5-dihydro-1H-imidazole-4-carboxylate (TCH 167 (*R,R,R*)) and (4S,5S)-(R)-sec-butyl 1-benzyl-2-(4-methoxyphenyl)-5-(4-nitrophenyl)-4-phenyl-4,5-dihydro-1H-imidazole-4-carboxylate (TCH 168 (*R,S,S*). To a flame dried flask under N_2, HCl salt **II-4** (1.59 g, 2.92 mmol) was dissolved in dry DCM (125 mL) and cooled to 0 ℃. Thereafter DMAP (0.570 g, 4.67 mmol), (*R*)-2-butanol (0.30 mL, 3.27 mmol) and EDCI hydrochloride (0.615 g, 3.20 mmol) were subsequently added. The mixture was allowed to warm to room temperature overnight and reacted for 13 h. The reaction was quenched with saturated $NaHCO_3$ (1 x 50 mL) and the organic layer was collected. The aqueous layer was extracted with additional DCM (2 x 50 mL). The combined organics were washed with Brine (1 x 50 mL), dried with Na_2SO_4 and concentrated *in vacuo*. The resulting oil was purified via flash chromatography (silica, 4:6 EtOAc:Hexanes) affording **TCH 167 (R,R,R)** and **TCH 168 (*R,S,S*)** (0.867 g combined mass of both diastereomers, 53% yield from **II-4**, oil). Note that it is important to run a long column (12 inches) in order for separation to occur. Multiple columns were necessary to obtain 0.867 g of the separated diastereomers. *Notebook reference: ML-II-62.*

TCH 167 (*R,R,R*): ^{1}H NMR (500 MHz) ($CDCl_3$) δ: 0.53 (t, J = 7.5 Hz, 3H), 0.86 (d, J = 6.3 Hz, 3H), 1.11 (ddt, J = 21.1, 13.9, 6.7 Hz, 2H), 3.83 (d, J = 15.7 Hz, 1H), 3.87 (s, 3H), 4.42 (dd, J = 12.5, 6.2 Hz, 1H), 4.64 (d, J = 15.7 Hz, 1H), 4.93 (s, 1H), 6.75 (d, J = 7.4 Hz, 2H), 7.02-7.16 (m, 5H), 7.29-7.37 (m, 3H), 7.59 (d, J = 8.3 Hz, 2H), 7.71-7.78 (m, 4H), 8.23-8.24 (m, 2H). ^{13}C NMR (125 MHz) ($CDCl_3$) δ: 9.3, 18.5, 28.0, 49.6, 55.5, 73.0, 73.7, 83.2, 114.2, 122.3, 123.7, 126.6, 127.3, 127.69, 127.70, 128.2, 128.6, 129.2, 130.5, 136.1, 161.5, 165.6, 170.1. IR (NaCl, neat): 2970, 2931, 1723, 1611, 1517, 1446, 1347, 1253 cm^{-1}. HRMS (ESI): m/z calcd for $C_{34}H_{34}N_3O_5$ $[M+H]^+$ 564.2498; found, 564.2484.

TCH 168 *(R,S,S)*: ^{1}H NMR (500 MHz) ($CDCl_3$) δ: 0.53-0.57 (m, 6H), 1.21-1.29 (m, 2H), 3.83 (d, J = 15.6 Hz, 1H), 3.88 (s, 3H), 4.42 (dd, J = 12.4, 6.3 Hz, 1H), 4.63 (d, J = 15.6 Hz, 1H), 4.97 (s, 1H), 6.77 (d, J = 7.3 Hz, 2H), 7.01-7.17 (m, 5H), 7.29-7.37 (m, 3H), 7.58 (d, J = 8.2 Hz, 2H), 7.71-7.77 (m, 4H), 8.23 (d, J = 8.9 Hz, 2H). ^{13}C NMR (125 MHz) ($CDCl_3$) δ: 9.3, 18.4, 28.4, 49.7, 55.5, 72.7, 73.6, 83.2, 114.2, 122.2, 123.8, 126.6, 127.4, 127.75, 127.77, 128.2, 128.6, 129.3, 130.6, 136.2, 143.7, 146.6, 147.9, 161.6, 165.5, 169.9. IR (NaCl, neat): 2971, 2931, 1734, 1611, 1517, 1446, 1347, 1252 cm^{-1}. HRMS (ESI): m/z calcd for $C_{34}H_{34}N_3O_5$ $[M+H]^+$ 564.2498; found, 564.2491.

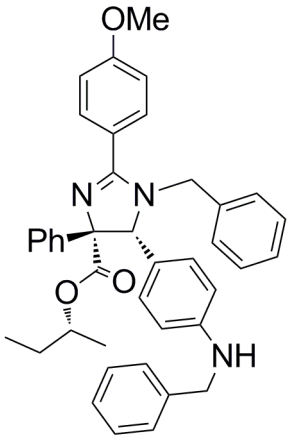

TCH 170 (*R,R,R*)

(4R,5R)-(R)-sec-butyl 1-benzyl-5-(4-(benzylamino)phenyl)-2-(4-methoxyphenyl)-4-phenyl-4,5-dihydro-1H-imidazole-4-carboxylate (TCH 170 (*R,R,R*)). To a flame dried flask under N_2, amine **II-6 (*R,R,R*)** (0.046 g, 0.087 mmol) was dissolved in dry DCM (4 mL). Thereafter anhydrous benzaldehyde (9 µL, 0.087 mmol) and $NaBH(OAc)_3$ (0.037 g, 0.17 mmol) were subsequently added. The mixture reacted for 14 h at room temperature. The reaction was quenched with saturated $NaHCO_3$ (10 mL). The aqueous layer was extracted with DCM (3 x 10 mL), dried with Na_2SO_4 and concentrated *in vacuo*. The crude material was purified via flash chromatography (silica neutralized with TEA, 1:1 EtOAc/Hexanes). The collected fractions were concentrated *in vacuo*, dissolved in boiling hexanes and placed in freezer. The collected precipitate afforded **TCH 170 (R,R,R)** (0.013 g, 24% yield from **II-6 (R,R,R)**, oil). *Notebook reference: ML-II-67.*

^{1}H NMR (500 MHz) ($CDCl_3$) δ: 0.56 (t, *J* = 7.5 Hz, 3H), 0.85 (d, *J* = 6.3 Hz, 3H), 1.02-1.19 (m, 2H), 3.79-3.84 (m, 4H), 4.13 (s, 1H), 4.35-4.42 (m, 3H), 4.57 (d, *J* = 15.9 Hz, 1H), 4.79 (s, 1H), 6.60 (d, *J* = 8.5 Hz, 2H), 6.76 (d, *J* = 7.2 Hz, 2H), 6.95 (d, *J* = 8.5

Hz, 2H), 7.06-7.18 (m, 5H), 7.23-7.38 (m, 9H), 7.69 (dd, J = 35.2, 7.9 Hz, 4H). ^{13}C NMR (125 MHz) ($CDCl_3$) δ: 9.4, 18.5, 28.1, 48.4, 55.5, 73.1, 73.7, 82.5, 112.8, 114.0, 123.5, 126.6, 127.0, 127.16, 127.23, 127.3, 127.4, 127.5, 127.9, 128.5, 128.8, 129.6, 130.4, 137.4, 139.5, 144.8, 148.3, 161.1, 165.1, 165.7, 170.7. IR (NaCl, neat): 3330, 3061, 3028, 2965, 2932, 1725, 1613, 1515, 1451, 1253, 1177 cm^{-1}. HRMS (ESI): m/z calcd for $C_{41}H_{42}N_3O_3$ $[M+H]^+$ 624.3226; found, 624.3228.

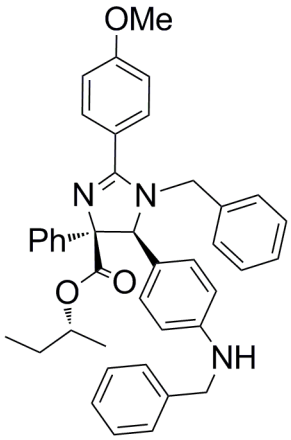

TCH 171 (*R,S,S*)

(4S,5S)-(R)-sec-butyl 1-benzyl-5-(4-(benzylamino)phenyl)-2-(4-methoxyphenyl)-4-phenyl-4,5-dihydro-1H-imidazole-4-carboxylate (TCH 171 (*R,S,S*)). To a flame dried flask under N_2, amine **II-7 (R,S,S)** (0.068 g, 0.13 mmol) was dissolved in dry DCM (4 mL). Thereafter benzaldehyde (13 µL, 0.13 mmol) and $NaBH(OAc)_3$ (0.054 g, 0.25 mmol) were subsequently added. The reaction stirred for 14 h at room temperature. Quenched the reaction with saturated $NaHCO_3$ (10 mL) and extracted the aqueous layer with DCM (3 x 10 mL). The combined organics were dried with Na_2SO_4 and concentrated *in vacuo*. The crude mixture was purified via flash

chromatography (silica neutralized with TEA, 1:1 EtOAc/Hexanes). The collected fractions were concentrated *in vacuo*, dissolved in boiling hexanes and placed in freezer. The collected precipitate afforded **TCH 171 (*R,S,S*)** (0.037 g, solid, 46% yield from **II-7 (*R,S,S*)**). *Notebook reference: ML-II-66.*

^{1}H NMR (500 MHz) ($CDCl_3$) δ: 0.54 (t, J = 7.4 Hz, 3H), 0.59 (d, J = 6.3 Hz, 3H), 1.25 (dq, J = 14.6, 7.3 Hz, 2H), 3.81-3.84 (m, 4H), 4.18 (s, 1H), 4.36 (s, 2H), 4.42 (dd, J = 12.4, 6.3 Hz, 1H), 4.58 (d, J = 15.9 Hz, 1H), 4.84 (s, 1H), 6.61 (d, J = 8.6 Hz, 2H), 6.80 (d, J = 7.0 Hz, 2H), 6.96 (d, J = 8.7 Hz, 2H), 7.09-7.19 (m, 5H), 7.24-7.39 (m, 9H), 7.67 (d, J = 8.7 Hz, 2H), 7.75 (d, J = 7.3 Hz, 2H). ^{13}C NMR (125 MHz) ($CDCl_3$) δ: 9.4, 18.4, 28.5, 48.3, 48.5, 55.4, 72.9, 73.2, 82.5, 112.9, 113.9, 123.4, 126.8, 127.0, 127.18, 127.24, 127.29, 127.35, 127.5, 127.9, 128.5, 128.7, 129.5, 130.4, 137.5, 139.5, 144.7, 148.3, 161.1, 164.8, 170.6. IR (NaCl, neat): 3401, 3061, 3029, 2972, 2935, 1731, 1615, 1516, 1449, 1252, 1177 cm^{-1}. HRMS (ESI): m/z calcd for $C_{41}H_{42}N_3O_3$ $[M+H]^+$ 624.3226; found, 624.3229. m.p. 56-58 °C.

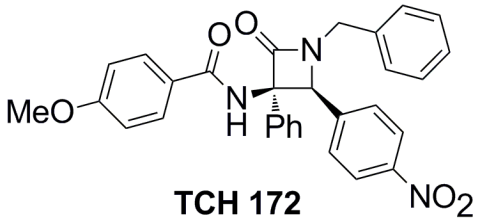

TCH 172
racemic

N-((2S,3R)-1-benzyl-2-(4-nitrophenyl)-4-oxo-3-phenylazetidin-3-yl)-4-methoxybenzamide (TCH 172). Isolated as a side product during the synthesis of **II-4** (refer to experimental procedure for **II-4**). During the workup of **II-4**, the EtOAc filtrate

was concentrated *in vacuo* and afforded β-lactam **TCH 172** (4.83 g, solid, 20% yield from phenylazlactone **II-2**). *Notebook reference: ML-II-75.*

^{1}H NMR (500 MHz) (d_6-DMSO) δ: 3.72 (s, 3H), 4.12 (d, J = 15.2 Hz, 1H), 4.72 (d, J = 15.2 Hz, 1H), 5.58 (s, 1H), 6.76-6.81 (m, 2H), 7.14-7.16 (m, 2H), 7.26-7.32 (m, 4H), 7.35-7.38 (m, 2H), 7.41-7.44 (m, 2H), 7.53-7.55 (m, 2H), 7.66-7.69 (m, 2H), 8.01-8.04 (m, 2H), 9.27 (s, 1H). ^{13}C NMR (125 MHz) (d_6-DMSO) δ: 44.4, 55.2, 64.9, 75.7, 113.1, 122.1, 125.8, 126.5, 127.5, 127.6, 128.2, 128.3, 128.6, 129.0, 130.3, 135.3, 137.2, 142.8, 146.8, 161.5, 165.3, 166.0. IR (NaCl, neat): 3299, 3062, 3031, 2938, 2839, 1747, 1663, 1606, 1521, 1497, 1347, 1255, 1175 cm^{-1}. HRMS (ESI): m/z calcd for $C_{30}H_{26}N_3O_5$ $[M+H]^+$ 508.1872; found 508.1873. m.p. 237-240 °C.

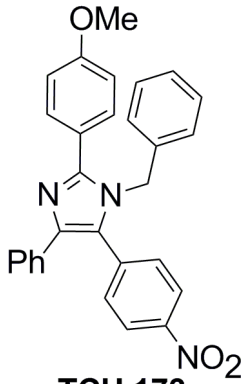

TCH 173

1-benzyl-2-(4-methoxyphenyl)-5-(4-nitrophenyl)-4-phenyl-1H-imidazole (TCH 173). *This was isolated as a side product during initial reaction conditions to form* ***TCH 167 (R,R,R)****and* ***TCH 168 (R,S,S)****.* To a flame dried flask under N_2, HCl salt **II-4** (0.118 g, 0.22 mmol) was dissolved in dry DCM (15 mL). The reaction mixture was cooled to 0 ℃ whereupon oxalyl chloride (50 µL, 0.65 mmol) was added dropwise followed by addition of anhydrous pyridine (66 µL, 0.82 mmol). After reacting for 2.5 h the reaction

mixture was concentrated *in vacuo* and placed on the vacuum pump for 1 hour. The crude mixture was then dissolved in dry DCM (10 mL) followed by the addition of (*R*)-2-butanol (60 µL, 0.65 mmol) at 0 ℃. The reaction mixture was allowed to warm to room temperature over 3 h. Thereafter the mixture was concentrated *in vacuo* and dissolved in DCM (15 mL). The organics were washed with saturated $NaHCO_3$ (2 x 10 mL), dried with Na_2SO_4 and concentrated *in vacuo.* The crude mixture was purified via flash chromatography (silica, 3:7 EtOAc/Hexanes) affording imidazole **TCH 173** (0.043 g, 43% yield from **II-4**). *Notebook reference: ML-II-56.*

^{1}H NMR (500 MHz) ($CDCl_3$) δ: 3.85 (s, 3H), 5.16 (s, 2H), 6.84-6.85 (m, 2H), 6.97 (d, J = 8.8 Hz, 2H), 7.22-7.29 (m, 7H), 7.37-7.39 (m, 2H), 7.52-7.54 (m, 2H), 7.64 (d, J = 8.8 Hz, 2H), 8.14-8.16 (m, 2H). ^{13}C NMR (125 MHz) ($CDCl_3$) δ: 48.8, 55.5, 114.3, 122.9, 124.0, 125.9, 127.2, 127.36, 127.39, 127.9, 128.4, 129.0, 130.6, 131.8, 133.9, 137.2, 138.3, 139.9, 147.6, 149.7, 160.6. IR (NaCl, neat): 1600, 1519, 1345, 1252 cm^{-1}. HRMS (ESI): m/z calcd for $C_{29}H_{24}N_3O_3$ $[M+H]^+$ 462.1818; found, 462.1828. m.p. 174-176 ˚C.

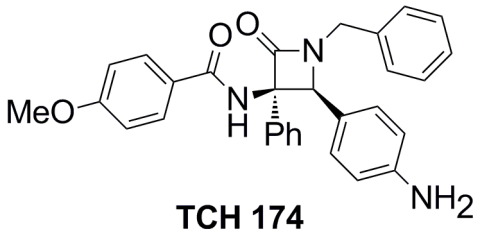

TCH 174
racemic

N-((2S,3R)-2-(4-aminophenyl)-1-benzyl-4-oxo-3-phenylazetidin-3-yl)-4-methoxybenzamide (TCH 174). To a flame dried flask under N_2, β-lactam **TCH 172**

(0.158 g, 0.311 mmol) was added to glacial acetic acid (4 mL) at room temperature. Thereafter zinc dust (0.732 g, 11.20 mmol) was added. After 45 minutes the mixture was filtered, and the filtrate was neutralized with saturated $NaHCO_3$ (30 mL plus additional $NaHCO_3$ (s) until pH = 9). The aqueous layer was extracted with DCM (3 x 15 mL). The organics were combined, dried with Na_2SO_4 and concentrated *in vacuo*. The crude solid was dissolved in minimal EtOAc with heating. Thereafter hexanes were added to the solution until cloudy, and the mixture was placed in the freezer. The resulting precipitate was collected affording **TCH 174** (54% yield from **TCH 172**). *Notebook reference: ML-II-79.*

^{1}H NMR (500 MHz) (d_6-DMSO) δ: 3.74 (s, 3H), 3.89 (d, J = 15.2 Hz, 1H), 4.68 (d, J = 15.2 Hz, 1H), 4.96 (s, 2H), 5.08 (s, 1H), 6.39 (d, J = 8.5 Hz, 2H), 6.81-6.85 (m, 2H), 7.04 (d, J = 8.5 Hz, 2H), 7.13-7.15 (m, 2H), 7.23-7.33 (m, 6H), 7.42-7.44 (m, 2H), 7.51-7.54 (m, 2H), 8.89 (s, 1H). ^{13}C NMR (125 MHz) (d_6-DMSO) δ: 43.4, 55.2, 66.2, 74.9, 113.00, 113.04, 120.5, 126.2, 126.5, 127.1, 127.5, 128.01, 128.03, 128.5, 129.1, 129.6, 135.8, 138.2, 148.3, 161.3, 165.0, 166.3. IR (NaCl, neat): 3448, 3353, 1741, 1654, 1608, 1520, 1497, 1253 cm^{-1}. HRMS (ESI): m/z calcd for $C_{30}H_{28}N_3O_3$ $[M+H]^+$ 478.2131; found, 478.2114. m.p. 176-178 °C.

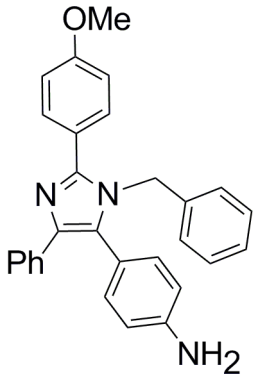

TCH 175

4-(1-benzyl-2-(4-methoxyphenyl)-4-phenyl-1H-imidazol-5-yl)aniline (TCH 175). To a flamed dried flask under N_2, imidazole **TCH 173** (0.033 g, 0.71 mmol) was dissolved in glacial acetic acid (2 mL). Thereafter zinc dust (0.167 g, 2.56 mmol) was added. After 30 minutes the mixture was filtered and the filtrate was neutralized with saturated $NaHCO_3$ (30 mL plus $NaHCO_3$ (s) until pH = 9). The aqueous layer was extracted with DCM (3 x 15 mL), and the combined organics were then washed with additional $NaHCO_3$ (1 x 20 mL). The organics were dried with Na_2SO_4 and concentrated *in vacuo.* The crude mixture was purified via flash chromatography (silica, 4:6 EtOAc/Hexanes) affording amine **TCH 175** (0.010 g, 34% yield from **TCH 173**). *Notebook reference: ML-II-77.*

^{1}H NMR (500 MHz) ($CDCl_3$) δ: 3.75 (bs, 2H), 3.81 (s, 3H), 5.06 (s, 2H), 6.59-6.62 (m, 2H), 6.84-6.91 (m, 4H), 6.96-6.99 (m, 2H), 7.12-7.24 (m, 6H), 7.54-7.57 (m, 2H), 7.61-7.64 (m, 2H). ^{13}C NMR (125 MHz) ($CDCl_3$) δ: 48.1, 55.4, 114.1, 115.4, 118.5, 120.9, 123.9, 126.1, 126.7, 127.3, 128.1, 128.7, 130.2, 130.5, 132.3, 135.1, 137.6, 138.2, 146.8, 147.7, 160.1. IR (NaCl, neat): 3463, 3376, 3216, 3059, 3031, 2927, 1612,

1514, 1489, 1446, 1294, 1251, 1178 cm^{-1}. HRMS (ESI): m/z calcd for $C_{29}H_{26}N_3O$ $[M+H]^+$ 432.2076; found, 432.2083. m.p. decomposed >190 °C.

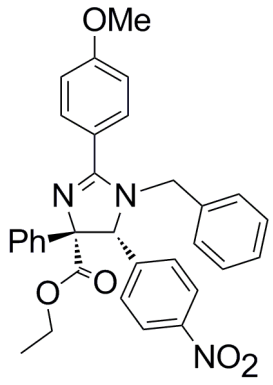

TCH 177 (*R,R*)

(4R,5R)-ethyl 1-benzyl-2-(4-methoxyphenyl)-5-(4-nitrophenyl)-4-phenyl-4,5-dihydro-1H-imidazole-4-carboxylate (TCH 177 (*R,R*)). In a flask under N_2, **TCH 167 (*R,R,R*)** (0.425 g, 0.754 mmol) was dissolved in a mixture of ethanol (20 mL) and 2 N NaOH (20 mL). The mixture was allowed to reflux for 10 h. Thereafter the mixture was cooled to 0 ℃ and concentrated HCl (~4 mL) was add ed dropwise until pH = 1. The aqueous mixture was extracted with DCM (3 x 25 mL). The combined organics were dried with Na_2SO_4 and concentrated *in vacuo.* The crude mixture (brown solid) was placed on the vacuum line for 1 h.

Thereafter, the crude mixture was dissolved in dry DCM (40 mL) and cooled to 0 ℃. To this mixture DMAP (0.147 g, 1.20 mmol), EDCI hydrochloride (0.160 g, 0.83 mmol) and anhydrous ethanol (10 mL) were subsequently added. The mixture was allowed to warm to room temperature and reacted for 10 h. The mixture was then quenched with saturated $NaHCO_3$ (20 mL) and stirred for 5 minutes. The aqueous layer was extracted with DCM (3 x 25 mL), and the combined organics were washed with Brine (30 mL) and

dried with Na_2SO_4. The crude material was purified via flash chromatography (silica, 4:6 EtOAc:Hexanes). Trace impurity was observed after the first column and was removed via flash chromatography (silica, 4:6 EtOAc/Hexanes) affording **TCH 177 (*R*,*R*)** (0.057 g, oily foam, 14% yield from **TCH 167 (*R,R,R*)**). *Notebook reference: ML-II-104.*

^{1}H and ^{13}C NMR spectra are consistent with racemic **TCH 152**. $[\alpha]_D^{20}$ = -11.2° (*All measurements were collected at 20℃ with a wavelength of 589 nm. All solution concentrations were 1 mg/mL.)*

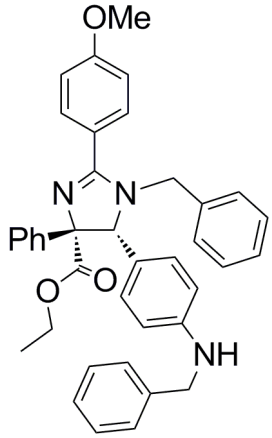

TCH 178 (*R,R*)

(4R,5R)-ethyl 1-benzyl-5-(4-(benzylamino)phenyl)-2-(4-methoxyphenyl)-4-phenyl-4,5-dihydro-1H-imidazole-4-carboxylate (TCH 178 (*R,R*)). Followed experimental procedure for racemic **TCH 165** using starting material **II-8 (*R,R*).** *Notebook reference: ML-II-109.*

^{1}H and ^{13}C NMR spectra are consistent with racemic **TCH 165**. $[\alpha]_D^{20}$ = -4.5° (*All measurements were collected at 20℃ with a wavelength of 589 nm. All solution concentrations were 1 mg/mL.)*

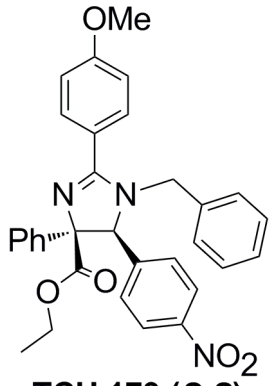

TCH 179 (*S,S*)

(4S,5S)-ethyl 1-benzyl-2-(4-methoxyphenyl)-5-(4-nitrophenyl)-4-phenyl-4,5-dihydro-1H-imidazole-4-carboxylate (TCH 179 (*S,S*)). TCH 168 (*R,S,S*) (0.336 g, 0.60 mmol) was dissolved in a mixture of ethanol (17 mL) and 2N NaOH (17 mL) under N_2. The mixture was allowed to reflux for 10 h. Thereafter the mixture was cooled to 0 ℃ and concentrated HCl (~3 mL) was added dropwise until pH =1. The aqueous mixture was extracted with DCM (3 x 20 mL). The combined organics were dried with Na_2SO_4 and concentrated *in vacuo*. The crude mixture (brown solid) was placed on the vacuum line for 20 minutes.

Thereafter, dry DCM (30 mL) was added to the crude mixture and cooled to 0 ℃. To this mixture DMAP (0.116 g, 0.95 mmol), EDCI hydrochloride (0.126, 0.66 mmol) and anhydrous ethanol (7 mL) were subsequently added. The mixture was allowed to warm to room temperature and reacted for 9 h. The reaction was quenched with saturated $NaHCO_3$ (20 mL) and stirred for 5 minutes. The aqueous layer was extracted with DCM (3 x 25 mL), and the combined organics were washed with brine (1 x 30 mL) and dried with Na_2SO_4. The organics were concentrated *in vacuo,* and the crude mixture was purified by flash chromatography (silica, 4:6 EtOAc/Hexanes). Trace impurity remained

after the first column and was removed via flash chromatography (silica, 4:6 EtOAc/Hexanes) affording **TCH 179 (*S,S*)** (0.034 g, oily foam, 11% yield from **TCH 168 (*R,S,S*)**. *Notebook reference: ML-II-105*.

^{1}H and ^{13}C NMR spectra are consistent with racemic **TCH 152**. $[\alpha]_D^{20}$ = +9.8° (*All measurements were collected at 20℃ with a wavelength of 589 nm. All solution concentrations were 1 mg/mL.)*

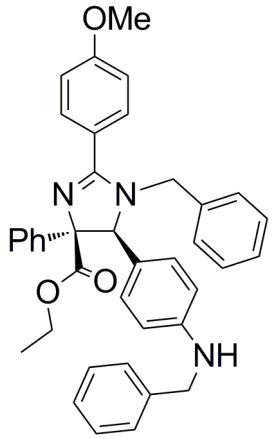

TCH 180 (*S,S*)

(4S,5S)-ethyl 1-benzyl-5-(4-(benzylamino)phenyl)-2-(4-methoxyphenyl)-4-phenyl-4,5-dihydro-1H-imidazole-4-carboxylate (TCH 180 (*S,S*)). Followed experimental procedure for racemic **TCH 165** using starting material **II-9 (*S,S*).** *Notebook reference: ML-II-110. .*

^{1}H and ^{13}C NMR spectra are consistent with racemic **TCH 165**. $[\alpha]_D^{20}$ = +3.0° (*All measurements were collected at 20℃ with a wavelength of 589 nm. All solution concentrations were 1 mg/mL.)*

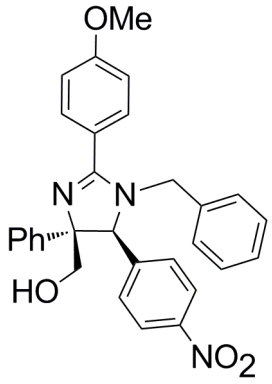

TCH 181
racemic

((4S,5S)-1-benzyl-2-(4-methoxyphenyl)-5-(4-nitrophenyl)-4-phenyl-4,5-dihydro-1H-imidazol-4-yl)methanol (TCH 181). In a flame dried flask under argon, ethyl ester **TCH 152** (0.250 g, 0.47 mmol) was dissolved in anhydrous THF (20 mL). The mixture was cooled to 0 ℃ and 2 M $LiBH_4$ in THF (0.25 mL, 0.50 mmol) was added dropwise. Immediately after addition of $LiBH_4$ the mixture was allowed to reflux for 3 h. Thereafter the mixture was cooled to 0 ℃ and quenched with NH_4Cl (20 mL). The aqueous mixture was extracted with DCM (3 x 25 mL). The combined organics were washed with brine (1 x 25 mL), dried with Na_2SO_4 and concentrated *in vacuo*. The crude mixture was purified via flash chromatography (silica, 4:1 EtOAc/Hexanes) affording **TCH 181** (0.128 g, solid, 56% yield from **TCH 152**). *Notebook reference: ML-II-97.*

^{1}H NMR (500 MHz) ($CDCl_3$) δ: 3.34 (dd, *J* = 49.5, 11.7 Hz, 2H), 3.82 (d, *J* = 15.6 Hz, 1H), 3.98 (s, 3H), 4.54 (s, 1H), 4.65 (d, *J* = 15.6 Hz, 1H), 6.70-6.71 (m, 2H), 7.03-7.14 (m, 5H), 7.18-7.21 (m, 1H), 7.27-7.28 (m, 4H), 7.77-7.80 (m, 2H), 8.22 (d, *J* = 8.3 Hz, 2H). ^{13}C NMR (150 MHz) ($CDCl_3$) δ: 50.3, 55.7, 66.3, 73.8, 78.0, 114.3, 122.7, 123.5,

125.5, 127.1, 127.79, 127.81, 128.6, 128.7, 129.4, 130.7, 135.6, 144.8, 146.3, 147.6, 161.6, 166.7. IR (NaCl, neat): 3189, 2927, 2857, 1615, 1517, 1447, 1346, 1253 cm^{-1}. HRMS (ESI): m/z calcd for $C_{30}H_{28}N_3O_4$ $[M+H]^+$ 494.2080; found, 494.2063. m.p. 176-178 °C.

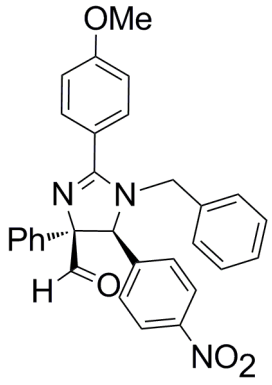

TCH 182
racemic

(4S,5S)-1-benzyl-2-(4-methoxyphenyl)-5-(4-nitrophenyl)-4-phenyl-4,5-dihydro-1H-imidazole-4-carbaldehyde (TCH 182). To a flame dried flask under argon, **TCH 181** (0.041 g, 0.083 mmol) was dissolved in EtOAc (5 mL) at room temperature. Thereafter IBX (0.067 g, 0.24 mmol) was added and the mixture reacted for 20 h. At this point additional IBX was added (0.075 g, 0.27 mmol), and the mixture reacted for 6 h at room temperature and refluxed for 1 h. Thereafter the reaction mixture was cooled and filtered to remove IBX. The organic filtrate was washed with Brine (20 mL), dried with Na_2SO_4 and concentrated *in vacuo*. The crude material was purified via column flash chromatography (silica, 4:6 EtOAc/Hexanes) affording **TCH 182** (0.024 g, solid, 59% yield from **TCH 181**). *Notebook reference: ML-II-95.*

^{1}H NMR (500 MHz) ($CDCl_3$) δ: 3.87-3.95 (m, 4H), 4.74 (d, J = 15.7 Hz, 1H), 4.76 (s, 1H), 6.73-6.75 (m, 2H), 7.02-7.14 (m, 5H), 7.28-7.55 (m, 7H), 7.82-7.90 (m, 2H), 8.25 (d, J = 8.8 Hz, 2H), 9.50 (s, 1H). ^{13}C NMR (125 MHz) ($CDCl_3$) δ: 49.9, 55.5, 73.8, 84.2, 114.4, 121.9, 124.1, 126.5, 127.4, 127.8, 128.0, 128.6, 128.8, 129.0, 130.5, 135.4, 141.0, 144.7, 147.8, 161.9, 167.7, 198.0. IR (NaCl, neat): 3062, 3030, 2925, 2852, 1729, 1610, 1517, 1347, 1254, 1174 cm^{-1}. HRMS (ESI): m/z calcd for $C_{30}H_{26}N_3O_4$ $[M+H]^+$ 492.1923; found, 492.1927. m.p. 48-51 °C.

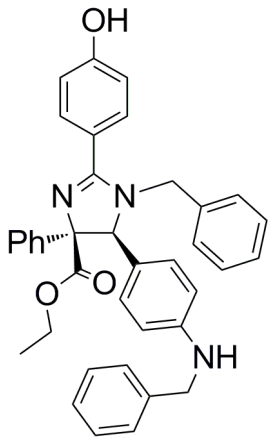

TCH 183
racemic

(4S,5S)-ethyl 1-benzyl-5-(4-(benzylamino)phenyl)-2-(4-hydroxyphenyl)-4-phenyl-4,5-dihydro-1H-imidazole-4-carboxylate (TCH 183). To a flame dried flask under argon, **TCH 165** HCl salt (0.100 g, 0.16 mmol) was dissolved in dry DCM (10 mL). The reaction mixture was cooled to 0 ℃ and BBr_3 (0.20 mL, 2.08 mmol) was added. After 1 h the reaction was quenched with H_2O (10 mL), and the aqueous mixture was extracted with DCM (3 x 15 mL). The combined organics were washed with brine (20 mL), dried with Na_2SO_4 and concentrated *in vacuo*. The crude material was purified

via flash chromatography (silica, 7:93 MeOH/DCM) affording **TCH 183** (0.017 g, solid, 19% yield from **TCH 165** HCl salt). *Notebook reference: ML-II-91.*

^{1}H NMR (600 MHz) ($CDCl_3$) δ: 0.72 (t, J = 7.1 Hz, 3H), 3.44-3.67 (m, 2H), 3.84 (d, J = 15.3 Hz, 1H), 4.36 (s, 2H), 4.70 (d, J = 15.3 Hz, 1H), 4.78 (s, 1H), 6.68 (d, J = 7.4 Hz, 4H), 6.92 (d, J = 8.2 Hz, 2H), 7.03-7.13 (m, 5H), 7.20-7.29 (m, 4H), 7.29-7.40 (m, 4H), 7.44 (d, J = 8.5 Hz, 2H), 7.53-7.54 (m, 2H). ^{13}C NMR (150 MHz) ($CDCl_3$) δ: 13.5, 29.7, 48.0,48.7, 61.4, 73.2, 116.8, 126.4, 127.2, 127.4, 127.6, 127.8, 128.3, 128.5, 128.6, 130.5, 139.1, 148.8, 166.0 (some peaks absent due to limited sample). IR (NaCl, neat): 3408, 3297, 3062, 3028, 2924, 2853, 1740, 1611, 1518, 1451, 1280, 1174 cm^{-1}. HRMS (ESI): m/z calcd for $C_{38}H_{36}N_3O_3$ $[M+H]^+$ 582.2757; found, 582.2752. m.p. 116-118 °C.

L. Spectra

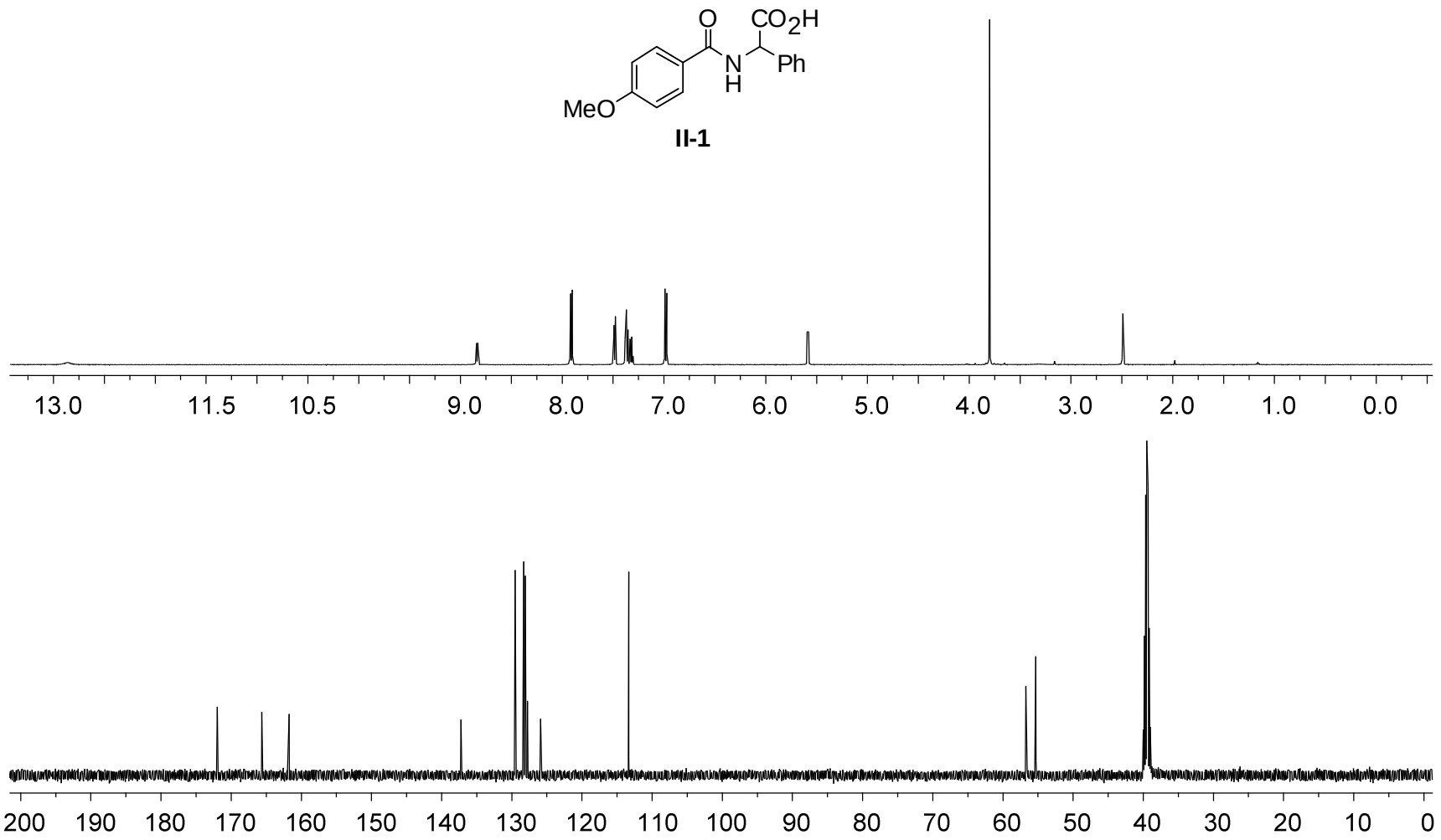

II-1

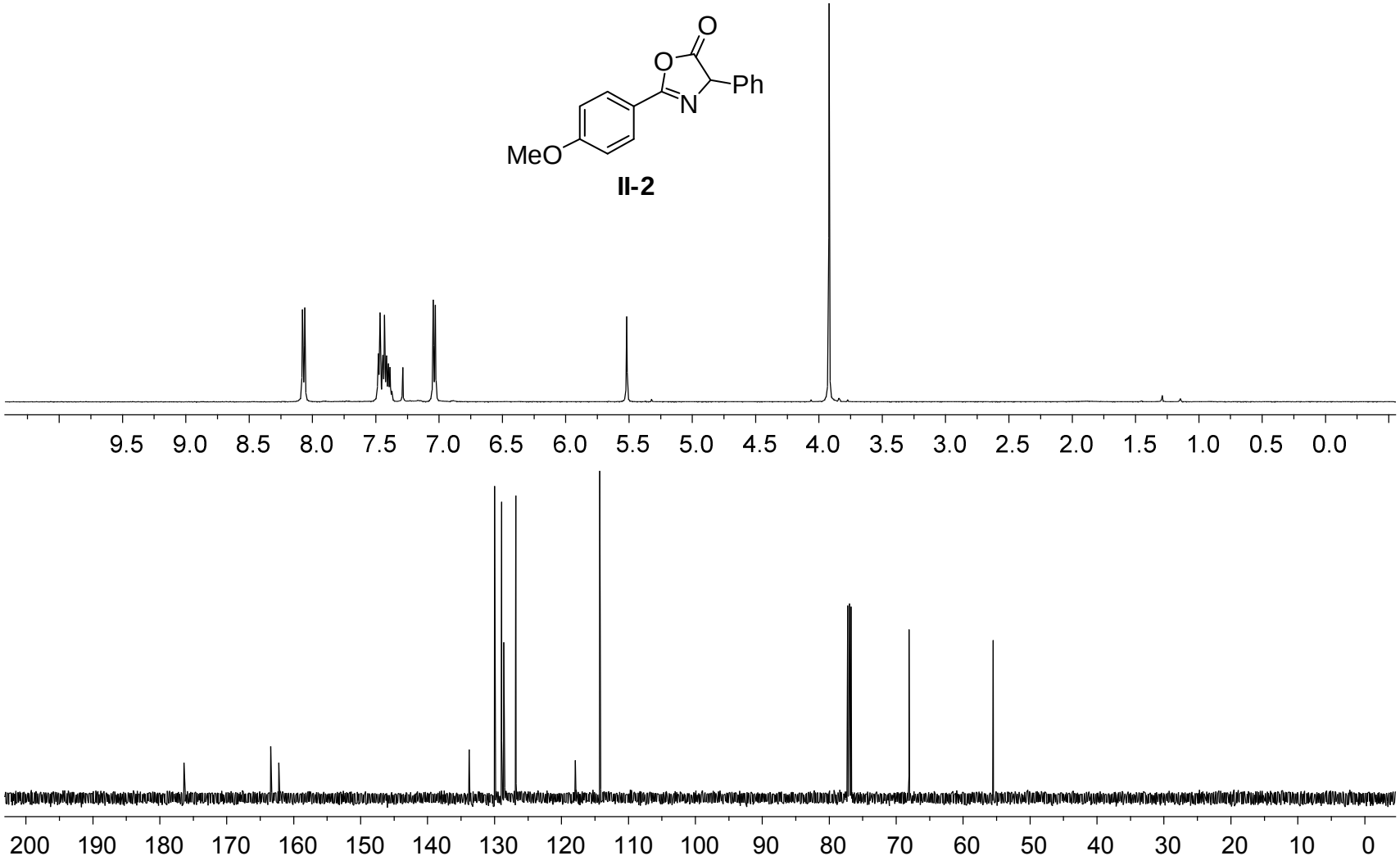
O
O
N
Ph
MeO
9.5 9.0 8.5 8.0 7.5 7.0 6.5 6.0 5.5 5.0 4.5 4.0 3.5 3.0 2.5 2.0 1.5 1.0 0.5 0.0
200 190 180 170 160 150 140 130 120 110 100 90 80 70 60 50 40 30 20 10 0

II-2

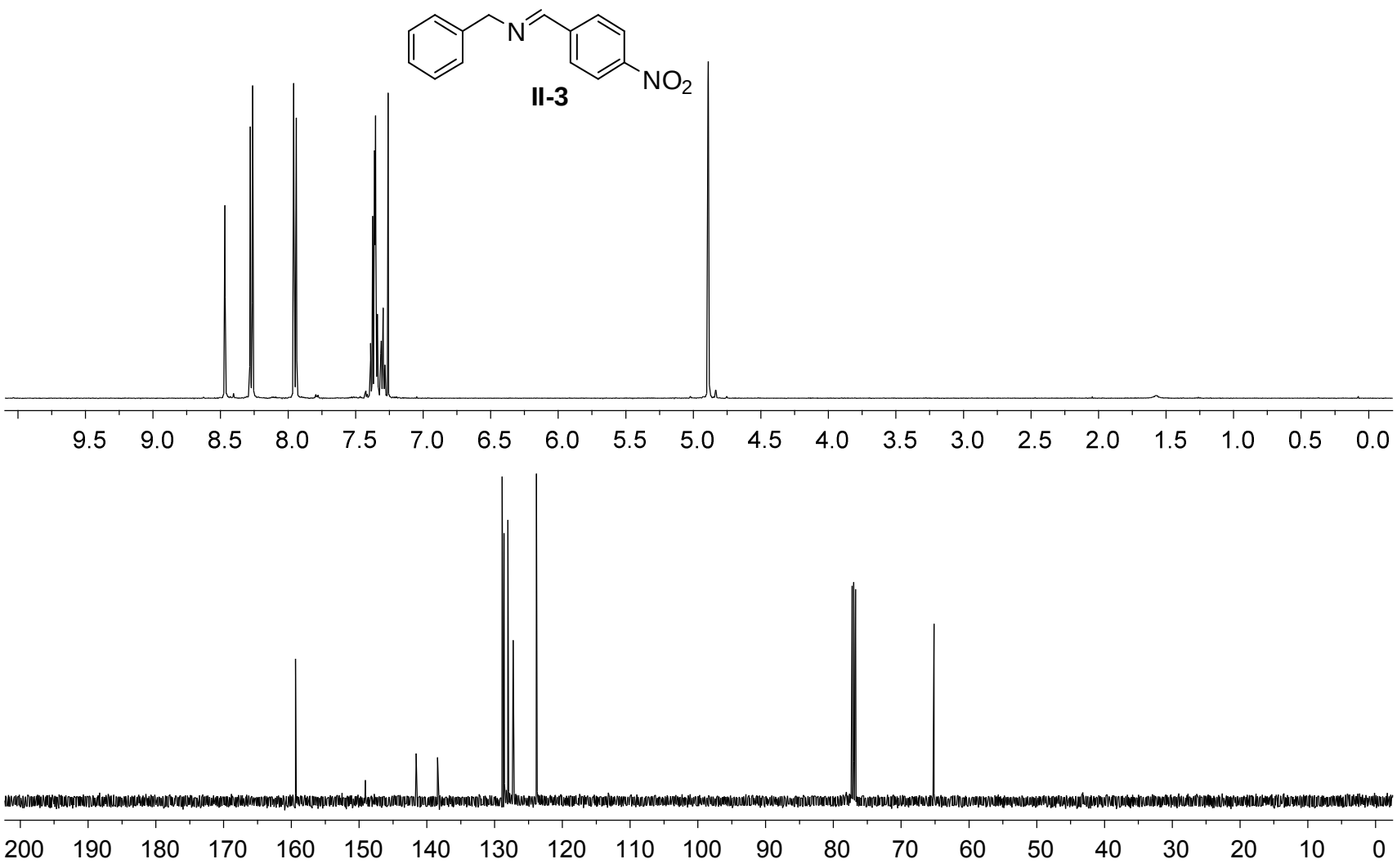
N
NO2
II-3
9.5 9.0 8.5 8.0 7.5 7.0 6.5 6.0 5.5 5.0 4.5 4.0 3.5 3.0 2.5 2.0 1.5 1.0 0.5 0.0
200 190 180 170 160 150 140 130 120 110 100 90 80 70 60 50 40 30 20 10 0

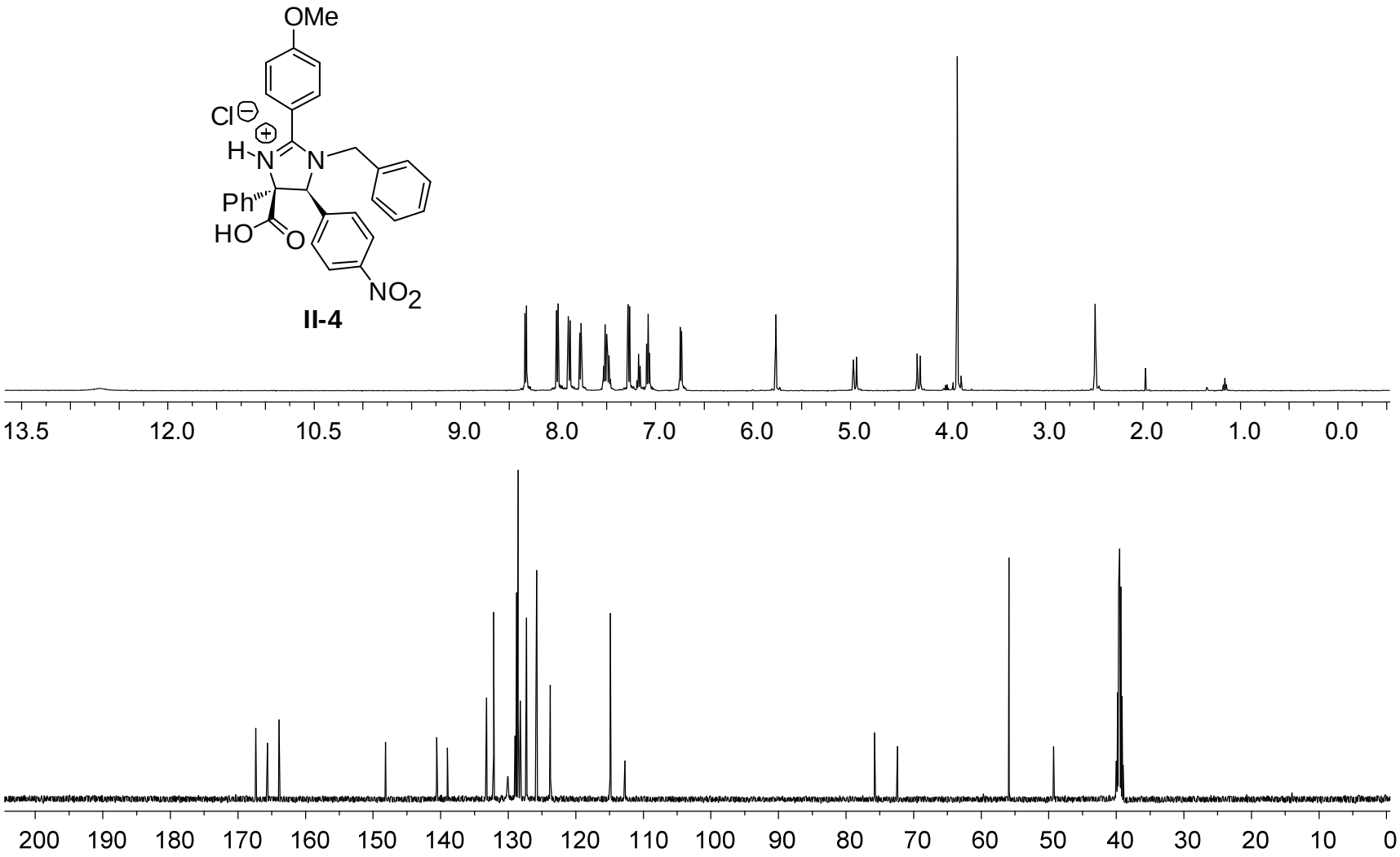
OMe
Cl
H
N
N
Ph
HO
O
NO2
II-4
13.5
12.0
10.5
9.0
8.0
7.0
6.0
5.0
4.0
3.0
2.0
1.0
0.0
200
190
180
170
160
150
140
130
120
110
100
90
80
70
60
50
40
30
20
10
0

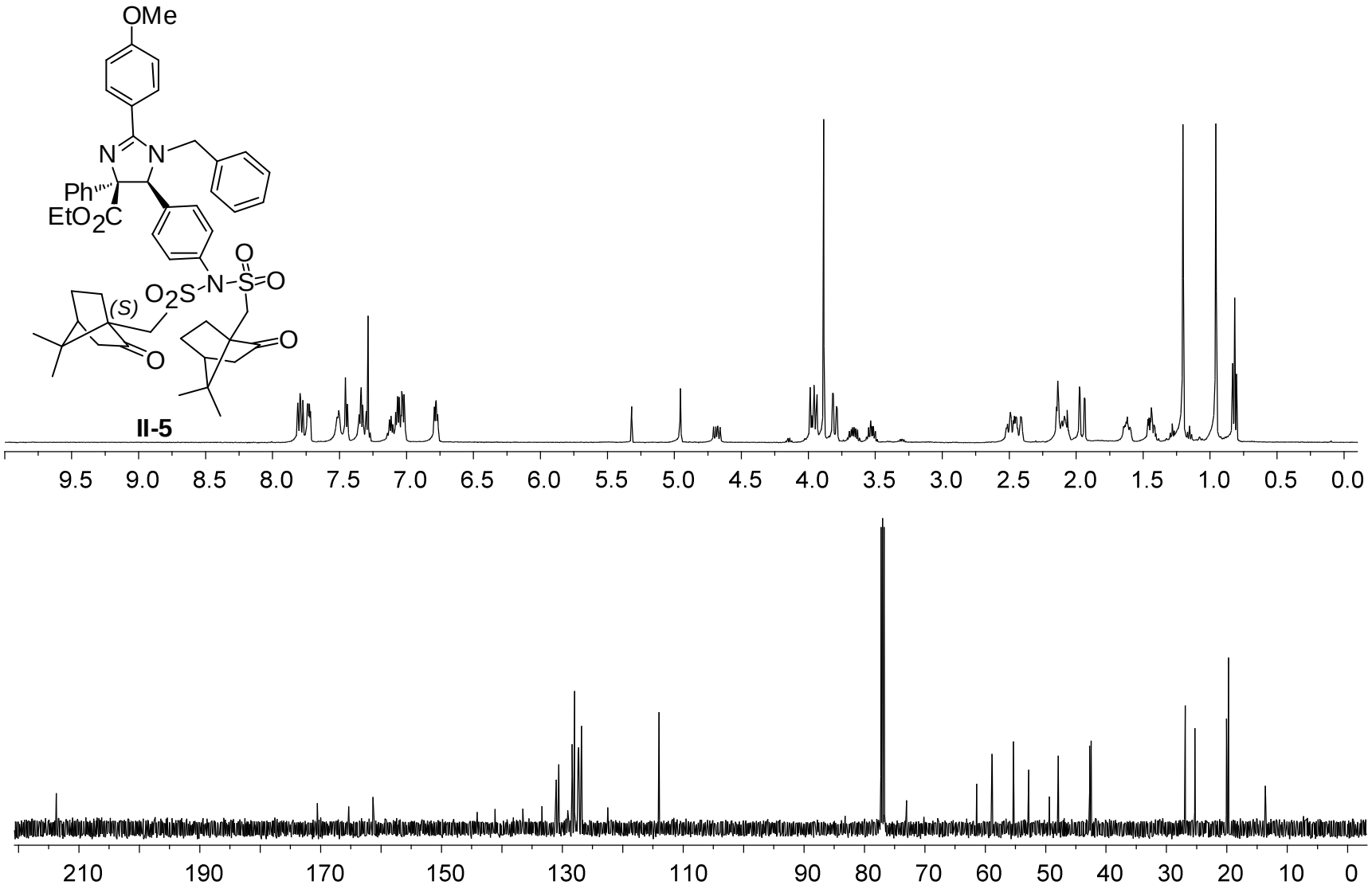
OMe
N
N
Ph
EtO2C
O
O2S
N
S
O
(S)
O
O
II-5
9.5 9.0 8.5 8.0 7.5 7.0 6.5 6.0 5.5 5.0 4.5 4.0 3.5 3.0 2.5 2.0 1.5 1.0 0.5 0.0
210 190 170 150 130 110 90 80 70 60 50 40 30 20 10 0

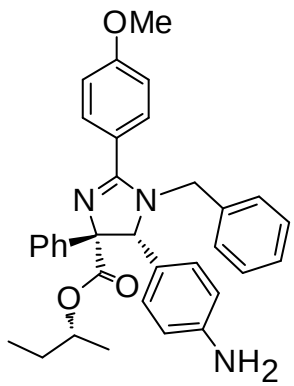
OMe
N
N
Ph
O
O
NH2

II-6 (*R*,*R*,*R*)

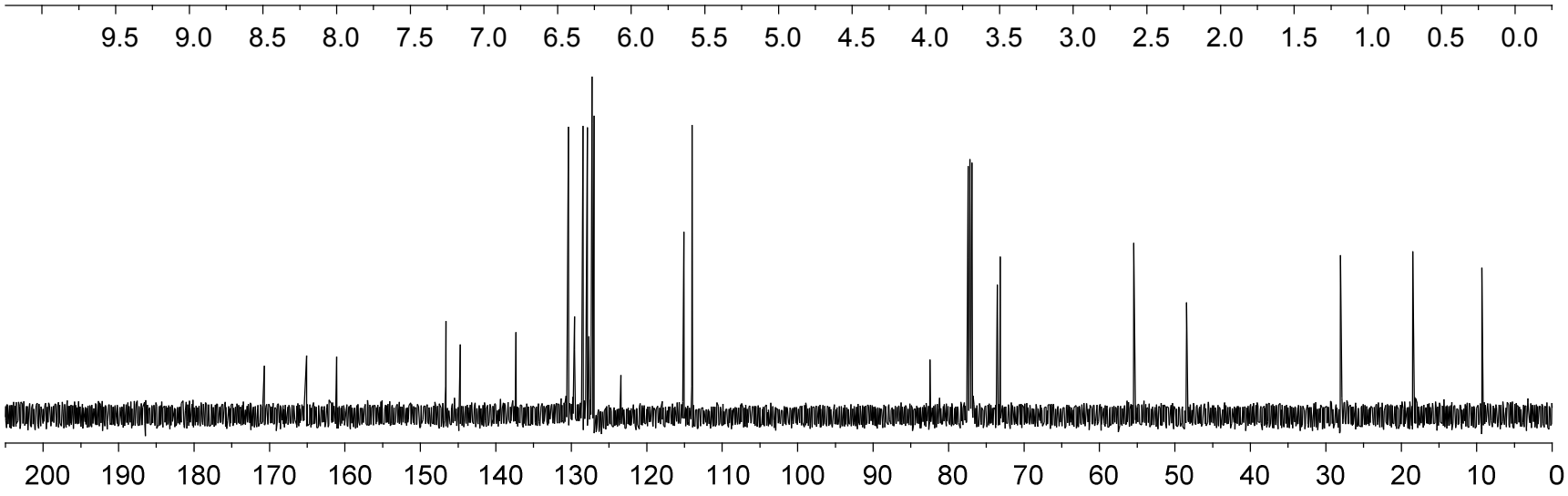
9.5 9.0 8.5 8.0 7.5 7.0 6.5 6.0 5.5 5.0 4.5 4.0 3.5 3.0 2.5 2.0 1.5 1.0 0.5 0.0

200 190 180 170 160 150 140 130 120 110 100 90 80 70 60 50 40 30 20 10 0

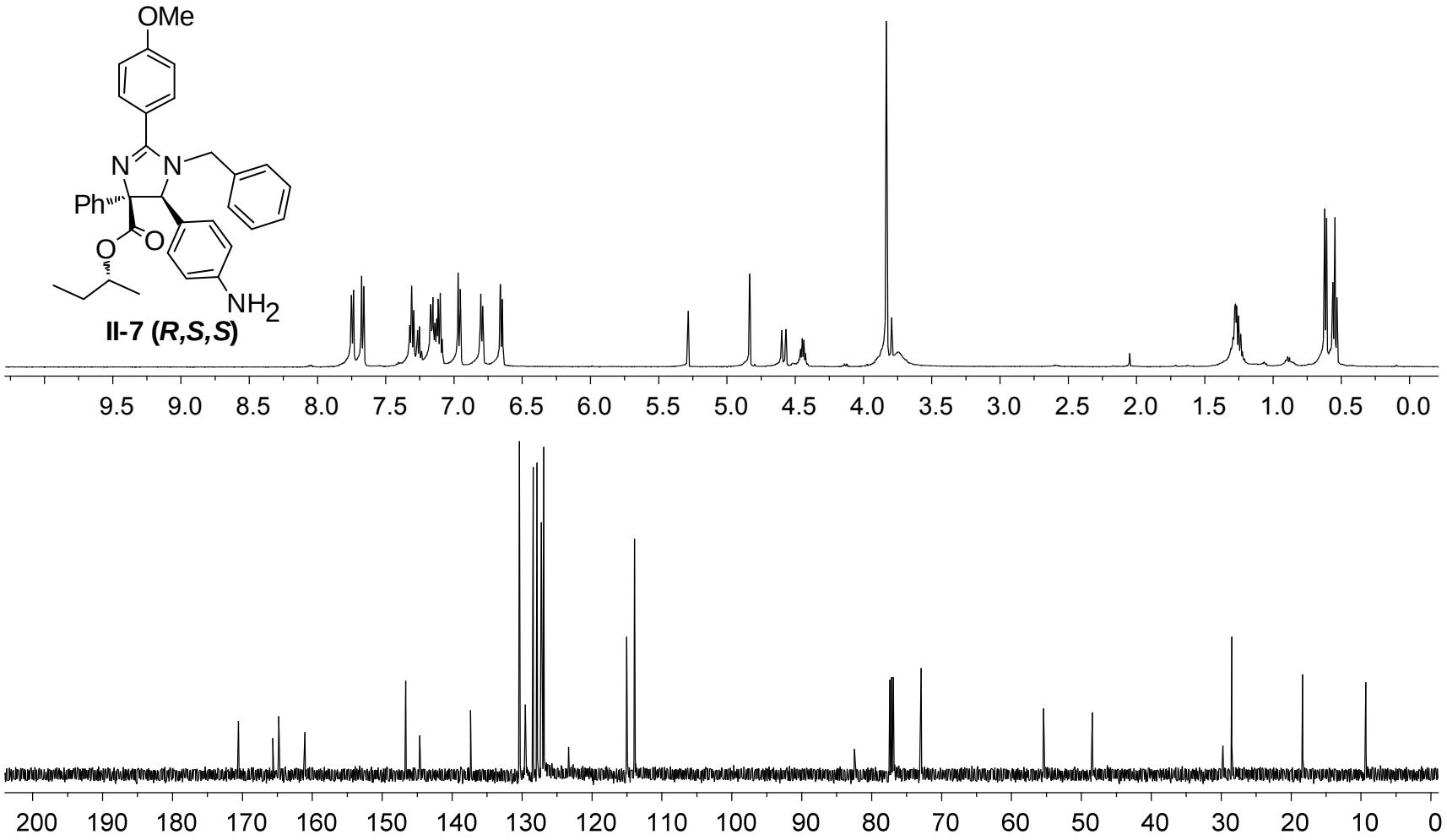
OMe
N
N
Ph
O
O
NH2
9.5 9.0 8.5 8.0 7.5 7.0 6.5 6.0 5.5 5.0 4.5 4.0 3.5 3.0 2.5 2.0 1.5 1.0 0.5 0.0
200 190 180 170 160 150 140 130 120 110 100 90 80 70 60 50 40 30 20 10 0

II-7 (*R*,*S*,*S*)

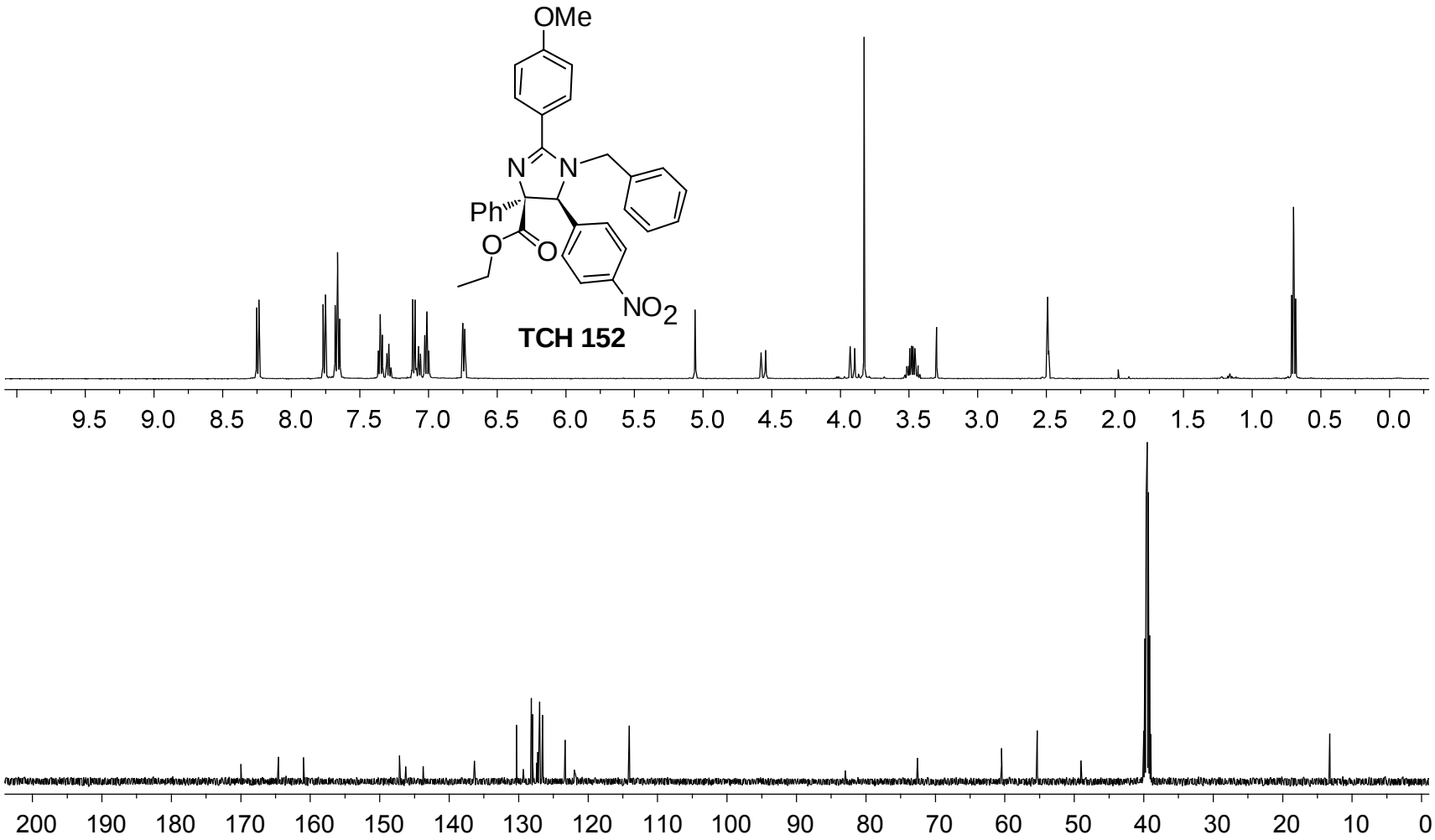
OMe
N
N
Ph
O
O
NO2
TCH 152
9.5 9.0 8.5 8.0 7.5 7.0 6.5 6.0 5.5 5.0 4.5 4.0 3.5 3.0 2.5 2.0 1.5 1.0 0.5 0.0
200 190 180 170 160 150 140 130 120 110 100 90 80 70 60 50 40 30 20 10 0

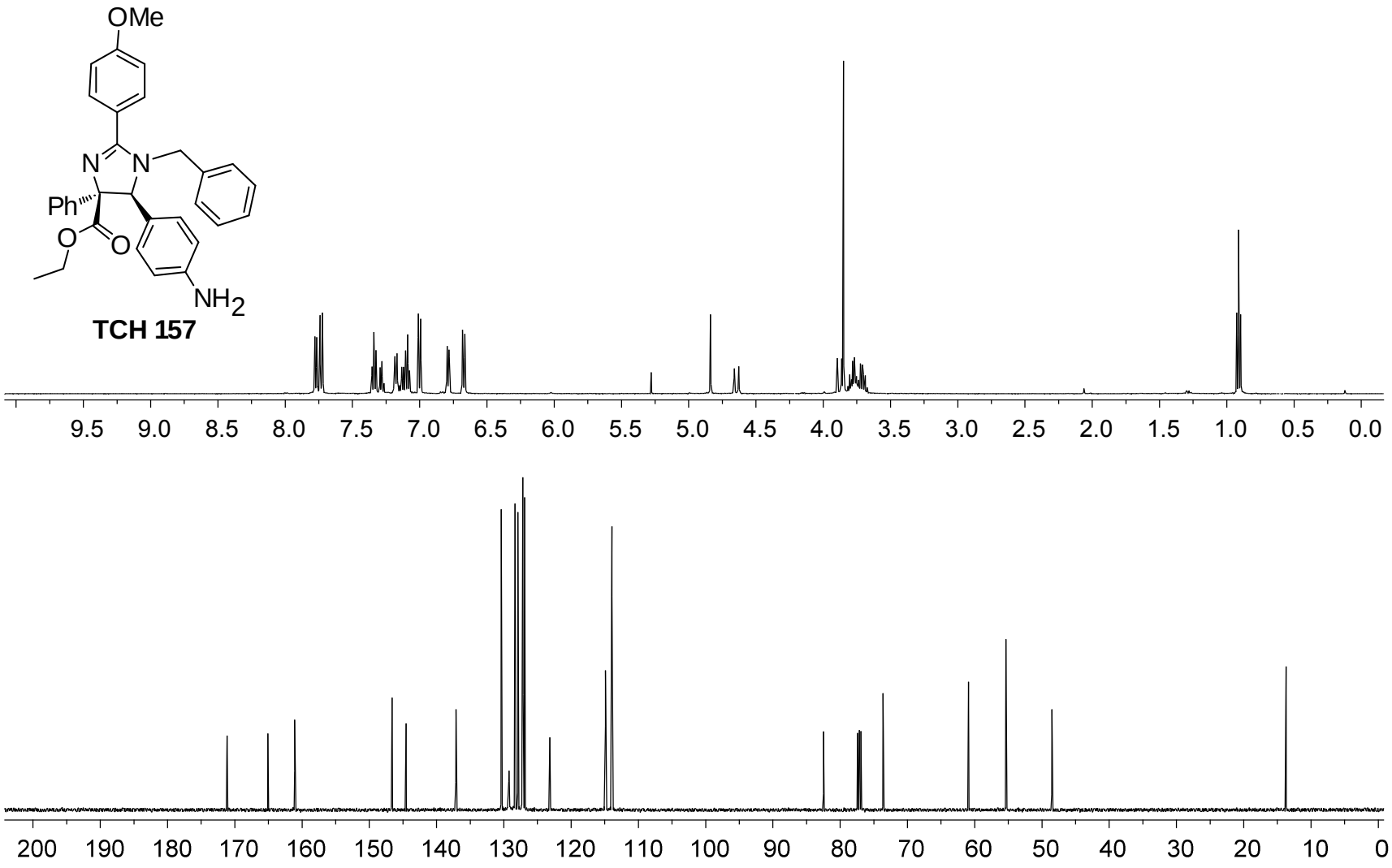
OMe
N
N
Ph
O
O
NH2
TCH 157
9.5 9.0 8.5 8.0 7.5 7.0 6.5 6.0 5.5 5.0 4.5 4.0 3.5 3.0 2.5 2.0 1.5 1.0 0.5 0.0
200 190 180 170 160 150 140 130 120 110 100 90 80 70 60 50 40 30 20 10 0

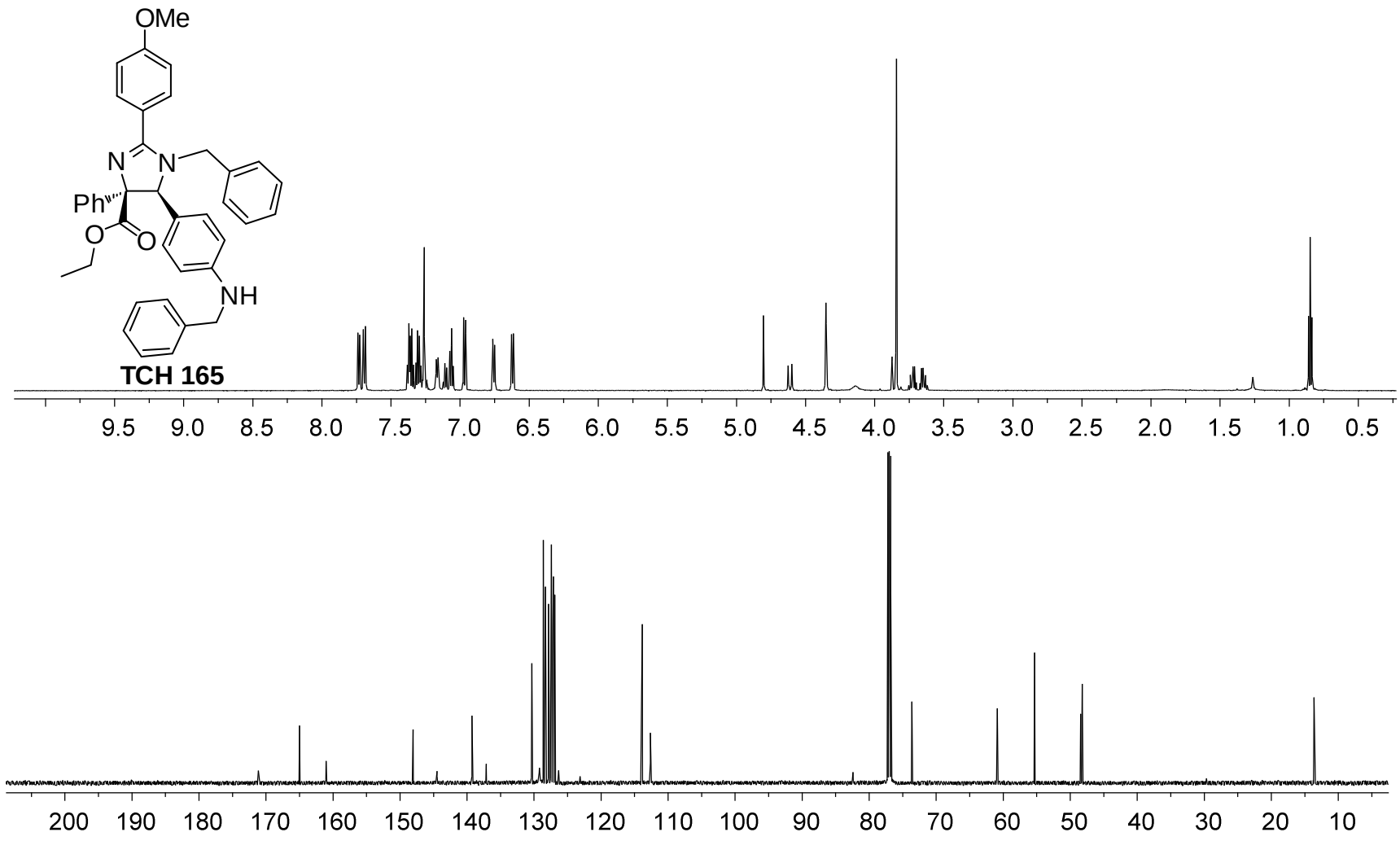
OMe
N
N
Ph
O
O
NH
TCH 165
9.5 9.0 8.5 8.0 7.5 7.0 6.5 6.0 5.5 5.0 4.5 4.0 3.5 3.0 2.5 2.0 1.5 1.0 0.5
200 190 180 170 160 150 140 130 120 110 100 90 80 70 60 50 40 30 20 10

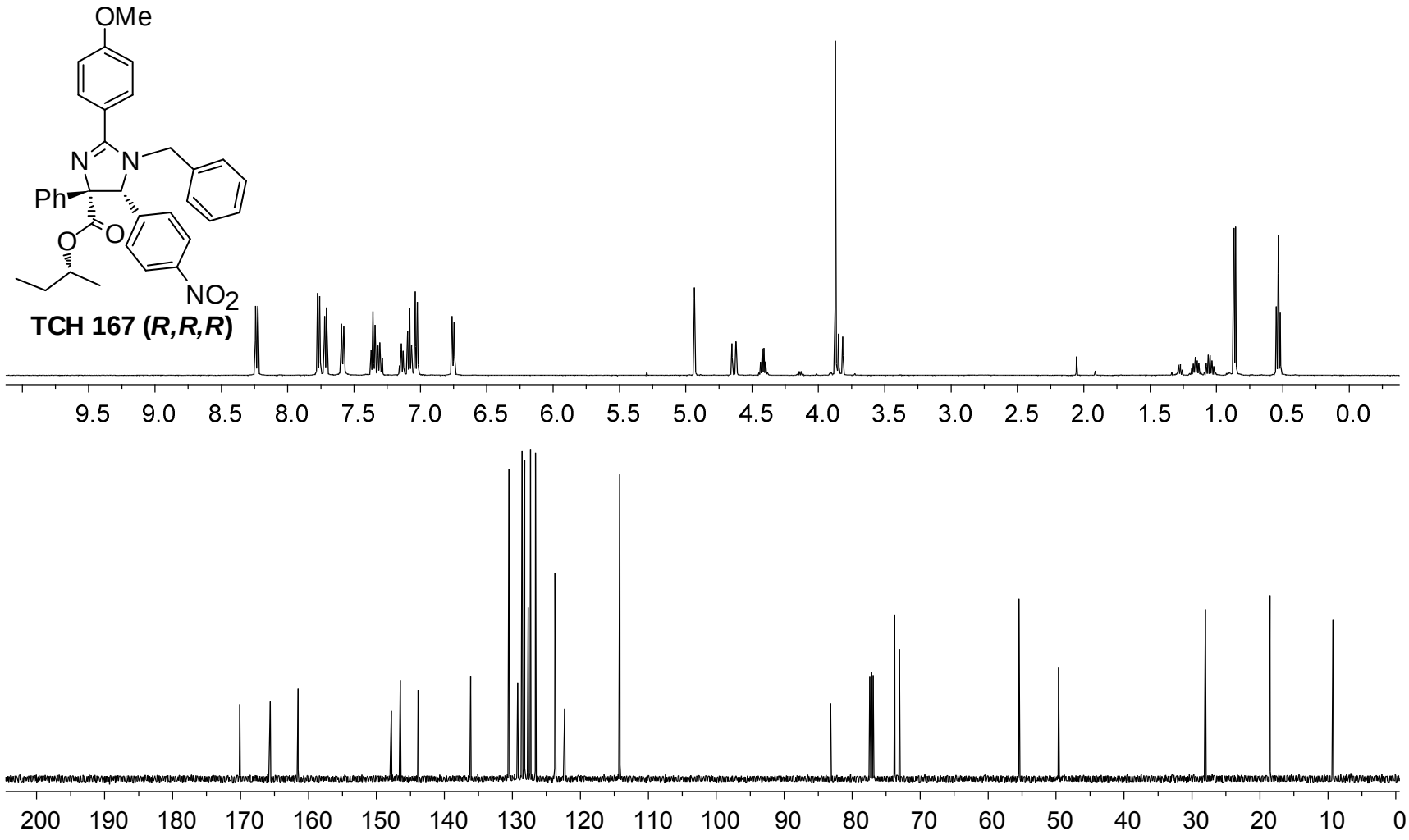
OMe
N
N
Ph
O
O
O
NO2
TCH 167 (R,R,R)
9.5 9.0 8.5 8.0 7.5 7.0 6.5 6.0 5.5 5.0 4.5 4.0 3.5 3.0 2.5 2.0 1.5 1.0 0.5 0.0
200 190 180 170 160 150 140 130 120 110 100 90 80 70 60 50 40 30 20 10 0

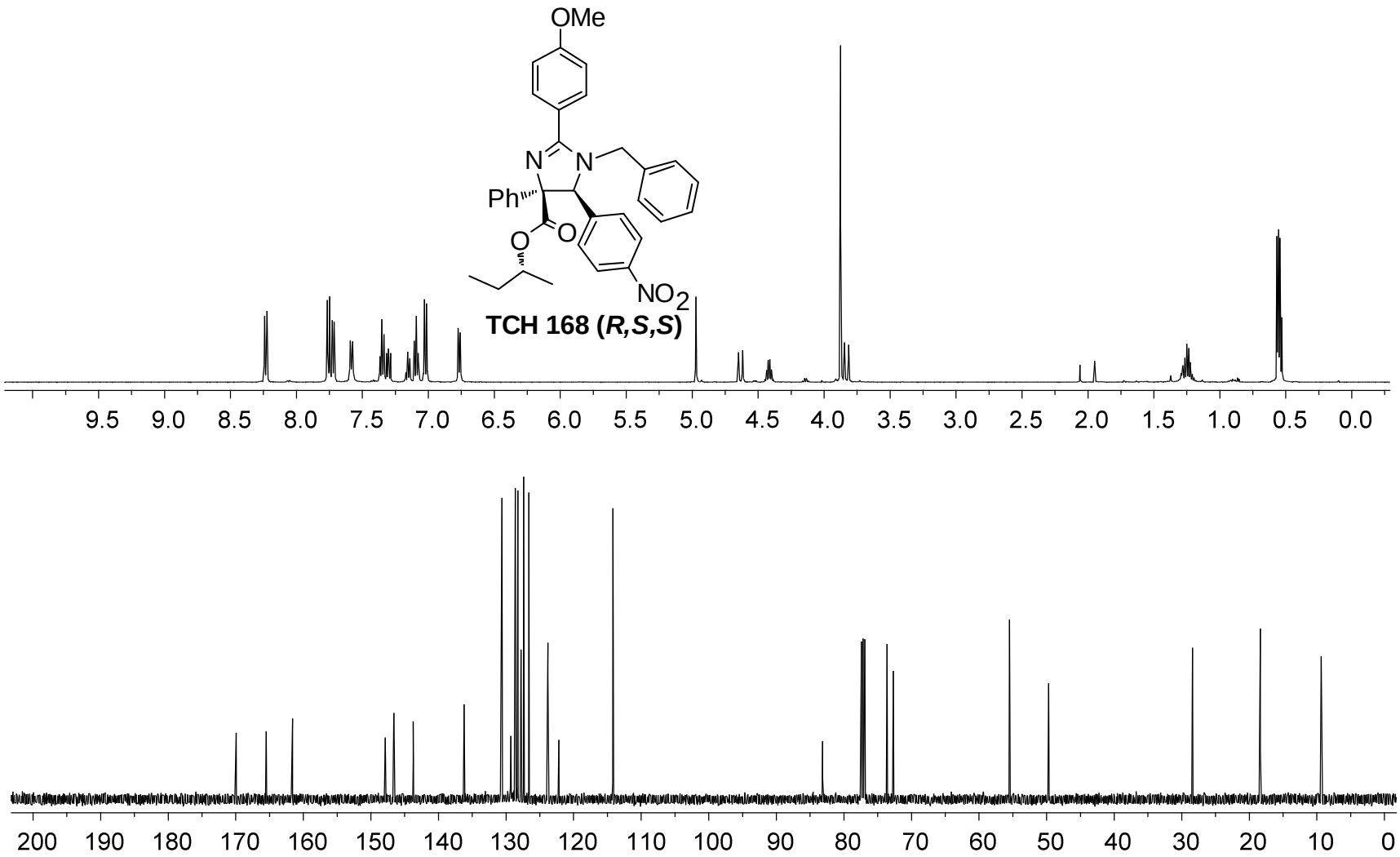
OMe
N
N
Ph
O
O
O
NO2
TCH 168 (R,S,S)
9.5 9.0 8.5 8.0 7.5 7.0 6.5 6.0 5.5 5.0 4.5 4.0 3.5 3.0 2.5 2.0 1.5 1.0 0.5 0.0
200 190 180 170 160 150 140 130 120 110 100 90 80 70 60 50 40 30 20 10 0

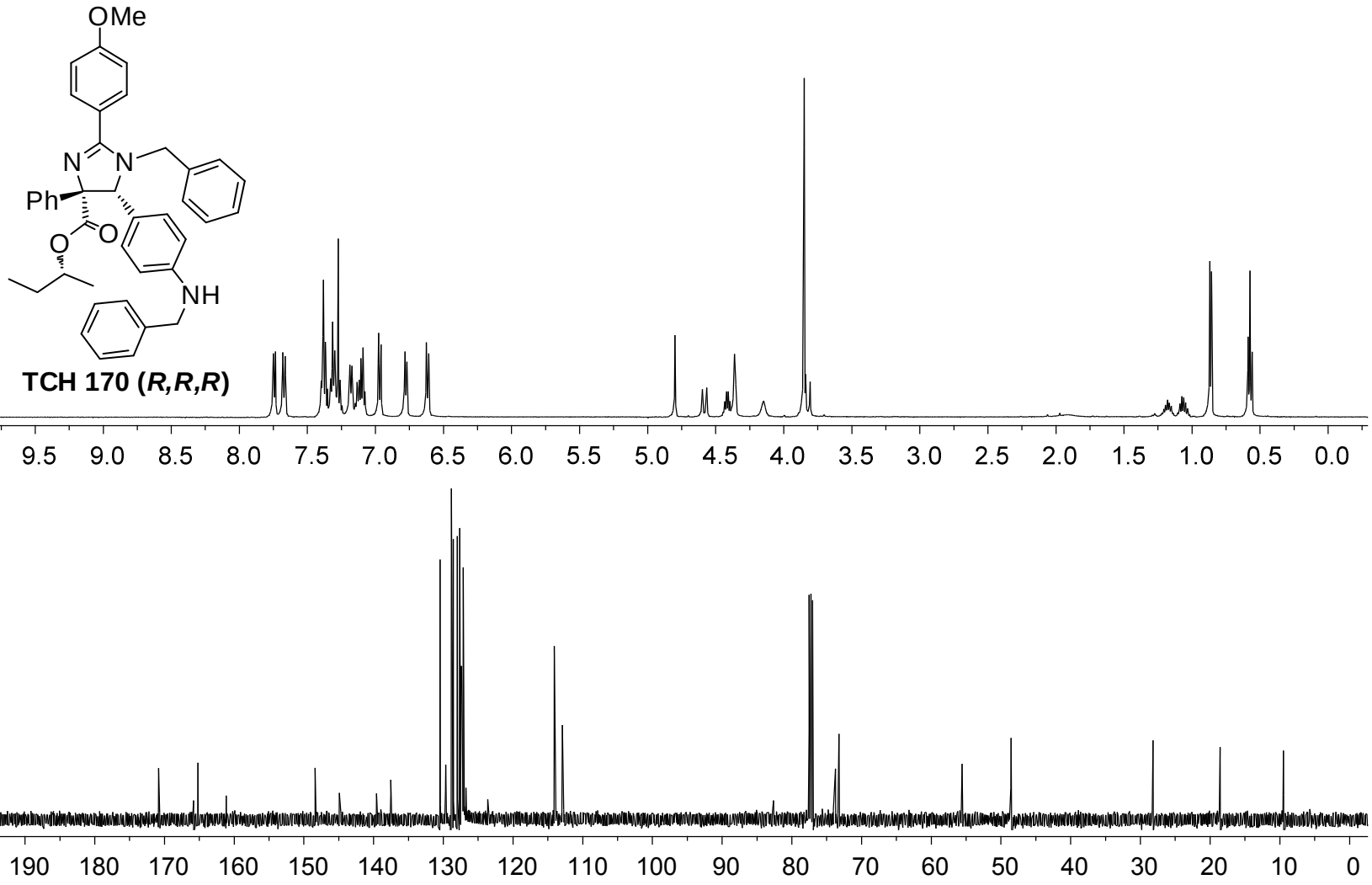
OMe
N
N
Ph
O
O
NH
TCH 170 (*R*,*R*,*R*)
9.5 9.0 8.5 8.0 7.5 7.0 6.5 6.0 5.5 5.0 4.5 4.0 3.5 3.0 2.5 2.0 1.5 1.0 0.5 0.0
200 190 180 170 160 150 140 130 120 110 100 90 80 70 60 50 40 30 20 10 0

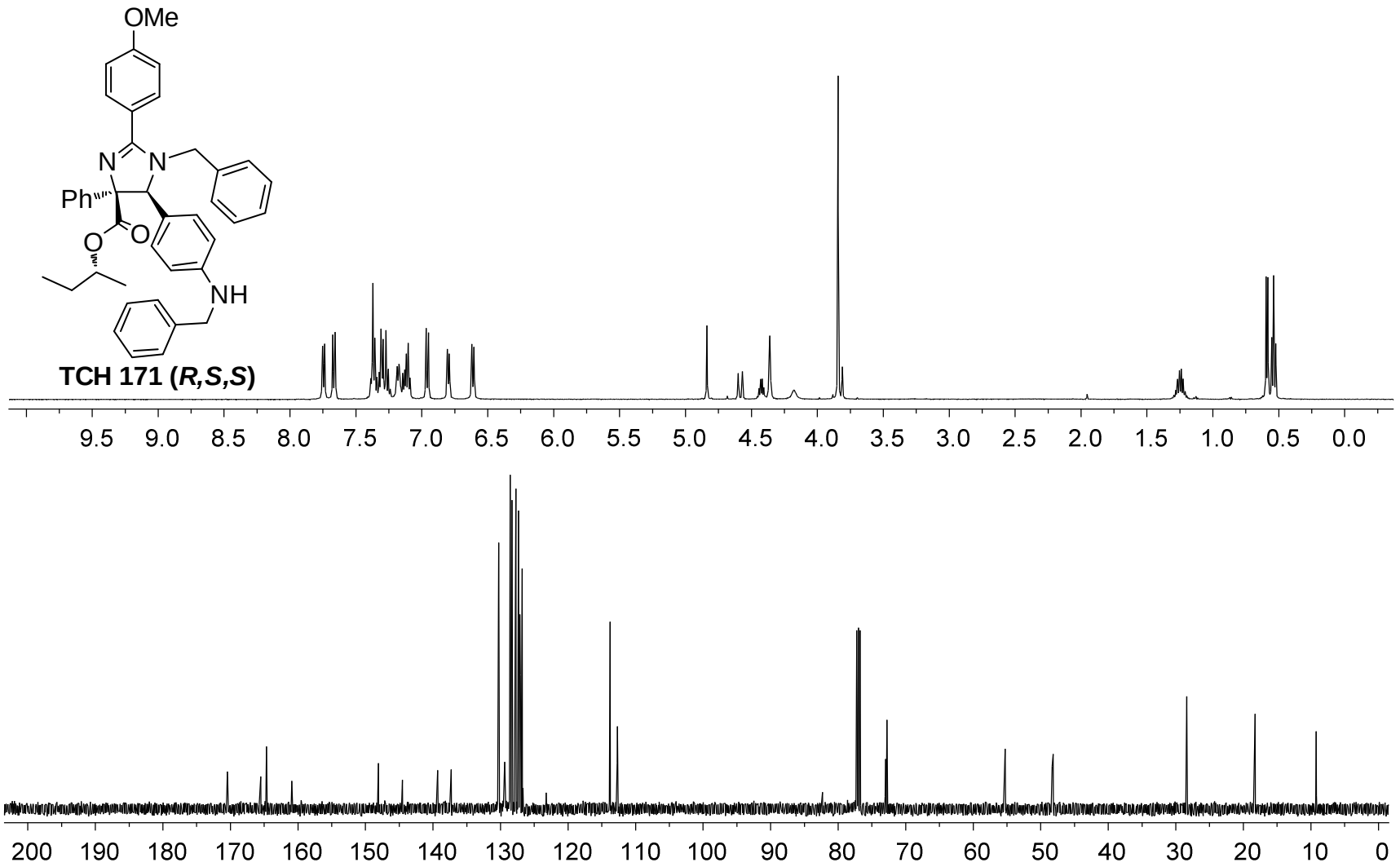
OMe
N
N
Ph
O
O
NH
TCH 171 (*R,S,S*)
9.5 9.0 8.5 8.0 7.5 7.0 6.5 6.0 5.5 5.0 4.5 4.0 3.5 3.0 2.5 2.0 1.5 1.0 0.5 0.0
200 190 180 170 160 150 140 130 120 110 100 90 80 70 60 50 40 30 20 10 0

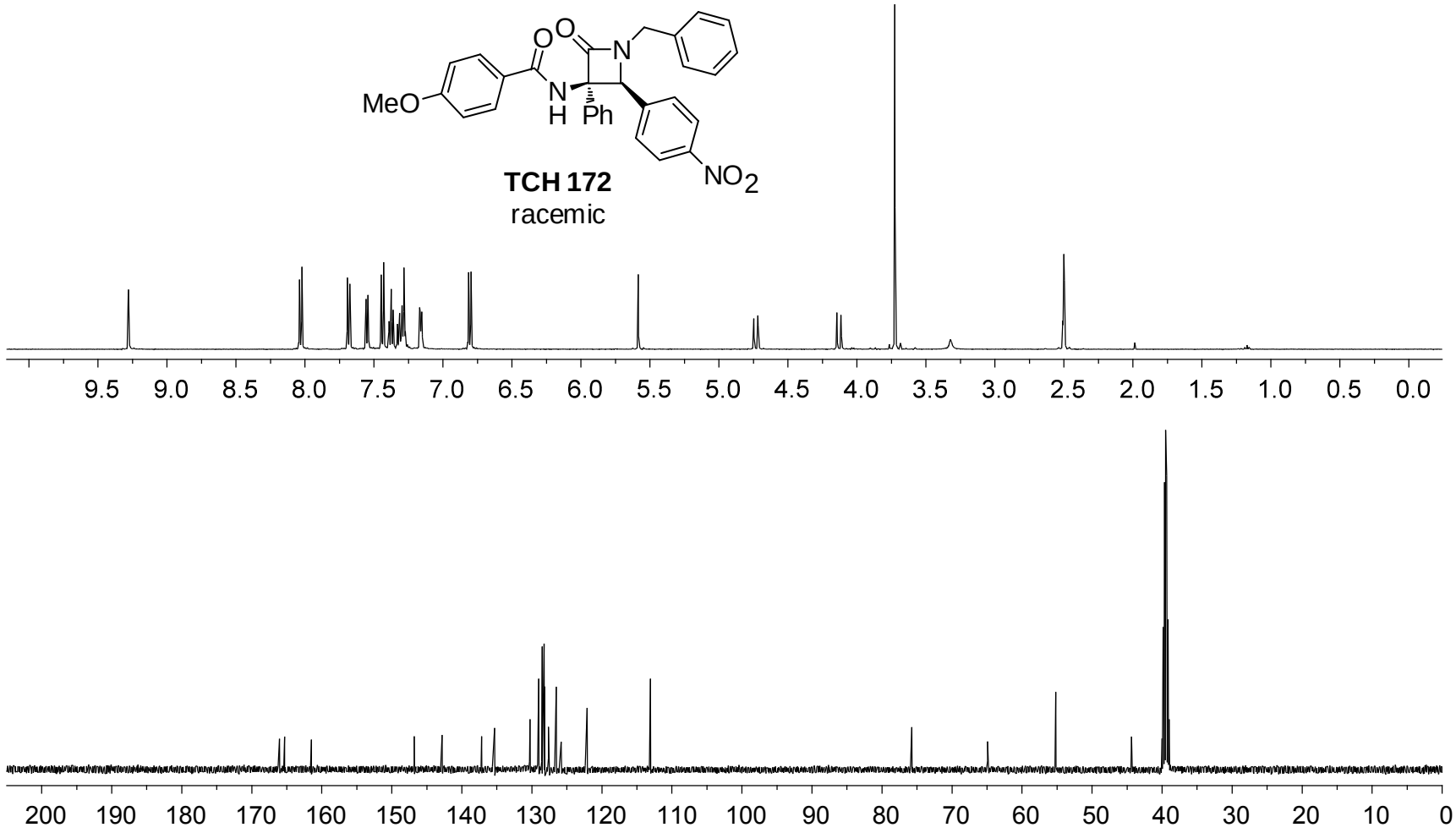
MeO
O
O
N
N
H
Ph
NO2
TCH 172
racemic
9.5 9.0 8.5 8.0 7.5 7.0 6.5 6.0 5.5 5.0 4.5 4.0 3.5 3.0 2.5 2.0 1.5 1.0 0.5 0.0
200 190 180 170 160 150 140 130 120 110 100 90 80 70 60 50 40 30 20 10 0

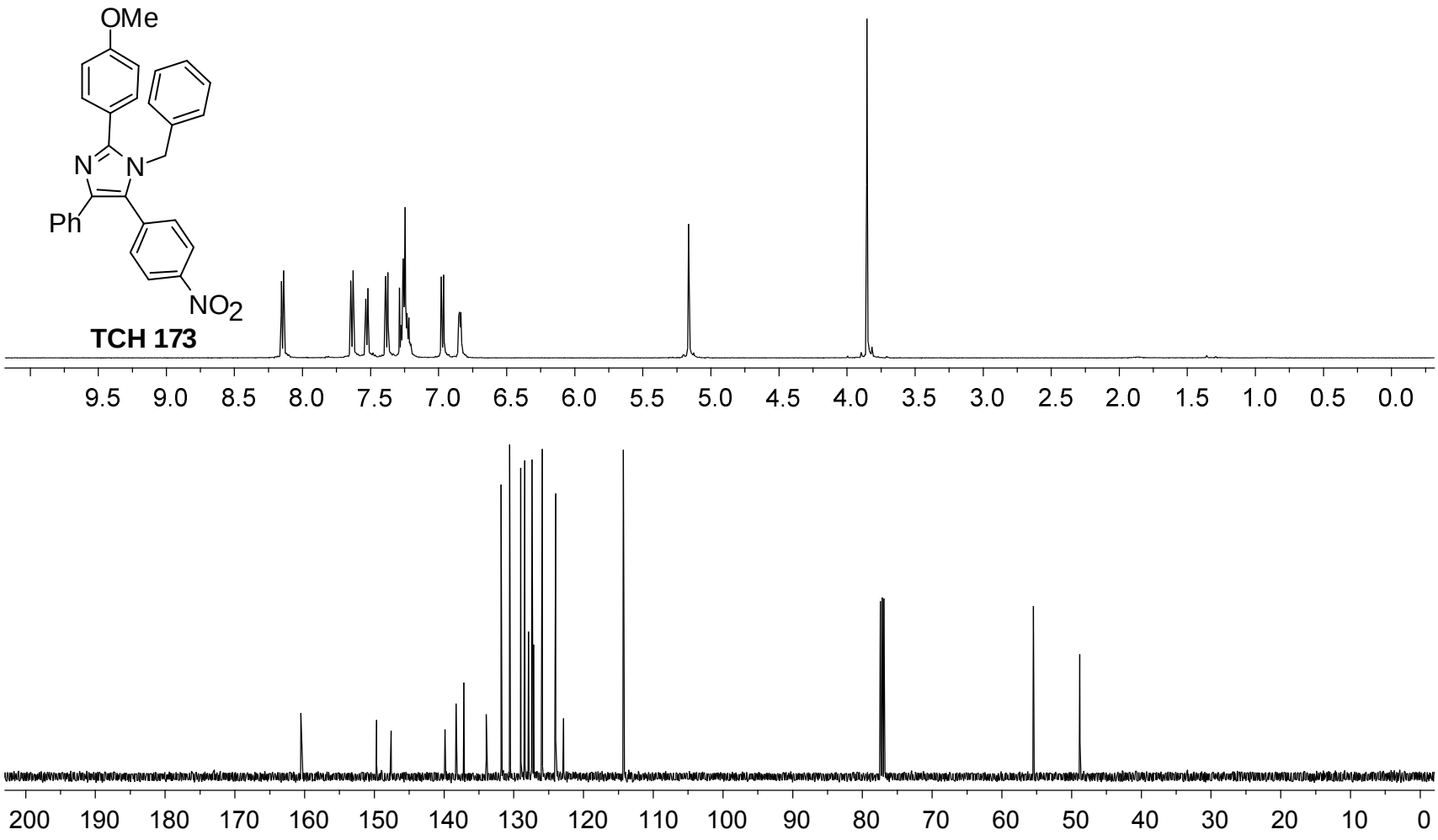
OMe
N
N
Ph
NO2
TCH 173
9.5 9.0 8.5 8.0 7.5 7.0 6.5 6.0 5.5 5.0 4.5 4.0 3.5 3.0 2.5 2.0 1.5 1.0 0.5 0.0
200 190 180 170 160 150 140 130 120 110 100 90 80 70 60 50 40 30 20 10 0

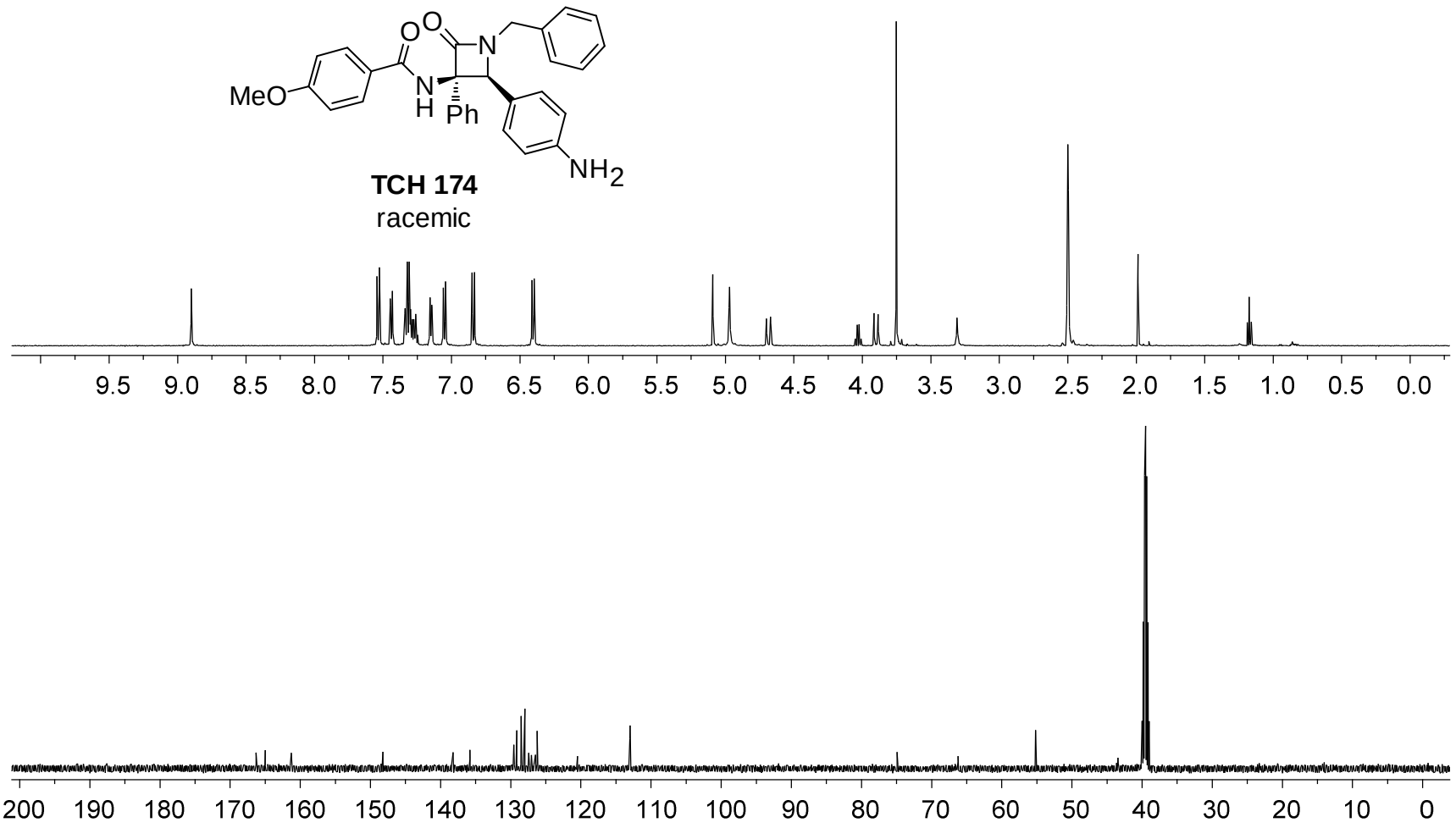
MeO
O
O
N
N
H
Ph
NH2
TCH 174
racemic
9.5 9.0 8.5 8.0 7.5 7.0 6.5 6.0 5.5 5.0 4.5 4.0 3.5 3.0 2.5 2.0 1.5 1.0 0.5 0.0
200 190 180 170 160 150 140 130 120 110 100 90 80 70 60 50 40 30 20 10 0

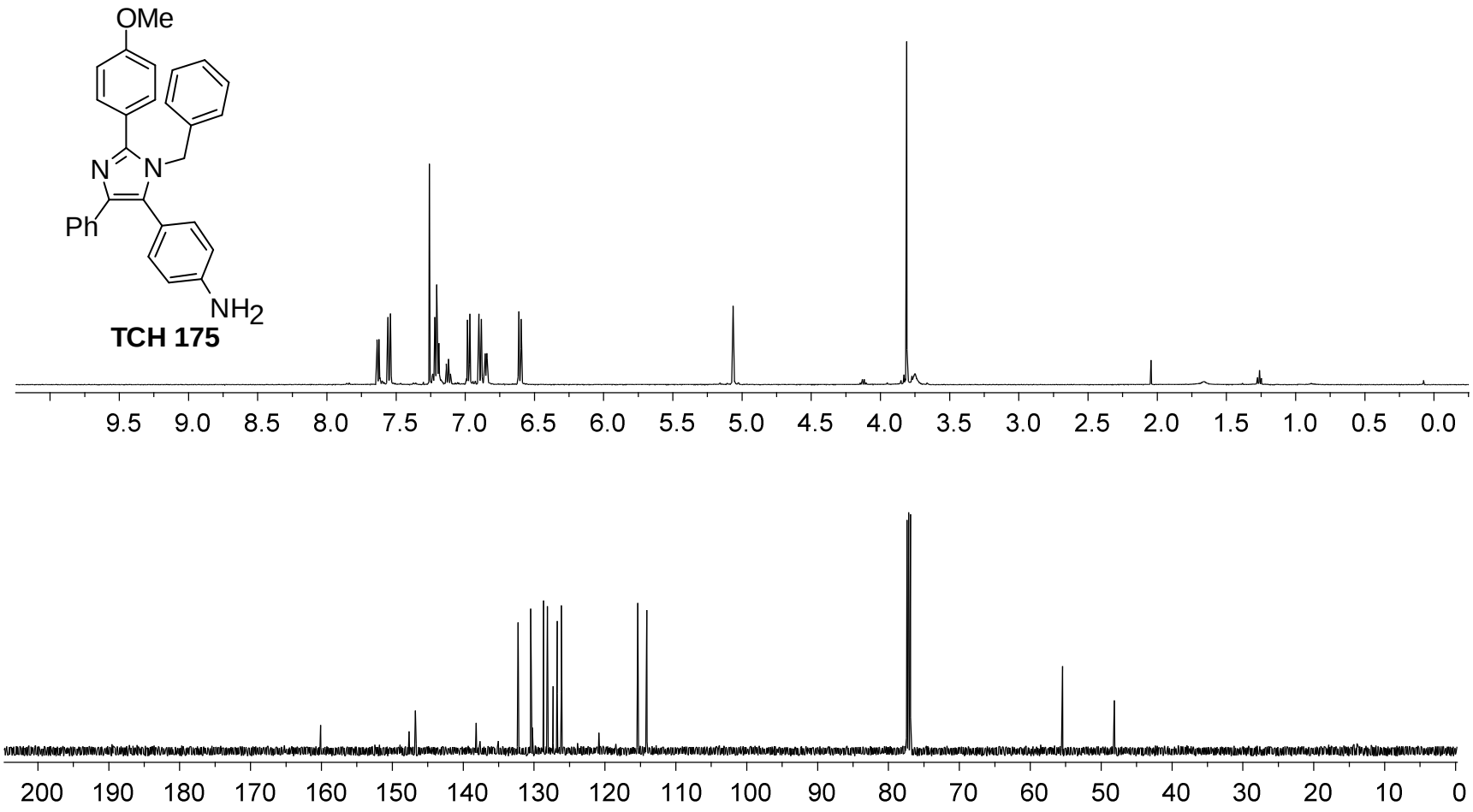
OMe
N
N
Ph
NH2
TCH 175
9.5 9.0 8.5 8.0 7.5 7.0 6.5 6.0 5.5 5.0 4.5 4.0 3.5 3.0 2.5 2.0 1.5 1.0 0.5 0.0
200 190 180 170 160 150 140 130 120 110 100 90 80 70 60 50 40 30 20 10 0

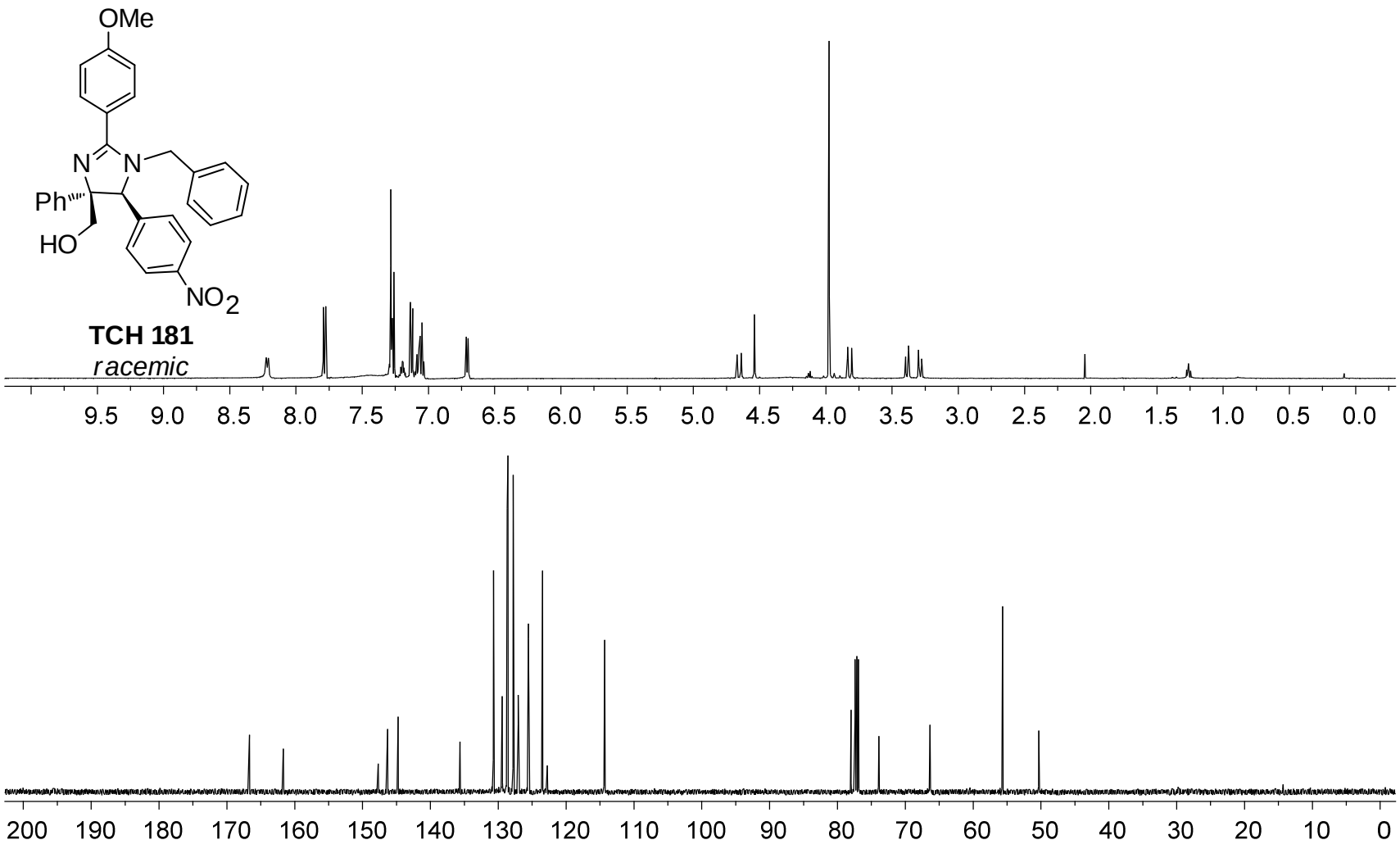
OMe
N
N
Ph
HO
NO2
TCH 181
racemic
9.5 9.0 8.5 8.0 7.5 7.0 6.5 6.0 5.5 5.0 4.5 4.0 3.5 3.0 2.5 2.0 1.5 1.0 0.5 0.0
200 190 180 170 160 150 140 130 120 110 100 90 80 70 60 50 40 30 20 10 0

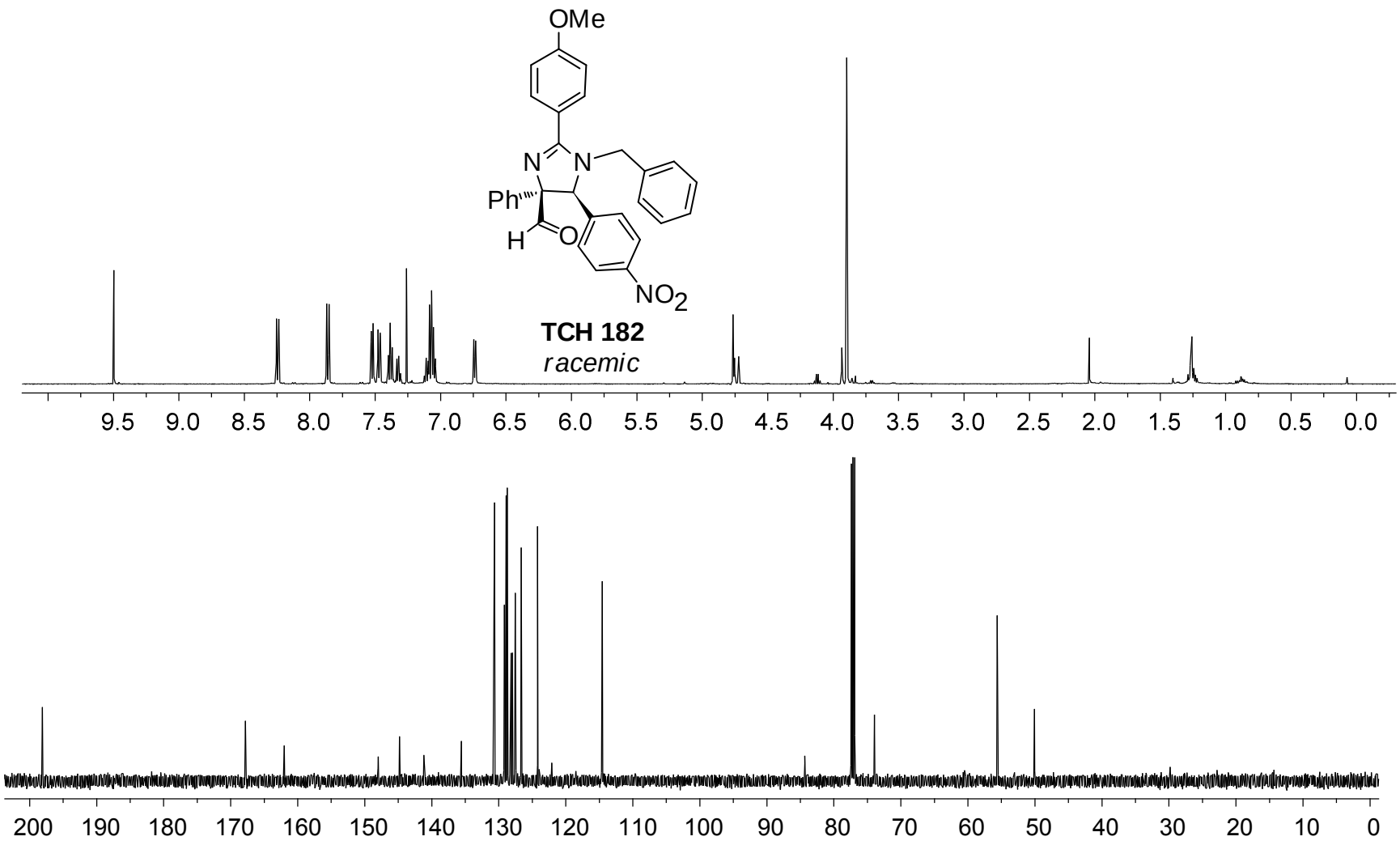
OMe
N
N
Ph
H
O
NO2
TCH 182
racemic
9.5 9.0 8.5 8.0 7.5 7.0 6.5 6.0 5.5 5.0 4.5 4.0 3.5 3.0 2.5 2.0 1.5 1.0 0.5 0.0
200 190 180 170 160 150 140 130 120 110 100 90 80 70 60 50 40 30 20 10 0

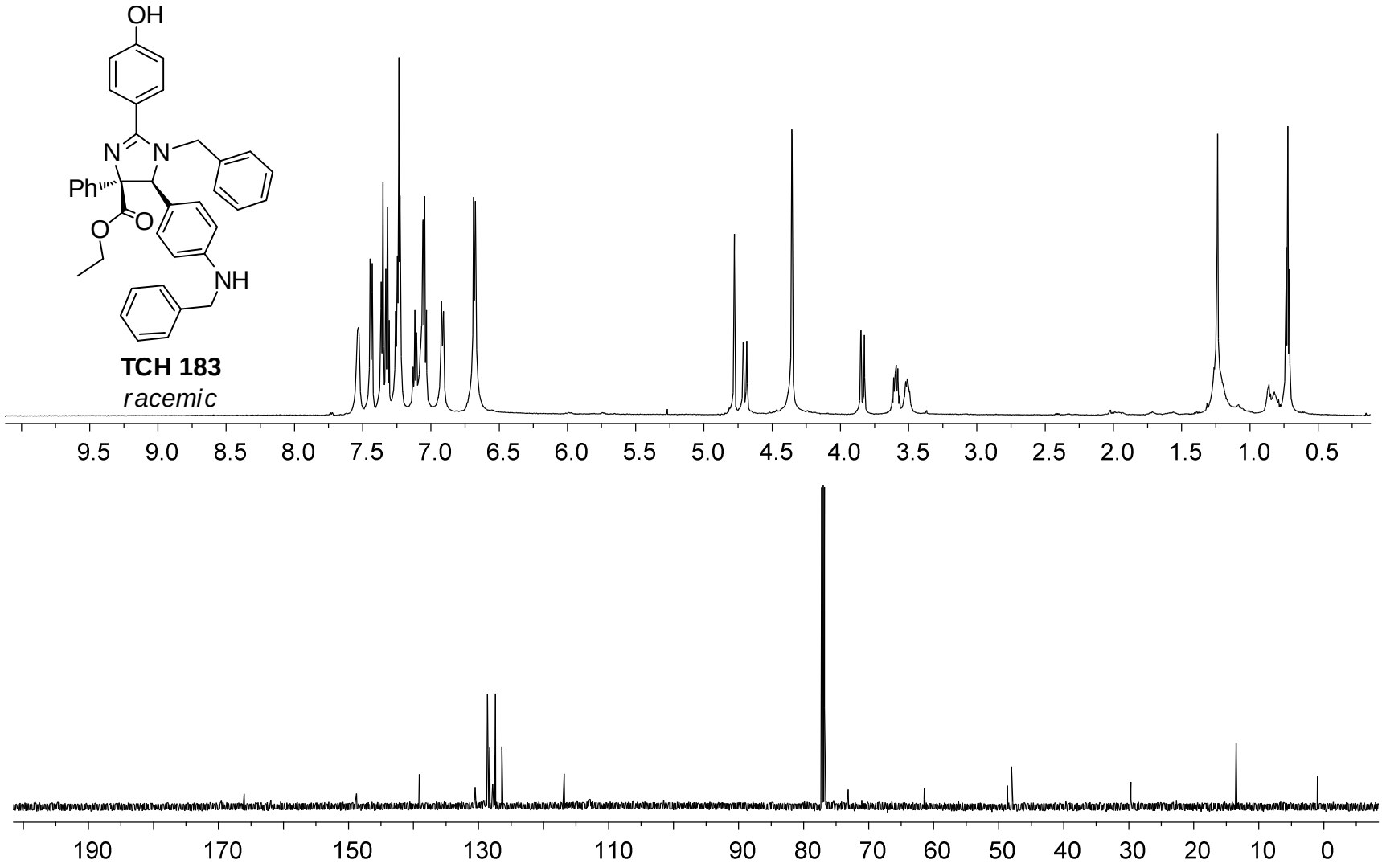
OH
N
N
Ph
O
O
NH
TCH 183
racemic
9.5 9.0 8.5 8.0 7.5 7.0 6.5 6.0 5.5 5.0 4.5 4.0 3.5 3.0 2.5 2.0 1.5 1.0 0.5
190 170 150 130 110 90 80 70 60 50 40 30 20 10 0

M. References

References

(1) Sharma, V.; Hupp, C. D.; Tepe, J. J. *Current Medicinal Chemistry* **2007**, *14*, 1061-1074.

(2) Sancar, A.; Lindsey-Boltz, L. A.; Unsal-Kacmaz, K.; Linn, S. *Annual Review of Biochemistry* **2004**, *73*, 39-85.

(3) Cusack, J. C.; Liu, R.; Baldwin, A. S. *Drug Resistance Updates* **1999**, *2*, 271-273.

(4) Sung, M. H.; Bagain, L.; Chen, Z.; Karpova, T.; Yang, X.; Silvin, C.; Voss, T. C.; McNally, J. G.; Van Waes, C.; Gordon, L. *Molecular Pharmacology* **2008**, *74*, 1215-1222.

(5) Burke, J. R.; Pattoli, M. A.; Gregor, K. R.; Brassil, P. J.; MacMaster, J. F.; McIntyre, K. W.; Yang, X.; Iotzova, V. S.; Clarke, W.; Strnad, J.; Qiu, Y.; Zusi, F. C. *Journal of Biological Chemistry* **2003**, *278*, 1450-1456.

(6) Ruggeri, B.; Miknyoczki, S.; Dorsey, B.; Hui, A.-M. *Adv Pharmacol* **2009**, *57*, 91-135.

(7) McNaught, K. S. P.; Olanow, C. W.; Halliwell, B.; Isacson, O.; Jenner, P. *Nature Reviews Neuroscience* **2001**, *2*, 589-594.

(8) Kahlon, D. K.; Lansdell, T. A.; Fisk, J. S.; Hupp, C. D.; Friebe, T. L.; Hovde, S.; Jones, A. D.; Dyer, R. D.; Henry, R. W.; Tepe, J. J. *Journal of Medicinal Chemistry* **2009**, *52*, 1302-1309.

(9) Pierce, J. W.; Schoenleber, R.; Jesmok, G.; Best, J.; Moore, S. A.; Collins, T.; Gerritsen, M. E. *Journal of Biological Chemistry* **1997**, *272*, 21096-21103.

(10) Yemelyanov, A.; Gasparian, A.; Lindholm, P.; Dang, L.; Pierce, J. W.; Kisseljov, F.; Karseladze, A.; Budunova, I. *Oncogene* **2005**, *25*, 387-398.

(11) Sharma, V.; Lansdell, T. A.; Peddibhotla, S.; Tepe, J. J. *Chemistry & Biology* **2004**, *11*, 1689-1699.

(12) Sharma, V.; Peddibhotla, S.; Tepe, J. J. *Journal of the American Chemical Society* **2006**, *128*, 9137-9143.

(13) Consult the Dissertation of Dr. Robert Mosey

(14) Dabiri, M.; Salehi, P.; Heydari, S.; Kozehgary, G. *Synthetic Communications* **2009**, *39*, 4350-4361.